CO_2 FLUXES FROM SOIL AND KARST CAVES: DETERMINATION OF SOURCES, PATHWAYS AND INTERACTIONS USING A STABLE ISOTOPE APPROACH

Bor Krajnc

Doctoral Dissertation
Jožef Stefan International Postgraduate School
Ljubljana, Slovenia

Supervisor: Prof. Dr. Nives Ogrinc, MPŠ and Jožef Stefan Institute, Ljubljana, Slovenia

Evaluation Board:
Prof. Dr. Janez Ščančar, Chair, MPŠ and Jožef Stefan Institute, Ljubljana, Slovenia
Prof. Dr. Janja Vaupotič, Member, MPŠ and Jožef Stefan Institute, Ljubljana, Slovenia
Prof. Dr. Annette Summers Engel, Member, Department of Earth and Planetary Sciences, University of Tennessee, USA

MEDNARODNA PODIPLOMSKA ŠOLA JOŽEFA STEFANA
JOŽEF STEFAN INTERNATIONAL POSTGRADUATE SCHOOL



Bor Krajnc

CO_2 FLUXES FROM SOIL AND KARST CAVES: DETERMINATION OF SOURCES, PATHWAYS AND INTERACTIONS USING A STABLE ISOTOPE APPROACH

Doctoral Dissertation

TOKOVI CO_2 IZ TAL IN KRAŠKIH JAM: DOLOČITEV VIROV, POTI IN INTERAKCIJ Z UPORABO STABILNIH IZOTOPOV

Doktorska disertacija

Supervisor: Prof. Dr. Nives Ogrinc

Ljubljana, Slovenia, October 2017

Svetu, po katerem bodo hodili Rujko in njegovi prijatelji

Acknowledgements

This doctoral thesis was performed at the Department of Environmental Sciences of the Jožef Stefan Institute. First of all, I want to sincerely thank my supervisor Prof. Dr. Nives Ogrinc for all the support, encouragement and patience during these years of study. I would also like to thank all the chair (Prof. Dr. Janez Ščančar) and the members of the committee (Prof. Dr. Janja Vaupotič and Prof. Dr. Annette Summers Engel) for the evaluation of the thesis and all the suggestions to improve the final version of the dissertation.

I would like to thank Prof. Dr. Radmila Milačič and Prof. Dr. Janez Ščančar who together with Nives saw the potential in me, encouraged me, and found the way for my enrolment to the doctoral study program.

I greatly appreciate all the support, laughs, and suggestions from my colleagues at the Organic Biogeochemistry group, especially Doris Potočnik, Janja Vrzel, Dr. Samo Tamše, Lidija Strojnik and Staša Gregorčič for a great company and their willingness to answer all my questions. I woud like to thank Staša also for checking the final version of the Dissertation. Beside our group I would like to thank also other fellow students and coworkers at our department, especially to Igor Živkovič and Lojze Gačnik for all the suggestions and brainstorming during our lunchbreaks.

I woud like to thank to Dr. David Heath for revising the Abstract

For technical assistance and all the explanations about practical work with IRMS machines a special thanks goes to Stojan Žigon.

I would like to thank again to Prof. Dr. Janja Vaupotič for generously sharing the knowledge and measurement equipment for radon measurements, and her young researcher Dafina Kikaj for all the brainstorming about radon levels in the cave. At the same time, I would like to thank Boštjan Črnič from the Department of Low and Medium Energy Physics for all the supplemental measurements in the cave, brainstorming and company at the fieldwork.

I would also like to thank Dr. Sonja Lojen and Dr. Tjaša Kanduč for constructive debates and their generous exchange of knowledge.

Many thanks go to Dr. Mitja Ferlan and Boštjan Zupanc from the Laboratory for Electronic Devices at the Slovenian Forestry Institute, for all the assistance while installing their soil CO_2 flux measurement devices and for helping me with data processing.

Special thanks go to Prof. Dr. Ryoko Fujiyoshi from the Division of Quantum Science and Engineering at Hokkaido University for all the help regarding the samples for 14C measurements.

Big thanks go also to Dr. Franci Gabrovšek from the Karst Research Institute for sharing the knowledge about processes happening in the caves and sharing results of his measurements in Pisani rov.

Thanks also to Dr. Iztok Jože Košir from the Slovenian Institute for Hop Research and Brewing for the pedological analysis of the soil and cave sediment.

For organizing cave visits, helping and accompanying me in the cave, I would like to thank the cave guides, especially Stanislav Glažar, Janez Margon and Erik Rebec.

I am greatly thankful to all of you who helped me out on the field. There are too many to list but I really appreciate you being willing to get some dirt on your boots. ☺

I would like to acknowledge the managers of Postojna Jama d.d. and Ministry of Agriculture and Environment of Slovenia for the permission to access and work in the cave, as well as the Farmland and Forest Fund of the Republic of Slovenia for the permission to do research in the forest.

This work has been financially supported by the Innovative scheme for co-financing of doctoral studies financed by the European Union through the European Social Fund and by the scholarship granted by the World Federation of Scientists. This study was performed within the H2020 MASTWIN project, the Japanese-Slovenian cooperation (*Dynamics of soil air components (radon, carbon dioxide, and its carbon isotopes) under semi-natural forest sites*), and O-2 research program group P1-0143 (*Kroženje snovi v okolju, snovna bilanca in modeliranje okoljskih procesov ter ocena tveganja*).

Finally, I thank my family and friends for all the support during the times of my study, and last but not least I would like to dedicate special acknowledgment to Irena for being the one that encouraged me to start all of this, for supporting me and surviving all the perks of being the PhD student's partner. At the end of my PhD studies our son Ruj has joined us who arrived just in time to enjoy the end of this adventure and I am grateful to him for making those moments one of the happiest ones.

Abstract

Global environmental change is one of the most pressing issues in Earth science research and significant effort has been devoted to understanding the role of the terrestrial reservoir in modulating carbon storage and cycling. Studies dedicated to CO_2 dynamics in terrestrial ecosystems have focused on either surface soils or on bedrock cavities. In karstic areas both systems exist and are inter-connected. It is assumed that soil CO_2 originates only from soil respiration. Recent studies have however revealed that abiotic terrestrial CO_2 exchange in carbonaceous areas can significantly influence and temporally even dominate soil CO_2. Likewise, ventilation of CO_2 from subterranean fissures and caves, which are capable of storing large amounts of CO_2, is a potential major source of soil CO_2.

This doctoral thesis sets out to investigate carbon fluxes and its sources in soils developed on geologically different parent material and assessing the influence of belowground processes. This thesis consists of five investigations where natural tracers were used to assess the relative contribution of different CO_2 sources to soil CO_2 fluxes and/or to assess carbon transport (e.g. in gas phase or in water phase) in soils formed on different geological materials. Cave air CO_2 dynamics were investigated as a possible source of soil CO_2 in karstic areas and soil CO_2 fluxes were also studied on the flanks of an active volcano to better understand the physio-chemical interactions occurring between deep CO_2 and the shallow environment of the volcano. Tracers included stable isotopes of carbon (^{12}C and ^{13}C), radiocarbon (^{14}C), radon (^{222}Rn), and stable isotopes of oxygen (^{16}O and ^{18}O).

First, CO_2 sources in forest soils developed on different parent materials in Slovenia were investigated. Isotopic analysis revealed that the CO_2 was young and there was no difference in the age of soil CO_2 above either carbonate or non-carbonate bedrock. Levels of ^{222}Rn in Karst soil, however, suggest that the ventilation of subterranean voids has a significant effect on soil CO_2. Second, a study of the dynamics of dissolved inorganic and organic carbon in forest soil revealed that local lithology, type of vegetation, soil texture and climate are important factors controlling the magnitude of carbon loss of both forms. The $\delta^{13}C_{DIC}$ values reveal that half of the dissolved inorganic carbon (DIC) derives from soil CO_2 such that 2 to 5 mol m^{-2} $year^{-1}$ of carbon is lost in the form of DIC due to carbonate dissolution. The loss of dissolved organic carbon at a soil depth of 5 cm was lower (1 mol m^{-2} $year^{-1}$) and shows no significant differences among the study sites. Third, soil CO_2 fluxes in forest soil above a known subterranean cave were studied. Findings reveal that cave ventilation affects soil CO_2 fluxes and temporally even dominates them. Fourth, a study of the sources and dynamics of cave air CO_2 in Pisani rov, a gallery of the Postojna Cave system, revealed that outside air temperature has a major influence on cave ventilation and that cave CO_2 is mainly CO_2 from soil respiration which directly enters into the cave. Carbon dioxide transported into the cave via dripwater has only a small effect on cave CO_2 levels. Finally, soil CO_2 efflux and its isotopic composition measurements from the flanks of Mount Etna (Italy) reveal the

different pathways of CO_2 from deep sources before reaching the surface and the influence that volcanic activity has on CO_2 effluxes and isotopic composition.

In summary, this thesis shows how natural isotope abundances can reveal important information about CO_2 fluxes and their driving forces above and below the ground.

Povzetek

Globalne okoljske spremembe so ena najpomembnejših tem, s katerimi se ukvarja okoljska znanost. Veliko truda je vloženega v razumevanje vloge zemeljskega rezervoarja ogljika pri modulaciji prevzemanja, shranjevanja in kroženja ogljika. Študije, ki se posvečajo dinamiki ogljikovega dioksida v kopenskih ekosistemih, se po navadi osredotočajo ali na dogajanja na površini ali na dogajanja v podzemlju. Na kraških območjih sta oba vidika nerazdružljivo povezana in ju je potrebno obravnavati istočasno. Kljub temu da se velikokrat predpostavlja, da zemeljski CO_2 izvira izključno iz dihanja tal, so nedavne študije pokazale, da lahko abiotski viri znatno vplivajo na talni CO_2 ter občasno celo prevladujejo. Pomemben dejavnik je tudi izhajanje CO_2 iz podzemnih razpok in jam ob njihovem prezračevanju, kar lahko predstavlja znaten vir CO_2 v tleh.

Doktorska disertacija preučuje vire in tokove ogljika v tleh, razvitih na različnih geoloških podlagah, in vpliv podzemnih procesov na njih. Delo je sestavljeno iz petih raziskav, v katerih so bili za oceno prispevka različnih virov CO_2 (tako v tleh kot v jami) ter za preučevanje transporta ogljika v tleh (bodisi v plinski ali tekoči fazi) uporabljeni različni naravni sledilci. Med drugim se je na kraškem območju kot možen vir talnega CO_2 preučeval CO_2 v jamskem zraku. Poleg tega so se preučevali tudi tokovi talnega CO_2 na vznožju aktivnega vulkana z namenom, da bi bolje razumeli fizikalno-kemijske interakcije, ki se pojavljajo med CO_2, ki izvira iz globokih virov, in plitvejšim delom geološke podlage v območju vulkana. Za sledilce so bili uporabljeni izotopi ogljika (^{12}C, ^{13}C in ^{14}C), radon (^{222}Rn) in stabilni izotopi kisika (^{16}O in ^{18}O).

V prvi raziskavi so bili preučevani različni možni viri CO_2 v gozdnih tleh na različnih matičnih podlagah v Sloveniji. Izotopska analiza je pokazala, da je bil CO_2 na preučevanih območjih mlajšega izvora in da v starosti talnega CO_2 ni bilo signifikantne razlike med tlemi, razvitimi na karbonatni ali na nekarbonatni podlagi. Kljub temu pa je raven ^{222}Rn na kraških tleh nakazovala na to, da bi lahko imelo prezračevanje podzemnih votlin pomemben učinek na talni CO_2. V drugi raziskavi je bila preučevana dinamika raztopljenega anorganskega in organskega ogljika v gozdnih tleh. Rezultati so pokazali, da so lokalna litologija, vrsta vegetacije, tekstura tal in podnebje pomembni dejavniki, ki vplivajo na izpiranje ogljika iz tal v obeh oblikah. Vrednosti $\delta^{13}C_{DIC}$ so pokazale, da polovica raztopljenega anorganskega ogljika (DIC) na karbonatnih tleh izvira iz ogljikovega dioksida, čigar vir je dihanje tal. Rezultati kažejo na to, da se zaradi raztapljanja karbonata izgubi 2 do 5 mol m^{-2} $leto^{-1}$ ogljika v obliki DIC. Izguba raztopljenega organskega ogljika na globini zemlje 5 cm je bila nekoliko nižja (1 mol m^{-2} $leto^{-1}$) in ni kazala bistvenih razlik med vzorčevalnimi mesti. V tretji raziskavi se je preučevalo tokove CO_2 v gozdnih tleh nad kraško jamo. Rezultati so pokazali, da prezračevanje jame vpliva na talni CO_2 in da lahko občasno v tleh celo prevladuje. V četrti raziskavi se je preučevala dinamika in viri CO_2 v jamskem zraku, v Pisanem rovu v Postojnski jami. Rezultati so pokazali, da je zunanja temperatura zraka glavni dejavnik, ki vpliva na prezračevanje jame. Vir jamskega CO_2 v preiskovani jami je bil predvsem CO_2, ki izvira iz dihanja tal in prispe neposredno v jamo. Ogljikov dioksid, ki se prenaša iz tal v jamo, raztopljen v prenikli vodi, je imel manj pomemben vpliv na raven CO_2 v

jamskem zraku. V zadnji, peti raziskavi so se merili tokovi in izotopska sestava CO_2 iz tal na vznožju vulkana Etne (Italija). Rezultati so nakazali na različne poti CO_2 iz globokih virov na površje ter vpliv aktivnosti vulkana na tokove CO_2 iz tal in njihovo izotopsko sestavo.

Če povzamemo, to delo prikazuje, kako lahko uporaba stabilnih izotopov pomaga razkriti pomembne informacije o tokovih CO_2 in dejavnikih, ki vplivajo nanj nad, v in pod tlemi.

Contents

List of Figures **xv**

List of Tables **xvii**

Abbreviations **xix**

1 Introduction **1**
1.1 The Global Carbon Cycle ... 1
1.2 Soil as Part of the Global Carbon Cycle ... 3
1.2.1 Soil CO_2 flux ... 3
1.2.1.1 Mechanisms of soil CO_2 fluxes ... 3
1.2.1.2 Measurements of CO_2 fluxes (micrometeorological methods) ... 4
1.2.1.2.1 Eddy covariance method ... 5
1.2.1.2.2 Chamber methods ... 6
1.2.1.2.3 Profile methods ... 7
1.2.1.3 Measurements of CO_2 concentrations ... 8
1.2.2 Sources of soil CO_2 ... 9
1.2.2.1 Atmosphere ... 9
1.2.2.2 Biogenic sources (soil respiration) ... 10
1.2.2.2.1 Factors controlling soil respiration ... 12
1.2.2.3 Geogenic sources ... 12
1.2.2.3.1 Deep sources ... 12
1.2.2.3.2 CO_2 from carbonate dissolution and precipitation processes ... 12
1.2.2.3.3 Caves as CO_2 sink or source ... 17
1.2.2.3.4 Cave ventilation ... 18
1.3 CO_2 Source Assessment ... 20
1.3.1 Stable isotopes in general ... 20
1.3.2 The use of stable isotopes in the environmental studies ... 21
1.3.3 Stable isotopes in terrestrial carbon cycle ... 23
1.3.3.1 Carbon isotopes in plants ... 23
1.3.3.2 Carbon isotopic composition of soil CO_2 ... 24
1.3.3.3 CO_2 sources in cave air ... 27
1.3.3.3.1 Degassing of CO_2 from dripwaters ... 28
1.3.4 Source partitioning of CO_2 ... 29
1.3.4.1 Radiocarbon (^{14}C) ... 30
1.3.4.2 Radon (^{222}Rn) activity ... 32
1.3.4.2.1 Radon in caves ... 33
1.3.5 Stable isotope measurement techniques ... 33
1.3.5.1 Isotope ratio mass spectrometry (IRMS) ... 33
1.3.5.2 Optical techniques of stable isotope analysis ... 35

2 Aims and Hypothesis **37**

3 Publications **39**

3.1 Scientific Paper: "Using ^{222}Rn and carbon isotopes (^{12}C, ^{13}C and ^{14}C) to determine CO_2 sources in forest soils developed on contrasting geology in Slovenia" 39

3.2 Scientific Paper: "Inorganic and organic carbon dynamics in forested soils developed on contrasting geology in Slovenia—a stable isotope approach" 51

3.3 Scientific Paper: "Soil CO_2 sources above subterranean cave - Pisani rov (Postojna Cave, Slovenia)" 67

3.4 Scientific Paper: "Sources, pathways and behaviour of cave air CO_2, using carbon isotopes" 79

3.5 Scientific Paper: "Temporal analysis of $\delta^{13}C_{CO2}$ and CO_2 efflux in soil gas emissions at Mt. Etna: a new tool for volcano monitoring" 137

4 Conclusions **171**

References **177**

Bibliography **187**

Biography **189**

List of Figures

Figure 1.1: Simplified schematic of the global carbon cycle. 2
Figure 1.2: A diagram of a typical nondispersive infrared gas analyzer (NIDR). 9
Figure 1.3: A Schematic diagram of the sources contributing to soil CO_2 efflux. 10
Figure 1.4: Relative abundance of dissolved inorganic carbon (DIC) ionic species 15
Figure 1.5: A diagram of thermally driven cave airflow. 19
Figure 1.6: A diagram of a »barometric cave«. 20
Figure 1.7: Chart of nuclides with percent natural abundance of stable isotopes. 21
Figure 1.8: Isotope composition of C, O and H pools in the carbon and water cycles... 23
Figure 1.9: Schematic diagram of the distribution of $\delta^{13}C_{CO2}$ and $\Delta^{14}C$ values 32
Figure 1.10: A diagram of the continuous flow-elemental analyzer inlet 35
Figure 1.11: A simplified diagram of the instruments 36

List of Tables

Table 1.1: List of methods used for measuring gas fluxes in natural systems 5
Table 1.2: Stochastic abundances of isotopologues of CO_2 22

Abbreviations

CA	... carbonate alkalinity
C_3	... C_3 plants, Calvin cycle
C_4	... C_4 plants, Hatch-Slack cycle
CAM	... crassulacean acid metabolism
CCS	... carbon capture and storage
CF-IRMS	... continuous flow IRMS
CO_2	... carbon dioxide
CRDS	... cavity ring-down spectroscopy
DIC	... dissolved inorganic carbon
DI-IRMS	... dual inlet IRMS
DOC	... dissolved organic carbon
δ	... delta, relative isotopic composition, value given in parts per thousand or "per mille" (‰)
$\delta^{13}C$	... isotopic composition of carbon
$\Delta^{14}C$	... ^{14}C isotopic ratio relative to the modern standard after correction for fractionation to $\delta^{13}C = -25‰$
EA	... elemental analyzer
EA-IRMS	... elemental analyzer IRMS
ε	... isotope enrichment factor
FTIR	... Fourier-transform infrared spectroscopy
HTP-IRMS	... high-temperature pyrolysis-IRMS
IPCC	... Intergovernmental Panel on Climate Change
IR	... infra-red
IRGA	... infrared gas analyzer
IRMS	... isotope ratio mass spectrometry
LIC	... lithogenic inorganic carbon
MRT	... mean residence time
NDIR	... nondispersive infrared gas sensor
NOAA	... National Oceanic & Atmospheric Administration
OA-ICOS	... off-axis integrated cavity output spectroscopy
Ω	... saturation state
pCO_2	... partial pressure of carbon dioxide, expressed as a mole fraction in dry air, µmol mol^{-1}, sometimes abbreviated as ppmv
PCP	... prior calcite precipitation
PIC	... pedogenic inorganic carbon
POC	... particulate organic carbon
QCL	... mid-infrared quantum cascade lasers
SOM	... soil organic matter
STP	... standard temperature (273.15 K) and pressure (100 kPa)
TA	... total alkalinity
TDLAS	... tunable diode laser absorption spectroscopy

TR ... turnover rate
VPDB ... Vienna Pee Dee Belemnite
VSMOW ... Vienna Standard Mean Ocean Water

Chapter 1

Introduction

1.1 The Global Carbon Cycle

The global carbon (C) cycle is a process where carbon moves between series of reservoirs of carbon in the earth system (see Figure 1.1). The exchanges of carbon between these reservoirs are called fluxes. If a certain reservoir either takes more carbon than it releases, or vice versa, that reservoir is considered as carbon sink or carbon source, respectively.

Based on the turnover rates, carbon reservoirs can be distinguished into two groups. The first group with "fast" turnover rate consists of carbon in atmosphere, oceans, land vegetation, soils and freshwaters where turnover rates range from a few years to millennia (IPCC, 2013). The second group with "slow" turnover rate consists of carbon stored in rocks and sediments. It has turnover rates of 10 000 years or longer. Natural exchange fluxes between the groups are considered to be relatively small on the global scale (IPCC, 2013) and may be important on the local scale. On the other hand anthropogenically induced exchanges have great global impact.

The first group can be further divided between three major carbon reservoirs: the ocean, the terrestrial biosphere and the atmosphere.

The largest reservoir is the ocean, where carbon is represented mainly in the form of dissolved inorganic carbon (DIC), dissolved organic carbon (DOC) and a small organic pool consisting of marine biota. Within the ocean reservoir carbon is transported by three mechanisms, the so-called: solubility pump, biological pump and the marine carbonate pump. With the atmospheric reservoir carbon exchanges mainly from the ocean surface in the form of CO_2 gas exchange.

The second largest reservoir is the terrestrial biosphere where the major part (cca. 70%) of its carbon is encountered in dead organic matter in litter and soils, while the remaining part is encountered as a living biomass in terrestrial vegetation. An additional amount of old soil carbon can be encountered in permafrost soils and wetland soils (IPCC, 2013).

Some amount of terrestrial carbon is transported from soils with water to rivers and lakes where: a) it can degas back to the atmosphere in the form of CO_2; b) it can be buried in freshwater sediments and/or transported to the oceans. The transport from the terrestrial reservoir to the costal oceans happens also through the rivers in the form of DIC, DOC and particulate organic carbon (POC) (Tranvik et al., 2009).

The smallest of the three carbon reservoirs is the atmosphere where carbon is mainly present in the form of CO_2, one of the most important greenhouse gases with annual mean concentration of 402.8 ± 0.10 µmol mol^{-1} determined in 2016 (NOAA, 2017). Other forms of carbon in the atmosphere include methane (CH_4), carbon monoxide (CO) and

smaller amounts of hydrocarbons, black carbon aerosols and organic compounds in the atmosphere (IPCC, 2013).

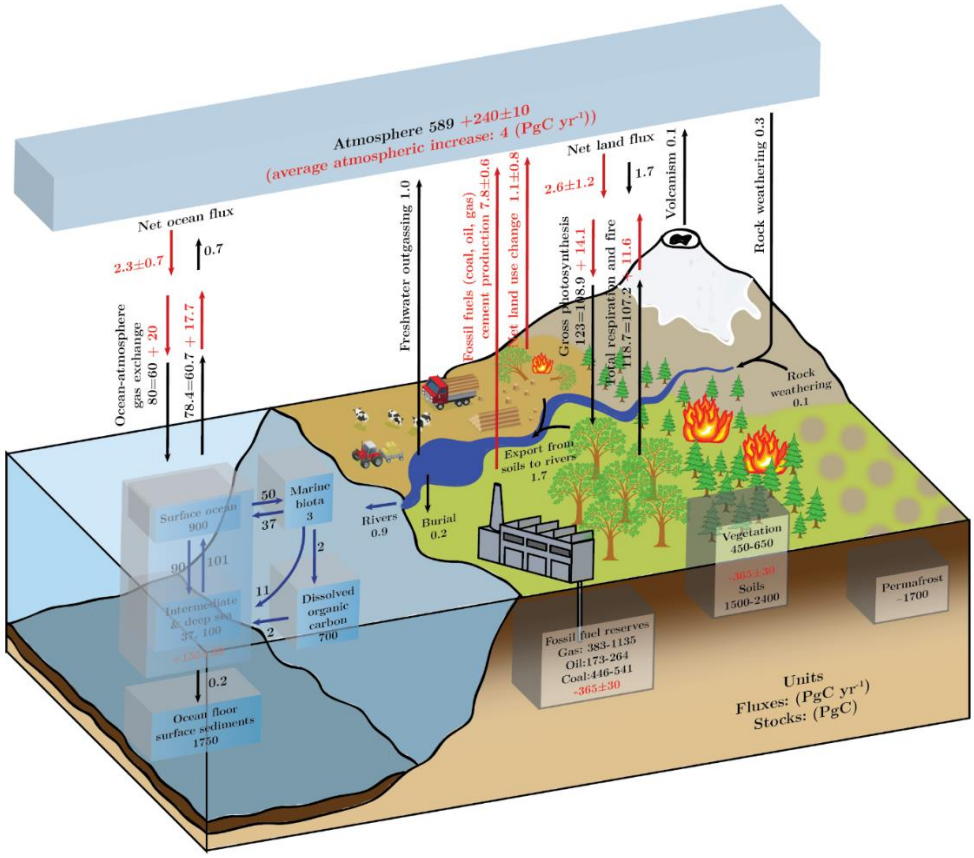


Figure 1.1: Simplified schematic of the global carbon cycle. Numbers in boxes represent carbon stocks (PgC) while numbers beside arrows represent annual exchange fluxes (PgC a^{-1}). Black numbers and arrows represent stocks and carbon fluxe estimated for the preindustrial era while the red numbers and arrows represent annual anthropogenic fluxes averaged over the 2000-2009 time period. Red numbers in the boxes indicate cumulative changes of anthropogenic carbon over the Industrial Period 1750-2011 (Figure adapted from IPCC (2013)).

The proposed PhD thesis deals with a better process-based knowledge of the terrestrial carbon cycle including the cave system, thus the following subchapters form the theoretical background providing the context for the role and behavior of the terrestrial C cycle. Special attention is paid to the determination of the sources of CO_2 using isotopes. Chapter 2 presents aims and objectives of the PhD thesis. Further chapters are related to the presentation of the work including five relevant publications.

In the first publication the sources of CO_2 in forest soil developed on carbonate and non-carbonate parent material were investigated using ^{222}Rn and carbon isotopes (^{12}C, ^{13}C and ^{14}C).

The second publication deals with organic and inorganic carbon transport in forest soils developed on different parent rock materials. Seasonal and spatial variations in soil organic carbon were investigated and sources and transport of DOC and DIC in soil water were evaluated using isotopic techniques.

In the third publication the use of carbon isotopes was used to detect a contribution of soil CO_2 originating from other sources than soil respiration. Special attention was paid to the contribution of CO_2 coming from the subterranean cave below the investigation site.

The fourth publication answers our question related to cave air CO_2 sources and dynamics in the cave chamber below the soil investigated in the third publication.

The fifth publication deals with the temporal variations of CO_2 effluxes and its stable carbon isotope composition on the flanks of the Etna volcano in Italy proposing the stable isotope analysis as a tool for monitoring volcano eruption.

Chapter 4 presents the conclusion of this work and identifies the possible future improvements.

1.2 Soil as Part of the Global Carbon Cycle

In the global carbon cycle soils play a very important role, because soil CO_2 efflux is considered the second largest flux in the terrestrial C cycle (IPCC, 2013). It is estimated that global soil CO_2 emissions are in the range of 98 ± 12 Pg/y, with annual increases of 0.1 Pg, which was suggested to be temperature associated (Bond-Lamberty & Thomson, 2010). Within the terrestrial ecosystems soils hold great amounts of C and can act as a source or as a sink of C through the CO_2 exchange with the atmosphere (Amundson, 2001), therefore even small changes in soil CO_2 production can affect atmospheric CO_2 concentrations. Although soil CO_2 respiration has a major role in the global C cycle, it is still one of the less understood ecosystem C fluxes (Luo & Zhou, 2006).

1.2.1 Soil CO_2 flux

Soil CO_2 efflux mainly consists of CO_2, which is produced by roots and decomposition of litter and soil organic matter (SOM). Soil temperature and soil moisture are considered as the most important abiotic parameters influencing soil respiration and its underlying processes (Kutsch, Bahn, & Heinemeyer, 2009). However, on specific soils also other processes that significantly contribute to soil CO_2 fluxes were identified. Recently it has been discovered that abiotic terrestrial CO_2 exchange can temporally even dominate the C fluxes in ecosystems on carbonaceous areas (Čater & Ogrinc, 2011; Kowalski et al., 2008; Plestenjak et al., 2012; Serrano-Ortiz et al., 2010).

Before further discussion on the soil CO_2 fluxes it is important to distinguish between the two terms that will be used hereafter: the "**soil CO_2**" and "**soil-respired CO_2**". Soil CO_2 is defined as CO_2 occupying soil pore spaces (Cerling, Solomon, Quade, & Bowman, 1991; Dörr & Münnich, 1986) and is a mixture of different sources. CO_2 from biogenic sources and their interactions i.e. produced by roots and decomposition of litter and SOM is defined as soil-respired CO_2 (Cerling et al., 1991; Dörr & Münnich, 1986).

1.2.1.1 Mechanisms of soil CO_2 fluxes

The main mechanisms of CO_2 transport from, to and within the soil are **diffusion**, **advection** and **CO_2 movement in water phase**. There are more types of diffusion that can be present in soils, i.e. **molecular diffusion**, **Kundsen diffusion** and **nonequimolar diffusion**. Molecular diffusion of CO_2 in soils is the process where CO_2 is transported from a region with a higher concentration to a region with a lower concentration. Therefore, transport by diffusion occurs when a concentration gradient is present and transport magnitude is proportional to this gradient. Here equimolar pairs of gases counter diffuse in pores whose size is much greater than that of the mean free path

of the gas molecules. In this case molecule-to-molecule collisions dominate over molecule-to-wall collisions. At steady state conditions this process can be described by the first Fick's law:

$$J_d = -D\nabla C \tag{1.1}$$

where J_d is the diffusive flux for unit area per unit time (mol m^{-2} s^{-1}), ∇C is the concentration gradient of gas (mol m^{-4}) and D is the bulk diffusion coefficient of the volume of the porous medium (m^2 s^{-1}). D depends on the molecular diffusion coefficient of the gas in question and properties of the porous medium like soil porosity, tortuosity and volumetric moisture.

Kundsen diffusive flux occurs when the gas mean free path is much greater than the pore radius and collision of molecules with pore walls dominates over collisions between molecules themselves. It depends on the molecular weights and temperatures of gases and the radius of the pores.

Nonequimolar diffusion occurs when gas components have different molecular weights. Lighter gas molecules have higher velocities than the heavier ones. In the binary mixture of nonequimolar gases, the more rapid diffusion of the lighter gas molecules results in a pressure gradient. The flux resulting from the build-up of pressure is diffusive and is called nonequimolar flux.

Advection of soil gas is the process where the gas is transported due to a pressure gradient and is described by Darcy's law:

$$\nu = -\frac{k}{\mu}\nabla p_z \tag{1.2}$$

where ν is gass velocity (m s^{-1}), ∇p_z is pressure gradient (Pa m^{-1}), μ is gas viscosity (Pa s) and k is the intristic permeability (m^2). Intrinsic permeability is a function of the soil properties such as air-filed porosity and tortuosity.

Molecular diffusion of CO_2 in water is smaller than in gases. The coefficient of molecular diffusion is smaller for liquids in a porous medium than in a pure liquid because a collision with the solids of the soil water medium obstructs diffusion.

Movement of CO_2 with water depends on different flow paths water takes in soil. Some of the flow paths are faster because they follow more direct paths through larger pores or through the center of pores. Other flow paths may be slower because they are closer to the grain boundaries. The different flow paths of the water cause the mechanical dispersion; a mechanical mixing within the bulk movement of soil water. Beside the movement of water also the uptake of water by plants plays an important role.

1.2.1.2 Measurements of CO_2 fluxes (micrometeorological methods)

Fluxes of gases between surface and atmosphere are measured using the micrometeorological methods. The scale to which the measurements are applied can range from several millimeters to up to a kilometer. The spatial scale and resolution depend on the needs of the measuring campaign and the size of the measuring plot. Several micrometeorological methods are being used in the field of the environmental sciences and some of them are listed in Table 1.1.

Table 1.1: List of methods used for measuring gas fluxes in natural systems (Table adapted from Arya (1988) and Burba & Anderson (2010)).

Method	**Short description**
Eddy covariance	Simultaneous and fast measuring of gas and 3D wind speed
Eddy accumulation	Fast measuring of vertical wind speed and proportional sampling of updraft and downdraft of gas
Relaxed eddy accumulation	Fast measuring of vertical wind speed and not proportional sampling of updraft and downdraft of gas
Aerodynamic method	Measurements of wind and gas profiles
Chamber methods	Measurements of changing gas concentrations in the chamber of known volume and area
Profile method	Measurements of gas concentrations on at least two levels
Resistance method	Measurements of gas and their resistance to transport
Mass balance for small areas	Measuring the differences in masses for certain parts of the ecosystem.

The methods that are currently most widely used for measuring CO_2 fluxes between vegetated surfaces (e.g. grasslands, croplands and forests) soils and atmosphere are Eddy covariance, Chamber methods and Profile method. Therefore, these methods will be described in more detail.

1.2.1.2.1 Eddy covariance method With the eddy covariance method the net exchange of gases between the ecosystem and the atmosphere is measured. Measurements are made above the ecosystem of interest (e.g. above tree canopy, shrubs or grasses) in the surface layer in which turbulence is more or less constant. With the appropriate position of the sensors above the measured system, different gases (e.g. CO_2, O_3, NO_x, CH_4, …), heat and water exchange can be measured. Wind speeds from all three directions (x, y, z), concentrations of gas and air temperatures are recorded with the sensors mounted on the flux towers at a frequency of at least 10 Hz. Gathered data is then processed using established methodologies such as proposed by Aubinet et al. (1999), Webb, Pearman, & Leuning (1980), Foken & Wichura (1996), Reichstein et al. (2005), Papale et al. (2006), Richardson & Hollinger (2007) and Lasslop et al. (2010). The height of the sensor placement is restricted from both top and bottom. From the top, it is restricted by the available upwind fetch for the area of interest, and from the bottom by the frequency response errors and related corrections. General guidelines are that height of the sensors should be 100 times lower than the desired fetch of the flux tower and at the same time it should ideally be twice the canopy height. If the terrain is patchy, with scattered bushes or trees, the ratio may need to increase to 5 times the canopy height (Burba & Anderson, 2010). Two different types of the instruments for measuring CO_2 and H_2O are generally used with the eddy covariance method: (I) the closed path and (II) the open path infrared gas analyzers (IRGA). The main factors that influence the decision in choosing either of the designs are the power availability and the frequency of the precipitation on the site.

Closed path (I) designs require more power since they operate an air pump that transports the air to the measuring cell form the measuring point near the anemometer. The main advantage of this design is that precipitation has no impact on the

measurements (limited only by the anemometer capability to operate during precipitation events).

Open path designs (II) have an actual open path analyzer in the immediate proximity of the anemometer. The analyzer design must be small enough and aerodynamic not to disturb the large eddies around it. The main advantage of the open path designs is the lower power consumption. The main disadvantage is that even light precipitation strongly influences the measurements.

1.2.1.2.2 Chamber methods As the name indicated special chambers that are placed on the soil surface are used. Efflux of gas of interest (e.g. CO_2) is assessed from the soil area enclosed by the chamber and measurements of the gas concentrations in air within or passing the chamber volume. CO_2 is mostly measured with different CO_2 sensors (subsection 1.2.1.3), however methods based on the absorption of CO_2 with alkali materials are still in use.

Chambers are made of different transparent or non-transparent materials. Some chambers use special collars that are placed into the soil to better insulate the chamber space. Some chambers are manually operated, while others are a part of a fully automated system. Different chamber techniques have been developed for measuring the soil CO_2 fluxes. According to the classification proposed by Livingston & Hutchinson (1995) three major chamber techniques can be distinguished:

- non-steady state non-through-flow chambers (closed static chambers);
- non-steady state through-flow chamber (closed dynamic chambers);
- steady-state through-flow chambers (open dynamic chambers).

When a non-steady chamber (static and dynamic) is used, a chamber is placed on the soil surface for a certain period of time. The CO_2 soil efflux is then determined from the rate of CO_2 concentration increase in that chamber. When a steady state chamber is used, the soil CO_2 efflux is calculated from the difference in concentrations at the inlet and the outlet of the chamber.

Each type of chamber has its benefits and drawbacks. For example, in the case of the non-steady-state chamber the CO_2 concentration in the chamber headspace changes, and therefore also the natural concentration gradient between the soil and "atmosphere" is changed, which affects the diffusion of gas from the soil (Davidson, Savage, Verchot, & Navarro, 2002; Livingston & Hutchinson, 1995; Nay, Mattson, & Bormann, 1994). Pressure differences between inside and outside of the steady-state chamber can cause mass flow of the gas into the chamber. Errors in CO_2 efflux measurements can be caused by pressure differences as low as 1 Pa (de Jong, Redmann, & Ripley, 1979; Fang & Moncrieff, 1998; Lund, Riley, Pierce, & Field, 1999).

1.2.1.2.3 Profile methods When the profile method (also known as gradient methods) is used for assessing the soil CO_2 flux, concentrations at least at two different depths should be measured and the CO_2 production and efflux is calculated from the vertical CO_2 diffusive flux divergence. The advantage of these methods is that in contrast to the eddy covariance and chamber methods they can reveal also certain information about CO_2 dynamics below the soil surface. For this calculation, the CO_2 concentration profiles and soil diffusive properties must be known. Soil CO_2 flux calculations (one dimensional, steady state) are generally made using the first Fick's law (see Eq. (1.1)), which can in the case of one-dimensional diffusion be written as (Drewitt, Black, & Jassal, 2005):

$$\sigma J_d = -D_{eff} \frac{\partial C}{\partial z} \tag{1.3}$$

where J_d is the diffusive flux (mol m^{-2} s^{-1}), D_{eff} stands for effective diffusivity coefficient (m^2 s^{-1}), C stands for CO_2 concentration (mol m^{-3}) and z for depth (m).

While CO_2 gradient $\frac{\partial C}{\partial z}$ is measured, the D_{eff} has to be assessed. Assessment of the diffusivity coefficient with confidence can be challenging and can lead to the major source of error associated with the profile methods (Koehler, Zehe, Corre, & Veldkamp, 2010).

There are also other more complex time-dependent models based on Fick's law, which account also for temporal changes of other factors controlling CO_2 flux in soils (Drewitt et al., 2005). In some cases, the Fick's law is insufficient to study multi-component gaseous diffusion in the soil and a more complex Stephan-Maxwell equation should be used (Jaynes & Rogowski, 1983). However, it has been shown by Freijer & Leffelaar (1996) that using the simpler calculations based on Fick's law generally introduces a relative error of only 5%. This is much lower than the error that is made due the measuring method alone (Nay et al., 1994), especially by the estimation of the diffusion coefficient (Risk, Kellman, & Beltrami, 2008).

To measure CO_2 concentrations below the surface, sample air is either extracted from soil or measured with sensors that are placed at different depths. In methods using the extraction, samples are either extracted by syringe from sampling tubes that are placed at different depths or soil horizons (Davidson & Trumbore, 1995; Drewitt et al., 2005; Koehler et al., 2010) or an automated system is in place which pumps soil air from sampling tubes and is connected to the instrument measuring CO_2 concentrations (e.g. IRGA) (Fang & Moncrieff, 1998; Hirsch, Trumbore, & Goulden, 2003). Extraction methods are considered as causing disturbance to the soil environment while sampling and can lead to bias in measurements. With profile methods using buried sensors, soil CO_2 concentrations sensors are placed at different depths where concentrations can be measured in shorter temporal intervals with no disturbance to the soil environment (Jassal et al., 2005; Liang et al., 2004; Ota & Yamazawa, 2010; Pingintha, Leclerc, Beasley Jr, Zhang, & Senthong, 2010). All methods usually require a soil pit excavation or drilling in order to place sampling tubes or CO_2 sensors.

1.2.1.3 Measurements of CO_2 concentrations

CO_2 concentration in environmental sciences is most commonly measured using two types of the CO_2 sensors:

- nondispersive infrared gas sensors (NDIR) such as found in the infrared gas analyzers (IRGA); and
- chemical gas sensors.

The method of choice for most scientific researches of CO_2 fluxes is the NDIR sensor, therefore this type of sensors is described in more detail in the following paragraph.

Nondispersive infrared gas sensors (NDIR). The most widespread sensors for measuring CO_2 concentrations for scientific purposes are the NDIR sensors. They offer high short-term repeatability of measurements and greater accuracy than other commercially available methods. At normal atmospheric CO_2 levels (cca. 400 µmol mol^{-1}) the state of the art instruments reach the accuracy < 3 µmol mol^{-1} (Peet & Krizek, 1997). Drawbacks of these instruments are their sensitivity to water vapor, drifts with time and changes in temperature. However, the newer models greatly improved against these flaws. CO_2 concentration is measured based on the absorption of the energy in the infrared region (IR) of the electromagnetic spectrum by CO_2 molecules. Absorption of the IR radiation during measurements with NIDR is compared between two gas cells: reference and sampling cell. IR radiation is alternately transmitted through each of those cells. In the reference cell the reference gas is either sealed or it is passed through the cell during the measurement. The concentration is then calculated from the values obtained from both sampling cells.

Basic components of NDIR sensors for scientific use are (see Figure 1.2): the IR radiation source, a spinning shutter disk, both (reference and sampling) gas cells, optical filter and CO_2 detector. A spinning shutter disk rotates between the source and both gas cells passing the IR beam alternately between the reference and the gas cell. The length of the cells can differ between the models where the newer instruments tend to have shorter cells with equal or even higher resolution than older instruments with longer cells. The interior of the cell is plated with reflective material (usually gold) to enhance the reflection. The optical filter reduces the interference from other gases (e.g. water) by transmitting and therefore tuning the detector to the CO_2 absorption band (4.26 µm). The detector is usually a solid state PbSe thermally stabilized detector. Modern NIDR devices can simultaneously analyze the CO_2 and water vapor, which allows monitoring the chamber relative humidity and therefore minimizing the effect of water vapor to the CO_2 measurement. In this case the instruments have two detectors (for CO_2 and for water) and their designated filters. A dichroic beam splitter splits the beam into two parts one of each goes to the detector filtered to detect radiation absorption one of CO_2 and the other of water (Peet & Krizek, 1997).

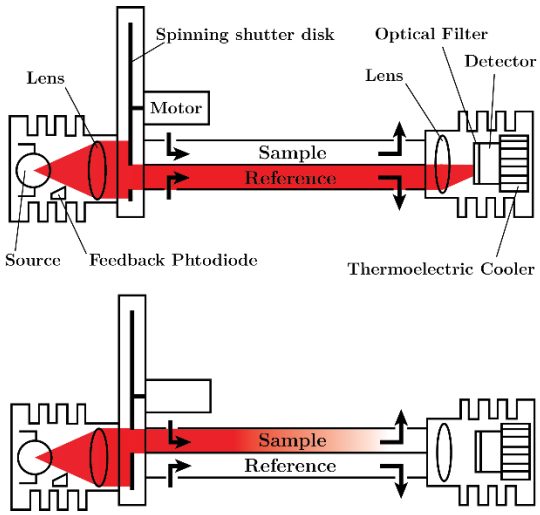


Figure 1.2: A diagram of a typical nondispersive infrared gas analyzer (NIDR). (Figure adapted from LI-COR Inc., Lincoln Nebraska).

1.2.2 Sources of soil CO_2

There are different sources that contribute to the overall soil CO_2 and consequently to soil CO_2 fluxes. First distinction can be made between biotic and abiotic sources. Biotic sources of soil CO_2 are represented by heterotrophic and autotrophic organisms in soils, while CO_2 from the atmosphere, carbonate dissolution/precipitation derived CO_2 and CO_2 from the deep sources are considered as abiotic sources. Carbonate dissolution/precipitation derived CO_2, as it will be discussed in this dissertation, are of special interest in karstic areas. Although deep CO_2 sources are pronounced particularly in the volcanic, seismic and geothermal areas, they can also be present in areas where tectonic faults are encountered.

Special contribution to the soil CO_2 in karstic areas can be CO_2 coming from subsurface air reservoirs, such as underground caves and cavities that accumulated CO_2 by different sources, which will be discussed in the following subsections.

Distinction between soil CO_2 sources and their controlling mechanisms is important because they condition different turnover rates for soil carbon and have different responses to changing environmental conditions. Understanding these mechanisms is essential to evaluate the soil and ecosystem CO_2 balance. Majority of the soil CO_2 evolves from biogenic sources and their interactions i.e. form autotrophic respiration of plant roots and heterotrophic respiration such as microbial decomposition of plant litter and SOM (Kuzyakov, 2006). Soil CO_2 can also mix with CO_2 from the atmosphere, which can come into soil via diffusion, convection or rain water. Besides that, also other abiotic CO_2 sources can be present, such as CO_2 from deep sources and CO_2 originating from water dissolution of the carbonate parent rock material and subsequent carbonate precipitation.

1.2.2.1 Atmosphere

In the upper layers of the soil profile, there is a sizeable atmospheric contribution to the soil CO_2. Contribution of atmospheric air within vertical soil profile depends on the efflux rate and soil porosity (Bertolini et al., 2006). Amundson, Stern, Baisden, & Wang (1998)

suggested a theoretical model to describe the vertical soil profile. With this model, a relative contribution of atmospheric CO_2 within the soil can be calculated.

1.2.2.2 Biogenic sources (soil respiration)

Organic carbon in soil can be divided into three major carbon pools: (1) **SOM**; (2) **above and belowground plant residues;** and (3) as **organic substances released by living roots**. These pools also represent the main sources of CO_2 fluxes from soil. In spite of that different carbon pools have different chemical compositions, different turnover rates, residence times and different ability to contribute to overall soil CO_2 flux, the boundaries between those pools are not always clear (Kuzyakov, 2006).

There are two main groups of organisms that contribute to soil CO_2 production: **heterotrophic** and **autotrophic** organisms. The most important heterotrophic organisms can be further subdivided into two broad groups: (1) soil microorganisms (bacteria fungi, actinomycetes and protozonas); and (2) soil macrofauna (macroscopic invertebrates and small mammals). The contribution of the macrofauna to the total CO_2 efflux from soils is very small. Most of the soil CO_2 efflux is contributed by the heterotrophic soil organisms (microbe respiration). The most important contributors to soil CO_2 from autotrophs are the plants with their root respiration. Contribution of other autotrophs like algae and chemolithotrophs is considered minimal (Kuzyakov, 2006).

According to Kuzyakov (2006) the soil respired CO_2 can be divided into five biotic sources (see Figure 1.3): (1) **basal respiration** (microbial decomposition of SOM in root free soil without undecomposed plant remains); (2) **rhizosphere priming effect** (microbial decomposition of SOM in root affected or plant residue affected soil); (3) **microbial decomposition of dead plant remains**; (4) **rhizomicrobial respiration** (microbial decomposition of rhizodeposits from living roots); and (5) **root respiration**.

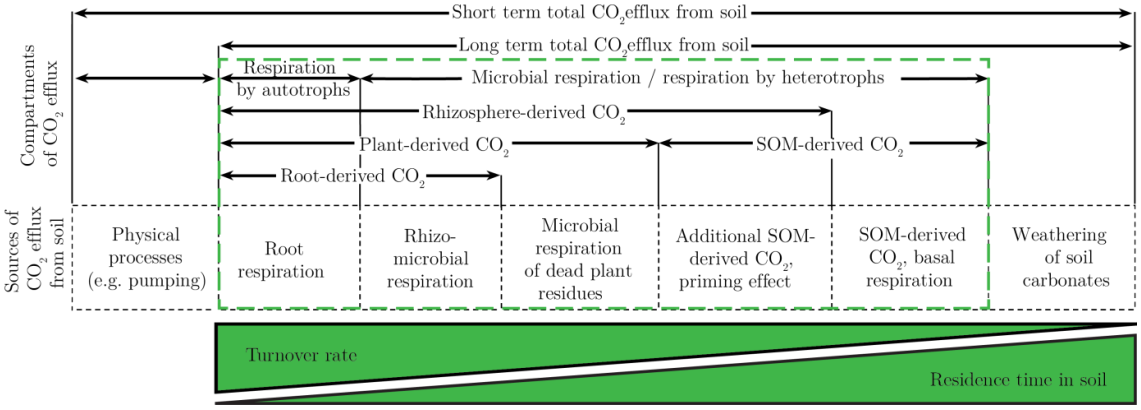


Figure 1.3: A Schematic diagram of the sources contributing to soil CO_2 efflux. The green dashed rectangle represents the biotic sources, while outside abiotic sources are represented. Each source also represents a relevant carbon pool with different turnover rates and residence time in soil (Figure adapted from Kuzyakov (2006)).

The last two biotic sources in the diagram originate from the process of the microbe decomposition of SOM, therefore CO_2 from this source can also be described as SOM originated CO_2. Other described biogenic CO_2 sources represent CO_2 originating from living or recently dead plant material. CO_2 coming from living plants can be joined into a group of root-derived CO_2. In soils without vegetation, the only source contributing to soil CO_2 efflux is the microbe decomposition of SOM without the influence of the roots. The contribution of other biotic sources depends on the presence of the vegetation. The

presence of the vegetation and the rhizodeposition of easily available carbon sources can substantially affect the microbial activity in the rhizosphere. The augmented microbial activity can change (increase or decrease) the intensity of SOM decomposition in the rhizosphere. Such change is called "the rhizosphere priming effect" (Kuzyakov, 2002). Four of the five biotic CO_2 sources depend on soil microorganisms, hence the name "microbial or heterotrophic respiration". Only the root respiration is attributed solely to the autotrophs.

One of the important differences concerning the soil CO_2 sources is the different turnover rate of their carbon pools. Turnover rate is the rate of cycling of C (or any other element or substance) in a pool or a system. If the pool is in steady state (input into the pool is equal to its decomposition), the value of the turnover rate (TR) is the ratio of the input amount per time unit to the total pool amount. Different turnover rates reflect the different mean residence time (MRT) of C in SOM pools which is inversely proportional to TR (MRT= 1/TR). MRT denotes the mean period of residence of C in the soil or in the SOM pool.

The shortest MRT in the plant-soil system is found for the root respiration and can range from several minutes to several hours. One of the examples are grasses where it takes only a day or two for carbon to be released through the root respiration back to the atmosphere (Cheng, Coleman, Carroll, & Hoffman, 1993). The MRT for tree roots is already longer and it can take up to four days (Ekblad & Högberg, 2001). Part of the carbon, which is assimilated by the plant, can be stored within the plant for a longer time period depending on the stress, such as mowing, grazing or unfavorable environmental factors, e.g. drought or frost. This stored carbon can be used for the needs of plant respiration (Kuzyakov, 2006).

The time required for degradation of root exudates is also in the range of several hours. Root exudates, which are composed of organic compounds of low molecular weight, such as carbohydrates, carboxylic acids and amino acids, are readily decomposed into CO_2 in several hours (Kuzyakov, Leinweber, Sapronov, & Eckhardt, 2003).

After the death of the plant, the majority of plant material ends up in the soil (if there is no anthropogenic interference such as mowing, grazing and wood cutting). The dead plant material in soil usually needs time of several weeks to several months for its total decomposition. Most rapid decomposition happens for dead plant material with high nitrogen and low lignin content. For these materials with high lignin content, such as needles from coniferous trees, more time for their decomposition is needed, even two to four years (Gaudinski, Trumbore, Davidson, & Zheng, 2000; Ogrinc, Simončič, & Kovač, 2012). Even slower decomposition happens in cold conditions or water saturated environments, such as peatlands, tundra, permafrost etc. (Dioumaeva et al., 2002). In such environments, cold and oxygen deficit inhibit microbial activity.

The longest MRT for biotic CO_2 sources in soil are characteristic for the priming effect and basal respiration. Depending on the local climate and soil clay content, it can take hundreds of years for its total decomposition. The average global turnover rate for soil organic carbon was estimated to be 32 years (Raich & Schlesinger, 1992). The assessment was done for several ecosystems and turnover rates range between 10 to 520 years (Raich & Schlesinger, 1992).

Considering the speed of SOM conversion, carbon pools can be divided into at least two or more pools, each with its different turnover rates. There are no standard definitions for these pools but they can be roughly divided into inert, recalcitrant resistant, decomposable, available, active, etc. The most persistent is the inert SOM pool, which is the most complex and tightly bound to clay minerals. It has a very slow decomposition rate with MRT of thousands of years and therefore only a minor contribution to annual soil CO_2 efflux (Kuzyakov, 2006).

1.2.2.2.1 Factors controlling soil respiration Soil respiration is generally controlled mainly by temperature, rainfall amount and its distribution, where soil temperature plays a major role and soil humidity gains more importance under drought conditions (Davidson, Belk, & Boone, 1998). Even very high soil water contents can restrict soil respiration. With low water contents metabolic activity of microbes and roots are inhibited, while at high soil water content soil respiration is reduced due to the lack of oxygen accumulation because of closed pore space. However, at conditions typically encountered in temperate forests, soil temperature is considered the most important environmental factor affecting soil respiration (Raich & Potter, 1995).

Many studies show a positive correlation between soil respiration and temperature (Raich & Schlesinger, 1992; Singh & Gupta, 1977). Some researchers have used linear regression analysis e.g. (Froment, 1972; Witkamp, 1966), while others have used the Q10 relationship, first developed by Van't Hoff (as cited in Lloyd & Taylor (1994)), where they assumed an exponential dependence of respiration on temperature. Q10 describes what the incensement of the soil CO_2 is if the temperature increases for 10 °C. Values of Q10 normally had a range between 1.3 and 3.3 with an average value of 2 (Raich & Schlesinger, 1992). There had been used also power relationships (Kucera & Kirkham, 1971) and relationships of the form proposed by Arrhenius (1889) with a basic parameter Q10. The greatest drawback of the Arrhenius function with basic parameter Q10 is that overestimates CO_2 flux from soils at greater temperatures (more than 25 °C) and overestimates fluxes at lower temperatures (0-15 °C). Lloyd & Taylor (1994) introduced a corrected model, in which modelled values coincide better with measured values along the entire temperature range. In ecosystems prone to droughts, the soil water content becomes an equally important factor as temperature. In such cases, the Lyod and Taylor model can be modified by adding a module (Gompertz function) that accounts also for soil water content (Bahn et al., 2008).

There are also other factors that influence soil CO_2 production, such as type and quantity of the microbial flora, pH value, C/N ratio of the decomposing organic matter, O_2 concentration in soil, presence of inhibitors or stimulants such as trace elements and antibiotics (Fang & Moncrieff, 1999).

1.2.2.3 Geogenic sources

In some soils, the biogenic and atmospheric sources are not the only sources of CO_2 (Mörner & Etiope, 2002), but also geogenic sources are present. Such sources are a consequence of geological processes in or below soil.

1.2.2.3.1 Deep sources One of them is CO_2 coming from deep sources (e.g. natural CO_2 springs). In this case the contribution to CO_2 flux comes mainly in the form of geogenic flux from the earth interiors where metamorphism of carbonate rocks under high temperatures and high pressures causes the release of large stocks of CO_2. Such CO_2 can be stored under different underground pools from where it can be released if it finds the way to the earth surface trough smaller or larger cracks and fissures. Such fluxes are most frequently encountered at locations where volcanic activity is or was present in the past. It can also be released through the tectonic faults.

1.2.2.3.2 CO_2 from carbonate dissolution and precipitation processes In the literature, there are several open discussions if precipitation of carbonates should be considered as a process of carbon stocking (Emmerich, 2003; Inglima et al., 2009) or should it be considered as a source of CO_2, while dissolution of carbonates represents a mechanism of CO_2 uptake (Kowalski et al., 2008; Schlesinger & Andrews, 2000). The

cause of this disagreement lies in the interpretation of two concepts of storage and emission of CO_2 during dissolution and precipitation of carbonates in soils and parent rock material. Difference between them is mainly by the duration of the incorporation of C into the geological reservoirs such as: (a) sequestration of CO_2 into the mineral phase through the formation of pedogenic inorganic carbon in soils, where it is stabilized for longer time periods; and(b) when CO_2 is stored in the soil solution over short time periods. Both processes are controlled by the carbonate-bicarbonate equilibria (see Eq. from 1.4 to 1.20).

First mechanism (a) affecting the carbon balance in soils can be encountered in soils of arid areas. Around 30% of global terrestrial area can be considered as arid areas. Soils in arid areas can contain large quantities of inorganic carbon in the form of carbonates (Schlesinger, 1985). Inorganic carbon in soil can be classified as lithogenic inorganic carbon (LIC) and pedogenic inorganic carbon (PIC). LIC is carbonate in soil that is inherited from the parent rock material e.g. limestone, while PIC can form through dissolution and precipitation processes of the carbonate parent material (Emmerich, 2003). PIC can also form with weathering of Ca/Mg bearing silicates and result in the precipitation of carbonate. This is the PIC, which is important for this paragraph. In such case the carbonate precipitation in the soil is favored by drying of the soil, decrease of the partial pressure of CO_2 in the soil, or increase of pH. Weathering of Ca^{2+} rich minerals of non-carbonate source (or an external source of Ca^{2+}) provides Ca^{2+} ions into the soil solution, which together with bicarbonate ions (HCO_3^-) can lead into precipitation of carbonate and therefore sequestration of carbon (Emmerich, 2003). Sequestration of carbon from CO_2 through formation of PIC can only happen in arid environments (favored precipitation). In these cases the source of Ca and/or Mg should not come from carbonate rocks (Emmerich, 2003). Sequestration of carbon from CO_2 through the formation of PIC can be considered as a global carbon sink with soil inorganic carbon turnover rates estimated from 120 years (Monger & Gallegos, 2000) to 85 000 years (Schlesinger, 1985). If the conditions are changed, such as increasing CO_2 concentration in soil (from atmosphere or additional organic matter), increased precipitation, hydrogen ions from acid precipitation or decomposing organic matter can shift carbonate-bicarbonate equilibrium reactions and the long-term carbon sink can become a source (Emmerich, 2003; Inglima et al., 2009).

Weathering processes in arid ecosystems, where calcite precipitation prevails, are complex. During the vegetation period, there is more pronounced dissolution of parent rock material that leads to lower CO_2 efflux from the soil. During the dry season the precipitation of carbonate minerals causes CO_2 efflux from soil. At the same time the additional Ca^{2+} ions from atmospheric deposition or from dissolution of silicates move the equilibrium to further precipitation of calcite and/or higher dissolution during the rainy season. The formation of secondary carbonates due to additional Ca^{2+} sources that do not come from carbonate parent rock thus contributes to stocking of carbon in soils on the long-term (Schlesinger, 1985), although it can also present a CO_2 source on a short time scale.

In the second case (b), when carbonate bedrock is present, we cannot consider carbonate dissolution/precipitation as a global sink, but rather as a local sink where CO_2 is stored in the soil solution over short-term periods. In this case when CO_2 and carbonate rocks are in equilibrium within the aqueous phase, for each molecule of $CaCO_3$ that is dissolved, one molecule of CO_2 is stored in the liquid phase. Such DIC can leave the local ecosystem by the underground water streams or can be degassed from water into subterranean reservoirs such as caves and cavities and its further fate depends on the ventilation regimes and mechanisms of such reservoirs. The dissolution of carbonates thus causes uptake of soil CO_2 (lowers the transport of soil respired CO_2 into the

atmosphere). At the same time the carbon originating from dissolving parent rock can be transported further below ground mainly in the form of bicarbonate ion.

Carbonate dissolution and precipitation is controlled by reactions involved in the three-component system of water (H_2O), carbon dioxide (CO_2) and calcium carbonate ($CaCO_3$) (Kaufmann & Dreybrodt, 2007). Due to the soil respiration, there is relatively a high amount of CO_2 accumulating in the soils. Soil CO_2 partial pressure can be 10 to 100 times higher from the atmospheric (Amundson & Davidson, 1990). The quantity of dissolved CO_2 in the water solution is proportional to partial pressure of the gas, which is in the equilibrium with the solution (Henry's law):

$$CO_{2(g)} \overset{K_0}{\Leftrightarrow} CO_{2(aq)} \tag{1.4}$$

where K_0 is the solubility coefficient of the CO_2 in water.

Carbonic acid itself is very unstable, and it readily dissociates to form H^+ and HCO_3^-. Because the dissociation constants for carbonic acid system do not differentiate between $CO_{2(aq)}$ and H_2CO_3 (Millero, 1995), and it is difficult to analytically distinguish between $CO_{2(aq)}$ and H_2CO_3, the sum of their concentrations is used and denoted by $[H_2CO_3^*]$ (see Eq. (1.5)) (Emerson & Hedges, 2008):

$$[H_2CO_3^*] = [CO_2] + [H_2CO_3] \tag{1.5}$$

The fugacity (f_{CO_2}) CO_2 is defined by relationship:

$$f_{CO_2} = \frac{[H_2CO_3^*]}{K_0} \tag{1.6}$$

Transport of CO_2 from the solution is slower than the uptake of CO_2 from the atmosphere (Cole, Caraco, Kling, & Kratz, 1994), especially in the non-saturated solutions. When CO_2 dissolves in water, it reacts with water and dissociates to form four different carbon species that form DIC (see Eq. (1.7)): dissolved CO_2 ($CO_{2(aq)}$), carbonic acid (H_2CO_3), bicarbonate ($HCO_3^-{}_{(aq)}$) and carbonate ($CO_3^{2-}{}_{(aq)}$), where, as already mentioned, the $CO_{2(aq)}$ and H_2CO_3 are usually considered together as $H_2CO_3^*$.

$$DIC = [H_2CO_3^*] + [HCO_3^-] + [CO_3^{2-}] \tag{1.7}$$

The carbonate species are related by the following equilibrium reactions:

$$CO_{2(aq)} + H_2O \overset{K_H}{\Leftrightarrow} H_2CO_3 \tag{1.8}$$

$$H_2CO_3^* \overset{K_1}{\Leftrightarrow} H^+ + HCO_3^- \tag{1.9}$$

$$HCO_3^- \overset{K_2}{\Leftrightarrow} H^+ + CO_3^{2-} \tag{1.10}$$

If it is assumed that the activity of water equals 1, the following equilibrium constants can be used for each of the equilibrium reactions at 25 °C (Appelo & Postma, 2005; Stumm & Morgan, 1981):

$$K_H = \frac{[H_2CO_3^*]}{[CO_2]_{aq}} \approx 10^{-1.5} \tag{1.11}$$

$$K_1 = \frac{[HCO_3^-][H^+]}{[H_2CO_3^*]} = \approx 10^{-6.3} \tag{1.12}$$

$$K_2 = \frac{[CO_3^{2-}][H^+]}{[HCO_3^-]} \approx 10^{-10.3} \tag{1.13}$$

where the equilibrium constants K_i are temperature, pressure and salinity dependent.

The DIC species in natural waters can be plotted as a function of pH in the Bjerrum diagram (see Figure 1.4) from where it can be seen that the majority of carbon in waters with pH values typically encountered in karst areas occurs as HCO_3^- ion.

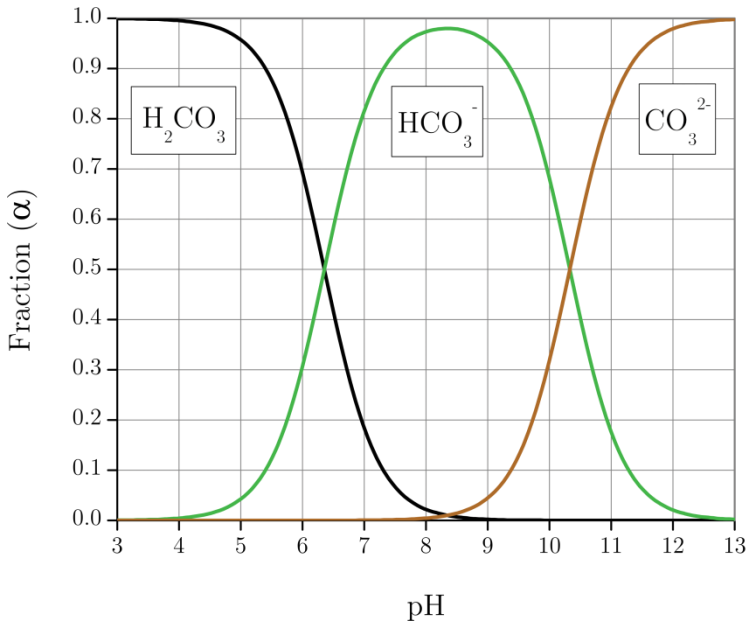


Figure 1.4: Relative abundance of dissolved inorganic carbon (DIC) ionic species in relation to pH in freshwater at 298 K (Ploted according to equations published in Plummer & Busenberg (1982)).

Carbonate equilibria is described by pH, fugacity of CO_2, DIC and total alkalinity (TA). If two of the listed parameters are measured, the other two can be calculated. Total alkalinity (TA) is defined as the sum of all bases that can accept the protons from carbonic acid (Dickson, 1981; Johansson & Wedborg, 1982) and represents the ability of water to resist pH change upon the addition of acid:

$$TA = [HCO_3^-] + 2[CO_3^{2-}] + [OH^-] - [H^+] + \ldots \tag{1.14}$$

In freshwaters including soil water, carbonate alkalinity (CA) almost equals the TA

$$CA = [HCO_3^-] + 2[CO_3^{2-}] \tag{1.15}$$

Beside the described carbonate equilibria, the reactions of calcite (and dolomite) dissolution and precipitation are very important mechanisms, which are governed by the following relation:

$$CaCO_{3(s)} \overset{K_{CaCO_3}}{\Longleftrightarrow} Ca^{2+} + CO_3^{2-} \tag{1.16}$$

where K_{CaCO_3} is the equilibrium constant or the solubility product for calcite (temperature, pressure and salinity dependent) and is expressed as:

$$K_{CaCO_3} = [Ca^{2+}][CO_3^{2-}] \tag{1.17}$$

where $[Ca^{2+}][CO_3^{2-}]$ are concentrations of Ca^{2+} and CO_3^{2-} ions in (mmol l^{-1}).

Dissolution of carbonate rocks is sensitive to the partial pressure of CO_2, therefore, the higher the CO_2 concentration, the greater the amount of calcite/dolomite dissolution (Clark & Fritz, 1997).

Solubility product can be further used to assess the solution saturation state, Ω, defined as:

$$\Omega = \frac{[Ca^{2+}][CO_3^{2-}]}{K_{CaCO_3}} \tag{1.18}$$

where Ω values of >1 correspond to supersaturation and potential formation of $CaCO_3$, while values <1 correspond to undersaturation and potential dissolution of $CaCO_3$. However, only the assessment of the saturation state is not a sufficient condition for mineral dissolution or precipitation. Important role is attributed also to the so-called inhibitors. For example, the speed of calcite precipitation in the supersaturated solution where Mg^{2+} ions are present is greatly inhibited. These ions hinder the growth of the calcite, because they adsorb on the surface of the crystal (Berner, 1975). In water environment rich in organic matter, the organic acids and phosphates inhibit the carbonate reaction, especially the precipitation of calcite (Stabel, 1986).

Additionally, the DIC concentration and calcite dissolution/precipitation processes depend on the "openness" of the investigated system. Open and closed systems are the two end-members of the range of the conditions that can be found in nature. In the open system, the carbonate dissolution proceeds with a constant supply from the gas phase reservoir (e.g. soil CO_2) and all three phases are simultaneously in equilibrium. Under closed system conditions the calcite dissolution is isolated from the gas phase, i.e. the CO_2 in water solution used for carbonate dissolution is not replenished by new amounts of CO_2. The equilibrium between the three phases does not occur simultaneously, but as

a series of two steps. First the equilibration between the gas phase and water solution occurs, which is followed by the equilibration between water solution and calcite. The effect on water solution composition caused by these two different conditions is significant. If, for example, the same partial pressure of CO_2 in the gas phase is considered, higher amounts of limestone will be dissolved under open system than under closed system conditions.

Weathering processes are on the longer time periods considered to be in equilibrium regarding the CO_2 (Berner, 2003). Dissolution of carbonates is in equilibrium with the precipitation of carbonate minerals in water systems. However, on the season or annual scale one of the processes that are important for the net CO_2 exchange in the system can prevail. Systems where (on the annual scale) calcite dissolution prevails act as a geochemical sink for CO_2. Soil CO_2 dissolves the carbonate rock and therefore the flux of CO_2 to the atmosphere is lower. The carbonate dissolution leads to the transport of carbon out of the soil. The dissolution of CO_2 into the solution strongly enhances calcite solubility. The overall reaction of calcite dissolution and precipitation in the carbonate system can be simplified as Eq. (1.19). As it can be seen from this reaction, one mole of CO_2 is used in order to dissolve one mole of limestone rock which can be leached out of the system in the form of bicarbonate (and other DIC species):

$$CaCO_3 + CO_2 + H_2O \Leftrightarrow Ca^{2+} + 2HCO_3^- \tag{1.19}$$

For dolomitic rocks ($CaMg(CO_3)_2$), reactions are analogous but with double molar requirements for consumption of CO_2 and water (see Eq. (1.20)), while precipitation prefers the formation of calcium carbonate rather than dolomite (Kowalski et al., 2008).

$$CaMg(CO_3)_{2(s)} + 2H_2CO_{3(aq)} \Leftrightarrow Ca^{2+}_{(aq)} + Mg^{2+}_{(aq)} + 4HCO^-_{3(aq)} \tag{1.20}$$

1.2.2.3.3 Caves as CO_2 sink or source Several studies, for example Kowalski et al. (2008), Serrano-Ortiz et al. (2010), Were et al. (2010), Kowalczk & Froelich (2010), Plestenjak et al. (2012), consider the possible influence of ventilation of CO_2 from subterranean cracks and caves where substantial amounts of CO_2 can be stored as a possible abiotic source of soil CO_2. Such storing and ventilation of subterranean CO_2 can be explained on an example where rainwater infiltrates and percolates through the soil, where there is higher CO_2 concentration (due to soil respiration) and reduced bicarbonate concentration (due to dilution). This moves the equilibrium described by reaction Eq. (1.19) to the right, which results in dissolution of soil CO_2 and production of DIC. This process represents a geochemical CO_2 sink, since the efflux of CO_2 from soil decreased. Water rich in CO_2 causes dissolution of the carbonate rock. Soil CO_2 and carbon from carbonate rock are transported within water in the form of DIC mainly in the form of HCO_3^- (see Figure 1.4). DIC together with Ca^{2+} and other ions percolates with drainage water and can eventually enter the cave where cave air CO_2 concentrations determine whether the reverse processes precipitate carbonate and degas CO_2 into the cave atmosphere and therefore augment the local CO_2 air concentration. During the events when caves ventilate, gaseous CO_2 escapes from caves (through different paths) into the atmosphere, and can produce sizeable upward fluxes in the atmospheric boundary layer. During the seasons with low cave air ventilation there are high cave CO_2 concentrations, and air in caves can represent sustained belowground sink for gaseous CO_2, whose magnitude may be important for the interpretation of net flux measurements. Another possible transport of CO_2 from soil into deeper layers of soil and eventually caves located

near the surface is by molecular diffusion. This mechanism of transport can be even more facilitated during the rain periods when soil pores are saturated by water, and thus the exchange of CO_2 with atmosphere is limited (Wood, 1985).

1.2.2.3.4 Cave ventilation Certain caves and other subterranean voids can create conditions that allow outside air or water to enter and purge the cave atmosphere. This is called the cave ventilation. The movement of cave air is induced by different environmental conditions. There is a variety of mechanisms that produce cave airflow, which mainly depend of the cave shape, number and location of entrances and local climatic conditions. Cave ventilation rates can be measured directly or through variations of cave air density, pressure or trace gas composition, such as CO_2 concentrations or ^{222}Rn activity concentrations.

The drivers for ventilation can be dynamic (moving fluids – water or wind), or static (variation of pressure, temperature or/and air composition). Examples of water induced flow of cave air are floodwaters changing the volume of the cave system, changing water level of the underground river, water entrainment airflow etc. Wind driven airflow mostly depends on the direction and shape of the cave and its entrances and consequently on the wind direction and speed.

In caves with temperature driven cave airflow (see Figure 1.5), the differences between air densities due to different temperatures of external air and cave air cause movement or stagnation of cave air (Badino, 2010; Cigna, 1968; Hakl, Csige, Hunyadi, Várhegyi, & Géczy, 1996; Kowalczk & Froelich, 2010; Wigley & Brown, 1976). Temperature can explain about 99% of the variation of the cave air density. However, also humidity or pCO_2 of the cave air, if it exceeds the atmospheric values by an order of magnitude, can influence the air density sufficiently to influence the cave airflow dynamics (Kowalski & Sánchez-Cañete, 2010; Sánchez-Cañete, Kowalski, Serrano-Ortiz, Pérez-Priego, & Domingo, 2013).

In the majority of cases the most present and important mechanism of cave airflow is the so-called "chimney effect" (Badino, 2010; Luetscher & Jeannin, 2004; Wigley & Brown, 1976). It is present in caves with more than one entrance in different elevations (see Figure 1.5). During the colder periods when the cave air is warmer and lighter than the colder outside air, cave air rises out the upper entrances, while outside air decreased in the lower entrances. During the warmer periods, the cave air is colder and denser than the outside air. Thus, the decrease of CO_2 at the lower entrances occurs pulling the outside air through the upper entrances (Covington & Perne, 2016). The entrances for air entering or leaving the cave system do not have to be largely visible since substantial airflow can be driven also through much more restricted pathways, such as soil, fissures, fractures or highly permeable rock (Covington & Perne, 2016; Spötl, Fairchild, & Tooth, 2005; Wigley & Brown, 1976). Under special conditions (mainly depending on the cave shape), the chimney effect can be active only during either cold or warm season. This can be the case where a cave passage connecting the entrances is situated significantly below or above its entrances and can represent a special case of cold (cave passage below the entrances) or warm trap (cave passage above the entrances).

Examples of cold and warm traps in caves with only one entrance can be the consequence of circulating convective airflow induced during either cold or warm period, and air stagnation in the opposite case (see Figure 1.5). Most frequently such airflows occur near large entrances to the cave preceding either downwards (cold trap) or upwards (warm trap). If the cave airflow goes downwards, air currents are active during cold periods, when cold and dry outside air sinks along the floor, while warmer and moister air rises outwards along the ceiling. If the cave airflow goes upwards, such ventilation occurs during the warm periods (Covington & Perne, 2016).

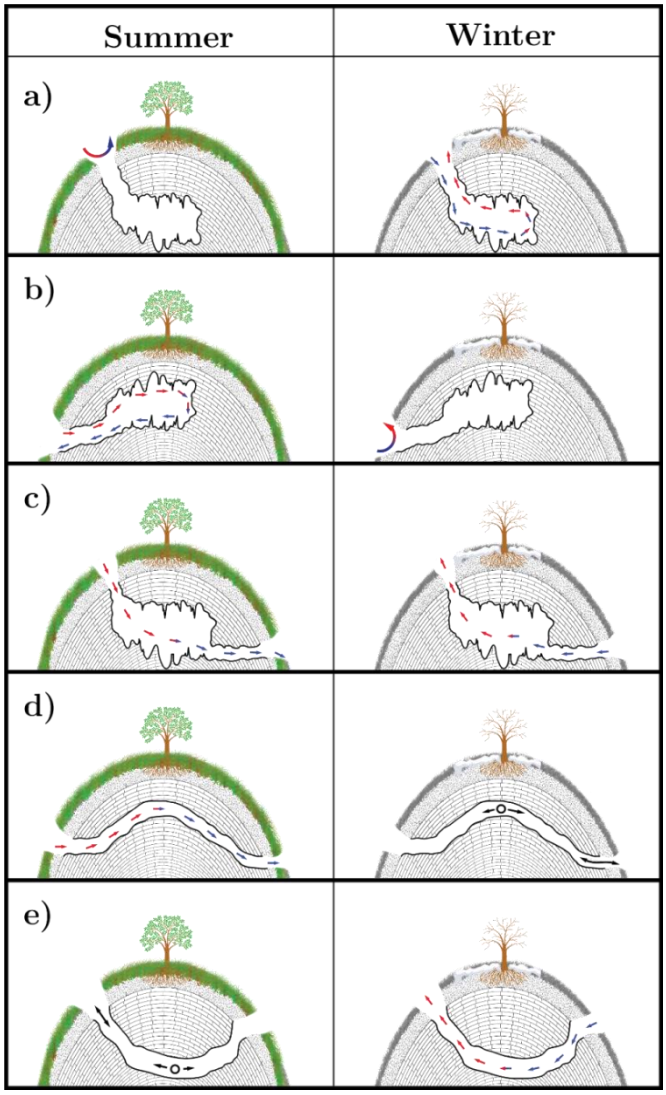


Figure 1.5: A diagram of thermally driven cave airflow. Airflow directions during warm external temperatures (summer) are shown in the left column and directions during cold external temperatures (winter) are shown in the right column. Red and blue arrows illustrate the relatively warm and cold air, respectively. (a) and (b) illustrate the circulating convection cells where the relative elevation of the cave and the cave entrance determine whether the convection is active in winter (a) i.e. »cold trap« or summer (b) i.e. warm trap. The rows from (c) to (e) show the chimney effect that occurs in caves with multiple entrances at different elevations. Chimney effect can cause opposite airflow on summer and winter mode, respectively. Depending on the cave geometry and the elevation differences the chimney effect can be less effective or even absent during summer (e) or during winter (d). In such cases when the passage connecting the entrances extends substantialy above (d) or below (e), the penetration of outside air into the inward drafting entrance can reduce or even stop the chimney effect flows. The black arrow at the entrances shows the zone of the winter and summer influences at the case (d) and (e), respectively, while the arrows in the midlle of the passage illustrate the movement of the air within the passage (Figure adapted from Covington & Perne (2016).

In the caves with large volumes connected by small passages, with one entrance or with very small entrances, the barometric circulation can also take place (see Figure 1.6).

In these cases, the ventilation is driven by pressure difference between the cave and outside atmosphere (Badino, 2010; Luetscher & Jeannin, 2004; Wigley, 1967).

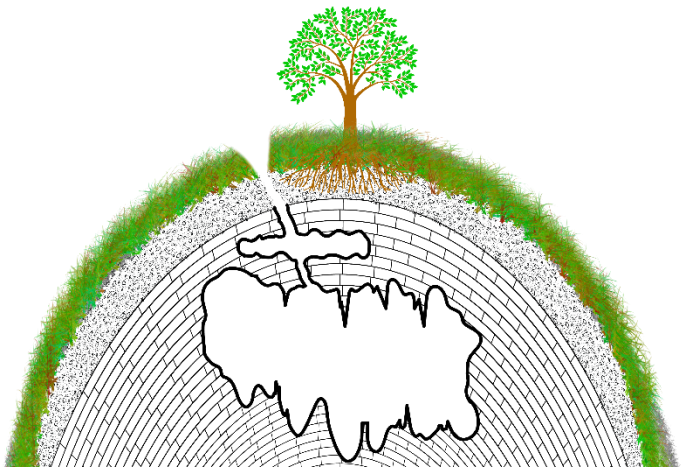


Figure 1.6: A diagram of a »barometric cave«. Barometric airflows dominate in caves which have large volumes but have narrow connections to the surface (Figure adapted from Covington & Perne (2016)).

1.3 CO_2 Source Assessment

The overall soil CO_2 and consequently soil CO_2 flux is thus composed of CO_2 from organic and inorganic sources, which interact with each other. Exact partition between organic and inorganic sources is difficult. To overcome this challenge the use of isotopic techniques can be of great help.

1.3.1 Stable isotopes in general

Isotopes are atoms whose nuclei contain the same number of protons but a different number of neutrons. They have the same atomic number but different atomic masses. Isotopes can be *stable* and *unstable* (radioactive) isotopes (see Figure 1.7). Unlike unstable isotopes, stable isotopes are not subjected to radioactive decay. Isotopologue is a molecular entity (e.g. CO_2) that differs only in isotopic composition (Muller, 1994). Different isotopes of the same element have differences in physical properties, while they have smaller but not always negligible changes in chemical behavior (Hoefs, 2008).

Slight difference in atomic mass causes difference in properties of substances containing different stable isotopes, resulting in different reaction kinetics and thermodynamic properties. This results in the "preference" of chemical and physical processes for one isotopologue over the other. These events are called fractionation events. Two major fractionation types are equilibrium fractionation and kinetic fractionation. Equilibrium fractionation occurs when a chemical reaction or a physical process is reversible and continues to occur in both directions, and the different isotopes accumulate on either side of the reaction or processes. Kinetic fractionation occurs during an irreversible process or during physical process (e.g. diffusion of CO_2 in air phase transitions with constant removal of one phase, or during chemical reactions like conversion of a substance to another).

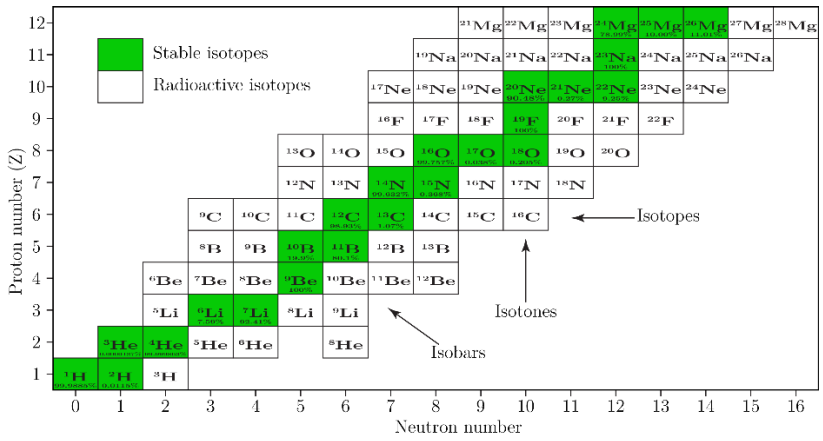


Figure 1.7: Chart of nuclides with percent natural abundance of stable isotopes. **Isotopes** are atoms that have the same atomic number but different mass number, **Isobars** are atoms that have the same mass but different atomic numbers due to different numbers of protons, and **Isotones** are atoms that have the same number of neutrons (Figure adapted from Michener & Lajtha (2008), percent natural abundances from Rosman & Taylor (1998)).

Stable isotope compositions are usually expressed in δ notation in per mille units (‰) relative to the internationally accepted standards (see Eq. (1.21)).

$$\delta(‰) = \left(\frac{R_{sample}}{R_{standard}} - 1\right) 10^3 \tag{1.21}$$

where R is the ratio of heavy/light isotope; R_{sample} is the ratio of the sample and $R_{standard}$ is the ratio of the standard. A positive δ value means that the sample has more of the heavy isotope than the standard and vice versa. Our study is oriented mainly toward the use of stable isotope composition of C and O, thus the R ratios could be related to $^{13}C/^{12}C$ and $^{18}O/^{16}O$. International accepted standard used for reporting carbon isotope composition is Vienna Pee Dee Belemnite (VPDB), while for the oxygen the standard is either Vienna Standard Mean Ocean Water (VSMOW) or in the case of carbonates it can be reported also relative to VPDB (Coplen, 2011; Craig, 1957; Farquhar, Ehleringer, & Hubick, 1989).

1.3.2 The use of stable isotopes in the environmental studies

The most common use in environmental researches is the use of stable isotopes of light elements such H, C, O, N and S. They are convenient to be used as tracers because of their abundance in biological compounds and because the percent increase in mass caused by the additional neutron is greater in lighter elements (Hoefs, 2008). In investigations of carbon cycles in natural ecosystems stable isotopes of C and O are the most commonly used. At this point also the third stable oxygen isotope has to be mentioned. This is the ^{17}O isotope. For terrestrial mass dependent fractionation the proportion of ^{17}O is related to the proportion of ^{18}O and is usually calculated. In some atmospheric photochemical processes there are mass independent fractionation processes that bring different proportions of ^{17}O than expected (Kawagucci et al., 2005). However if the investigation is oriented toward terrestrial systems, the mass independent fractionation is generally neglected.

When using stable isotopes in environmental research, bulk compositions of natural samples are usually used. Bulk composition of measured gases depends on abundances of molecules containing one rare isotope (e.g. $^{13}C^{16}O^{16}O$ or $^{12}C^{18}O^{16}O$). However, also molecules that have more than one rear isotope exist (e.g. $^{13}C^{18}O^{16}C$ or $^{12}C^{18}O^{17}O$), but are present in very low concentrations (Hoefs, 2008). Stochastic abundances of isotopologues of CO_2 are presented in Table 1.2.

The use of stable isotopes in environmental research can be roughly divided into two fundamental groups: use of isotopes at naturally occurring levels, i.e. "**natural abundance**", and the use of "labelled samples" at levels much greater than those naturally occurring, i.e. "**enriched levels**".

Table 1.2: Stochastic abundances of isotopologues of CO_2 (Eiler, 2007).

Mass	Isotopologue	Relative abundance
44	$^{12}C^{16}O_2$	98.40%
	$^{13}C^{16}O_2$	1.11%
45	$^{12}C^{17}O^{16}O$	748 ppm
	$^{12}C^{18}O^{16}O$	0.40%
	$^{13}C^{17}O^{16}O$	8.4 ppm
46	$^{12}C^{17}O_2$	0.142 ppm
	$^{13}C^{18}O^{16}O$	44.4 ppm
	$^{12}C^{17}O^{18}O$	1.5 ppm
47	$^{13}C^{17}O_2$	1.6 ppb
	$^{12}C^{18}O_2$	3.96 ppm
48	$^{13}C^{17}O^{18}O$	16.8 ppb
49	$^{13}C^{18}O_2$	44.5 ppb

Stable isotopes at natural abundances can be used as natural integrators and as tracers of ecological processes. When used as **integrators** they can help us to evaluate the net outcome of many time and space variable processes, without disturbance to the natural activity or behavior of the observed element in that system (Handley & Raven, 1992; Högberg, 1998; Robinson, 2001). When stable isotopes are used as **tracers**, they are used to follow fates and transformations of a certain source. When using natural abundances, two crucial conditions must be satisfied: (1) different potential sources have to have repeatable and distinct δ values that are broader than the natural range of plant measured δ at the research area; and (2) there must be no significant fractionation or mixing of sources during the steps involved from the source to the part that is measured. When these conditions cannot be met, it is better to use the enriched isotope approach (Dawson, Mambelli, Plamboeck, Templer, & Tu, 2002).

With the **enriched isotope approach**, a trace amount of a labelled substance is applied. With these approaches, flows and fates of an element without altering its natural behavior can be followed (Schimel, 1993). Because substances are enriched relative to the variation caused by fractionation, the problems arising from fractionation among pools that mix are minimized. Flow of elements through a system can be traced and rates of biological processes within the system can be determined (Dawson et al., 2002).

1.3.3 Stable isotopes in terrestrial carbon cycle

Along the pathway of carbon and oxygen from the atmosphere through the plant into the soil and back to the atmosphere or further underground, different fractionation processes occur. These processes are associated with diffusion, phase transition and enzyme activities in leaves, non-green plant parts and soil. Therefore, stable isotope techniques can be used to better understand the complexity of atmosphere-plant-soil interactions in the global terrestrial carbon cycle (see Figure 1.8).

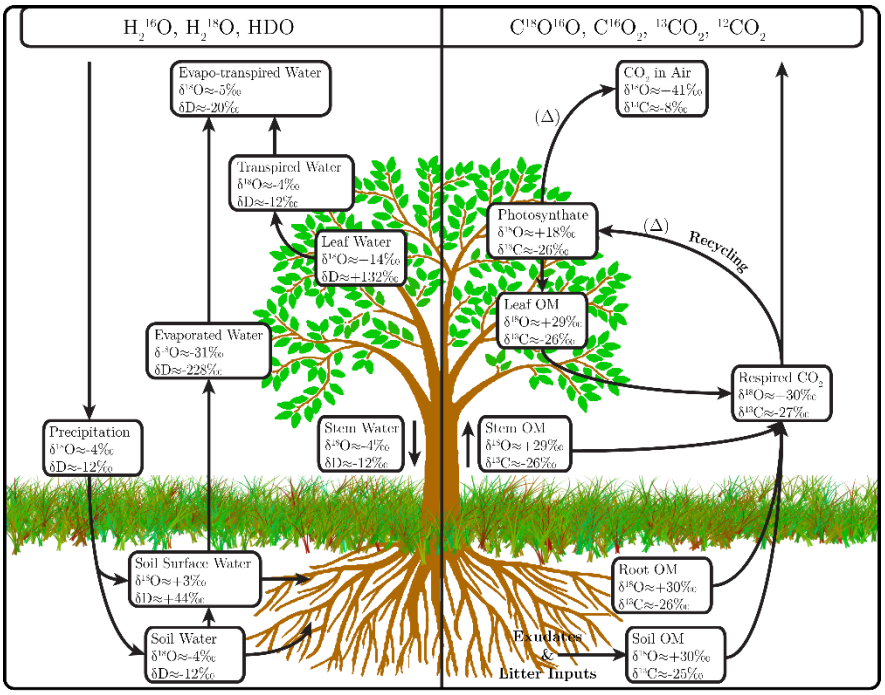


Figure 1.8: Isotope composition of C, O and H pools in the carbon and water cycles. Values are approximate and can vary greatly with geographical location and environmental conditions (Figure adapted from Dawson, Mambelli, Plamboeck, Templer, & Tu (2002)).

Since there are several difficulties concerning the use of oxygen isotopes to partition between different sources of soil CO_2 they are generally not used. One of the important factors that make this kind of a source partitioning difficult and unreliable is ^{18}O isotopic exchange between CO_2 and soil water. Other confounding factors include significant ^{18}O isotopic discrimination of CO_2 due to dissolution of CO_2 in soil water, isotopic discrimination of CO_2 during diffusion through the soil profile, incomplete equilibrium between CO_2 and water in leaves, and diurnal variations of the $\delta^{18}O$ of water pools (Amundson et al., 1998). A more common use of stable isotopes of oxygen is based on the water cycle and transport of the water in soil and plants (see Figure 1.8).

1.3.3.1 Carbon isotopes in plants

Plant material has more negative $\delta^{13}C$ values than atmospheric CO_2 because processes involved in the CO_2 uptake discriminate against ^{13}C. Several processes affect the fractionation of carbon isotopes during plant fixation of CO_2 from the atmosphere. Fractionation before carboxylation occurs during the diffusion through the boundary layer into the leaves through stomata, during the dissolution of CO_2 and diffusion

through the liquid phase (Farquhar, O'Leary, & Berry, 1982). However, the most important step concerning the isotopic fractionation is carboxylation. Based on the plant carboxylation three different photosynthetic pathways and therefore three different types of plants are distinguished. These are C_3, C_4 and CAM plants. Each type of plants has an isotopic composition of their plant material within a characteristic interval for its type.

C_3 plants use the so-called Calvin photosynthetic pathway with one CO_2 fixation step where the reaction is catalyzed by ribulose bisphosphate carboxylase known as Rubisco. Rubisco enzyme significantly discriminates against ^{13}C, leading to lighter carbon isotopic composition of plant material. Typical $\delta^{13}C$ values of plant material for C_3 plants are within a range from $-35‰$ to $-20‰$, with an average value of $-27‰$ (Deines, 1980; O'Leary, 1988).

C_4 plants use Hatch–Slack photosynthetic pathway with two CO_2 fixation steps. Atmospheric CO_2 is fixed by the phosphoenolpyruvate carboxylase producing organic acid with four carbons. This product is further moved deeper in the leave, broken down and CO_2 is released within the bundle sheath cells where it is fixed for the second time by the rubisco enzyme. Rubisco carboxilisation is similar to that in C_3 plants but since the first fixation step in C_4 plant is irreversible and the CO_2 accumulates in the bundle sheath cells the discrimination against ^{13}C by Rubisco is minimal. Therefore, the fractionation during CO_2 fixation in C_4 plants is mainly governed by the first step where phosphoenolpyruvate carboxylase discriminates very little against ^{13}C. Typical $\delta^{13}C$ values of plant material for C_4 are therefore less negative than of C_3 plants within the range from $-17‰$ to $-9‰$ with an average value of about $-13‰$ (Deines, 1980).

CAM (Crassulacean acid metabolism) plants fix CO_2 at night by phosphoenolpyruvate carboxylase. Similarly as in C_4 plants this enzyme discriminates very little against ^{13}C. During the day when and if the plant closes its stomatal pores the product from the first step is broken down and the released CO_2 is fixed by rubisco. If stomatal pores are closed during the day, the discrimination against ^{13}C will be small and similar to that in C_4 plants. However, some CAM plants do open their stomatal pores at different times of the day or switch to C_3 photosynthesis in certain periods of the year. Carbon isotopic composition of these plants is more similar to that of C_3 plants. CAM plant material $\delta^{13}C$ values can therefore range from values typical for C_3 plants to values typical for C_4 plants (Farquhar et al., 1989).

1.3.3.2 Carbon isotopic composition of soil CO_2

Soil CO_2 carbon stable isotope composition depends on several factors. As already mentioned soil CO_2 is a mixture of different CO_2 sources, which can include soil respired CO_2, atmospheric CO_2, cave CO_2 and other abiotic sources such as carbonate derived CO_2 and CO_2 from deep sources. The most important factor affecting its isotopic composition is the soil-respired CO_2.

Since plants are the main carbon sources for most soils, the carbon isotope of a soil respired CO_2 is mainly dominated by the $\delta^{13}C$ value of the local flora. Respiration of plant roots produces CO_2, which has $\delta^{13}C$ values similar to that of the plant material (Cerling et al., 1991). In soils at steady state also microbial decomposition of SOM produces CO_2 with $\delta^{13}C$ values similar to that of the above and below ground litter inputs (Amundson et al., 1998). Although SOM can be slightly enriched in ^{13}C relative to litter inputs during aerobic decomposition, the humification and other microbial processes during the incorporation of plant-derived C into SOM usually affect its isotopic composition for less than $2‰$ (Kuzyakov, 2006). $\delta^{13}C$ values of SOM commonly slightly increase with depth therefore also $\delta^{13}C$ of microbial respiration may deviate from the litter value in a particular soil layer, or at a particular time. However, in most cases $\delta^{13}C$

of soil respired CO_2 is nearly the same as that of the flora at the site (Cerling et al., 1991). Soil CO_2 has a different isotopic composition than soil respired CO_2 due to the different diffusivities of $^{12}CO_2$ in comparison to $^{13}CO_2$ in the soil pore space. If soil respired CO_2 would be the only source of soil CO_2, this would result in an isotopic composition of soil CO_2 approximately 4.4‰ higher than soil-respired CO_2 (Cerling & Quade, 1993; Davidson & Trumbore, 1995).

The next important source affecting soil CO_2 isotopic composition is the atmospheric CO_2, which can enter soil via diffusion, convection or dissolved in rainwater. Atmospheric CO_2 is less depleted in ^{13}C than soil-respired CO_2. According to GLOBALVIEW-CO_2C13 (2009), the average global atmospheric CO_2 isotopic composition ($\delta^{13}C_{atm}$) was about -8‰ and is getting even lower due to the anthropogenic CO_2 emissions. Its presence in soil increases the $\delta^{13}C$ value of soil CO_2. The proportion of atmospheric CO_2 in soil CO_2 at certain soils mostly depends on soil depth and soil respiration rate: lower soil CO_2 respiration rates and smaller depths greater proportion of atmospheric CO_2 is encountered (Amundson & Davidson, 1990). In reality the ^{13}C fractionation between soil CO_2 and its source (i.e. soil-respired CO_2) is not constant but varies due to the difference between atmospheric and soil gas CO_2 concentrations. This relationship can be expressed by Eq. (1.22) proposed by Davidson & Trumbore, (1995):

$$\delta^{13}C_{soil} = 1.0044\ \delta^{13}C_{resp} + \frac{C^{12}_{atm}}{C^{12}_{soil}}(\delta^{13}C_{atm} - 1.0044\ \delta^{13}C_{resp} - 4.4) + 4.4 \quad (1.22)$$

where $\delta^{13}C$ is the carbon isotopic composition of CO_2, C^{12} is the $^{12}CO_2$ concentration which can be approximated by the total CO_2 concentration (naturally occurring CO_2 is almost 99% $^{12}CO_2$, which means that the bulk measurements of CO_2 can be used in place of the C^{12} and the error introduced by this replacement is less than 0.001 ‰ (Davidson & Trumbore, 1995)). The subscripts *soil*, *atm* and *resp* represent soil, atmospheric and respired CO_2, respectively.

There is another source of soil CO_2, which has been generally neglected or considered of minor importance (Kuzyakov, 2006) and is originating from the carbonate bedrock weathering. There is a growing number of studies reporting its significance to soil CO_2 fluxes (Čater & Ogrinc, 2011; Kowalski et al., 2008; Plestenjak et al., 2012; Serrano-Ortiz et al., 2010). Stable carbon isotopes are a useful tracer for this source since the $\delta^{13}C$ value of the carbonate bedrock normally has a narrow, close to zero range (0‰ - 4‰). Due to this rather large difference relative to biogenic sources, the abiotic source from carbonate weathering can be detected in soil CO_2 isotopic signature even at low contributions.

The main mechanism affecting this source in karst areas in temperate zone is the dissolution of carbonate bedrock by infiltrating rainwater and subsequent degassing and precipitation of carbonates. As described in paragraph 1.2.2.3.2, rainwater in soil encounters places with higher partial pressures of CO_2 originating mainly from soil respiration. CO_2 in infiltrating water forms a weak carbonic acid (H_2CO_3*), and other species of DIC. The H_2CO_3* in percolating water dissolves carbonate bedrock (e.g. $CaCO_3$ in limestone) (see Eq. (1.19) and (1.20)). Part of the carbon in the bicarbonate on the right side of the reaction therefore originates from the dissolved $CaCO_3$ and part from the dissolved CO_2. If water later encounters places with lower pCO_2 (e.g. caves, subterranean voids, etc.) or places with higher temperatures, this causes degassing of CO_2 from water and depending on the saturation state of the water also carbonate precipitation. Since part of the DIC and consequently part of degassed CO_2 comes from dissolution of carbonate bedrock, it can be, in certain conditions, traced by the use of stable carbon isotopes. The influence of carbon from carbonate bedrock to the isotopic composition of

the evolving CO_2 also depends on the state of the reaction. The processes of carbonate dissolution in soil and epikarst range between (a) open system and (b) closed system. In open system dissolution, a complete isotopic equilibrium occurs between soil CO_2 and inorganic carbon species in the solution, while the pCO_2 of the gas phase is fixed, i.e. does not decrease since a large CO_2 reservoir is constantly resupplying the CO_2 taken up by the carbonate dissolution. Therefore, the isotopic composition of DIC and subsequently of CO_2 degassing from water is not influenced by the isotopic composition of the dissolving $CaCO_3$, but depends only on the isotopic composition of soil CO_2 (Deines, Langmuir, & Harmon, 1974; Salomons & Mook, 1986). In the case of closed system dissolution however, water first equilibrates with soil CO_2 and is later isolated from it, so the water has no connections with the soil CO_2 reservoir during the $CaCO_3$ dissolution (Deines et al., 1974; Salomons & Mook, 1986). In this case the stoichiometry of the carbonate dissolution (see Eq. (1.19)) dictates that half of carbon in HCO_3^- originates from H_2CO_3* and half from $CaCO_3$ which affect the isotopic composition of HCO_3^- (Jin et al., 2009) as follows:

$$\delta^{13}C_{DIC} = \left(\delta^{13}C_{H_2CO_3} + \ \delta^{13}C_{CaCO_3}\right)/2 \tag{1.23}$$

The proportion of different DIC species in percolating water primarily depends on its pH (see Figure 1.4). Isotopic composition of each of DIC species depends on several reactions generally considered being at isotopic equilibrium. Isotope enrichment factors (ε) between the DIC species and gaseous CO_2 dissolving in water are mainly temperature dependent. These fractionations are described with the following equations described by Zhang, Quay, & Wilbur (1995):

$$\varepsilon CO_{2(gas)}(CO_2) = (0.0049 \pm 0.0015)T - 1.31 \pm 0.005 \tag{1.24}$$

$$\varepsilon CO_{2(gas)}(HCO_3^-) = (-0.1141 \pm 0.0028)T + 10.78 \pm 0.04 \tag{1.25}$$

$$\varepsilon CO_{2(gas)}(CO_3^{2-}) = (-0.052 \pm 0.021)T + 7.22 \pm 0.38 \tag{1.26}$$

where T is expressed in °C. Isotope enrichment factors for calcite-bicarbonate and aragonite-bicarbonate are independent of temperatures in conditions usually encountered in caves (10-40 °C). These factors are 1.0±0.2‰ and 2.7±0.6‰ for calcite-bicarbonate and aragonite-bicarbonate, respectively (Romanek, Grossman, & Morse, 1992).

When percolating water encounters places with lower pCO_2 or places with higher temperatures, this causes degassing of CO_2. This can happen e.g. in cold seasons when water drains from colder upper parts of soil into warmer deeper parts or when water encounters subterranean voids such as karstic caves with lower pCO_2. These voids can at certain conditions expulse the accumulated CO_2 through the soil back to the atmosphere i.e. affecting the soil CO_2 flux and its isotopic composition. This can happen for example if extensive rainfall fills the subterranean CO_2 reservoirs or in the case of the cave ventilation already discussed.

1.3.3.3 CO_2 sources in cave air

CO_2 in the cave air can originate from different sources and can be transported through different pathways (Frisia et al., 2011): (I) CO_2 from the external atmosphere; (II) input of CO_2 from the overlaying soil and epikarst; (III) degassing of CO_2 from dripwaters; (IV) cave visitors; (V) biotic CO_2 production in cave; (VI) deep CO_2 sources.

More sources that are potentially present, more tracers (e.g. ^{13}C, ^{14}C, radon) should be used if the goal is to assess the contribution of each of these sources. This will be explained in more detail in subsection 1.3.4. Not all of these sources are present in all the caves. Depending on the type of research one can chose a cave where some of the sources are obviously not present. For example, when studying natural carbon fluxes in a certain ecosystem with no interest in assessing the impact of the cave visitors, the caves where there are no tourist visits are chosen. Similarly if no organic matter (e.g. plant litter, sediment reach in organic matter etc.) is found in the cave, no biotic CO_2 production is expected.

Atmospheric CO_2 and CO_2 from soil respiration have been already explained in subsections 1.2.2.1 and 1.2.2.2. Further since the most important sources for this dissertation were atmospheric, and soil respired CO_2 coming to cave either directly or via percolating water, other sources are just briefly explained.

CO_2 exhaled by cave visitors. If the number of visitors is known and if the isotopic composition of exhaled air is sufficiently different from the other source, it is possible to use stable isotope techniques to assess the contribution of CO_2 exhaled by the visitors. The isotopic composition of exhaled air is mainly defined by the diet. Due to differences in diet in different parts of the world also isotopic composition of exhaled air varies regionally. Isotopic composition of exhaled air in populations of European countries averages at $\sim -23‰$, the United States at $\sim -21‰$, and Japan falling somewhere between these two countries (Bütz, Casperson, & Whigham, 2014; Nakamura, Schoeller, Winkler, & Schmidt, 1982). The average adult human respiration produces $\sim$480 L h^{-1} with a concentration of 36000 µmol mol^{-1} CO_2 (Kivastik, 1998).

Biotic CO_2 production in caves. If similar conditions for microbial decomposition of organic matter in cave as in the soil are assumed, isotopic composition of CO_2 biotic production in the cave mainly depends on the isotopic composition of the organic material and produces CO_2 with $\delta^{13}C$ values similar to the organic matter present. This source can be found for example in vertical caves or caves with entrances or other conduits that enable plant litter and other organic material to fall or be otherwise transported into the cave. Other examples are the caves where flowing waters or animals living in the cave deposit organic material e.g. bat colonies.

Deep CO_2 sources. There can be different sources of deep CO_2 where this CO_2 of geologic origin is typically ^{13}C enriched relative to biogenic sources. The $\delta^{13}C$ of CO_2 degassing from the upper mantle has values ≈ -6.5 ‰ (Sano & Marty, 1995) or even higher if deep source CO_2 is undergoing secondary methanogenesis following hydrocarbon biodegradation (Etiope, Nakada, Tanaka, & Yoshida, 2011). Deep CO_2 may also derive from limestone or organic carbon from sedimentary rocks in island arcs and subduction-related volcanism (Hoefs, 2008), where the thermos-metamorphism of carbonate rock typically produces CO_2 with $\delta^{13}C_{CO2} \approx 0‰$ while organic carbon from sedimentary rocks has $\delta^{13}C$ values typically lower than $-20‰$ (Sano & Marty, 1995). In this case it is therefore difficult to differentiate between sources of CO_2 from soil respiration based only on stable carbon isotope composition.

1.3.3.3.1 Degassing of CO_2 from dripwaters Processes in soil and epikarst, discussed in subsection 1.3.3.2, determine the water chemistry and its carbon isotopic composition to the karst. Water is expected to be in equilibrium with calcite before it arrives into the cave environment (Fairchild & Baker, 2012). Once water leaves the soil and its "infinitive" CO_2 reservoir, the carbonate system for the carbon is closed (Dreybrodt, 2011). This means that when the dissolution of carbonate is completed the carbon isotope composition remains the same until favorable conditions cause degassing or calcite precipitation. If this happens before water reaches the cave, this can lead to prior calcite precipitation (PCP). PCP is a consequence of water degassing into air spaces before water arrives to the cave, which changes its chemical composition and its isotopic signature before the water is sampled. It is possible to detect PCP in sampled drip water using the concentrations of elements such as Mg^{2+} (or Sr^{2+}) and relate them with Ca^{2+} concentrations. Because the distribution coefficient for Mg^{2+} (and Sr^{2+}) is much smaller than 1, much larger reduction in Ca^{2+} than that of the element could be expected causing an increase in the ratio of the selected element to Ca^{2+} in the solution. Negative correlation between Ca^{2+} concentration and Mg^{2+}/Ca^{2+} (and Sr^{2+}/Ca^{2+}) concentration ratio of the drip water would indicate the presence of PCP (above cave or inside the cave prior to drip water collection) (Fairchild & Treble, 2009). A test for PCP is made by comparison of the measured data by PCP lines calculated by:

$$\left(\frac{[Mg^{2+}]}{[Ca^{2+}]}\right)_{water} = \left(\frac{[Mg^{2+}]}{[Ca^{2+}]}\right)_{water_o} - ([Ca_o^{2+}] - [Ca^{2+}])_{water} D_{Mg} \tag{1.27}$$

where $[Mg^{2+}]$ and $[Ca^{2+}]$ are concentrations of Mg^{2+} and Ca^{2+} ions (mol dm^{-3}) in the solution, D_{Mg} represents the partition coefficient for Mg and the suffix o refers to the original conditions.

Once water gets in contact with the cave atmosphere (with lower pCO_2) i.e. enters the cave ceiling, the CO_2 degassing started. The first step is the degassing by molecular diffusion directly from water. This is a fast process completed in time scales of 10 s for the thin water films. If the water film is thicker, it can also be completed in the time scales of 100 s (Dreybrodt, 2011). The CO_2 expelled from the water is isotopically light, therefore in the solution higher $\delta^{13}C_{DIC}$ values are expected. Initially $\delta^{13}C_{DIC}$ value increases rapidly due to the release of large amounts of isotopically lighter CO_2. Then the increase in $\delta^{13}C_{DIC}$ value is slower since the $CO_{2(w)}$ reservoir is exhausted and the outgassing is controlled by the HCO_3^- ions. The flux of CO_2 out of the solution is much larger than the flux back to the solution, therefore, CO_2 already present in the cave atmosphere has a negligible influence on the isotopic composition of the solution (Dulinski & Rozanski, 1990). When degassing is completed, the pH and DIC species are not in equilibrium due to the lower CO_2 concentration. Establishing the chemical and isotopic equilibrium causes an increase in pH and calcite supersaturation. Equilibrium is established at a time scale of 100 s (Dreybrodt, 2011). When supersaturation is achieved, calcite begins to precipitate, which again causes degassing of CO_2. Solutions that had higher pCO_2 at their formation begin to precipitate calcite earlier than solutions that had lower pCO_2. One molecule of CO_2 is released for each $CaCO_3^-$ unit that is attached to the calcite surface. This is a process that is completed at the time scales of 1000 s (Dreybrodt, 2011). Although in some caves there is clear evidence of a preceding degassing phase and increase in $\delta^{13}C_{DIC}$ before calcite precipitations take place, there are caves, where there is no clear evidence if these two phases are happening separately. The modelling of $\delta^{13}C$ values in such cases can be done assuming simultaneous $CaCO_3$

precipitation with CO_2 degassing (Bar-Matthews, Ayalon, Matthews, Sass, & Halicz, 1996).

The loss of CO_2 from the solution and the increase in $\delta^{13}C_{DIC}$ before calcite precipitation is a process that can likely cause kinetic fractionation. These effects can lower $\delta^{13}C$ values of the degassed CO_2 than expected under equilibrium conditions and consequently cause ^{13}C enrichment of DIC in the solution. Further, these processes can be so effective that they can even mask the distinctive isotopic signature controlled by C_3 or C_4 vegetation.

CO_2 degassing and precipitation of calcite with CO_2 degassing can be described in terms of Rayleigh distillation fractionation (see Eq. (1.28)). Here isotopic species (e.g. ^{13}C or ^{12}C) are selectively removed from the solution (e.g. precipitating and degassing) and are continuously in thermodynamic and isotopic equilibrium with those remaining in the system at the moment of removal. Such reactant should, for ideal »Rayleigh fractionation«, also not back-react with the product (Clark & Fritz, 1997).

$$log\left(1+\frac{\delta^{13}C}{1000}\right) = log\left(1+\frac{\delta^{13}C_o}{1000}\right) + \varepsilon log f \tag{1.28}$$

where $\delta^{13}C_0$ refers to the initial $\delta^{13}C$, f is the remaining fraction of carbon in the system and ε is the isotope enrichment factor.

If there are more fractionation reactions happening at the same time, the isotope enrichment factor of the Rayleigh distillation should have the mean value related to fractionations of all reactions according to the mass balance (Fairchild & Baker, 2012). Since pH of the solution and speciation of carbon in DIC can change during such reactions, these changes should also be considered when calculating the isotopic composition of the products of the reaction. The most comprehensive, less time consuming and less error prone way to do this kind of calculations is to use special speciation software such as PHREEQC (Appelo & Postma, 2005).

1.3.4 Source partitioning of CO_2

The partition techniques can be divided into (1) natural abundance and (2) labelling techniques. Labeling techniques include different methods such as tracer methods and dilution methods. In tracer methods a certain quantity of material with significantly different isotopic composition than the natural background is added to the labeled pool, and observation of the change in isotopic signature in the recipient pool after a certain amount of time is made. Isotope dilution methods consist of the labelling of a pool that is the product of the transformation of interest and the measuring of how fast the added isotope is diluted by influx of the natural isotope into the pool over time.

In natural abundance methods, that is also the subject of the proposed thesis, the source partition is made based on the different isotopic compositions of the pools that are naturally present, e.g. carbon originating from carbonate bedrock versus carbon fixed by C_3 plants or carbon from atmospheric CO_2.

In the situations where only two sources are present the contribution of each source can be assessed using a simple isotopic mass balance mixing equations:

$$\delta_t = f_A \delta_A + f_B \delta_B \tag{1.29}$$

$$1 = f_A + f_B \tag{1.30}$$

where δ_t is the observed isotopic value, δ_A, and δ_B are the isotopic values of two different sources A and B, while f_A and f_B are a corresponding fraction of the sources contributing to the observed value.

When more than two different sources are present and only one tracer (e.g. ^{13}C) is available, assessing the proportional use of each becomes much more challenging. In that case more complex models must be used. These models require additional information about the spatial and temporal variation of the sources within a system; they may be the only way to quantitatively access resource use and partitioning among multiple end-members and species, within an ecosystem. In some instances, there may be several different interpretations, and simple two- or even three-source models cannot and should not be applied. In these cases one may still be able to arrive at a best-case interpretation with model developed by Phillips & Gregg (2003). With this approach possible combinations of source proportions are calculated iteratively and compared to measured values. Possible solutions are calculated within a proposed tolerance. With this kind of calculations it is possible to obtain some interval of maximum and minimum values of possible contributors. Width of this interval can be different with different input values of the contributors.

The best solution in cases where more than two sources are present is to include more tracers that are suitable for the given research e.g. radiocarbon (^{14}C) and/or radon (^{222}Rn) in the case of assessment of the influence of subterranean caves to soil CO_2 fluxes. These two tracers are also the subject of the present thesis.

1.3.4.1 Radiocarbon (^{14}C)

The third of the three principal isotopes that occur in nature is the ^{14}C, which is unlike the other two (^{12}C and ^{13}C) radioactive i.e. unstable. It is the most rear of the three isotopes with its natural abundance of one part per trillion. ^{14}C is formed in the upper atmosphere through the effect of cosmic ray neutrons on nitrogen-14 (^{14}N). The formed ^{14}C rapidly oxidizes to $^{14}CO_2$, which is eventually distributed throughout the global atmosphere and enters the plant and animal life through photosynthesis and food chain. ^{14}C also enters the world's waters with an atmospheric exchange as DIC. DIC and therefore ^{14}C in soil water principally comes from organic matter via soil respiration. Plants and animals take up ^{14}C carbon during their lifetimes and are in equilibrium with the ^{14}C concentration of the atmosphere. When a plant or animal dies, the metabolic function of carbon uptake no longer works therefore in their tissue there is only decay of ^{14}C without its replenishment. When ^{14}C decays back to ^{14}N it emits a weak beta particle (160 keV). The ^{14}C half-life is 5730 $\pm$ 40 years (Godwin, 1962).

The $\delta^{13}C_{CO2}$ values together with $\Delta^{14}C$ can be used to evaluate the relative contribution of different sources to soil and cave CO_2 gas. Three different main sources are considered: (a) atmospheric air; (b) young organic carbon derived from contemporary C_3 plants; and (c) weathered carbonates and carbonate rocks. Thus, a triple mixing model can be applied using the following equations:

$$\delta^{13}C_t = f_A\delta^{13}C_A + f_B\delta^{13}C_B + f_C\delta^{13}C_C \tag{1.31}$$

$$\Delta^{14}C_t = f_A\Delta^{14}C_A + f_B\Delta^{14}C_B + f_C\Delta^{14}C_C \tag{1.32}$$

$$f_A + f_B + f_C = 1 \tag{1.33}$$

where subscript "t" refers the observed isotopic value of the sample and the subscripts "A", "B" and "C" in this case refer to (a) atmospheric air, (b) young organic carbon and (c) weathered carbonates.

Global atmospheric CO_2 has $\delta^{13}C$ values around −9‰, but can be lower in polluted areas due to the presence of ^{13}C-depleted CO_2 originating from the burning of fossil fuels (Allison, Francey, & Krummel, 2003). Atmospheric CO_2 as well as respiratory sources will contain modern ^{14}C from nuclear testing, and since root and most microbial respiration is fueled by recently synthesized organic matter, the $\Delta^{14}C$ of respiratory CO_2 will be close to that of the atmosphere (ca. +125‰) representing the young, ^{14}C-active C. Another source is slowly decomposing organic matter, which is more depleted in ^{14}C (Dörr & Münnich, 1986) and CO_2 originating from carbonate bedrock, which is composed of ancient, ^{14}C-dead C and has a $\Delta^{14}C$ of –1000‰ (Lambert & Aharon, 2011). The range of $\delta^{13}C$ values of marine carbonate bedrock is narrow i.e., 0 to 4‰ (Lambert & Aharon, 2011).

Figure 1.9 shows the relationship between $\delta^{13}C_{CO2}$ and $\Delta^{14}C$ values in soil gas. The contribution of carbonate-derived C to the total soil CO_2 pool can be quantified as a mixing line between modern ^{14}C and ancient carbonate. The equilibration of soil CO_2 with carbonate minerals *via* carbonic acid weathering will shift soil CO_2 towards the carbonate end-member.

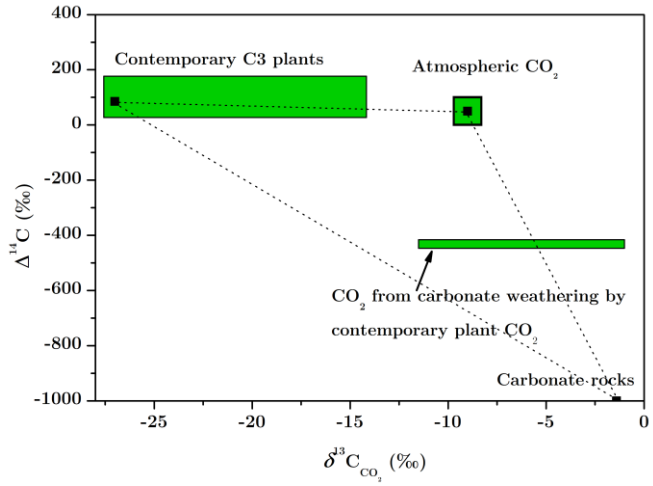


Figure 1.9: Schematic diagram of the distribution of $\delta^{13}C_{CO2}$ and $\Delta^{14}C$ values for different carbon sources with the following isotopic values ($\delta^{13}C_{CO2}$ and $\Delta^{14}C$) of individual end-member (−9, 49.5), (−27, 85.1) and (−1.4, −1000) for open air, young organic carbon and deep mineral (carbonate rock) sources, respectively. The values were derived from the literature (Krajnc, Ferlan, & Ogrinc, 2017; Levin et al., 2010; Liu, Moriizumi, Yamazawa, & Iida, 2006).

1.3.4.2 Radon (^{222}Rn) activity

Radon is very popular and useful tracer gas in environmental sciences, due to some of its properties such as: it is a noble gas (thus chemically inert), it is radioactive, and has a relatively short half-life. Its radioactivity makes its detection relatively easy. While the short half-life makes it useful for investigation of dynamics of several processes in the lithosphere, hydrosphere and atmosphere. Radon is generated from the alpha transformation of radium. It has three isotopes which originate from three natural decay chains. When radon is used in the environmental sciences as a tracer, this is most often the ^{222}Rn which is also the most abundant of the three isotopes. It originates from ^{238}U decay chain and has a half-life of 3.82 days. The second one ^{220}Rn is also called thoron since it originates from the ^{232}Th chain. It has a half-life of 55.6 seconds. The third, ^{219}Rn, originates from the ^{235}U decay chain and has a half-life of 3.9 second and is called action. Radon is a colorless gas. It is the heaviest gas in nature with a density of 9.73 kg m^{-3} (STP). It has a relatively high solubility in water (230 cm^3 kg^{-1} at 20 °C).

The amounts of ^{222}Rn in nature depend primarily on the concentrations of uranium (^{238}U) in the soils and rocks. ^{238}U with a half-life of 4.47 x 10^9 years is the forerunner of ^{222}Rn. It is present in all types of rocks and soils. The immediate precursor of ^{222}Rn is Radium (^{226}Ra). ^{226}Ra has a half-life of 1602 years. Due to the particular geologic history of certain types of rock and soils, some types can have enhanced concentrations of uranium and therefore radium and radon. For example granite, where uranium is present in accessory minerals, is relatively rich in uranium. On the other hand certain rocks such as basalt and carbonate rocks are relatively poor in uranium (Wilkening, 1990). Besides the uranium (and therefore radium) content in soils and rocks is the ^{222}Rn concentration in soil gas dependent on intergranular and fissure porosity and permeability, location of tectonic faults, fracture zones, volcanic pipes, soil gas and ground-water fluxes.

The proportion of radon produced by radium decay that escapes a solid grain or material is described by emanation coefficient (also known as emanation factor or emanation power). During the creation of ^{222}Rn atom by α-transformation of ^{226}Ra, they receive 86 keV recoil energy which enables those that are close enough to the grain surface to emanate from the grain into the void space between the grains. The recoil distance depends on the density and composition of the material. Emanation coefficient also depends on other factors such as grain size and radium distribution (Sakoda et al., 2010), moisture content (Barillon, Özgümüs, & Chambaudet, 2005; Stranden, Kolstad, & Lind, 1984), and temperature (Iskandar, Yamazawa, & Iida, 2004; Stranden et al., 1984).

Radon gas that is eventually released to the capillaries and pores in the soil and rock can reach levels of the order of 1000 times that of the atmospheric values. However, its actual concentration is still relatively low comparing to other gases (orders of 10-10 µmol mol^{-1}). ^{222}Rn atoms can migrate from soil pores or rock fissures by diffusion and/or advection. Diffusion comes more to the fore on a short scale distance while for longer distances radon is transported mainly by advection. However, the amount of radon alone is too small to react to pressure gradients, thus if radon is transported by advection, it must be carried by a flow of carrier gases (Kristiansson & Malmqvist, 1982) (e.g. CO_2, CH_4, N_2) or dissolved in water. Gaseous mixture, formed of a carrier gas and a rare gas (e.g., He, Rn), is referred to as a "geogas" (Etiope & Martinelli, 2002). If CO_2 is the carrier gas, then a significant correlation exists between the levels of both gases in the soil. Recent studies of radon emanation from soil in Slovenia (Kardos et al., 2015) and the distribution of radionuclides in soils (Kovács et al., 2013) reveal soil gas radon concentrations to be highly heterogeneous and emphasize the important contribution of long-range radon transport.

1.3.4.2.1 Radon in caves Karstic caves can have relatively high radon concentrations (in respect to the outside air) although the quantities of ^{238}U in limestone are generally very low (1.3-2.5 µmol mol^{-1}) (Cigna, 2005; Gillmore, Phillips, Denman, & Gilbertson, 2002; Hakl et al., 1997). This can be attributed to low ventilation of those caves and constant emission from surfaces, drip waters and fractures. Concentration of radon in the cave thus depends on the radon source, the cave ventilation and its radioactive decay. Because of that radon can be used as an excellent tracer for air movement in the cave environment (Cigna, 2003; Cunningham & LaRock, 1991; Gregorič, Zidansek, & Vaupotic, 2011; Gregorič, Vaupotič, & Gabrovšek, 2013; Gregorič, Vaupotič, & Šebela, 2014; Hakl et al., 1996; Kowalczk & Froelich, 2010; Perrier, Richon, Crouzeix, Morat, & Le Mouël, 2004). The ventilation characteristics of a cave can be reflected in the fluctuation of radon concentration as long as the turnover time is shorter than five mean lives of ^{222}Rn which is approximately four weeks (Kowalczk & Froelich, 2010).

1.3.5 Stable isotope measurement techniques

There are two most commonly used techniques for isotope measurements:

- isotope ratio mass spectrometry (IRMS) and
- optical isotope measurement systems.

1.3.5.1 Isotope ratio mass spectrometry (IRMS)

In IRMS techniques the charged atoms or molecules are separated based on their mass-to-charge ratios and motions in the presence of a strong magnetic field (Dawson & Brooks, 2001). It is used for precise and accurate measurements of isotopic ratios of light

elements, i.e. H, C, N, O and S. Precision of IRMS systems ranges from 0.02‰ to 0.1‰ for $\delta^{13}C_{CO2}$ and from 0.05‰ to 0.2‰ for $\delta^{18}O_{CO2}$ (Griffis, 2013), while typical precision for $\delta^{2}H_{H2O}$ and $\delta^{18}O_{H2O}$ is 0.5 - 1‰ and 0.03 - 0.1‰, respectively (Lee, Sargent, Smith, & Tanner, 2005; Wang, Caylor, & Dragoni, 2009; Yakir & Wang, 1996). IRMS comprises three main sections: Ion source, mass analyzer and ion collection assembly (see Figure 1.10). It is critical that the sample is processed before entering the mass spectrometer so that only a single chemical species enters at a given time. Samples are generally combusted or pyrolyzed and the desired gas species is purified by means of traps, filters, catalysts and/or chromatography. Gas suitable for isotopic analysis of the desired element (i.e. H_2, N_2, CO_2, CO, N_2O, NO, O_2 and SO_2 or SF_6) is introduced into the ionization chamber. An electron beam, which enters the ionization chamber, is generated by thermionic emission from a heated filament. When ionization occurs, the ions are accelerated through a flight tube between the poles of an electromagnet, where they are separated according to their mass-to-charge ratio (m/z). In the magnetic field the lighter ions follow a path with a smaller radius than the heavier ions. Finally the ions are collected by collectors (Faraday cups) (Benson, Lennard, Maynard, & Roux, 2006; Rao, 2012). There are two common designs of IRMS that mainly differ in the sample introduction method. For both of these IRSM designs the samples, either in solid, liquid or gaseous form, need to be first converted into pure gases. The two most common designs of IRMS are Dual Inlet IRMS (DI-IRMS) and Continuous Flow IRMS (CF-IRMS). Under ambient conditions gases would naturally move into the ionization chamber by molecular flow and if they were of different masses, fractionation would occur. To avoid this problem the gas is either temporarily stored in a variable volume bellows for dual DI-IRMS, or placed within a continuous flow of an inert carrier gas (He) for CF-IRMS.

DI-IRMS. DI-IRMS is the oldest and still considered the most precise method for measuring isotope ratios of light elements. The drawback is that it requires larger sample sizes and greater sample preparation time, more skilled operator and is thus generally more expensive. With DI-IRMS the isotope ratios from pure gases are determined by alternately introducing sample gas and a reference gas into IRMS. Both gases enter the spectrometer under nearly identical conditions. This allows high precision isotope ratio measurements. 5 to 10 alternate measurements of sample and reference gas isotope ratio measurements are typically made for one sample (Carter & Barwick, 2011).

Measurements are typically performed on samples of pure gas, which has to be prepared “offline”. Several clean-up processes and reactions may be performed to convert a sample (solid, liquid, gas mixture or dissolved gases) into a pure gas. These procedures are usually very time consuming. However some of the common preparation methods have been adapted for automated DI-IRMS e.g. oxygen isotope ratio measurements of waters by CO_2 equilibration, C and O isotope ratio measurements of carbonates and carbon and oxygen isotope ratio measurements of atmospheric CO_2 (Carter & Barwick, 2011).

CF-IRMS. CF-IRMS systems employ an elemental analyzer (EA) where two types of EA are available. In the first type simply known as EA-IRMS, the sample undergoes combustion (900-1050 °C) in an oxygen atmosphere and is hence useful for the analysis of carbon and nitrogen. The reactor typically consists of a two-reactor system, where a “combustion” reactor is followed by the “reduction” reactor. In the combustion reactor the CO_2, NO_x and H_2O gases are produced and in the reduction reactor the excess oxygen is removed and NO_x is reduced to N_2. The reactors are followed by a water separation device (water trap containing magnesium perchlorate) and by packed GC column to separate the evolved gases. When only nitrogen isotope ratios are to be determined the CO_2 is removed from the gas stream using a chemical trap containing soda lime. In the

second system, the sample undergoes a high temperature thermal conversion with pyrolysis and is therefore known as high-temperature pyrolysis-IRMS (HTP-IRMS). The thermal conversion happens at temperatures between 1350 and 1450 °C, where both organic and inorganic compound are converted to H_2, N_2 and CO gases. The evolved gases are separated with an isothermal packed GC before they are introduced into IRMS.

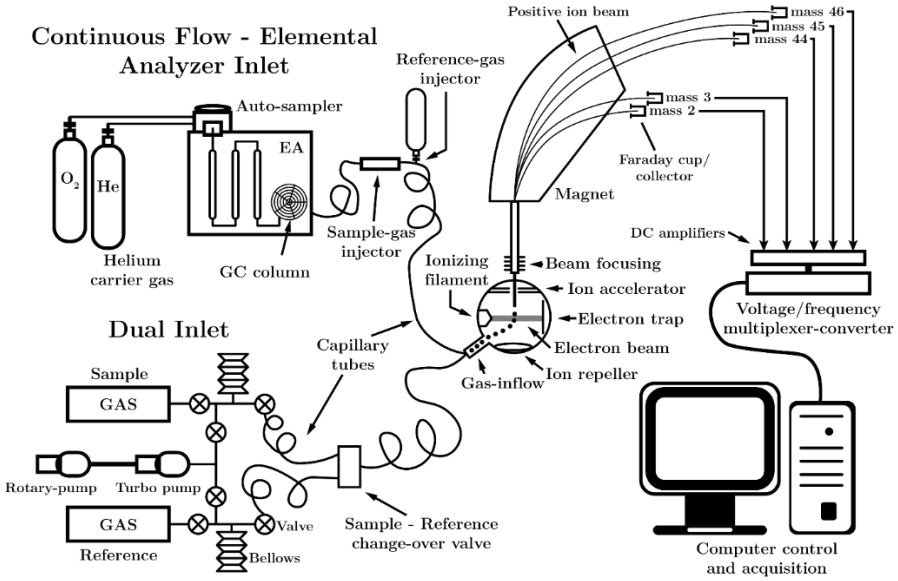


Figure 1.10: A diagram of the continuous flow-elemental analyzer inlet (top left) and dual inlet (bottom left) that interface to the isotope ratio mass spectrometer (IRMS) (Figure adapted after Dawson & Brooks (2001)).

1.3.5.2 Optical techniques of stable isotope analysis

Although these techniques have a generally lower precision than IRMS, the optical isotope measurements systems can have advantages over the IRMS systems in the case where a high frequency of the measurements is required and, due to their mobility, where in-situ measurements are required. Furthermore these systems have a very simple sampling methodology, since the special pre-treatment of the sample is generally not required. Besides that the overall cost of the instrument and of the sample measurement is lower than for the IRMS methods. Those methods continue to develop and therefore also the precision of these methods is expected to improve over time. Even nowadays some of the techniques have a precision comparable to the IRMS. The basic principle of the optical technologies consists of the detection of radiation absorbed and emitted by the target gas species. The two most popular commercially available optical techniques are (1) the tunable diode laser absorption spectroscopy (TDLAS) and (2) Fourier-transform infrared spectroscopy (FTIR).

TLDAS. All TLDAS systems use a tunable laser and an absorption spectrometer to measure the absorption spectrum. This technique is based on detecting the molecular absorption of radiation that is tuned into the rotational-vibrational frequency of the molecule of interest (Griffis, 2013). Unique rotational-vibrational frequencies, which are specific for each isotopologue, can be measured independently under the condition that there is minimal interference from other molecules. The measurement is based on the concentration measurement of each isotopologue (not ratios as with IRMS) and of the

major challenge for these techniques is the need to measure the major and minor isotopologues near-simultaneously.

Different laser types have been used for these systems. The most widely used were/are: the Lead–salt tunable diode laser systems, Cavity ring-down spectroscopy (CRDS), Off-axis integrated cavity output spectroscopy (OA-ICOS), and Mid-infrared quantum cascade lasers (QCL).

The Lead–salt tunable diode laser systems were one of the first systems for in-situ isotope measurements. These systems are not produced any more. One of the main drawbacks of these systems was the need of cryogens for lasers. For some species such as water vapor also the detectors need to be cooled using liquid nitrogen. Furthermore, these systems were very sensitive to temperature fluctuations.

The CRDS systems use a continuous wave laser and the rate of change in the absorbed radiation of laser that is temporarily "trapped" within a highly reflective sample cell (optical cavity) is measured. Basic procedure here is that near-IR laser is turned for the time until the laser emission inside the sample cell builds up to a critical threshold detected by a photo detector. When the laser is turned off, the decay time required for light to escape the cell is measured. This decay is exponential and related to the fact that the mirrored sample cell does not have a perfect reflectivity. If the target gas is present in the sampling cell, the decay rate increases due to the gas absorption of the light (Griffis, 2013). The higher the concentration of the target gas in the sampling cell, the more rapid the decay time ("ring-down").

The OA-ICOS is a similar technique as CRDS with this difference that here the laser beam travels off the main sample cell axis (see Figure 1.11). This helps prevent the so-called "cavity resonance" (light interfering with itself).

QCL systems are somehow more expensive TDLAS systems that are becoming more affordable in the last years. The highest advantage over other systems is that they have a stronger output and can be operated at near-room temperature, therefore the need for cryogens can be avoided (Griffis, 2013).

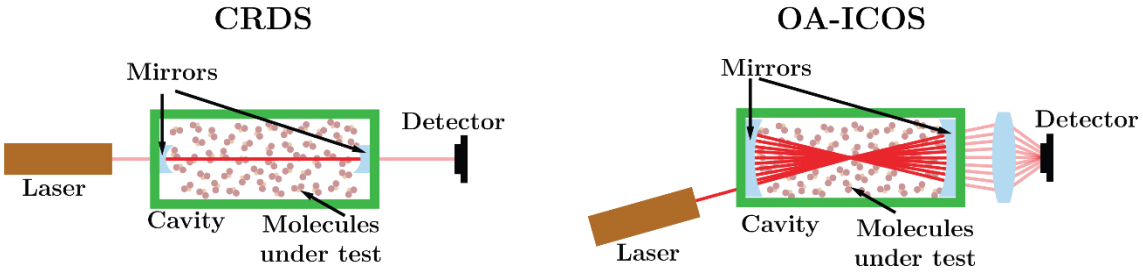


Figure 1.11: A simplified diagram of the instruments used for Cavity ring-down spectroscopy (CRDS) on the left and for the Off-axis integrated cavity output spectroscopy (OA-ICOS) on the right. (Figure adapted from LGR (2013)).

FITR. FITR systems are optical systems that use broadband blackbody as a source. Here, stronger molecular absorption in the mid-infrared wavebands can be achieved. These instruments measure a much wider spectral range, but with lower resolution. The major advantage of these instruments is the possibility of simultaneous measurement of many species (Griffis, 2013).

Chapter 2

Aims and Hypothesis

More than 40% of the Slovenian territory lies on carbonate rocks (limestone and dolomite). Although it is often claimed that our karst is one of the most thoroughly investigated worldwide, there is no information available about the overall C balance in the karstic areas: we do not know whether our karst is a source or a sink for atmospheric CO_2. Soil respiration and soil atmosphere have recently been thoroughly investigated in karstic forest areas and grasslands (Čater & Ogrinc, 2011; Plestenjak et al., 2012). It was found that a considerable part of the soil CO_2 derives from carbonate weathering, where the contribution of geogenic CO_2 depends upon vegetation, soil type and temperature. The influence of carbonate bedrock processes was, however, not included in these studies. This thesis will contribute to filling the gap in the knowledge of the potential of temporal storage of CO_2 within the karstic aquifer in a humid forested karstic area underlain by a cave system. With a detailed study of the in-aquifer and in-cave processes in the carbonate system, where biogenic (soil organic matter) and geogenic (bedrock dissolution) C sources will be separated, we will be able to identify the contribution of biotic and abiotic CO_2 to the net CO_2 fluxes and exchange with the atmosphere in the forested karstic areas.

The main objective of the proposed thesis is to test if it is possible to detect the influence of cave ventilation to soil CO_2 fluxes and to understand the biogeochemical processes, which govern the soil CO_2 fluxes above the caves. Furthermore, we want to better understand the carbon dynamics in the soil-cave system. Although a great number of studies were performed in karst areas, there are still a lot of gaps and assumptions that could be tested for our particular site. One of the important purposes of this work is also to better study the ventilation and dripwater characteristics and parameters influencing them in the cave system.

Thus the specific objectives of the proposed dissertation are as follows:

- to provide improved methodology and tools to estimate the soil-atmosphere carbon exchange in karst landscapes;
- to explain the contributions of geochemical and biological processes in carbon cycling, their interdependencies and underlying mechanisms that govern the overall carbon fluxes in the karst area;
- to investigate the CO_2 sources in soils and cave atmosphere using carbon isotopes;
- to detect the contributions of cave ventilation to soil CO_2 fluxes in karst area; and to determine the transport pathways of carbon from the surface atmosphere (air, precipitation) through the soil to the cave – and back to the atmosphere.

Within the proposed thesis the following hypotheses will be tested:

1. cave ventilation is a significant source of soil CO_2 in karst region;
2. soil CO_2 is the main source of cave air CO_2 transported by diffusion or flowing down from the soil;
3. the process of cave ventilation forces degassing of CO_2 from the dripwater, prior to any calcite precipitation, causing kinetic isotope fractionation.

Chapter 3

Publications

3.1 Scientific Paper: "Using ^{222}Rn and carbon isotopes (^{12}C, ^{13}C and ^{14}C) to determine CO_2 sources in forest soils developed on contrasting geology in Slovenia"



In this chapter the paper entitled "Using ^{222}Rn and carbon isotopes (^{12}C, ^{13}C and ^{14}C) to determine CO_2 sources in forest soils developed on contrasting geology in Slovenia" by Bor Krajnc, Ryoko Fujiyoshi, Janja Vaupotič, Hikaru Amano, Yousuke Sakuta, Asta Gregorič, and Nives Ogrinc is presented. The paper was published in Environmental Earth Sciences, 2016 and describes the first research conducted during my PhD.

In the presented study, carbon isotopes and ^{222}Rn were used to distinguish between different sources of CO_2 in forest soils with a different bedrock geology at seven locations across Slovenia. Carbon isotopes at their natural abundance level were used to distinguish between three possible sources (1) soil organic matter and root respiration, (2) the atmosphere and (3) carbonate dissolution/precipitation processes (in the presence of carbonate bedrock). Additionally the ^{222}Rn concentration in soil gas was measured to reveal if the origin of CO_2 (which is one of the carrier gases for ^{222}Rn) comes from the deeper part of the earth crust, ventilation of CO_2 from subterranean voids (pores, fissures or cavities) or comes together with CO_2 from shallow biological sources.

The investigation based on measured isotopic data revealed that there was no statistically significant difference between soil CO_2 in carbonate and non-carbonate soils since at all sites the CO_2 was "young". Although δ^{13}C values of gas above carbonate bedrock were higher and therefore suggesting the influence of CO_2 derived from carbonates, the addition of Δ^{14}C data indicated that soil CO_2 was young i.e. originating from root respiration and decomposition of relatively young organic matter. This data also suggested that there was a substantial influence of atmospheric air at the sampling sites on carbonate bedrock. A possible way of atmospheric air coming to those sampling sites is either from the atmosphere above the soil or from below; from fissures, cracks or subterranean cavities (which can be essentially a mixture of atmospheric and soil respiration derived CO_2). Although the first possibility seems more reasonable, the high ^{222}Rn concentrations suggest that the ventilation of subterranean voids had a significant influence. Carbonate bedrocks are generally known to hold low concentrations of ^{226}Ra, which is the immediate precursor of ^{222}Rn. Therefore this indicates that ^{222}Rn (and

therefore its carrier gas CO_2) originates from poorly ventilated fractures and/or subterranean caves. On soils developed on non-carbonate bedrock also the contribution of organic matter degradation to root respiration was estimated (since carbonate endmember is not present). Root respiration of the newly produced photo assimilates accounted for at least 70 % of total soil respiration.

The presented study revealed the presence additional mechanisms that add to the complexity of soil-air CO_2 system and the necessity of including several tracers for investigation of carbon cycle pathways in soils.

In this paper, the candidate developed the research question, , conducted sampling in the field and analyzed the samples. He together with Ryoko Fujiyoshi and Janja Vaupotič selected the sampling sites around Slovenia, installed the sampling tubes and preformed the sampling. The candidate sampled the soil air for isotope analysis. He conducted $\delta^{13}C$ measurements using isotope ratio mass spectrometry, while ^{14}C analysis was made with Tandetron Accelerator Mass Spectrometer (AMS) at the Japan Atomic Energy Agency in Mutsu, Japan. Further, he collected the samples for radon measurements using scintillation cells and later in the laboratory analyzed them by alpha counter. He performed data analysis using different statistical approaches in R statistical environment (R Core Team, 2014). The candidate interpreted the data and wrote the manuscript.

Environ Earth Sci (2016) 75:1068
DOI 10.1007/s12665-016-5866-0

ORIGINAL ARTICLE

Using ^{222}Rn and carbon isotopes (^{12}C, ^{13}C and ^{14}C) to determine CO_2 sources in forest soils developed on contrasting geology in Slovenia

Bor Krajnc[1] · Ryoko Fujiyoshi[2] · Janja Vaupotič[1,3] · Hikaru Amano[4] · Yousuke Sakuta[2] · Asta Gregorič[5] · Nives Ogrinc[1,3]

Received: 29 April 2015 / Accepted: 2 July 2016 / Published online: 9 July 2016
© Springer-Verlag Berlin Heidelberg 2016

Abstract Global carbon estimates have identified abiotic CO_2 as a potentially significant source of atmospheric CO_2, albeit little is known about its origin. The aim of this study was to identify the origin of soil CO_2 using carbon isotopes and ^{222}Rn data. The study involved collecting data from seven Slovenian forest soils developed over bedrock with contrasting geology where different origin of soil CO_2 was expected; two sampling sites were located on soils formed above carbonate bedrock, one above metamorphic bedrock and the remainder above clastic sedimentary rocks. Analysis of soil gas including the levels of CO_2, carbon isotope measurements (^{12}C, ^{13}C and ^{14}C) and ^{222}Rn activity was recorded at a soil depth of 80 cm. Isotopic analysis revealed that the CO_2 was young and there was no difference in the age of soil CO_2 above either carbonate or non-carbonate bedrock. The data also suggest that the ^{13}C-enrichment in soil CO_2, above carbonate bedrock was a consequence of the mixing of soil CO_2 with atmospheric CO_2 and/or the ventilation of subterranean CO_2 from pores, fissures and cavities. The latter effect was supported by the high ^{222}Rn concentrations observed at these sites. Based on the $\delta^{13}C_{CO_2}$ data, photosynthesis prevailed over microbial respiration accounting for the majority (>70 %) of total soil CO_2 over non-carbonate bedrock—at least at the time of sampling. Overall, results from this study could represent useful information for global carbon cycle models used to predict the impacts of climate changes.

Keywords Soil gas · CO_2 · Carbon isotopes · ^{222}Rn · Geology · Slovenia

✉ Nives Ogrinc
nives.ogrinc@ijs.si

[1] Jožef Stefan International Postgraduate School, Jamova 39, 1000 Ljubljana, Slovenia

[2] Faculty of Engineering, Hokkaido University, Sapporo 060-8628, Japan

[3] Department of Environmental Sciences, Jožef Stefan Institute, Jamova 39, 1000 Ljubljana, Slovenia

[4] Japan Chemical Analysis Center, Inage-ku, Chiba 263-0002, Japan

[5] Center for Atmospheric Research, University of Nova Gorica, Vipavska 13, 5000 Nova Gorica, Slovenia

Introduction

Global environmental change has been identified as one of the most urgent issues in Earth science research (Ciais et al. 2013). A considerable amount of research effort has gone into understanding the role of the terrestrial reservoir in modulating carbon storage, and how the rapid cycling of carbon at the Earth's surface over the next few 100 years will affect the Earth's surface environment (Trumbore 2006; Bond-Lamberty and Thomson 2010). The CO_2 efflux originates from different sources including plant-root, heterotrophic and mycorrhizal respiration (Kuzyakov 2006). Root-associated and mycorrhizal respiration (autotrophic) are strongly linked to photosynthetic activity (Högberg et al. 2006; Kuzyakov and Gavrichkova 2010), while heterotrophic respiration originates from the decomposition of soil organic matter (SOM). This respiration depends on the amount of SOM and on the soil organic carbon (SOC) pool, SOM nutrient value, degree of stabilization and microbial activity (e.g., Davidson and Janssens 2006; Reichstein and Beer 2008). Recent studies of carbonate ecosystems reveal that abiotic exchange processes can contribute temporally to net CO_2 exchange

(Stone 2008; Wohlfahrt et al. 2008; Xie et al. 2008). The main abiotic processes involved in net ecosystem CO_2 exchange include geochemical weathering processes such as the dissolution and precipitation of carbonates. Silicate weathering is generally accepted as the main long-term CO_2 sink operating on a geological timescale, whereas carbonates dissolve and precipitate at a much higher rate and represent a short-term contribution to the overall net ecosystem CO_2 balance. At present, there exists no agreement among the scientific community as to whether regional carbonate dissolution is actually a sink or a source of CO_2. This is because on an annual scale, neither dissolution nor precipitation prevails. Equally, their contributions cannot explain the large magnitude of daytime CO_2 emissions from karst regions (Serrano-Ortiz et al. 2009). Serrano-Ortiz et al. (2010) suggest that the ventilation of subterranean CO_2 from the pores, fissures and cavities present in the karst regions influences the amount of soil CO_2 and subsequent CO_2 efflux at the ecosystem level. As a first approximation, their estimates indicate that this source accounts for more than half of the total CO_2 content of the atmosphere (Serrano-Ortiz et al. 2010). Partitioning of the total CO_2 efflux, therefore, into the contributions derived from individual sources (autotrophic vs. heterotrophic; biotic vs. abiotic) is highly important, especially to predict the net response of soil carbon stores to climate change.

To estimate the relevance and contribution of each of these processes occurring in carbonate and karst systems, methodologies that can discriminate between biological and abiotic-derived CO_2 fluxes are needed. In this context, an additional natural tracer such as radioactive gas radon (^{222}Rn), which originates in the Earth's crust by radioactive decay of radium (^{226}Ra), can be used. Only a portion of the radon atoms, called the emanation fraction, f_{em} (or emanation factor or emanation power), can escape from mineral grains of soils and bedrock into the void space, from where it migrates to the surface. The radon, which is dissolved either in water or in a carrier gas (e.g., CO_2, CH_4 and N_2), rises toward the surface through cracks or faults by diffusion over short distances and by advection over longer distances. This gaseous mixture, formed of a carrier gas and a rare gas (e.g., He, Rn), is referred to as a "geogas" (Etiope and Martinelli 2002). Radon, which is a noble gas, passes through the medium and does not react chemically with it; however, it does undergo alpha decay with a half-life of 3.82 days. If CO_2 is the carrier gas, then there exists a significant correlation between the levels of both gases in the soil. Recent studies of radon emanation from soil in Slovenia (Kardos et al. 2015) and the distribution of radionuclides in soils (Kovács et al. 2013) reveal soil gas radon concentrations to be highly heterogeneous and emphasize the important contribution of long-range radon transport.

The measurements of the stable carbon isotopes (^{13}C and ^{12}C) and radiocarbon (^{14}C) can discern the different processes that occur during carbon cycling in the soil. From the natural abundance levels of three isotopes, it is possible to distinguish between the following sources of soil CO_2: (1) soil organic matter and root respiration, (2) the atmosphere and (3) carbonate dissolution/precipitation processes (in the presence of carbonate bedrock). The isotope composition of SOC and root-derived CO_2 is also dependent on the types of photosynthetic vegetation (Kuzyakov 2006). For example, in temperate forest ecosystems like in Slovenia (mid-eastern Europe), mainly C3 type plants predominate with $\delta^{13}C$[1] values of about −27 ‰ (−35 ‰ ≤ $\delta^{13}C$ ≤ −20 ‰). The SOC developed under C3 vegetation has a similar $\delta^{13}C$ value, since the isotope fractionation from decomposition of plant material is negligible, i.e., typically <2 ‰ (Kuzyakov 2006). Root-derived CO_2 has nearly the same $\delta^{13}C$ values as the flora (Cerling et al. 1991). Atmospheric CO_2 has $\delta^{13}C$ values around −9 ‰, but can be lower in polluted areas due to the presence of ^{13}C-depleted CO_2 originating from the burning of fossil fuels (Allison et al. 2003). Atmospheric CO_2 as well as respiratory sources will contain modern ^{14}C from nuclear testing, and since root and most microbial respiration is fueled by recently synthesized organic matter, the $\Delta^{14}C$ of respiratory CO_2 will be close to that of the atmosphere (ca. +125 ‰) representing the young, ^{14}C-active C. Another source is slowly decomposing organic matter, which is more depleted in ^{14}C (Dörr and Münnich 1986) and CO_2 originating from carbonate bedrock, which is composed of ancient, ^{14}C-dead C and has a $\Delta^{14}C$ of −1000 ‰ (Bond-Lamberty and Thomson 2010). The range of $\delta^{13}C$ values of marine carbonate bedrock is narrow, i.e., 0–4 ‰ (Bond-Lamberty and Thomson 2010). The respective contributions of these different sources can be obtained using different mixing models.

The aim of this work was to distinguish between different sources of CO_2 in forest soils with different bedrock geology (carbonates vs. non-carbonate bedrock) using carbon isotopes and ^{222}Rn measurements. It is hypothesized that at carbonate sites, inorganic sources contribute significantly to overall CO_2, since CO_2 acts as a carrier gas for ^{222}Rn transport from the deeper parts of the Earth's crust to the surface. A strong correlation between radon and CO_2 is often observed over faults and areas of high hydrothermal activity (Etiope and Lombardi 1995), and the existence of a similar strong correlation would reveal a common source of radon and an inorganic source of CO_2 as a carrier gas. On the other hand, the fraction of non-

[1] $\delta^{13}C$ (‰) = $[(^{13}C/^{12}C)_{sample}/(^{13}C/^{12}C)_{std}-1]$ *1000, where $(^{13}C/^{12}C)_{sample}$ and $(^{13}C/^{12}C)_{std}$ are abundance ratios of the sample and reference standard (V-PDB), respectively.

correlated CO_2 and ^{222}Rn originates from shallow biological sources of CO_2 and the local source of ^{222}Rn due to emanation form soil mineral grains.

Materials and methods

Study area

Geological setting

Slovenia is situated at the junction between the Alpine and the Dinaridic regions, which include the Southern Alps, Eastern Alps, the Pannonian basin, Dinarides and the Adriatic–Apulia foreland (Placer 2008; Fig. 1). The western and southwestern part of Slovenia is characterized by NW–SE trending dextral strike-slip faults [sampling sites Idrija (ID), Žirovski vrh (ZV) and Rakitna (RA); Fig. 1], accompanied by wide fault deformation zones, such as the Idrija fault zone. In the northeastern part of Slovenia is tectonically more stable the Pannonian basin, which is characterized by individual depressions originating from the early Palaeogene and Neogene era. This region corresponds to the subsequent sampling sites Gorišnica (GO), Ptujska Gora (PG) and Otovci (OT) (Fig. 1). These sampling sites are filled with sediments from the Paratethys ocean deposited on subsided continuations of the Eastern and Southern Alps and Dinarides (Placer 2008). The final sampling site Pohorje (PO) is located in the northeastern part of Slovenia on the outskirts of the Pannonian basin.

Description of sampling sites and sampling procedures

Sampling took place at seven forest research plots each differing in terms of geology, soil type and vegetation (Table 1). Each sampling site was divided according to bedrock soil formation as follows: ID and RA sampling sites were located on carbonate bedrock soils, PO was located on metamorphic bedrock and ZV, GO, PG and OT sites were all located on soils formed on clastic sedimentary rocks (Fig. 1). Soil depth varied from 48 to 245 cm with the shallowest soils observed at ID and the deepest at GO (Table 2), although at ID, deeper soil pockets also exist (>80 cm). The pH values of the carbonaceous soils at ID (pH 6.85) and RA (pH 6.99) were higher than for clayey and other soil types (pH 3–4) at PO, ZV, GO, PG and OT. This reflects the carbonate equilibrium in the soil solution systems of carbonaceous soils (Fujiyoshi et al. 2012; Ogrinc et al. 2016). At all of the sampling sites, the amount of SOC decreases with soil depth, and at a depth of 80 cm, the SOC content was from 4.5 to 14.7 gC kg^{-1} of soil, with the lowest value observed at ZV and the highest at RA (Fujiyoshi et al. 2012). At each site, the level of soil CO_2 was measured in situ, while gas samples were transferred to the laboratory for radon and isotopic composition analysis. Soil and carbonate rock samples were also collected for analysis.

Sampling was performed in September 2011, during late summer conditions. At each site, samples were collected within a grid pattern comprising of nine points (two squares of four points, 1 m and 4 m from the central point)

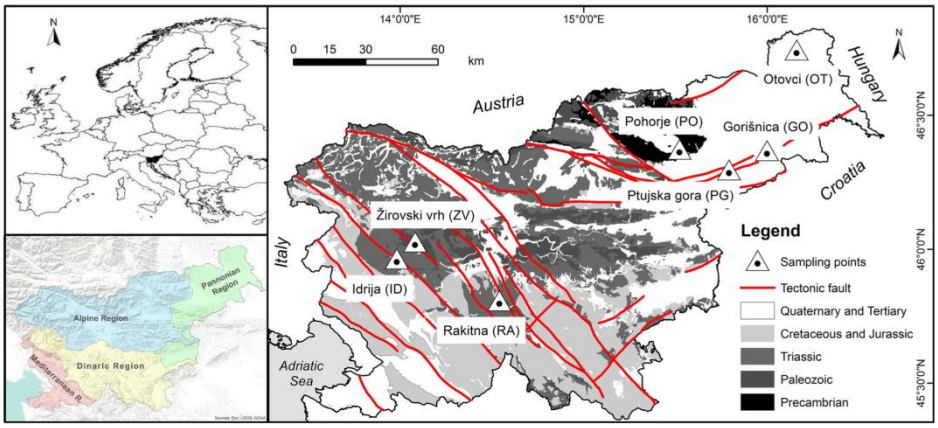


Fig. 1 Landscape and geological map of Slovenia with sampling sites

Table 1 Description of investigated locations with mean annual values of precipitation and temperature, soil type, geology and forest vegetation

Location name (abbreviation)	Location (WGS84)	Mean annual precipitation (mm)	Mean annual temperature (°C)	Soil type	Geology	Forest vegetation
Rakitna (RA)	45°54′15.09″N 14°26′42.73″E	1500	8.5	Chromic cambisol and rendzina	Triassic dolomite	European beech (*Fagus sylvatica* L.) European spruce (*Picea abies* (L.) H.Karst.
Idrija (ID)	45°59′46.51″N 13°59′23.82″E	2300	6.9	Chromic cambisol and rendzina	Anisian dolomite, dolomite conglomerate and limestone	European beech (*Fagus sylvatica* L.) European ash (*Fraxinus excelsior* L.) Sycamore maple (*Acer pseudoplatanus* L.)
Žirovski vrh (ZV)	46°4′59.88″N 14°4′59.88″E	1500	6.9	Dystric cambisol	Permian Gröden formation (siliciclastic, predominant red-colored sandstone)	Sessile oak (*Quercus petraea* (Mattuschka) Liebl.)
Pohorje (PO)	46°25′52.02″N 15°30′18.42″E	1300	9.4	Dystric cambisol	Pohorje metamorphic assemblage (gneiss and schist)	Scots pine (*Pinus sylvestris* L.)
Gorišnica (GO)	46°22′9.62″N 15°59′50.48″E	1100	10.4	Glaysol, fluvisol	Quaternary fluvial deposits (gravel, sand, silt, clay)	European beech (*Fagus sylvatica* L.) Sessile oak (*Quercus petraea* (Mattuschka) Liebl.
Ptujska Gora (PG)	46°21′9.2″N 15°46′17.3″E	1335	11.1	Dystric cambisol	Quaternary (Pliocene, Pleistocene) – clay, clayey silt, quartz gravel and silicate rocks)	European beech (*Fagus sylvatica* L.)
Otovci (OT)	46°47′50.73″N 16°8′40.96″E	1094	10.7	Eutric cambisol	Middle Pliocene – gravel, sand and sandy clay	Scots pine (*Pinus sylvestris* L.) European beech (*Fagus sylvatica* L.)

Table 2 Sampling soil depth and horizon [classification after Urbančič et al. (2005)], lithology, texture, stable isotope composition of soil organic carbon ($\delta^{13}C_{SOC}$) and radon emanation fraction (f_{em}) (Kardos et al. 2015) at selected sites

Location name	Soil depth (cm)	Soil horizon	Lithology	Texture	$\delta^{13}C_{SOC}$ (‰)	f_{em}
Rakitna (RA)	94	$C(B)_{rz}$	C	Clay loam	−25.0	0.186
Idrija (ID)	48	$C(B)_{rz}$	C	Loam	−27.5	0.186
Žirovski vrh (ZV)	152	$(B)_v$	B2	Clay loam	−26.0	0.056
Pohorje (PO)	80	$(B)_v$	D	Silty clay loam	−25.0	0.029
Gorišnica (GO)	245	Bg	B1	Silty clay	−25.8	0.089
Ptujska Gora (PG)	100	$(B)_v$	B1	Silty clay loam	−26.3	0.089
Otovci (OT)	113	$(B)_v$	B2	clay loam	−27.9	0.056

Bedrock lithology was assigned to different classes according to classification based on the study published by Kovács et al. (2013)

B1 clastic sediments containing clay, *B2* coarse clastic sediments, *C* carbonate rocks and *D* metamorphic rocks

in order to obtain a statistically significant number of measurements. All samples were collected from a depth of 80 cm, also at ID, where the samples were taken from deep soil pockets (Table 2). The characteristics of each sampling sites/points, e.g., variations in moisture content in soils on non-carbonate rocks, shallow soil layers and the presence

of stones on carbonate rocks, meant that sampling conditions varied significantly within each grid, but with minimal effect on the overall results presented. Soil gas samples were obtained from a limited number of sampling points: three at RA, two at ID and five from ZV, PO, GO, PG and OT. All gas samples were collected using a Neznal's probe (Neznal and Šmarda 1991), which consists of a metal tube (length 1.10 m, inner diameter 12 mm) with a removable conical metal tip. Radon sampling was performed using the same probe with an additional gas pump connected to an alpha scintillation cell (Lucas type). Soil gas was flushed through either a 0.70 dm^3 (Vaupotič et al. 1992) or 0.31 dm^3 (Quindós-Poncela et al. 2003) scintillation cell at a flow rate of 1 dm^3 min^{-1}, for 1.5 to 3 min, which is the time required to exchange the air in the cell with the soil gas.

Samples for determining CO_2 concentration and isotope measurements were taken immediately after the radon activity measurements. To avoid possible contamination with gas from the sampler tube, the system was purged twice with the soil gas. Samples collected for stable isotope analysis were transferred immediately into pre-evacuated 12-ml glass serum vials. The septum penetration needles allow direct delivery of the gas sample into the pre-evacuated vial thereby minimizing potential contamination with atmospheric air (Torn et al. 2003).

The $\Delta^{14}C$ measurements were performed only at RA, ID, ZV, OT and GO. For these measurements, soil CO_2 was pumped out of the Neznal's probe through a Dreschel bottle containing a 0.1 M NaOH aqueous solution (100 cm^3), while taking precautions not to contaminate the samples with atmospheric air. The time needed for air sampling was dependent on the amount of CO_2 in the soil gas. The formed sodium carbonate was then transferred into a beaker, and the pH adjusted to 10.5 using a 1 M NH_4Cl solution. The $CaCO_3$ was precipitated after the addition of 1 M $CaCl_2$. The solution was then filtered, and the $CaCO_3$ dried in an oven at 110 °C. The weight of the carbonate precipitate was measured and retained for carbon isotope analysis.

Analytical methods

Radon activity measurements

The radon activity in the scintillation cells was determined after three hours (when the secular equilibrium between radon and its products was achieved) using a PRM-145 alpha counter (AMES, Slovenia). The alpha scintillation cells were calibrated in the KR-600 Radon Chamber at the Henryk Niewodniczański Institute of Nuclear Physics, PAN, Kraków, Poland (Kozak et al. 2009). Cell efficiencies were around 2 s^{-1} Bq^{-1}, which gives a lower limit of detection of 20–50 Bq m^{-3} for a 10 min counting time at a 1–2 min^{-1} background.

Soil CO_2 concentration measurement

Carbon dioxide in the soil gas was measured using a non-dispersive infrared (IR) absorption sensor (TESTO-453, TESTO, Germany). The time interval and resolution of each measurement were 10 min and 1 μmol mol^{-1}, respectively. The same probe was also used to measure the relative humidity and the temperature of the soil gas. Probe calibration was performed by TESTO, Germany.

Stable carbon isotope measurements

The stable isotope composition of CO_2 ($\delta^{13}C_{CO_2}$) was determined according to the methods of Knohl et al. (2004) and Spötl (2004). Measurements were made using a Europa Scientific 20–20 isotope-ratio mass spectrometer (IRMS) coupled to an ANCA-TG preparation module.

For $\delta^{13}C_{SOC}$ measurements, soil samples were first sieved (2 mm) and 1 M HCl was added to remove any carbonate. The $\delta^{13}C$ values were then determined using a Europa Scientific 20–20 IRMS coupled with an ANCA-SL preparation module. The reference materials IAEA-CH-7 (−32.15 ± 0.05 ‰) and IAEA-CH-6 (−10.45 ± 0.03 ‰) were used for calibration.

To determine the isotope composition of the carbonate rock ($\delta^{13}C_{Ca}$), powdered rock samples (2 mg) were placed into sealed ampoules and allowed to react with anhydrous H_3PO_4 for 24 h at 25 °C under He. The $\delta^{13}C$ in the released CO_2 was then measured using IRMS. Reference materials NBS 18 and NBS 19 with $\delta^{13}C$ values of −5.014 ± 0.035 and 1.95 ‰, respectively, were used for calibration. Measurement precision for $\delta^{13}C_{CO_2}$, $\delta^{13}C_{SOC}$ and $\delta^{13}C_{Ca}$ was ± 0.2 ‰.

Radiocarbon measurements

The $\Delta^{14}C$ measurements were taken at the Japan Atomic Energy Agency (JAEA, Mutsu, Japan) using a Tandetron Accelerator Mass Spectrometer (AMS) (Model 4130, High Voltage Engineering Europe). The $CaCO_3$ samples (3–100 mg C) were combusted under vacuum overnight at 900 °C in the presence of an Ag plate and CuO powder. The released CO_2 was dehydrated using a mixture of ethanol and dry ice and purified with liquid nitrogen. Samples of CO_2 were then reduced to graphite at 650 °C with H_2 gas using iron powder (>99.000 %), which was packed in a small aluminum "target" for AMS measurement. A reference ^{14}C oxalic acid (NIST-SRM-4990C) was used to evaluate the carbon isotope data. All the reported

$\Delta^{14}C$ values calculated from the $^{14}C/^{12}C$ ratios were corrected for fractionation using the $\delta^{13}C$ value of each sample. The precision of the $\Delta^{14}C$ values obtained was typically below ±1.0 (0.3–1.0) ‰ at 1 σ of the counting statistics.

Statistical analysis

The collected data (90 samplings) were statistically analyzed, and basic statistics were computed (mean, standard deviation, minimum and maximum values). A Duncan's multiple range test was used to determine any significant differences of the variables between the sampling sites, while multiple linear regressions using the least squares were used to obtain the relationship between CO_2 concentrations, $\delta^{13}C_{CO_2}$ values and ^{222}Rn. A 95 % confidence interval was chosen for the confidence level.

All statistical analyses were performed using the STATISTICA software package v.7 (StatSoft Inc., Tulsa, OK, USA).

Results and discussion

The average CO_2 concentration and ^{222}Rn activity at each site are presented in Fig. 2a, b, while Fig. 2c, d shows the $\delta^{13}C_{CO_2}$ and $\Delta^{14}C_{CO2}$ values. The highest average CO_2 concentrations were found at ZV (7383 ± 1895 µmol mol^{-1}) followed by PO (6151 ± 2092 µmol mol^{-1}) and OT (6115 ± 607 µmol mol^{-1}). The lowest average CO_2 concentrations were observed at ID (3530 ± 932 µmol mol^{-1}), PG (3732 ± 756 µmol mol^{-1}) and RA (3967 ± 285 µmol mol^{-1}). The highest mean ^{222}Rn activity was recorded at RA (60.1 ± 13.8 kBq m^{-3}) and the lowest mean values at GO (7.3 ± 2.3 kBq m^{-3}) and PG (8.0 ± 6.0 kBq m^{-3}).

According to a Duncan's multiple range test, the $\delta^{13}C_{CO_2}$ values of the soil gas in soils on carbonate bedrock (Fig. 2c) are significantly higher than in soils formed over non-carbonate bedrock ($\alpha = 0.05$). The $\Delta^{14}C$ measurements were from 97.7 at ID to 105.8 ‰ at OT. The $\delta^{13}C_{SOC}$ values were from −27.9 to −25.0 ‰ (Table 2), while the average value of $\delta^{13}C_{Ca}$ was −1.4 ± 0.5 ‰.

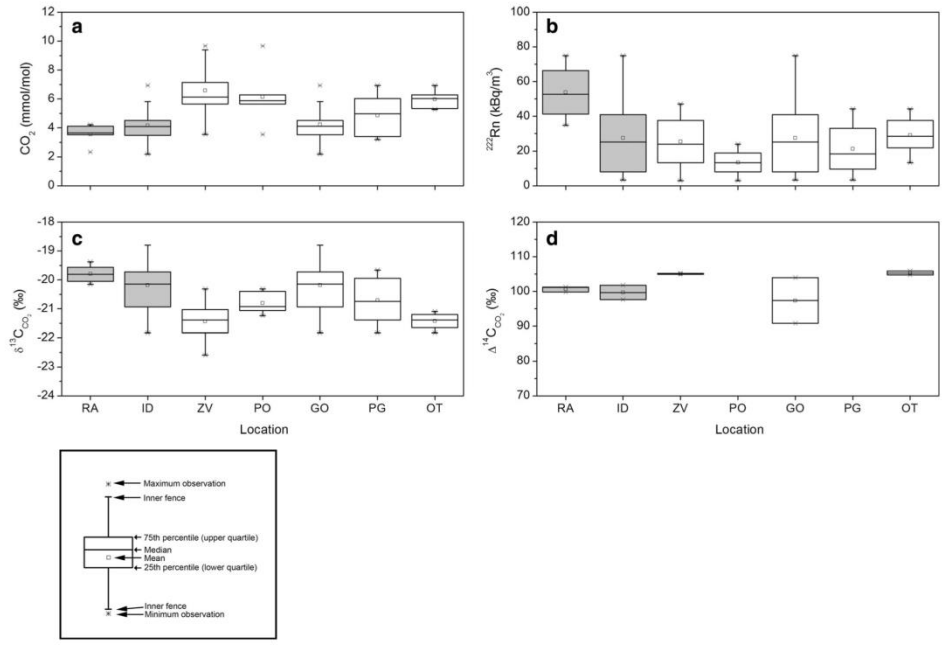


Fig. 2 Box plot of **a** CO_2 concentrations; **b** ^{222}Rn activity; **c** $\delta^{13}C$ values; and **d** $\Delta^{14}C$ values with the mean, maximum and minimum values at selected sites in September 2011. The *box* plots at carbonaceous soils are presented in *gray color*

Correlations between the measured data were obtained using a simple multiple linear regression analysis of CO_2 concentrations, $\delta^{13}C_{CO_2}$ values and ^{222}Rn. The statistical parameters are given in Table 3. The data suggest that at all sites, a significant correlation exists between the CO_2, $\delta^{13}C_{CO_2}$ values and ^{222}Rn values.

The highest radon concentrations were measured at RA and ID, which are both located on soils formed above carbonate bedrock. These high concentrations are consistent with previous radon measurements in soil gas in Slovenia (Vaupotič et al. 2008). Dolomite bedrock is also more prone to mechanical weathering (as compared to limestone, where chemical weathering prevails), which means that dolomite rock is also more susceptible to fracturing than limestone rock. Fractured bedrock allows radon transport from the Earth's crust to the surface and finally to the atmosphere. Limestone bedrock is characterized by underground cavities resulting from chemical weathering. These cavities represent a trap for radon-rich air, causing high radon exhalation at sites where a connection between such cavities and the surface exists. The Žirovski vrh (ZV) sampling site is located on the bedrock of the Permian Gröden formation and comprises red-colored sandstone, characterized locally by uranium enrichment, which was exploited by the former Žirovski vrh uranium mine. The main source of radon at ZV is most likely from the radionuclides present in the bedrock and soil, which is also evident from the modest correlation between CO_2 and ^{222}Rn (R^2 (adj.) = 0.57, $p = 0.087$). The site OT has a similar radon concentration. Here, the bedrock is highly permeable consisting of sandy gravel quaternary material. This permeable bedrock allows a higher advective flux of gasses from the Earth's crust to the surface, resulting in the strongest correlation between CO_2 and ^{222}Rn (R^2 (adj.) = 0.92, $p = 0.007$).

Table 3 Correlations between CO_2 concentrations, $\delta^{13}CO_2$ values and ^{222}Rn (for 90 measured data) at selected sites using a multiple linear regression analysis

Location	$CO_2 = A0 + A1 * \delta^{13}C_{CO_2} + A2 * {}^{222}Rn$				
	$A0$	$A1$	$A2$	R^2 (adj.)	p
RA	0	−174	0.002	0.99	0.0001
ID	0	−216	0.002	0.96	0.0001
ZV	0	−234	0.063	0.95	0.0001
PO	0	−243	0.088	0.87	0.0021
GO	0	−216	0.008	0.95	0.0001
PG	0	−171	0.008	0.99	0.0001
OT	0	−220	0.005	0.99	0.001

A p value < 0.05 shows there is statistically significant correlation

Low radon concentrations occurred at sites PO, GO and PG. Soils formed on metamorphic rocks have a low emanation fraction (Table 2) and is the most likely reason for the low levels of radon in the soil gas at PO. The low permeability of bedrock also hinders convective radon transport. Low permeability is also characteristic of clastic sediments, especially in the presence of fine-grained sediments such as marls or clays. Furthermore, low levels of radionuclides are present in soils from the northeastern part of Slovenia (Kovács et al. 2013), which means that the soil itself contributes little to the overall levels of radon in soil gas.

The $\delta^{13}C_{CO_2}$ values of soil gas in soils formed over carbonate bedrock were statistically higher than in soils formed over non-carbonate bedrock (Fig. 2c). A statistically significant correlation was observed between CO_2 concentrations, ^{222}Rn activity and $\delta^{13}C_{CO_2}$ values ($p < 0.03$) at non-carbonate sites. At carbonate sites, the only correlation was between CO_2 concentrations and $\delta^{13}C_{CO_2}$ values ($p < 0.0001$). The three main sources of soil CO_2 include the decomposition of organic matter, respiration of plant roots and atmospheric CO_2 (Werth and Kuzyakov 2008, 2010). At a depth of 80 cm, the contribution from atmospheric CO_2 is negligible. In addition, the abiotic CO_2 efflux is thought to be of minor importance compared to biotic CO_2 fluxes (Kuzyakov 2006). Despite this, the contribution of abiotic processes such as weathering and storage/ventilation in karst systems can be significant and should be taken into account when making an assessment of the soil CO_2 carbon budget (Emmerich 2003; Serrano-Ortiz et al. 2010; Čater and Ogrinc 2011; Plestenjak et al. 2012). This is especially the case when the external air temperature is lower than the air temperature in the cave. This difference in air density both triggers and drives the ventilation of the cave air. Whether temperature driven ventilation happens during cold or during warm periods depends on both the location and shape of the cave.

The $\delta^{13}C_{CO_2}$ values together with $\Delta^{14}C$ in soil gas provide further information about the sources of soil CO_2. Previous investigations of forest soils, abundant in carbonate minerals, involving simple thermal and chemical treatment indicated that at least two major carbon sources exist: (1) carbonates (dolomite) and (2) soil organic carbon from C3 plants (Fujiyoshi et al. 2012). Figure 3 shows the relationship between $\delta^{13}C_{CO_2}$ and $\Delta^{14}C$ values in soil gas at selected sites. The $\Delta^{14}C$ values of atmospheric air, contemporary C3 plants and weathered carbonates and carbonate rocks are taken from the literature (Liu et al. 2006; Levin et al. 2010), while $\delta^{13}C_{SOC}$ and $\delta^{13}C_{Ca}$ values were determined in this study. The contribution of carbonate-derived C to the total soil CO_2 pool can be quantified as a mixing line between modern ^{14}C and ancient carbonate

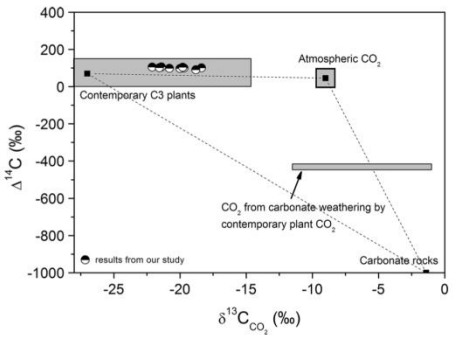


Fig. 3 Schematic diagram of the distribution of $\delta^{13}C_{CO_2}$ and $\Delta^{14}C$ values for different carbon sources with the following isotopic values ($\delta^{13}C$, $\Delta^{14}C$) of individual end-member (**−9**, **49.5**), (−27, **85.1**) and (−1.4, **−1000**) for open air, young organic carbon and deep mineral (carbonate rock) sources, respectively. The *bold values* were derived from the literature (Liu et al. 2006; Levin et al. 2010), while the $\delta^{13}C_{SOC}$ and $\delta^{13}C_{Ca}$ values were obtained within this study

(Fig. 3). The equilibration of soil CO_2 with carbonate minerals via carbonic acid weathering will shift soil CO_2 toward the carbonate end-member.

The results from this study indicate that the CO_2 collected at a depth of 80 cm is young and there is no difference between carbonate and non-carbonate soil CO_2. In contrast in a cool-deciduous stand in Sapporo, Japan, CO_2 from the depth of 100 cm was old, especially in winter, when the ground surface was covered by snow (Fujiyoshi et al. 2009). Similar observation like in the present study was obtained in the study of a semiarid region in the Yatir Forest, northern Negev, Israel, where the main source of soil CO_2 was found to be young and of biogenic origin. The abiotic source of CO_2 was found deeper in the soil profile accounted for 16 to 22 % (Carmi et al. 2013). The data from the present study plot along the mixing line between soil and atmospheric CO_2 (Fig. 3), indicating that carbonate mineral has no influence on soil CO_2 in carbonate soils and the ^{13}C-enrichment in soil CO_2 observed at these sites derives from the atmosphere, even though at a depth of 80 cm atmospheric CO_2 contribution should be of minor importance. The reason is that the soil texture at these sites is heterogeneous comprising of pores and fissures, which allows air to penetrate deeper into the soil. Another potential source is from the ventilation of subterranean CO_2 from the pores, fissures and cavities. The highest radon concentrations at RA and ID provide an indication of a direct contribution of deep CO_2 to the soil CO_2 pool.

The contribution of organic matter degradation to root respiration was estimated based on $\delta^{13}C_{CO_2}$ values, but only at non-carbonate sites. In this calculation, the $\delta^{13}C_{SOC}$ values were used as an end-member for degraded organic matter (Table 2), since heterotrophic respiration is assumed to be a non-fractionating process. The highest $\delta^{13}C$ value of −21 ‰ observed in C3 plants was used as an end-member for photosynthesis, since this value is unknown (Ekblad and Högberg 2001). Data from September 2011 suggest that root respiration of the newly produced photoassimilates accounted for at least 70 % of total soil respiration. This finding is in agreement with the previous investigation, where root respiration was the dominant process influencing soil respiration during the growing season in several forest soils in Slovenia (Čater and Ogrinc 2011). These are, however, only rough estimates, and there is a need for further investigations of root and soil respiration $\delta^{13}C$ to better understand the conditions and the processes affecting carbon fractionation of below ground respiration.

Conclusions

A combination of isotopic, CO_2 and ^{222}Rn measurements provided new insights into the dynamics of the carbon cycle in forest soils in Slovenia. Isotope analysis revealed that CO_2 collected at a depth of 80 cm was consistently young and there was no observable difference between carbonate and non-carbonate soil CO_2 in September 2011. Even in carbonate soils, the carbonate mineral had no influence on soil CO_2. The ^{13}C-enrichment in soil CO_2 observed at these sites was likely a consequence of the mixing of soil CO_2 with atmospheric CO_2, although the highest radon concentrations indicated that the ventilation of subterranean CO_2 from pores, fissures and cavities also occurred. The soil itself contributed little to soil gas radon concentration. Soil respiration was also strongly related to root respiration, contributing >70 % of the total soil CO_2.

This preliminary study indicates that the soil–air ventilation system is too complex to explain the sources of the gaseous components. Nevertheless, the data can represent a useful input to global carbon cycle models where stable isotope composition data are included and indicate that these models should include both biological and non-biological CO_2 production to predict the response of soil CO_2 to climate change.

Acknowledgments This work was partially supported by the Slovenian Research Agency within the program no. P1-0143, the Slovenia-Japan cooperation in science and technology within the bilateral project BI-JP-10-12-002 and by the Japan Atomic Energy Agency (JAEA) for measuring carbon isotopes by AMS (2012A-F02, 2014A-F04). We would like to thank the staff members of the Mutsu AMS facility of the JAEA (Aomori Prefecture, Japan) for providing C isotope data of excellent quality. The study represents part of the

doctoral dissertation research of B. Krajnc, which was supported by the Innovative schemes for co-financing of doctoral studies financed by the European Union through the European Social Fund.

References

Allison CE, Francey RJ, Krummel PB (2003) $\delta^{13}C$ in CO_2 from sites in the CSIRO atmospheric research GASLAB air sampling network, in trends: a compendium of data on global change, carbon dioxide Inf. Anal. Cent., Oak Ridge Natl. Lab., U.S. Dep. of Energy, Oak Ridge, TN. http://cdiac.ornl.gov/trends/co2/allison-csiro/allcsiro-alt.html. Accessed 21 Mar 2015

Bond-Lamberty B, Thomson A (2010) Temperature-associated increases in the global soil respiration record. Nature 464:579–582

Carmi I, Yakir D, Yechieli Y, Kronfeld J, Stiller M (2013) Variations in soil CO_2 concentrations and isotopic values in a semi-arid region due to biotic and abiotic processes in the unsaturated zone. Radiocarbon 55:932–942

Čater M, Ogrinc N (2011) Soil respiration rates and $\delta^{13}C_{CO2}$ in natural beech forest (*Fagus sylvatica* L.) in relation to stand structure. Isot Environ Health Stud 47:221–237. doi:10.1080/10256016.2011.578214

Cerling TE, Solomon DK, Quade J, Bowman JR (1991) On the isotopic composition of carbon in soil carbon dioxide. Geochim Cosmochim Acta 55:3403–3405. doi:10.1016/0016-7037(91)90498-T

Ciais P, Sabine C, Bala G, Bopp L, Brovkin V, Canadell J, Chhabra A, DeFries R, Galloway J, Heimann M, Jones C, Le Quéré C, Myneni RB, Piao S, Thornton P (2013) Carbon and other biogeochemical cycles. In: Stocker TF, Qin D, Plattner G-K, Tignor M, Allen SK, Boschung J, Nauels A, Xia Y, Bex V, Midgley PM (eds) Climate change 2013: the physical science basis. Contribution of working group I to the fifth assessment report of the intergovernmental panel on climate change. Cambridge University Press, Cambridge, New York, pp 465–570

Davidson EA, Janssens IA (2006) Temperature sensitivity of soil carbon decomposition and feedbacks to climate change. Nature 440:165–173

Dörr H, Münnich KO (1986) Annual variations of the ^{14}C content of soil CO_2. Radiocarbon 2A:338–345

Ekblad A, Högberg P (2001) Natural abundance of ^{13}C in CO_2 respired from forest soils reveals speed of link between tree photosynthesis and root respiration. Oecologia 127:305–308. doi:10.1007/s004420100667

Emmerich WE (2003) Carbon dioxide fluxes in a semiarid environment with high carbonate soils. Agr Forest Meteorol 116:91–102. doi:10.1016/S0168-1923(02)00231-9

Etiope G, Lombardi S (1995) Evidence for radon transport by carrier gas through faulted clays in Italy. J Radioanal Nucl Chem 193:291–300. doi:10.1007/BF02039886

Etiope G, Martinelli G (2002) Migration of carrier and trace gases in the geosphere: an overview. Phys Earth Planet Inter 129:185–204. doi:10.1016/S0031-9201(01)00292-8

Fujiyoshi R, Haraki Y, Sumiyoshi T, Amano H, Kobal I, Vaupotič J (2009) Tracing the sources of gaseous components (^{222}Rn, CO_2 and its carbon isotopes) in soil air under a cool-deciduous stand in Sapporo, Japan. Environ Geochem Health 32:73–82. doi:10.1007/s10653-009-9266-1

Fujiyoshi R, Amano H, Yousuke S, Okamoto K, Sumiyoshi T, Kobal I, Vaupotič J (2012) Practical evaluation of carbon sources of forest soils in Slovenia from stable and radio-carbon isotope measurements. Environ Earth Sci 67:133–140. doi:10.1007/s12665-011-1486-x

Högberg P, Buchmann N, Read DJ (2006) Comments on Yakov Kuzyakov's review 'sources of CO_2 efflux from soil and review of partitioning methods' [Soil Biology & Biochemistry 38, 425–448]. Soil Biol Biochem 38:2997–2998. doi:10.1016/j.soilbio.2006.04.001

Kardos R, Gregorič A, Jónás J, Vaupotič J, Kovács T, Ishimori Y (2015) Dependence of radon emanation of soil on lithology. J Radioanal Nucl Chem 304:1321–1327. doi:10.1007/s10967-015-3954-3

Knohl A, Werner RA, Geilmann H, Brand WA (2004) Kel-F (TM) discs improve storage time of canopy air samples in 10-mL vials for CO_2-delta C-13 analysis. Rapid Commun Mass Spectrom 18:1663–1665

Kovács T, Szeiler G, Fábián F, Kardos R, Gregorič A, Vaupotič J (2013) Systematic survey of natural radioactivity of soil in Slovenia. J Environ Radioact 122:70–78. doi:10.1016/j.jenvrad.2013.02.007

Kozak K, Mazur J, Vaupotič J, Kobal I, Janik M, Kochowska E (2009) Calibration of the IJS-CRn and IFJ-PAN radon measuring devices in the IFJ-KR-600 radon chamber. Jožef Stefan Institute Report IJS-DP-10103

Kuzyakov Y (2006) Sources of CO_2 efflux from soil and review of partitioning methods. Soil Biol Biochem 38:425–448. doi:10.1016/j.soilbio.2005.08.020

Kuzyakov Y, Gavrichkova O (2010) Time lag between photosynthesis and carbon dioxide efflux from soil: a review of mechanisms and controls. Global Change Biol 16:3386–3406

Lambert WJ, Aharon P (2011) Controls on dissolved inorganic carbon and $\delta^{13}C$ in cave waters from DeSoto Caverns: implications for speleothem $\delta^{13}C$ assessments. Geochim Cosmochim Acta 3:753–768. doi:10.1016/j.gca.2010.11.006

Levin I, Naegler T, Kromer B, Diehl M, Francey RJ, Gomez-Pelaez AJ, Steele PL, Wagenbach D, Weller R, Worthy DE (2010) Observations and modelling of the global distribution and long-term trend of atmospheric $^{14}CO_2$. Tellus 62B:26–46

Liu W, Moriizumi J, Yamazawa H, Iida T (2006) Depth profiles of radiocarbon and carbon isotopic compositions of organic matter and CO_2 in a forest soil. J Environ Radioact 90:210–223

Neznal M, Šmarda J (1991) Radon infiltration risk from the ground in Chaby, Prague. In: Barnet I (ed) Radon investigations in Czechoslovakia II. Geological Survey, Prague, pp 34–39

Ogrinc N, Kanduč T, Krajnc B, Vilhar U, Simončič P (2016) Inorganic and organic carbon dynamics in forested soils developed on contrasting geology in Slovenia—a stable isotope approach. J Soils Sediments 16:382–395. doi:10.1007/s11368-015-1255-7

Placer L (2008) Principles of the tectonic subdivision of Slovenia. Geology 51:205–217. doi:10.5474/geologija.2008.021

Plestenjak G, Eler K, Vodnik D, Ferlan M, Čater M, Kanduč T, Simončič P, Ogrinc N (2012) Sources of soil CO_2 in calcareous grassland with woody plant encroachment. J Soils Sediments 12:1327–1338. doi:10.1007/s11368-012-0564-3

Quindós-Poncela LS, Fernandez PL, Sainz C, Arteche J, Arozamena JG, George AC (2003) An improved scintillation cell for radon measurements. Nucl Instrum Method A 512:606–609. doi:10.1016/S0168-9002(03)02049-7

Reichstein M, Beer C (2008) Soil respiration across scales: the importance of a model–data integration framework for data interpretation. J Plant Nutrit Soil Sci 171:344–354

Serrano-Ortiz P, Domingo F, Cazorla A, Were A, Cuezva S, Villagarcıa L, Alados- Arboledas L, Kowalski AS (2009) Interannual CO_2 exchange of a sparse Mediterranean shrubland on a carbonaceous substrate. J Geophys Res 114:G04015. doi:10.1029/2009JG000983

Serrano-Ortiz P, Roland M, Sanchez-Moral S, Janssens IA, Domingo F, Godderis Y, Kowalski AS (2010) Hidden, abiotic CO_2 flows

and gaseous reservoirs in the terrestrial carbon cycle: review and perspectives. Agric Forest Meteorol 150:321–329. doi:10.1016/j.agrformet.2010.01.002

Spötl C (2004) A simple method of soil gas stable carbon isotope analysis. Rapid Commun Mass Spectrom 18:1239–1242. doi:10.1002/rcm.1468

Stone R (2008) Have desert researchers discovered a hidden loop in the carbon cycle? Science 320:1409–1410

Torn MS, Davis S, Bird JA, Shaw MR, Conrad ME (2003) Automated analysis of C-13/C-12 ratios in CO_2 and dissolved inorganic carbon for ecological and environmental applications. Rapid Commun Mass Spectrom 17:2675–2682. doi:10.1002/rcm.1246

Trumbore S (2006) Carbon respired by terrestrial ecosystems—recent progress and challenges. Global Change Biol 12:141–153

Urbančič M, Simončič P, Prus T, Kutnar L (2005) Atlas gozdnih tal Slovenije. Zveza gozdarskih društev Slovenije/GIS, Ljubljana

Vaupotič J, Ančik M, Škofljanec M, Kobal I (1992) A method for determination of indoor radon concentrations using α-scintillation cells. J Environ Sci Health A 27:15–35. doi:10.1016/0160-4120(88)90013-X

Vaupotič J, Žvab P, Gregorič A, Kobal I, Kocman D, Kotnik J, Križman M (2008) Radon mapping in Slovenia based on its levels in soil gas. In: 33rd International geological congress abstract CD-ROM. X-CD Technologies, Oslo, pp EGG03742P

Werth M, Kuzyakov Y (2008) Root-derived carbon in soil respiration and microbial biomass using ^{14}C and ^{13}C. Soil Biol Biochem 40:625–637. doi:10.1016/j.soilbio.2007.09.022

Werth M, Kuzyakov Y (2010) ^{13}C fractionation at root-microorganisms-soil interface: a review and outlook for partitioning studies. Soil Biol Biochem 42:1372–1384. doi:10.1016/j.soilbio.2010.04.009

Wohlfahrt G, Fenstermaker LF, Arnone JA (2008) Large annual net ecosystem CO_2 uptake of a Mojave Desert ecosystem. Glob Change Biol 14:1475–1487. doi:10.1111/j.1365-2486.2008.01593.x

Xie J, Li Y, Zhai C, Li CZL (2008) CO_2 absorption by alkaline soils and its implication to the global carbon cycle. Environ Geol 56:953–961. doi:10.1007/s00254-008r-r1197-0

3.2 Scientific Paper: "Inorganic and organic carbon dynamics in forested soils developed on contrasting geology in Slovenia—a stable isotope approach"

In this chapter the paper entitled "Inorganic and organic carbon dynamics in forested soils developed on contrasting geology in Slovenia—a stable isotope approach" by Nives Ogrinc, Tjaša Kanduč, Bor Krajnc, Urša Vilhar, Primož Simončič and Lixin Jin is presented. The paper was published in the Journal of Soils and Sediments, 2015.

The dynamics of organic and inorganic carbon at four forest soils developed on different bedrocks were studied. Sampling locations were situated on magmatic granodiorite bedrock, on carbonate bedrock in the karstic-dinaric area (two locations) and on Pleistocene coalluvial terraces. Soil and plant material was collected for stable isotope analysis of organic carbon and total nitrogen. Several parameters (Temperature, pH, total alkalinity, Ca^{2+}, $Mg^{2+}$and Cl^{-} concentrations, dissolved organic carbon and $\delta^{13}C$) were measured in throughfall and soil water every month from June to November during 2005-2007. The main objectives were to characterize the stable isotopic values in soil and soil waters, to investigate seasonal and spatial variations in soil organic carbon, and to evaluate the sources and transport of DIC and DOC in soil waters.

The DOC isotopic composition indicated no significant isotopic differentiation between the DOC and its presumed soil organic matter source. The typical incensement of $\delta^{13}C$ values of DOC were observed as the water percolated from upper organic rich layers toward the deeper mineral layers. The DOC data suggested that the water input is the main driving factor for controlling DOC fluxes moving carbon from soil profiles to underlying groundwater reservoirs, likely more than the actual DOC concentration and its temporal variation. Thus, factors that control water budget and transport such as soil texture may be more significant in controlling DOC transport. The loss of DOC at 5 cm was in the order of 1 mol m^{-2} $year^{-1}$ at all four sites. Only a small fraction of DOC remained in soil waters with the majority, either sorbed on mineral surfaces, respired or re-assimilated. The drainage of water in locations with sandy soil can flush out a substantial amount of DOC. DIC fluxes were highest at deeper soils especially on soils developed on carbonate bedrock where calcite and dolomite dissolution dominates. In those locations also the isotopic composition of DIC indicates that half of the DIC was from soil CO_2 and other half from carbonate minerals. In soils developed on carbonate bedrock 2 to 5 mol m^{-2} $year^{-1}$ of CO_2 was estimated to be lost via soil waters in dissolved inorganic form. Soil waters remained unsaturated with respect to calcite and dolomite at the lowest sampling depth, thus the dissolution of these minerals and CO_2 uptake may continue down water percolating pathway. On the other two locations the DIC fluxes were much lower, ~0.2 mol m^{-2} $year^{-1}$ which is consistent with the slow silicate kinetics. And also the isotopic composition of DIC at those locations indicated that DIC is isotopically equilibrated with ^{13}C-enriched soil CO_2.

This investigation clearly identified that local lithology, type of vegetation, soil texture and climate are important factors controlling the magnitude of carbon loss in dissolved organic and inorganic forms.

In this paper, the candidate performed stable isotope measurements in soil water and helped with the interpretation of the data. Ca^{2+}, Mg^{2+}, Cl^{-} and DOC concentrations in waters were measured at the University of Michigan (USA).

J Soils Sediments (2016) 16:382–395
DOI 10.1007/s11368-015-1255-7

SOILS, SEC 1 • SOIL ORGANIC MATTER DYNAMICS AND NUTRIENT CYCLING • RESEARCH ARTICLE

Inorganic and organic carbon dynamics in forested soils developed on contrasting geology in Slovenia—a stable isotope approach

Nives Ogrinc[1,2] · Tjaša Kanduč[1] · Bor Krajnc[2] · Urša Vilhar[3] · Primož Simončič[3] · Lixin Jin[4]

Received: 23 April 2015 / Accepted: 2 September 2015 / Published online: 16 September 2015
© Springer-Verlag Berlin Heidelberg 2015

Abstract
Purpose Soil carbon dynamics were studied at four different forest stands developed on bedrocks with contrasting geology in Slovenia: one plot on magmatic granodiorite bedrock (IG), two plots on carbonate bedrock in the karstic-dinaric area (CC and CD), and one situated on Pleistocene coalluvial terraces (FGS).
Materials and methods Throughfall (TF) and soil water were collected monthly at each location from June to November during 2005–2007. In soil water, the following parameters were determined: *T*, pH, total alkalinity, concentrations of Ca^{2+} and Mg^{2+}, dissolved organic carbon (DOC), and Cl^- as well as $\delta^{13}C_{DIC}$. On the other hand, in TF, only the Cl^- content was measured. Soil and plant samples were also collected at forest stands, and stable isotope measurements were performed in soil and plant organic carbon and total nitrogen and in carbonate rocks. The obtained data were used to calculate the dissolved inorganic carbon (DIC) and DOC fluxes. Statistic analyses were carried out to compare sites of different lithologies, at different spatial and temporal scales.
Results and discussion Decomposition of soil organic matter (SOM) controlled by the climate can explain the ^{13}C and ^{15}N enrichment in SOM at CC, CD, and FGS, while the soil microbial biomass makes an important contribution to the SOM at IG. The loss of DOC at a soil depth of 5 cm was estimated at 1 mol m^{-2} $year^{-1}$ and shows no significant differences among the study sites. The DOC fluxes were mainly controlled by physical factors, most notably sorption dynamics, and microbial–DOC relationships. The pH and pCO_2 of the soil solution controlled the DIC fluxes according to carbonate equilibrium reactions. An increased exchange between DIC and atmospheric air was observed for samples from non-carbonate subsoils (IG and FGS). In addition, higher $\delta^{13}C_{DIC}$ values up to −19.4‰ in the shallow soil water were recorded during the summer as a consequence of isotopic fractionation induced by molecular diffusion of soil CO_2. The $\delta^{13}C_{DIC}$ values also suggest that half of the DIC derives from soil CO_2 indicating that 2 to 5 mol m^{-2} $year^{-1}$ of carbon is lost in the form of dissolved inorganic carbon at CC and CD after carbonate dissolution.
Conclusions Major difference in soil carbon dynamics between the four forest ecosystems is a result of the combined influence of bedrock geology, soil texture, and the sources of SOM. Water flux was a critical parameter in quantifying carbon depletion rates in dissolved organic and inorganic carbon forms.

Keywords Carbon cycle · DIC · DOC · Forest ecosystem · SOM · Stable isotopes

Responsible editor: Woo-Jung Choi

Electronic supplementary material The online version of this article (doi:10.1007/s11368-015-1255-7) contains supplementary material, which is available to authorized users.

✉ Nives Ogrinc
nives.ogrinc@ijs.si

[1] Department of Environmental Sciences, Jožef Stefan Institute, Jamova 39, 1000 Ljubljana, Slovenia

[2] Jožef Stefan International Postgraduate School, Jamova 39, 1000 Ljubljana, Slovenia

[3] Slovenian Forestry Institute, Večna pot 2, 1000 Ljubljana, Slovenia

[4] Department of Geological Science, University of Texas at El Paso, El Paso, TX 79968-0555, USA

1 Introduction

Accumulation of greenhouse gases (CO_2) in the atmosphere from fossil fuel burning is the major driver of global warming

and leads to changes in terrestrial ecosystem functioning (IPCC 2013). Recently, the international community began developing management strategies for terrestrial ecosystems, aimed at the mitigation of and the adaptation to potential climate change (IPCC 2013). Most researchers agree that the terrestrial organic carbon reservoir, one of the largest organic carbon storage pool in the world, is a good candidate for carbon sequestration (Myneni et al. 1997; Fan et al. 1998; Houghton et al. 1998, 1999; Barber et al. 2000). Forests cover nearly one third of Earth's land area, containing up to 80 % of the total aboveground terrestrial carbon and 40 % of belowground carbon, thus having a critical role in the global carbon cycle (Dixon et al. 1994), especially in controlling the concentrations of greenhouse gases in the atmosphere.

Soil carbon dynamics vary regionally under the influence of climatic and geological conditions, and types of land use (Wang and Hsieh 2002 and references therein; Wynn et al. 2006). Organic carbon cycle in the terrestrial ecosystems includes short-term plant growth and decay, and longer-term variability of soil carbon storage. This organic carbon cycle is closely linked to the inorganic carbon cycle through release of soil-respired CO_2 to atmosphere and through the dissolution of soil-respired CO_2 to form dissolved inorganic carbon (DIC) in natural soil waters. As the climate changes and atmospheric CO_2 concentration increases, there is a potential to sequester more carbon in forest biomass, litter, and soil (e.g., Nadelhoffer et al. 1999; Richter et al. 1999; Giardina and Ryan 2000; Schimel et al. 2000), and it is critical to understand the complex feedbacks that exist between the inorganic carbon system and the soil organic carbon as discussed below. Although an increase in terrestrial biomass may result from the "fertilization" effect of elevated CO_2 levels on photosynthesis, a large portion of this increase takes place in the belowground biomass (e.g., Van Veen et al. 1991; Bowden et al. 1993). Plants grown in elevated CO_2 atmospheres also have higher root and microbial respiration rates, which can increase the pCO_2 values in the soil (Hungate et al. 1997; Powers and Schlesinger 2002). This increase in soil gas CO_2 can result in an enhanced flux back to the atmospheric reservoir through diffusion (e.g., Trumbore et al. 1996) as well as driving an increased carbon flux to the soil carbon pool and/or to groundwater systems as dissolved inorganic and organic carbon (e.g., Richter et al. 1999; Andrews et al. 2000).

Enhanced carbonate and silicate mineral dissolution rates, and enhanced CO_2 consumption rates have recently been documented in experimental tree growth mesocosms at elevated air CO_2 and soil nitrogen fertility levels (Andrews et al. 2000; Hamilton et al. 2002; Williams et al. 2006). In this case, soil zone pCO_2 is controlled by root and microbial respiration rates which increase with enhanced growth under elevated CO_2 (the "fertilization effect") and with N fertility (Pregitzer et al. 2000). Dissolved organic carbon (DOC) has a complex role in soil C cycling as it can either serve as an easily decomposable substrate for soil microorganisms to form CO_2, or become a soil organic matter (SOM) stabilizing component when transported to a mineral soil (Kaiser and Guggenberger 2000; Marschner and Kalbitz 2003; Cleveland et al. 2004; Sanderman and Amundson 2008). Laboratory experiments have shown that most mineral soils have a high tendency to absorb DOC (Cleveland et al. 2004). In addition, DOC collected within the mineral soil is chemically more similar to SOM than it is to fresh litter leachates (Sanderman and Amundson 2008 and the references therein).

The spatial and temporal trends of the carbon isotopic composition of SOM provide the main tool in understanding the terrestrial carbon dynamics and help in desiphering the biogeochemical processes and fluxes in a dynamic soil system (Bird and Pousai 1997; Bird et al. 2001; Powers and Schlesinger 2002; Wynn et al. 2006). The isotopic composition of soil CO_2 varies temporally and spatially and depends on the source of organic matter and microbial respiration, which is also influenced by the photosynthetic pathway (Vogel 1993). In most terrestrial ecosystems, the C3 photosynthetic pathway dominates and produces vegetation with $\delta^{13}C$ value of about −27‰ (Vogel 1993). As infiltrating waters dissolve soil $CO_2(g)$, the speciation of DIC (relative proportion of dissolved CO_2, bicarbonate (HCO_3^-), and carbonate (CO_3^{2-}) ions) depends on pH and on temperature (Stumm and Morgan 1996). The enrichment factor in ^{13}C between $CO_2(aq)$ and HCO_3^- is about 9‰ (Clark and Fritz 1997). Also, bedrock geology is a crucial factor affecting soil carbon dynamics (interactions between bedrock–soil–soil waters and soil gas) and the isotopic composition of carbon. In forest soils, developed on silicate bedrock, the isotopic composition of soil CO_2 largely reflects the decomposition of organic matter and root respiration (Amiotte-Suchet et al. 1999). In the case of carbonate bedrock, the dissolution of carbonate minerals will influence the isotopic composition of soil CO_2 and C dynamics in the soil profile: carbonate mineral dissolution increases the concentrations of dissolved inorganic carbon ($DIC=[HCO_3^-]+[CO_3^{2-}]+[H_2CO_3^*]$) and concentrations of divalent cations (Ca^{2+}, Mg^{2+}) in soil water, and pH until carbonate mineral saturation is reached.

Carbon isotope studies have focused mainly on riverine waters, with little information available for waters in soil profiles that represent the critical zone of carbon transformation (Jin et al. 2009; Arai and Tokuchi 2010; Jin et al. 2014). In this study, we investigated the dynamics of organic and inorganic carbon in four forest soils developed on different geological bedrock: one plot on magmatic granodiorite bedrock, two on carbonate bedrock in a karstic-dinaric area, and one situated on Pleistocene colluvial terraces. These sites allow a comparison of soil water chemistry and a study of carbon dynamics in environments of contrasting geological composition, soil texture, and vegetation. This is the first systematic study of soils

developed in forest ecosytems with different geological compositions in Slovenia, including the use of stable isotopes as tracers for C source identification. We hypothesize that DIC fluxes in soils vary significantly with bedrock lithology (carbonate-bearing versus carbonate-free), whereas DOC fluxes are sensitive to vegetation coverage. Thus, the main objectives of the present study are to (1) characterize the stable isotopic values in soil and soil water, (2) investigate seasonal and spatial variations in soil organic carbon, and (3) evaluate the sources and transport of DIC and DOC in soil waters on bedrocks with different geological compositions.

2 Materials and methods

2.1 Sampling sites

The four forest research plots chosen in this study differ in terms of vegetation and geology (Fig. 1 and Table 1). Two plots are located in the Dinaric fir-beech forests in Kočevski Rog, one located on the southern edge of a virgin forest reserve known as Rajhenavski Rog and the other in a forest managed for silviculture known as Snežna jama. Both sites are situated on carbonate bedrock with various amounts of dolomite and calcite. At Snežna jama, the presence of calcite and dolomite rocks (gravels and sand) was observed at depths >40 cm (Ogrinc et al. 2012), while at Rajhenavski Rog, calcite dominates. At these two sites, rendzinas and eutric brown soils with up to 35 cm thick dominate, with 25 and 10 % of the surface covered by bare rock at Snežna jama and Rajhenavski Rog. The third research plot, Kladje, is located in spruce monocultures at mountain habitats of acidophilic beech on Pohorje. The soils in this site are a clayey dystric cambisol 60 to 70 cm in thickness above a granodiorite bedrock (igneous rock alumosilicates). An intensively monitored plot at Brdo in Kranj, developed on fluvioglacial sediments (gravel and sand composed of carbonate rocks), was selected as the fourth field site. The main tree species is *Pinus sylvestris* and the forest community is *Vaccinio myrtilli-Pinetum*. Soils at Brdo are dystric cambisol with the thickness ranging from being nonexistent to 100 cm thick. The mineral content at all selected locations consists mainly of clays (gibbsite), kaolinite, and quartz (Ogrinc et al. 2012).

In order to facilitate the discussion of the obtained results in connection to bedrock lithology, the following abbreviations were used for selected research plots: Rajhenavski Rog as CC (carbonate calcite), Snežna jama as CD (indicating dolomite contribution), Kladje as IG (igneous rock), and Brdo as FGS (fluvioglacial sediments). Three different sampling locations were selected in FBS, labeled as FGS-A, FGS-B, and FGS-C, respectively.

2.2 Collection of soil and soil water samples

Soil samples were collected from soil pits at distinct horizons at the four different locations (Fig. 1). Samples were then passed through a 2-mm sieve (dry sieving) to remove large organic material and rock fragments. Representative fresh terrestrial plants were also collected during the growing season by randomly picking leaves. Soil and plant samples were air-dried and ground to a fine powder with a mill ready for elemental and isotopic analyses. Carbonate bedrocks (n=4) samples were taken from carbonate outcrops at CD and CC.

Throughfall (TF) and soil water samples were collected monthly at each location from June to November during 2005–2007. Soil water was obtained using ICP Forest low-tension lysimeters (P80) with ceramic suction cup and plate (Nieminen 2011). Samples were taken from two depths of 5 and 50 cm beneath the organic matter–mineral soil interface at locations CD, CC, and IG, and at depths 5, 20, and 40 cm at FGS-A, FGS-B, and FGS-C. Temperature and pH of soil waters were measured in the field. Solution samples were stored in pre-cleaned HDPE bottles after filtering through 0.45-μm Whatman millipore filters. For Cl^- and alkalinity analyses, samples needed no further treatment, while for the determination of cations, water samples were acidified using several drops of ultrapure HNO_3. The DOC samples were acidified with HCl and stored at about 4 °C before analysis, while samples for carbon isotope analyses of DIC ($\delta^{13}C_{DIC}$) were stored in sealed glass serum vials with no headspace.

2.3 Characterization of throughfall and soil waters

The concentrations of Ca^{2+} and Mg^{2+} in soil waters were determined by atomic absorption spectrometry (AAS), with a precision of ±5 %, while Cl^- was measured using Dionex ion chromatography with a precision of ±5 %. For TF, only concentrations of Cl^- were determined. Total alkalinity (approximate for carbonate alkalinity=$[HCO_3^-]+2[CO_3^{2-}]$) was measured by Gran titration with a precision of ±10 % (Gran 1952). DOC concentrations of soil water were determined with a Shimadzu TOC-5000A dissolved carbon analyzer. The isotopic composition of DOC ($\delta^{13}C_{DOC}$) was determined only for samples collected in 2005 from FGS-A, FGS-B, and FGS-C. To determine $\delta^{13}C_{DOC}$ values, samples were filtered and acidified to pH <2 using 5 % phosphoric acid and then freeze-dried to a powder. These powdered samples were then prepared for analysis in the same manner as the solid samples (Sanderman and Amundson 2008).

The $\delta^{13}C_{DIC}$ values were measured using a Europa Scientific 20–20 Isotope Ratio Mass Spectrometer (IRMS) coupled with an Automated Nitrogen Carbon Analyser for Trace Gases (ANCA-TG) preparation module for trace gas samples equipped with a Gilson autosampler (Kanduč et al. 2007). Briefly, into a series of glass septum tubes (Exetainer

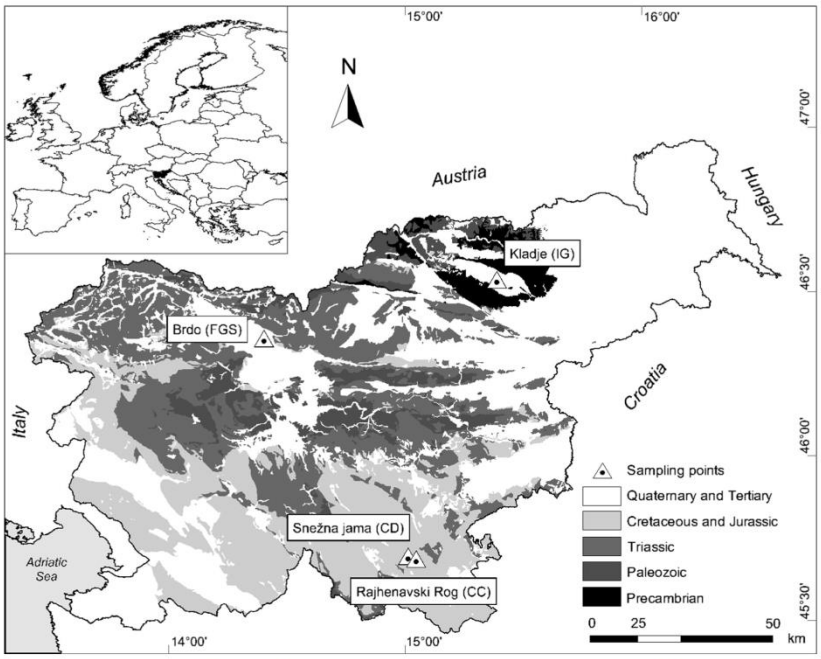


Fig. 1 Geological map of Slovenia with sampling locations in four different research plots: Kladje (IG), located in area composed of aluminosilicate bedrock; Brdo (FGS), located in area composed of alluvial bedrock; and Snežna jama (CD) and Rajhenav (CC), located in area composed of carbonate bedrock

Septum Tubes, Labco Limited, UK), 100 % phosphoric acid was added (100–200 μl) and the tubes were purged with pure He. Five milliliters of water sample was then introduced into each tubes by a syringe. The acid–water reaction began immediately upon injection. The isotope ratio of CO_2 was then determined directly from the headspace. To determine the optimal extraction procedure for the water samples, a standard solution was prepared with Na_2CO_3 of known $\delta^{13}C_{DIC}$ value of −10.8±0.2‰ (Waldron et al. 2014).

The concentration of dissolved inorganic carbon (DIC), partial pressure of CO_2 (pCO_2), and saturation indexes of calcite ($SI_{calcite}$) and dolomite ($SI_{dolomite}$) were calculated using water chemistry data (pH, alkalinity, and concentrations of major ions) and soil water temperature by PHREEQC software for Windows (Parkhurst and Appelo 1999).

2.4 Characterization of vegetation, soils, and carbonate rocks

The organic carbon (OC) content and $\delta^{13}C$ values of soils and plant organic matter were measured after treatment with 1 M HCl to remove carbonate material, while total nitrogen (TN) content and the isotopic ratios of nitrogen ($\delta^{15}N$) were determined on the bulk samples without acid treatment. Sample concentrations of OC and TN were determined using a LECO 2000 CNS elemental analyzer with a ±3 % precision.

The $\delta^{13}C$ and $\delta^{15}N$ values in soil and plant debris and $\delta^{13}C_{DOC}$ were measured with an IRMS ANCA-SL preparation module for solid and liquid samples. Analyses were calibrated against reference materials: IAEA NBS 22 (oil) and IAEA-CH-7 for carbon and IAEA-N1, IAEA-N2, and IAEA-NO-3 for nitrogen.

The isotopic composition of carbonate rock ($\delta^{13}C_{Ca}$) was also determined. Samples were prepared by grinding into a powder in an agate mortar; 2 mg of sample was then placed into ampoules, which were capped, flushed with helium, and then reacted with anhydrous H_3PO_4 for 1 day at 25 °C. The released CO_2 was then measured with IRMS with an ANCA-TG preparation module for trace gas samples. NBS 18 and NBS 19 were used as reference materials.

All stable isotope results are reported using conventional delta (δ) notation in permil (‰) relative to a suitable standard: VPDB for $\delta^{13}C$ and AIR for $\delta^{15}N$. The precision of measurements was ±0.2‰ for all $\delta^{13}C$ analyses and ±0.3‰ for $\delta^{15}N$ analyses.

Table 1 General characteristics of the four forest research plots in Slovenia

Plot name	Snežna jama	Rajhenavski Rog	Brdo	Kladje
Abbreviation	CD	CC	FGS	IG
Latitude (m)	+45° 39′ 17″	+45° 39′ 44″	+46° 17′ 14″	+46° 28′ 26″
Longitude (m)	+15° 1′ 39″	+15° 0′ 35″	+14° 24′ 00″	+15° 23′ 51″
Altitude (m)	880	860	471	1300
Slope inclination	15°	10°	5°	0°
Average amount of precipitation (mm year^{-1})	1300–1400	1300–1400	1400–1500	1300–1500
Average air temperature (°C)	12	12	15	8
Soil thickness (cm)	Up to 35	Up to 35 cm	Up to 100 cm	Up to 70 cm
Rock cover (%)	25	10	0	0
Aspect	E	E	SSW	SW
Parent material	Limestone & dolostone	Limestone & dolostone	Fluvioglacial gravels & sands	Dioritoid (Tonalite)
Dominant soil types	Rendzinas, eutric brown soils, luvisols	Rendzinas, eutric brown soils	Dystric Cambisols	Dystric brown soils, dystric rankers
Soil texture	Clay loam	Loam	Silty loam	Sandy loam
Forest community	*Omphalodo-Fagetum*	*Omphalodo-Fagetum*	*Vaccinio myrtilli-Pinetum*	*Avenello flexuosae-Piceetum* acidophilous altimountain beech forest (*Luzulo albidae-Fagetum*)
Main tree species	Fir-beech	Fir-beech	*Pinus sylvestris*	Spruce-beech

2.5 Flux models

The flux of percolating water was calculated assuming Cl^- as a conservative anion (Nilsson et al. 1998) using the following equation:

$$WF_Z = [C1^-]TF{\cdot}X{\cdot}WF_{TF}/[C1^-]_Z \quad (1)$$

where WF_z is the annual water flux (mm) at z depth (cm) (z=5, 20, or 40 cm or z=5, or 50 cm below ground surface), while $[Cl^-]_{TF}$ and $[Cl^-]_z$ are concentrations of Cl^- (mmol l^{-1}) in throughfalls (TF) and in percolation water (PW) at z depth (cm), respectively. The DOC fluxes, F_z (mmol m^{-2} $year^{-1}$), were calculated using DOC concentrations at a z depth and WF_z for each sampling period and summed over 1 year:

$$F_Z = [DOC]_Z{\cdot}X{\cdot}WF_Z \quad (2)$$

This method assumed that Cl^- is a conservative tracer, and not involved in any biogeochemical processes, and provided a rough estimate of DOC transport with an uncertainty of 10 % calculated by propagation of error. DOC fluxes within the forest soil were assumed to be zero in winter when the soil was frozen. The DIC fluxes were also estimated using the same approach, but only at IG, CC, and CD.

2.6 Statistics

Spatial and temporal variabilities were tested for statistical significance using the non-parametric Kruskal–Wallis test, while differences between sampling depths were analyzed with the non-parametric Mann–Whitney U test. The tests were carried out with the Statistica version 7 software (Statsoft, Tulsa, USA).

3 Results

3.1 Soil C and N isotopes and C/N ratios

The depth profiles of SOC, carbon, and nitrogen isotopic composition of soil ($\delta^{13}C_{soil}$, $\delta^{15}N_{soil}$), and soil organic C/N (molar) ratios are presented in Fig. 2. At all sites, the concentrations of SOC decrease with soil depth, while values of $\delta^{13}C_{soil}$ increase from −27.7 to −23.8‰ at IG, −29.3 to −25.1‰ at CD, −29.9 to −24.4‰ at CC, and −28.9 to −23.8‰ at FGS. Similarly, an increase in $\delta^{15}N_{soil}$ was also observed with depth, i.e., −6.3 to 5.9‰ at IG, −3.2 to 4.4‰ at CD, −2.9 to 4.7‰ at CC, and −5.6 to 6.1‰ at FGS. C/N ratios are significantly greater in organic horizons than those in the underlying mineral soils, with almost constant C/N ratios in deeper soil layers. An exception are IG soils, where a slight increase in the C/N ratio with depth was observed.

The stable carbon isotope composition of plant material ($\delta^{13}C_{plant}$) from locations CD and CC varied from −34.8 to −25.8‰, with an average of −30.9±2.3‰ (n=39) (Table 2). The isotopic composition of nitrogen in plant material ($\delta^{15}N_{plant}$) showed less variations, with values from −6.9 to −1.7‰, with an average of −3.6±1.8‰. The isotopic

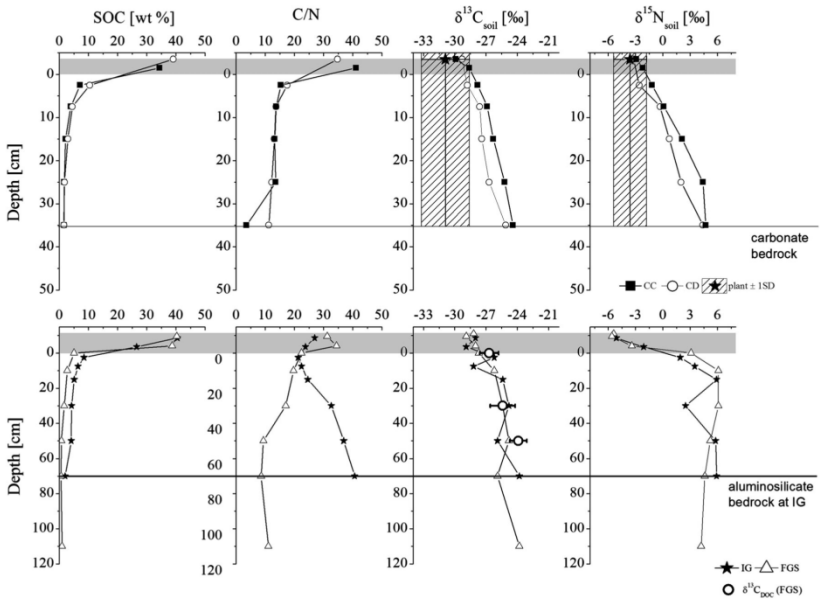


Fig. 2 Depth profiles of soil organic carbon content (SOC), C/N molar ratios, and the isotopic composition of soil organic carbon ($\delta^{13}C_{soil}$) and nitrogen ($\delta^{15}N_{soil}$) at all four sampling locations. *Solid lines* represent soil bedrock boundaries, while *shaded area* show the upper organic layer

composition of carbonate rocks ($\delta^{13}C_{ca}$) was −1.4‰ at CD and 1.2‰ at CC.

3.2 Soil water chemistry and isotopes

Soil water temperature, pH, and concentrations of Ca^{2+}, Mg^{2+}, DOC, alkalinity, and pCO_2 together with $\delta^{13}C_{DIC}$ values for IG, CC, and CD are given in Table S1 and for FGS in Table S2 (see Electronic Supplementary Material). At all sites, no statistically significant differences in temporal variability were observed in measured parameters.

Significant higher pH values were observed at CC and CD ($p<0.0001$) than those at IG and FGS. Indeed, pH was between 4.18 and 6.80 in all the soil water samples from IG and at FGS, similar to the pH values of precipitation (Tables S1 and S2, Electronic Supplementary Material). At IG or FGS, no statistically significant difference in soil water pH was observed among different depths ($p=0.543$ at IG, $p=0.547$ at FGS). In contrast, marked difference between two depths was observed at CC and CD (both $p<0.0001$). The pH of the soil waters collected at a depth of 5 cm at CC and CD ranged between 5.40 and 7.50 and increased to a range from 7.10 to 8.23 at a depth of 50 cm resulting from the direct contact with the carbonate bedrock.

Concentrations of Ca^{2+} and Mg^{2+} in all soil water of four sites ranged from 0.004 to 2.001 mmol l^{-1} and from 0.002 to 0.974 mmol l^{-1}, respectively (Supplementary Tables S1 and S2). Statistically significant spatial differences were observed in Ca^{2+} and Mg^{2+} concentrations, where Ca^{2+} concentrations at CC and CD were higher and differed significantly from IG and FGS sites ($p<0.0001$) and Mg^{2+} concentrations at CD differed significantly from CC, IG, and FGS ($p<0.0001$). The variation of Ca^{2+} concentrations with depth was statistically significant at CC, CD, and IG ($p<0.0001$ at CC and CD; $p=0.035$ at IG), with higher Ca^{2+} concentrations observed at a depth of 50 cm at CC and CD and at a depth of 5 cm at IG. Statistically higher Mg^{2+} concentrations were also observed at a depth of 50 cm at CD ($p<0.0001$), while no statistically significant differences in Mg^{2+} concentrations with depth were observed at CC and IG ($p=0.129$; $p=0.134$). The depth distribution in Ca^{2+} and Mg^{2+} concentrations were not statistically significant at FGS ($p=0.202$ for Ca^{2+}, $p=0.131$ for Mg^{2+}).

Statistically significant differences were observed in DOC concentrations at four sites, where the lowest concentrations were observed at CD ($p<0.0001$). Depth distribution indicated that DOC concentrations at CD, IG, and FGS were statistically higher in shallow soil horizons but decline sharply with

Table 2 Isotopic composition of C and N of characteristic plant material at CC and CD

Plant material	$\delta^{13}C$ (‰)	$\delta^{15}N$ (‰)
Leaves (*Fagus sylvatica* L.)	−31.3	−3.1
Needles (*Abies alba* Mill.)	−32.0	−2.9
Undergrowth (*Euphorbia amygdaloides* L., *Aremonia agrimonioides* (L.) DC., *Sanicula europaea* L., *Cardamine trifolia* L., *Senecio fuchsia* Gmelin, *Elymus caninus* L., *Daphne laureola* L., *Daphne mezereum* L., *Galium odoratum* (L.) Scop., *Oxalis acetosella* L., *Lactuca muralis* (L.) Gaertn., *Omphalodes verna* Moench., *Salvia glutinosa* L., *Paris quadrifolia* L., *Juncus effuses* L., *Circaea lutetiana* L., *Calamintha grandiflora* (L.) Moench.	−32.8±1.1	−2.8±1.5
Litterfall	−27.0	−2.5
Moss	−26.4	−5.9

depth (Fig. 3). No such significant trend in DOC concentrations was observed at CC (p=0.725), although at this site the highest DOC concentrations were observed for both shallow (5 cm) and deep (50 cm) soils. We observed no correlation between DOC and SOC for each site. The $\delta^{13}C_{DOC}$ values were between −28.2 and −26.0‰ at location FGS during 2005 and are similar to the isotopic composition of the top soil layers (Fig. 2). With soil depth, the DOC became ^{13}C-enriched with the $\delta^{13}C_{DOC}$ values between −27.4 and −22.8 ‰. This trend is similar to the depth profile of $\delta^{13}C_{soil}$ (Fig. 2).

Vertically infiltrating DOC fluxes were estimated at depths of 5 and 50 cm at IG, CC, and CD and at 5 and 40 cm at FGS for each sampling period (Fig. 4). An important factor in controlling the DOC flux calculation in soil water is the amount of water percolating (WF_z) down through the soil determined using Eq. (1). The DOC fluxes at a depth of 5 cm ranged from 1.40 to 2.31 mol DOC m^{-2} $year^{-1}$, while at 50 cm, the fluxes were consistently much lower from 0.3 to 1.7 mol DOC m^{-2} $year^{-1}$ (Fig. 4). The decline in the DOC flux with depth was due primarily to a significant decrease in DOC concentrations with water flux playing only a minor role.

At FGS, where only silicate dissolution occurs, alkalinity, dissolved Ca^{2+} and Mg^{2+}, and pH are low (Fig. 3). In contrast, soil waters at CC and CD that are dominated by carbonate dissolution are characterized by higher concentrations of divalent cations and alkalinity, with higher pH (Fig. 3). At all four sites, the carbonate alkalinity of the shallow soil water was low (0.02 to 1.40 meq l^{-1}) due to a low pH and the presence of dissolved organic acids in the shallow soil zones (Cai et al. 1998). Statistically significant differences in alkalinity with depth were observed for CC and CD sites, but not for IG (p=0.077). In the carbonate-bearing CC and CD soils, higher alkalinity was determined at a depth of 50 cm (up to 4.55 meq l^{-1} in November 2005 at CD) (Table S1, Electronic Supplementary Material).

The partial pressure of CO_2 (pCO_2) and concentrations of DIC in soil waters were calculated with alkalinity and pH using the PHREEQC speciation program (Parkhurst and Appelo 1999). The calculation was not performed for FGS soils because of the high uncertainty in the alkalinity data. The soil pCO_2 values (550 to about 39,811 ppmv) were from 2 to >100 times higher than the atmospheric pCO_2 of about 400 ppm. The pCO_2 was the highest in soil from IG and increased with depth. The same observation was found at CC, while at CD, the pCO_2 decreased with depth in the soil. However, the differences related to site were not statistically significant (p=0.774) nor were the differences related to depth (p=0.399 at IG; p=0.071 at CC; p=0.344 at CD).

In the soil water at the measured pH, the predominant DIC species are $H_2CO_3^*$ and HCO_3^-. The DIC fluxes estimated at IG, CC, and CD are presented in Fig. 4. They were generally greater at a depth of 50 cm at CC and CD than the DOC fluxes. The exception was in acidic soil (IG), where DIC accounted for <30 % of total dissolved carbon. The $\delta^{13}C_{DIC}$ values in soil water varied with site and depth (Figs. 3 and 5), but the differences related to season $\delta^{13}C_{DIC}$ were not statistically significant (p=0.960). Indeed, statistically significant differences were related to site, where CC and CD differed from IG and further CC, CD, and IG differed from FGS (p<0.0001). In carbonate-bearing soils (CC and CD), the $\delta^{13}C$ values in the soil water are higher (from −16.5 to −11.7‰) than those in silicate soils (IG and FGS) (Tables S1 and S2, Electronic Supplementary Material). The $\delta^{13}C_{DIC}$ values ranged from −23.3 to −13.7‰, and from −26.9 to −12.2‰ at locations IG and FGS, respectively (Tables S1 and S2, Electronic Supplementary Material). At both locations, the $\delta^{13}C_{DIC}$ values were lower in shallow soil waters compared to those in deeper horizons. However, statistically significant differences in $\delta^{13}C_{DIC}$ values with depth were observed only at FGS (p<0.0001) and CD (p=0.008).

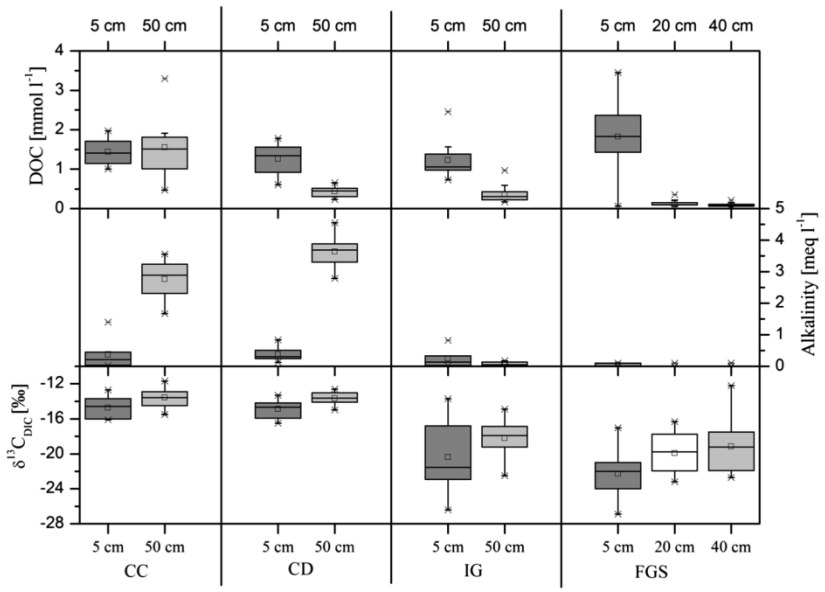


Fig. 3 Box plots of the concentrations of DOC, alkalinity, and $\delta^{13}C_{DIC}$ with the mean, maximum, and minimum values observed at 5 and 50 cm at IG, CC, and CD and 5, 20, and 40 cm at FGS during 2005–2007

4 Discussion

4.1 General distribution of soil nitrogen and organic carbon

The differences between $\delta^{13}C$ and $\delta^{15}N$ of SOM and vegetation (Fig. 2) have been also observed elsewhere and are thought to arise from fractionation during litter decomposition and SOM oxidation (Nadelhoffer and Fry 1988; Balesdent and Mariotti 1996; Buchmann et al. 1997; Ehleringer et al. 2000; Makarov et al. 2008). The increase in $\delta^{15}N_{soil}$ values with depth of 5–10‰ that we observed is consistent with other studies of well-drained, undisturbed forest soils (Nadelhoffer and Fry 1988; Högberg 1997; Boström et al. 2007). Explanations for ^{13}C and ^{15}N isotopic enrichment include (a) fractionation by microbial decomposition, (b) preferential decomposition of isotopically lighter fractions of the organic material, and (c) soil carbon mixing dynamics and changes in the organic carbon sources over time (Nadelhoffer and Fry 1988; Wedin et al. 1995). Alternatively, the microbial biomass itself may be the origin of isotopically enriched organic material since the enrichment in ^{13}C and especially in ^{15}N relative to the fresh plant litter has been observed in microbial biomass in different soil types (Dijkstra et al. 2006; Williams et al. 2006; Boström et al. 2007). This also explains the significant changes in C/N ratios with the depth at IG. Large C/N ratios indicate poorly degradable litter, slow transformation, and recycling of OM.

Preferential degradation alone could account for a decreasing ^{13}C abundance with humification and explaining lower $\delta^{13}C$ values observed at the surface (Ehleringer et al. 2000), but the mechanisms for this are not fully understood (Melillo et al. 1989). Lipids and lignin tend to be ^{13}C-depleted and degrade slowly, whereas cellulose and carbohydrates tend to be enriched in ^{13}C and degrade more rapidly (Ehleringer et al. 2000; Adams and Grierson 2001). An alternative explanation for ^{13}C enrichment observed with depth is the preferential utilization of ^{12}C compounds by soil microorganisms during decomposition (Stout et al. 1981; Kramer and Gleixner 2008). The microbial biomass in carbonate-rich soils shows no significant ^{13}C enrichments (Dijkstra et al. 2006). Thus, at CC and CD, the increase in $\delta^{13}C$ and $\delta^{15}N$ values with soil depth could be a consequence of the isotopic fractionation during decomposition resulting in the gradual enrichment in ^{13}C and ^{15}N of the residual OM (Högberg 1997).

4.2 Dissolved organic carbon fluxes and sorption processes

The production of DOC is closely linked to SOM decomposition and is important in the carbon cycling processes. The

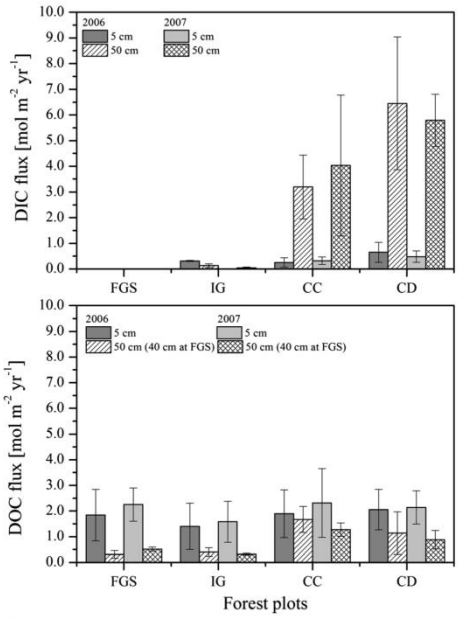


Fig. 4 DIC and DOC fluxes with soil depth in 2006 and 2007. *Error bars* represent the uncertainty due to temporal variability of concentrations

DOC concentrations in the four studied soils decrease with depth (Fig. 3) and the calculated DOC fluxes are comparable with the data obtained for other EU forests (Lindroos et al. 2008; Sanderman and Amundson 2008; Kindler et al. 2011). The highest DOC concentrations were observed at CC, for both shallow (5 cm) and deep (50 cm) soils, which is probably a result of a large amount of aboveground biomass and forest floor C pools. The OM content at CC was the highest in comparison to that in other locations (Urbančič et al. 2009). The highest DOC percolation fluxes were also observed at CC. The differences in DOC fluxes between 2006 and 2007 varied from 4 to 24 % at all depths with the highest variation observed at a depth of 50 cm at CC. There is a positive correlation (r^2=0.78, p<0.012) between soil C/N ratios and DOC concentrations at FGS, CC, and CG, but not at IG. This positive correlation could be explained by the faster processing of nitrogen-poor OM resulting in the production of more soluble residues. The topsoils and organic layers are regarded as the soil compartments that are the most important for DOC generation (Guggenberg and Kaiser 2003). More rapid degradation of OM was observed at IG, despite less favorable C/N ratios and the higher content of surface lipids and cutin than at CC (Ogrinc et al. 2012). The results of the study performed by Aneja et al. (2006) indicate that abiotic and microbial communities in mixed stands (such as IG) promote decomposition rates and the rates are higher than those found in pure stands of beech (such as CC). Thus, it seems that at IG, where the soil thickness is up to 70 cm thick formed on dioritoid-tonalite (Table 1), most of the carbon associated with processed SOM is either respired or re-assimilated as indicated also by high pCO_2 values.

At CC and CD, the DOC fluxes decrease with depth less sharply than at IG and FGS. In general, different studies have concluded that the decrease in DOC concentrations is a consequence of adsorption processes, particularly at low pH and in sandy soils, like that at FGS (Kalbitz et al. 2000; Michalzik et al. 2001; Peichl et al. 2007). The $\delta^{13}C$ values of DOC indicated no significant isotopic differentiation between the DOC and its presumed source of SOM (Fig. 2), which was also found in a coniferous forest catchment in the Morban Mountains of France (Amiotte-Suchet et al. 2007). Our data show how $\delta^{13}C_{DOC}$ values become more positive (enriched in ^{13}C by 1–3.5‰) as water percolates from the upper organic-rich layers toward the deeper mineral layers. This enrichment could be explained by selective sorption of the ^{13}C-depleted hydrophobic fraction (Kaiser et al. 2001; Sanderman and Amundson 2008), which acts to stabilize DOC against decomposition. Iron and aluminum (hydr)oxides with high specific surface areas in soils are considered the most important sorbents for DOC in soils (Kaiser et al. 2001). The FT-IR spectra obtained at FGS indicates the presence of aluminum (hydr)oxides that can act as sorbents for DOC (Kovač, personal communication). Our observation of ^{13}C enrichment of DOC with depth disagrees with the findings of Ludwig et al. (2000) and Amiotte-Suchet et al. (2007), who found that $\delta^{13}C_{DOC}$ decreases with depth as a consequence of sorptive retention of DOC.

In addition, our estimates suggest that water input is a driving factor for controlling DOC fluxes that move carbon from soil profiles to underlying groundwater reservoirs, likely more than the actual DOC concentration and its temporal variation. Thus, factors that control water budget and transport such as soil texture may be more significant in controlling the DOC transport. The drainage of water via macropores in sandy soils present at IG and FGS may flush out a substantial amount of DOC and could explain the more rapid decrease in DOC fluxes with depth compared to that in CC and CD.

4.3 Dissolved inorganic carbon fluxes and chemical weathering

Soil CO_2 can be lost to the atmosphere by diffusion or to soil water DIC by reacting with minerals in the soil profile. The formation of DIC in soil solution can be described with the following reactions (Stumm and Morgan 1996): $CO_{2(g)}+H_2O \Leftrightarrow H_2CO_3 \Leftrightarrow H^+ + HCO_3^- \Leftrightarrow 2H^+ + CO_3^{2-}$. This is important

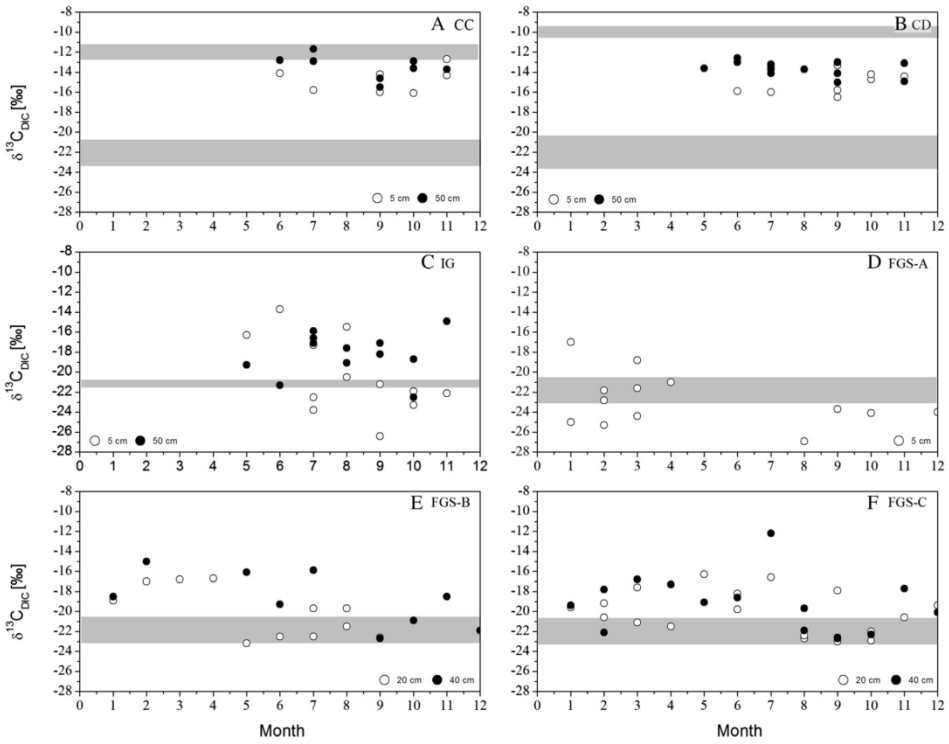


Fig. 5 Temporal variation of $\delta^{13}C_{DIC}$ in soil water at (**a**) CC, (**b**) CD, (**c**) IG, (**d**) FGS-A, (**e**) FGS-B, and (**f**) FGS-C during 2005–2007. The shaded areas in the figures represent the range of isotopic composition of soil CO_2. For CC and CD, the theoretical carbon isotopic composition of a 1:1 mixing between soil CO_2 and carbonate dissolution is also shown as *dark shaded area*

when carbonate minerals are present, which are reactive and readily soluble using H_2CO_3, and thus, their dissolution consumes more CO_2 than silicate weathering. We consider carbonate system parameters together with stable C isotope compositions to identify sources of soil water DIC and to determine the extent of equilibration with soil CO_2. Isotopic equilibrium between soil CO_2 and soil water DIC is expected because (1) soil gas is a large C reservoir while the consumption of CO_2 by silicate dissolution is slow, and (2) soil water stays in the soil profile for days (Jin et al. 2009), providing sufficient time to reach isotopic equilibrium with soil CO_2. If DIC in natural waters does not attain isotopic equilibrium with soil CO_2, for example, in a closed system, then $\delta^{13}C_{DIC}$ is controlled by the isotopic composition of its carbon sources. In the case of silicate weathering with soil CO_2, the $\delta^{13}C_{DIC}$ equals $\delta^{13}C_{CO2}$ (Ca silicate$+CO_2+H_2O \Leftrightarrow Ca^{2+} + HCO_3^- +$ secondary clay). In the case of carbonate weathering with CO_2 ($MgCa(CO_3)_2+H_2O+2CO_2 \Leftrightarrow Mg^{2+} + Ca^{2+} + 4HCO_3^-$), the $\delta^{13}C_{DIC}$ equals ½ ($\delta^{13}C_{CO2}+\delta^{13}C_{Ca}$). Thus, before interpreting the $\delta^{13}C_{DIC}$ data, the isotopic composition of the source materials (two C end members: CO_2 and carbonate) must be identified. Assuming an isotopic enrichment of +4.4 ‰ between soil-respired CO_2 and its organic matter sources (Cerling 1991) induced by CO_2 diffusion, the $\delta^{13}C$ of the soil CO_2 produced by SOM mineralization in our study sites should range from −25.5 to −19.4‰ with an average value of −22.5‰. These are typical of soil $\delta^{13}C_{CO2}$ values reported in the literature for sites with predominantly C3 type of vegetation (Cerling et al. 1991; Amundson et al. 1997; Andrews et al. 2000). Because partial pressures of CO_2 in soil air are higher than atmospheric partial pressures, the direct influence of atmospheric CO_2 on DIC concentrations in soil is negligible (Table S1, Electronic Supplementary Material). For carbonate end member, $\delta^{13}C_{ca}$ value of −1.4‰ was used for CD and 1.2‰ for CC.

Variations in $\delta^{13}C_{DIC}$ values in soil water at IG and FGS indicate that DIC is isotopically equilibrated with ^{13}C-enriched soil CO_2 as a result of the higher concentrations of $H_2CO_3^*$ relative to HCO_3^-. The $\delta^{13}C_{DIC}$ values are close to equilibrium with soil $\delta^{13}C_{CO2}$ (Fig. 5). This also implies that soil CO_2 is the major source of DIC in shallow soils, and the contribution of atmospheric CO_2 is insignificant. The $\delta^{13}C_{DIC}$ values were higher at both locations CC and CD due to the influence of carbonate mineral dissolution. Previous studies have shown that pCO_2 concentration is the major factor controlling the solubility and reactivity of carbonate minerals (Palmer and Cherry 1984). The concentrations of Ca^{2+} and Mg^{2+} increased at a depth of 50 cm close to where the soil contacts the carbonate bedrock at both locations, reflecting the effect of soil solution pCO_2 on carbonate dissolution, with the minerals including calcite or dolomite. The calculated SIs of soil solutions were −1.3±1.0 for calcite and −3.5±1.8 for dolomite. At both locations, the data plot slightly above the 2:1 line for carbonate mineral dissolution with an alkalinity of 0.03–4.6 meq l^{-1} (Fig. 6a). Dolomite dissolution, calcite dissolution, and dolomite and calcite dissolution in equal amounts would produce waters with Mg^{2+}/Ca^{2+} molar ratios of 0, 1, and 0.33, respectively. As shown in Fig. 6b, the Mg^{2+}/Ca^{2+} ratio at CC and CD is <0.1, suggesting that the dissolution of calcite is the main source of the DIC flux. However, some data at CD indicate the relative contribution of Mg-rich carbonates (dolomite) to DIC flux.

Contribution of carbonate dissolution to DIC is also observed by the $\delta^{13}C_{DIC}$ values in shallow and deep soil waters. The data lie close to equilibrium with soil CO_2 and the mixing line between soil CO_2 and DIC from carbonate dissolution (Fig. 5a, b).

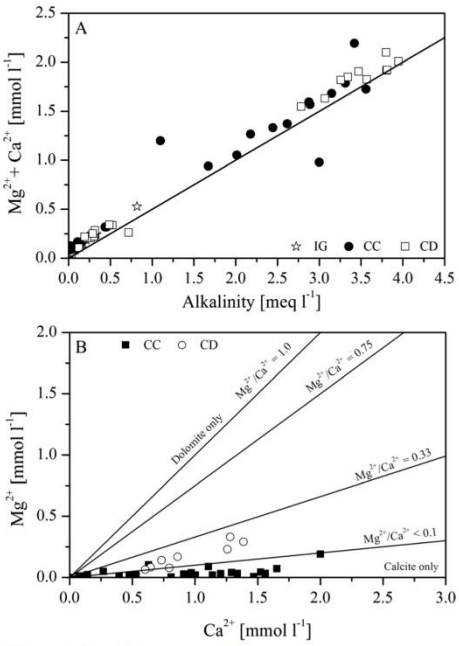


Fig. 6 **a** $Mg^{2+}+Ca^{2+}$ versus alkalinity in soil waters at different sampling sites during the sampling period (2005–2007). The $2HCO_3^-$:1($Ca^{2+}+Mg^{2+}$) relationship is shown as a *solid line* on the plot; **b** concentrations of Mg^{2+} versus Ca^{2+} in soil solutions at CC and CD in Kočevski Rog, with Mg^{2+}/Ca^{2+} ratios of 0.33, 0.75, and 1.0 shown for reference

4.4 Microbial processes and CO_2 outgassing

Comparing the data plots (Fig. 5c–f) between IG and FGS reveals that in the shallow soil at IG, CO_2 has an isotopic signature similar to that of vegetation in winter, with low fractionation or contribution of atmosphere CO_2, while in summer, the soil CO_2 is enriched in ^{13}C by +4 to +8‰ compared to soil carbon. This seasonal variation agrees with the findings of Amiotte-Suchet et al. (1999) who studied in a small granitic catchment in France, but disagrees with the findings of Solomon and Cerling (1987) and Cerling et al. (1991) for a site where soil activity was low during the winter. In our study, the autumnal respiration rate was low (Čater and Ogrinc 2011), and isotopic fractionation accompanying molecular diffusion was insignificant. As a result, the isotopic composition of CO_2 is similar to that of the SOM. At depth, the $\delta^{13}C_{DIC}$ values of soil water are between −21.3 and −14.9 ‰ and show little variation but are higher during the autumn. Higher $\delta^{13}C_{DIC}$ values compared to those in the shallow soil waters indicate an open system equilibration of the DIC with soil CO_2, so that the DIC is enriched in ^{13}C by about 9‰.

At FGS, the trend in seasonal changes of $\delta^{13}C_{DIC}$ is opposite and at all three locations (FGS-A, FGS-B, and FGS-C), and in all three depth profiles, the $\delta^{13}C_{DIC}$ values are higher during the autumn, while during the summer, the average $\delta^{13}C_{DIC}$ values approach the isotopic signature of soil CO_2. Studies have found that the $\delta^{13}C$ of soil becomes less negative during colder months (Reardon et al. 1979; Prada et al. 1983; Solomon and Cerling 1987; Cerling et al. 1991). During these months, CO_2 production is lower, and the shift in $\delta^{13}C$ values is, at least in a part, due to the diffusion of CO_2 from the atmosphere into the soil (Amundson et al. 1997). At FGS, the coarse soil texture composed of fluvioglacial gravels, sands, and coalluvial deposits permits outgassing, which is most pronounced at a depth of 20 cm (Fig. 5f). Further lighter texture soils such as sand loam present at IG and at the depth of 20 cm at FGS respond with more sensitivity to meteorological conditions, and these larger interconnecting pores allow water and air to move freely into and out of the soil representing even the source of CO_2 in the environment.

Alternatively, data presented by Andrews et al. (2000) suggest that this is a result of a temperature-dependent shift in the active microbial community, resulting in remineralization of the C pool.

Also at CC and CD, the $\delta^{13}C_{DIC}$ values of soil waters vary seasonally (Fig. 5a, b) with higher $\delta^{13}C_{DIC}$ values during colder months and lower values in the summer when the amount of SOM degradation and respiration rates are higher (Čater and Ogrinc 2011). The soil texture is loam at CC and clay loam at CD, which is characterized by good structure stability, high porosity, and good water-holding capacity. These characteristics limit isotopic exchange between DIC and atmospheric air.

5 Conclusions

Terrestrial carbon reservoirs in forests respond to climate change and human perturbation in complex ways, with long-term turnover around soil organic matter and short-term dynamics around the plants. This study focused on carbon reservoirs in four forest soils developed on contrasting bedrock geology and the transport of dissolved organic and inorganic when soil waters infiltrate and move to groundwaters and streams. The aim was to better understand carbon dynamics and processes in the soil profiles, sources and transformation of DIC and DOC in soil waters, and the CO_2 consumption by chemical weathering.

The loss of DOC at 5 cm was in the order of 1 mol m^{-2} $year^{-1}$ at all four study sites, although the vegetation coverage varies among sites. Only a small fraction of the DOC remained in soil waters with the majority either sorbed on mineral surfaces, respired, or re-assimilated. A sharp decrease in DOC fluxes observed at IG and FGS is also related to the amount of water percolating through the soil. The drainage of water via macropores in sandy soils present at IG and at the depth of 20 cm at FGS may flush out a substantial amount of DOC.

DIC fluxes followed an opposite trend to DOC fluxes, as the highest DIC fluxes were observed at deeper soils (50 cm), especially at CD and CC, where dolomite and calcite dissolution dominates. Indeed, the C isotope composition of DIC at CD and CC suggested that half of the DIC was from soil CO_2 and the other half from carbonate minerals. Thus, 2 to 5 mol m^{-2} $year^{-1}$ of CO_2 was estimated to be lost through soil waters in dissolved inorganic form. More importantly, the soil waters at CD and CC remained unsaturated with respect to dolomite and calcite, and the continuous dissolution of these carbonate minerals would continue to dissolve more CO_2 until equilibration is reached and thus on a global scale acting as a sink of C. At study sites IG and FGS, however, the DIC fluxes were much lower, ~0.2 mol m^{-2} $year^{-1}$, consistent with slow silicate dissolution kinetics.

This investigation clearly identified local lithology (carbonate-bearing vs carbonate free rocks), types of vegetation (spruce, beech), soil texture (clay, silt, sand), and climate (i.e., water fluxes through balances of precipitation and evapotranspiration) as important factors controlling the magnitude of carbon losses in dissolved organic and inorganic forms. Such studies are crucial in modeling carbon cycling–climate feedbacks.

Acknowledgements The authors are thankful to Mr. Stojan Žigon for technical support. This research was conducted in the framework of two projects, L4-6232 and J7-7397, funded by the Slovenian Research Agency (ARRS). The study is a part of research doctoral dissertation of B. Krajnc supported by Innovative schemes for co-financing of doctoral studies financed by the European Union through the European Social Fund. Special thanks are given to David J. Heath for linguistic corrections, the Editor, and two anonymous reviewers for their constructive comments that improved the quality of the paper.

References

Adams MA, Grierson PF (2001) Stable isotopes at natural abundance in terrestrial plant ecology and ecophysiology: an update. Plant Biol 3: 299–310

Amiotte-Suchet P, Aubert D, Probst JL, Gauthier-Lafaye F, Probst A, Andreux F, Viville D (1999) $\delta^{13}C$ pattern of dissolved inorganic carbon in small granitic catchment: the Strengbach case study (Vosges mountains, France). Chem Geol 159:129–145

Amiotte-Suchet P, Linglois N, Leveque J, Andreux F (2007) ^{13}C composition of dissolved organic carbon in upland forested catchments of the Morvan Mountains (France): influence of coniferous and deciduous vegetation. J Hydrol 335:354–363

Amundson R, Stern L, Baisden T, Wang T (1997) The isotopic composition of soil and soil-respired CO_2. Geoderma 82:83–114

Andrews JA, Matamala R, Westover KM, Schlesinger WH (2000) Temperature effects on the diversity of soil heterotrophs and the $\delta^{13}C$ of soil-respired CO_2. Soil Biol Biochem 32:699–706

Aneja MK, Sharma S, Fleischmann F, Stich SS, Heller W, Bahnweg G, Munch JC, Schloter M (2006) Microbial colonization of beech and spruce litter—influence of decomposition site and plant litter species on the diversity of microbial community. Microb Ecol 52:127–135

Arai H, Tokuchi N (2010) Factors contributing to greater soil organic carbon accumulation after afforestation in a Japanese coniferous plantation as determined by stable and radioactive isotopes. Geoderma 157:243–251

Balesdent J, Mariotti A (1996) Measurement of soil organic matter turnover rate using ^{13}C natural abundance. In: Boutton TW, Yamasaki S-I (eds) Mass spectrometry of soils. Marcel Dekker, New York, pp 83–111

Barber VA, Juday GP, Finney BP (2000) Reduced growth of Alaskan white spruce in the twentieth century from temperature-induced drought stress. Nature 405:668–673

Bird MI, Pousai P (1997) Variations of $\delta^{13}C$ in the surface soil organic carbon pool. Glob Biogeochem Cycles 11:313–322

Bird MI, Šantrůčková H, Lloyd J, Veenendaal EM (2001) Global soil organic carbon pool. In: Schulze E-D et al. (eds) Global Biogeochemical Cycles in the Climate System. Academic Press, pp 185–197

Boström B, Comstedt D, Ekblad A (2007) Isotope fractionation and ^{13}C enrichment in soil profiles during the decomposition of soil organic matter. Oecologia 153:89–98

Bowden RD, Nadelhoffer KJ, Boone RD, Melillo JM, Garrison JB (1993) Contributions of aboveground litter, below ground litter, and root respiration to total soil respiration in a temperate mixed hardwood forest. Can J For Res 23:1402–1407

Buchmann N, Kao W-Y, Ehleringer J (1997) Influence of stand structure of carbon-13 of vegetation, soils, and canopy air within deciduous and evergreen forests in Utah, United States. Oecologia 110:109–119

Cai WJ, Wang Y, Hodson RT (1998) Acid–base properties of dissolved organic matter in the estuarine waters of Georgia, USA. Geochim Cosmochim Acta 62:473–483

Čater M, Ogrinc N (2011) Soil respiration rates and $\delta^{13}C_{CO2}$ in natural beech forest (*Fagus sylvatica* L.) in relation to stand structure. Isot Environ Health Stud 47:221–237

Cerling TE (1991) Carbon dioxide in the atmosphere; evidence from Cenozoic and Mesozioc Paleosols. Am J Sci 291:377–400

Cerling TE, Solomon DK, Quade J, Borman JR (1991) On the isotopic composition of carbon in soil carbon dioxide. Geochim Cosmochim Acta 55:3403–3405

Clark I, Fritz P (1997) Environmental isotopes in hydrology. Lewis Publishers, New York

Cleveland CC, Neff JC, Townsend AR, Hood E (2004) Composition, dynamics, and fate of leached dissolved organic matter in terrestrial ecosystems: results from a decomposition experiment. Ecosystems 7:275–285

Dijkstra P, Ishizu A, Doucett R, Hart SC, Schwartz E, Menyailo OV, Hungate BA (2006) ^{13}C and ^{15}N natural abundance of the soil microbial biomass. Soil Biol Biochem 38:3257–3266

Dixon RK, Solomon AM, Brown S, Houghton RA, Trexier MC, Wisniewski J (1994) Carbon pools and flux of global forest ecosystems. Science 263:185–190

Ehleringer JR, Buchmann N, Flannagan LB (2000) Carbon isotope ratios in belowground carbon processes. Ecol Appl 10:412–422

Fan S, Gloor M, Mahlman J, Pacala S, Sarmiento J, Takahashi T, Tans P (1998) A large terrestrial carbon sink in North America implied by atmospheric and oceanic carbon dioxide data and models. Science 282:442–446

Giardina CP, Ryan MG (2000) Evidence that decomposition rates of organic carbon in mineral soil do not vary with temperature. Nature 404:858–861

Gran G (1952) Determination of the equivalence point in potentiometer titration. Part II, Analyst 77:661–671

Guggenberg G, Kaiser K (2003) Dissolved organic matter in soil: challenging the paradigm of sorptive preservation. Geoderma 113:293–310

Hamilton JG, DeLucia EH, George K, Naidu SL, Finzi AC, Schlesinger WH (2002) Forest carbon balance under elevated CO_2. Oecologia 131:250–260

Högberg P (1997) ^{15}N natural abundance in soil-plant systems. New Phytol 137:179–203

Houghton RA, Davidson EA, Woodwell GM (1998) Missing sinks, feedbacks, and understanding the role of terrestrial ecosystems in the global carbon balance. Global Biogeochem Cycles 12(1):25–34

Houghton RA, Hackler JL, Lawrence KT (1999) The U.S. carbon budget: contributions from land-use change. Science 285:574–578

Hungate BA, Holland EA, Jackson RB, Chapin FS, Mooney HA, Field CB (1997) The fate of carbon in grasslands under carbon dioxide enrichment. Nature 388:576–579

IPCC (2013) Climate Change 2013: The Physical Science Basis. Contribution of Working Group I to the Fifth Assessment Report of the Intergovernmental Panel on Climate Change. Stocker TF, Qin D, Plattner G-K, Tignor M, Allen SK, Boschung J, Nauels A, Xia Y, Bex V, Midgley PM (eds) Cambridge University Press, Cambridge, United Kingdom and New York, NY, USA, Chapter 6: Carbon and Other Biogeochemical Cycles, pp 514–552

Jin L, Ogrinc N, Hamilton SK, Szramek K, Kanduč T, Walter LM (2009) Inorganic carbon isotope systematics in soil profiles undergoing silicate and carbonate weathering (Southern Michigan, USA). Chem Geol 264:139–153

Jin L, Ogrinc N, Yesavage T, Hasenmueller EA, Ma L, Sullivan PL, Kaye J, Duffy C, Susan L, Brantley SL (2014) The CO_2 consumption potential during gray shale weathering: insights from the evolution of carbon isotopes in the Susquehanna Shale Hills critical zone observatory. Geochim Cosmochim Acta 142:260–280

Kaiser K, Guggenberger G (2000) The role of DOM sorption to mineral surfaces in the preservation of organic matter in soils. Org Geochem 31:711–725

Kaiser K, Gugenberger G, Haumaier L, Zech W (2001) Isotopic fractionation of dissolved organic carbon in shallow forest soils as affected by sorption. Eur J Soil Sci 52:585–597

Kalbitz K, Solinger S, Park JH, Michalzik B, Matzner E (2000) Controls on the dynamics of dissolved organic matter in soils: a review. Soil Sci 165:277–304

Kanduč T, Szramek K, Ogrinc N, Walter LM (2007) Origin and cycling of riverine inorganic carbon in the Sava River watershed (Slovenia) inferred from major solutes and stable carbon isotopes. Biogeochem 86:137–154

Kindler R, Siemens J, Kaiser K, Walmsley DC, Bernhofer C, Buchmann N, Cellier P, Eugster W, Gleixner G, Grünwald T, Heim A, Ibrom A, Jones SK, Jones M, Klumpp K, Kutsch W, Larsen KS, Lehhuger S, Loubert B, McKenzie R, Moors E, Osborne B, Pilegaard K, Rebmann C, Saunders M, Schmidt MWI, Schrumpf M, Deyeferth J, Skibas U, Soussana J-F, Sutton MA, Tefs C, Vowinckel B, Zeeman MJ, Kaupenjohhann M (2011) Dissolved carbon leaching from soil is a crucial component of the net ecosystem carbon balance. Glob Change Biol 17:1167–1185

Kramer C, Gleixner G (2008) Soil organic matter in soil depth profiles: distinct carbon preferences of microbial groups during carbon transformation. Soil Biol Biochem 40:425–433

Lindroos A-J, Derome J, Mustajärvi K, Nöjd P, Beuker E, Helmisaari H-S (2008) Fluxes of dissolved organic carbon in stand throughfall and percolation water in 12 boreal coniferous stands on mineral soils in Finland. Boreal Environ Res 13(suppl B):22–34

Ludwig N, Heil B, Flessa H, Beese F (2000) Dissolved organic carbon in seepage water—production and transformation during soil passage. Acto hydrochimica et hydrobiologica 28:77–82

Makarov MI, Malysheva TI, Cornelissen JHC, van Logtestijn RSP, Glasser B (2008) Consistent patterns of ^{15}N distribution through soil profiles in diverse alpine and tundra ecosystems. Soil Biol Biochem 40:1082–1089

Marschner B, Kalbitz K (2003) Controls of bioavailability and biodegradability of dissolved organic matter in soils. Geoderma 113:211–235

Melillo JM, Aber JD, Linkins AE, Ricca A, Fry B, Nadelhoffer K (1989) Carbon and nitrogen dynamics along the decay continuum: plant litter to soil organic matter. Plant Soil 115:189–198

Michalzik B, Kalbitz K, Park JH, Solinger S, Matzner E (2001) Fluxes and concentrations of dissolved organic carbon and nitrogen—a synthesis for temperate forests. Biogeochem 52:173–205

Myneni RB, Keeling CD, Tucker CJ, Asrar G, Nemani RR (1997) Increased plant growth in the northern high latitudes from 1981 to 1991. Nature 386:698–702

Nadelhoffer KJ, Fry B (1988) Controls of natural nitrogen-15 and carbon-13 abundances in forest soil organic matter. Soil Sci Soc Am J 52:1633–1640

Nadelhoffer KJ, Emmett BA, Gundersen P, Kjonaas OJ, Koopmans CJ, Schleppi P, Tietema A, Wright RF (1999) Nitrogen deposition makes a minor contribution to carbon sequestration in temperate forests. Nature 398:145–148

Nieminen TM (ed) (2011) Soil solution collection and analysis. Addentum to: ICP Forests (201). Manual on Methods and Criteria

for Harmonized Sampling, Assessment, Monitoring and Analysis of the Effects of Air Pollution on Forest. UNECE ICP Forests Programme. Co-ordinating Centre Hamburg. www.icp-forests.org/manual.html

Nilsson SI, Berggren D, Westling O (1998) Retention of deposited NH_4-N and NO_3-N in coniferous forest ecosystems in southern Sweden. Scand J For Res 13:393–401

Ogrinc N, Simončič P, Kovač N (2012) Soil organic matter characterization at different forest stands in Slovenia. In: Björklund PA, Mello FV (eds) Soil organic matter: ecology, environmental impact and management. Nova Science Publishers, New York, pp 89–110

Palmer CD, Cherry JA (1984) Geochemical evolution of groundwater in sequence of sedimentary rocks. J Hydrol 75:27–65

Parkhurst DL, Appelo CAJ (1999) User's guide to PHREEQC (version 2) – a computer program for speciation, batch – reaction, one – dimensional transport, and inverse geochemical calculations. Water – Resources Investigations Report 99–4259

Peichl M, Moore TR, Arain A, Dalva M, Brodkey D, McLaren J (2007) Concentrations and fluxes of dissolved organic carbon in an age-sequence of white pine forests in Southern Ontario, Canada. Biogeochem 86:1–17

Powers JS, Schlesinger WH (2002) Geographic and vertical patterns of stable carbon isotopes in tropical rain forest soils of Costa Rica. Geoderma 109:141–160

Prada CB, Long A, Davis SN (1983) Stable-isotopic composition of soil carbon dioxide in the Tucson Basin, Arizona, USA. Isot Geochem 1: 219–236

Pregitzer KS, Zak DR, Maziasz J, DeForest J, Curtis PS, Lussenhop J (2000) Interactive effects of atmospheric CO_2 and soil-N availability on fine roots of Populus tremulodies. Ecol Appl 10:18–33

Reardon EJ, Allison GB, Fritz P (1979) Seasonal chemical and isotopic variations of soil CO_2 at Trout Creek, Ontario. J Hydol 43:355–371

Richter DD, Markewitz D, Trumbore SE, Wells CG (1999) Rapid accumulation and turnover of soil carbon in a re-establishing forest. Nature 400:56–58

Sanderman J, Amundson R (2008) A comparative study of dissolved organic carbon transport and stabilization in California forest and grassland soils. Biogeochem 89:309–327

Schimel D, Melillo J, Tian H, McGuire AD, Kicklighter D, Kittel T, Rosenbloom N, Running S, Thornton P, Ojima D, Parton W, Kelly R, Sykes M, Neilson R, Rizzo B (2000) Contribution of increasing CO_2 and climate to carbon storage by ecosystems in the United States. Science 287:2004–2006

Solomon DK, Cerling TE (1987) The annual carbon dioxide cycle in a montane soil: observations and implications for weathering. Water Res 23:2257–2265

Stout JD, Goh KM, Rafter TA (1981) Chemistry and turnover of naturally occurring resistant organic compounds in soil. In: Paul EA, Ladd JN (eds) Soil biochemistry. Marcel Dekker, New York, pp 1–73

Stumm W, Morgan JJ (1996) Aquatic chemistry: chemical equilibria and rates in natural waters, 3rd edn. Wiley, New York

Trumbore SE, Chadwick OA, Amundson R (1996) Rapid exchange between soil carbon and atmospheric carbon dioxide driven by temperature change. Science 272:393–396

Urbančič M, Kobal M, Vilhar U, Simončič P (2009) Zaloge organske snovi v izbranih sestojih na bukovih rastiščih – Evaluation of the organic matter at selected research objects of beech sites. Trajnostna raba lesa v kontekstu sonaravnega gospodarjenja z gozdom, pp 15–25

Van Veen JA, Liljeroth E, Lekkerkerk LJA, van de Geijn SC (1991) Carbon fluxes in plant-soil systems at elevated atmospheric CO_2 levels. Ecol Appl 1(2):175–181

Vogel JC (1993) Variability of carbon isotope fractionation during photosynthesis. In: Ehleringer JR, Hall AE, Farquar GD (eds) Stable isotopes and plant carbon-water relations. Academic Press, San Diego, pp 29–38

Waldron S, Scott EM, Vihermaa LE, Newton J (2014) Quantifying precision and accuracy of measurements of dissolved inorganic carbon stable isotopic composition using continous-flow-isotope-ratio mass spectrometry. Rapid Commun Mass Spectrom 28:1117–1126

Wang Y, Hsieh Y-P (2002) Uncertainties and novel prospects in the study of the soil carbon dynamics. Chemosphere 49:791–804

Wedin DA, Tieszen LL, Dewey B, Pastor J (1995) Carbon isotope dynamics during grass decomposition and soil organic matter formation. Ecology 76:1383–1392

Williams MA, Rice CW, Owensby CE (2006) Natural ^{15}N abundance in a tallgrass prairie exposed to 8-y of elevated atmospheric CO_2. Soil Biol Biochem 38:409–412

Wynn JG, Harden JF, Fries TL (2006) Stable carbon isotope depth profile and soil organic carbon dynamics in the lower Mississippi Basin. Geoderma 131:89–109

3.3 Scientific Paper: "Soil CO_2 sources above subterranean cave - Pisani rov (Postojna Cave, Slovenia)"



In this chapter the paper entitled "Soil CO_2 sources above subterranean cave - Pisani rov (Postojna Cave, Slovenia" by Bor Krajnc, Mitja Ferlan and Nives Ogrinc is presented. The paper was published in the Journal of Soils and Sediments, 2016.

The objective of this research was to detect possible abiotic CO_2 sources of soil CO_2 above a subterranean cave. Recent studies of carbonate ecosystems have revealed that although the biological sources (soil respiration) represent the main contributors of soil CO_2, the abiotic exchange processes can in certain locations temporarily significantly contribute to net CO_2 exchange. Those events were observed by several researchers that were investigating soil CO_2 fluxes in karstic areas. Some of these researches assumed the subterranean caves as temporary means of CO_2 storage. When subterranean caves ventilate, they may represent the abiotic mechanism influencing soil CO_2.

The presented research was performed on the forest soil above Pisani rov (Postojna Cave) and in the Pisani rov. Soil gas, atmospheric air and cave air CO_2 carbon stable isotope composition and CO_2 concentrations were measured together with several meteorological parameters, at locations above the cave and at the control sampling location.

As the first step, the correlations of soil CO_2 concentrations with meteorological data that are known to control the biotic CO_2 source (temperature and soil water content) were compared between test and control sampling location. Data showed that at the location above the cave the variance of the CO_2 in certain occasions in fall could not be explained by meteorological factors, indicating that there must be additional mechanisms influencing the soil CO_2 concentrations above the cave.

The second step was to use the stable isotope approach. Stable isotopes are a very useful tool for detecting the presence of CO_2 with distinct isotopic composition (in relation to soil respired CO_2), e.g. CO_2 coming from carbonate dissolution precipitation processes. Two-end-member model was used in the time series of carbon isotopic compositions of soil CO_2 to assess the moment when the unknown source with distinct isotopic composition affects the overall soil CO_2 isotopic composition. The idea was that end-members in the two-end-member model should be constant if indeed only two end-members are present. In the case of the presence of the third end-member, with distinctive isotopic signature, the value of the "constant" end-member should suddenly change. This shift was observed for the soil CO_2 above the cave. The highest changes were observed in fall and spring, which are the typical transitional periods when most of the cave ventilation happens. The time of the "shifts" also coincided with the observed cave ventilation below the sampling location, suggesting that cave ventilation is the mechanism affecting the soil CO_2. A rough estimate indicates that if the assumptions are correct, the cave air CO_2 can account for up to 80% of the overall soil CO_2 during the ventilation.

Part of this work was also presented as an oral presentation at the 22nd International Symposium on Environmental Biogeochemistry (ISEB22), 28 September – 2 October 2015 in Piran, Slovenia, and as an oral and poster presentation at the 8th Jožef Stefan

International Postgraduate School Students' Conference, 31 May – 1 June 2016 in Ljubljana, Slovenia.

In this paper, the candidate developed the research question, the method for continuous measurements and collection of the field data of soil temperature, moisture and soil CO_2 fluxes. Further, he installed the instruments for continuous field measurements at two sites (sampling site above the cave and control site), together with the power supply installation (Solar cell, batteries chargers and regulators) and maintenance. The candidate also collected all the required documents and permissions for installation of the measurement systems in the forest. He performed all the drillings used for installation for the temperature sensors. He organized all the field trips and performed all additional sampling collections, data collections and additional manual measurements every two weeks. The candidate installed the sampling tubes in the soil and performed sampling of soil air and atmospheric air every two weeks. For $\delta^{13}C$ measurements he collected the soil air samples into pre-evacuated 12 ml glass vials, soil samples, and rock samples. He performed all laboratory preparation of the samples prior to analysis and conducted the analysis using IRMS. Soil samples for pedological analysis were sent to the Laboratory of Slovenian Institute of Hop Research and Brewing in Slovenia. He performed raw-data manipulation (from the continuous measuring instruments) and data analysis using different statistical approaches in R statistical environment (R Core Team, 2014). The candidate interpreted the data and wrote the manuscript..

J Soils Sediments (2017) 17:1883–1892
DOI 10.1007/s11368-016-1543-x

ISEB 2015: BIOGEOCHEMICAL DYNAMICS OF SEDIMENT-WATER SYSTEMS: PROCESSES AND MODELLING

Soil CO_2 sources above a subterranean cave—Pisani rov (Postojna Cave, Slovenia)

Bor Krajnc[1,2] · **Mitja Ferlan**[3] · **Nives Ogrinc**[1,2]

Received: 7 March 2016 / Accepted: 29 August 2016 / Published online: 10 September 2016
© Springer-Verlag Berlin Heidelberg 2016

Abstract
Purpose The objective of this research is to detect abiotic sources of soil CO_2 above a subterranean cave in the Slovenian karst region.
Materials and methods The research was performed in the forest above Pisani rov (Postojna Cave) near the town of Postojna (SW Slovenia) and also in the cave. Soil gas, atmospheric air and cave air carbon stable isotope composition ($\delta^{13}C_{CO2}$) and CO_2 concentration were measured. Sampling and measurements were performed bi-monthly at the test and control sites above the cave. The abiotic source of soil CO_2 was estimated using a stable isotope mass balance calculation.
Results and discussion Similar seasonal patterns of soil CO_2 and $\delta^{13}C_{CO2}$ values were observed at both the test and control sites until spring, with higher levels of CO_2 observed in summer and lower in winter. The $\delta^{13}C_{CO2}$ showed the opposite trend, i.e. lower values (−26 to −20 ‰) in summer and higher values (up to −17 ‰) in winter and early spring. In spring, the soil CO_2 concentration decreases and the $\delta^{13}C_{CO2}$ value increases only at the control site. A time series of a modelled "isotopically light" endmember revealed large shifts in the data values, due to the presence of an abiotic CO_2 source. Results suggest that the subterranean CO_2 pool and its ventilation is the main source of soil CO_2, accounting for up to 80 % of the soil gas during cold periods.
Conclusions Ventilation from subterranean cavities is an important source of soil CO_2 in karstic areas and should be taken into account during carbon cycling studies.

Keywords Abiotic sources · Karst region · Soil CO_2 · Stable isotopes · Ventilation

Responsible editor: Jadran Faganeli

✉ Bor Krajnc
bor.krajnc@ijs.si

[1] Jožef Stefan International Postgraduate School, Jamova 39, 1000 Ljubljana, Slovenia

[2] Department of Environmental Sciences, Jožef Stefan Institute, Jamova 39, 1000 Ljubljana, Slovenia

[3] Slovenian Forestry Institute, Večna pot 2, 1000 Ljubljana, Slovenia

1 Introduction

Understanding the global carbon cycle is gaining importance due to increasing atmospheric CO_2 concentrations. Soil plays a significant role in the carbon cycle (Raich and Schlesinger 1992), since it acts as both a major sink and source of atmospheric CO_2 (Amundson 2001; Raich et al. 2002). The distinction between soil CO_2 sources and their controlling mechanisms is important because soil carbon has a different turnover rate and responds differently to changing environmental conditions. Most soil CO_2 is derived from the interaction of two biological sources: autotrophic respiration from plant roots and heterotrophic respiration, i.e. microbial decomposition of plant litter and soil organic matter (SOM) (Kuzyakov 2006). The CO_2 from these sources is defined as soil-respired CO_2 (Doerr and Münnich 1986; Cerling et al. 1991). Soil CO_2 also mixes with CO_2 from the atmosphere, which can enter soil via diffusion, convection or rain water. Recent studies of carbonate ecosystems have revealed that abiotic exchange processes can also contribute temporally to net CO_2 exchange, and although, on a global scale, this is considered of minor importance (Kuzyakov 2006), there are a growing number of studies reporting its significance to soil CO_2 fluxes (Kowalski et al. 2008; Serrano-

Ortiz et al. 2010; Čater and Ogrinc 2011; Plestenjak et al. 2012). Several studies have focused on subterranean cavities as a temporary means of CO_2 storage and as an abiotic mechanism influencing soil CO_2 (Kowalski et al. 2008; Serrano-Ortiz et al. 2010). As a first approximation, estimates indicate that the ventilation of subterranean CO_2 from the pores, fissures and cavities present in the karst environment accounts for more than half of the total CO_2 content of the atmosphere (Serrano-Ortiz et al. 2010). Subterranean caves can act as a temporal reservoirs accumulating CO_2 from different sources, e.g. atmosphere, soil respiration, dissolution of carbonate rock, via percolating water, diffusion or advection. The CO_2 that accumulates in caves can be "exhaled" back to the atmosphere. Different environmental conditions such as temperature, atmospheric pressure changes, rainfall and wind can regulate this cave ventilation. In addition, the ventilation depends on the shape and position of the cave, its passages, entrances and other connections with the outside atmosphere. The ventilation of Pisani rov was observed also in the study performed by Gregorič et al. (2013). In their study, it was found that the main trigger for ventilation was the outside temperature, i.e. the difference between densities of cold and warm air. In the case when outside temperatures were lower than cave temperatures, the colder outside air caused the increase of warmer cave air, which escaped the cave through vertical cracks and fissures. When outside temperatures were below freezing point, the snow layer and frozen water prevented cave ventilation. During warmer periods, when outside temperatures were higher than cave temperatures, CO_2 in Pisani rov started to accumulate again. Rainfall and air pressure changes have no significant influence on cave ventilation in Pisani rov. These observations are typical for so-called thermal caves, where during the warm season CO_2 accumulates and during the cold season, the cave ventilates (Domínguez-Villar et al. 2015).

Chemical reactions, along with different physical and biological processes that affect soil CO_2 can be studied using stable isotopes. Stable carbon isotope composition of soil CO_2 ($\delta^{13}C_{CO2}$) depends on several factors starting with soil-respired CO_2 that reflects the $\delta^{13}C$ values of the local flora. Root respiration and SOM microbial decomposition produce CO_2 with $\delta^{13}C$ values similar to plant material at a specific location (Cerling et al. 1991). The possible fractionation effects during decomposition of plant litter into SOM are usually less than 2 ‰ (Kuzyakov 2006). Isotopic composition of plant material mostly depends on the different photosynthetic pathways, which help plants to avoid the photorespiration. On the base of those pathways, C3, C4 and CAM plants can be distinguished, where C3 plants are the most prone to photorespiration, especially in hot and dry conditions. At these conditions, C4 and CAM plants have developed different more efficient mechanisms for carbon fixation, which are on the other hand also more energy demanding. Therefore, C4 and CAM plants are more frequent in hot and dry environments, while C3 plants are widely represented in cold and temperate environments, e.g. Slovenia. Because C3 plants are less efficient during CO_2 fixation from the atmosphere, also carbon isotopic fractionation is higher in C3 plants than in C4 plants. The $\delta^{13}C$ values of plant tissues from C3 plants are about −27 ‰ (−35 to −20 ‰); from C4 plants, values are around −13 ‰ (−15 to −7 ‰) (Kuzyakov 2006), while those values from CAM plants are between them. Another important factor affecting the isotopic composition of soil CO_2 are the different diffusivities of $^{12}CO_2$ in comparison to $^{13}CO_2$ in the soil pore space, which results in an isotopic composition of soil CO_2 approximately 4.4 ‰ higher than soil-respired CO_2 (Cerling and Quade 1993; Davidson 1995). The isotopic composition of soil CO_2 also depends on the proportion of atmospheric CO_2 in the soil CO_2, which increases the soil $\delta^{13}C$ value. According to GLOBALVIEW-CO2C13 (2009), the average global atmospheric CO_2 isotopic composition ($\delta^{13}C_{atm}$) is about −8 ‰. GLOBALVIEW-CO2C13 is a database of spatial and temporal distribution of atmospheric CO_2 and its stable isotopic compositions on a global scale. This database is operated by the University of Colorado (CU), Institute of Arctic and Alpine Research (INSTAAR), Stable Isotope Laboratory (SIL). The proportion of atmospheric CO_2 in soil CO_2 depends on soil depth and soil respiration rate. The final factor affecting soil CO_2 $\delta^{13}C$ values is the contribution of CO_2 derived from carbonate weathering. The $\delta^{13}C$ value of the carbonate bedrock ($\delta^{13}C_{CaCO3}$) has normally a narrow, close-to-zero range (0–4 ‰). Due to this rather large difference, relative to biogenic sources, the formation of CO_2 from carbonate bedrock dissolution and precipitation processes can influence the isotopic signature of soil CO_2 even at low contributions.

The aim of this study is to determine the influence that cave ventilation has on soil CO_2 using a stable isotope approach and to understand the biogeochemical processes that govern the soil CO_2 flux balance. More than 40 % of the Slovenian territory is situated on carbonate bedrock (limestone and dolomite) and although Slovenian karst is one of the most studied worldwide, no information exists about the overall carbon mass balance in karst areas. Our recent studies indicate that the abiotic pool contributes significantly to the soil CO_2 flux (on average 12 %) in karst forested areas (Čater and Ogrinc 2011) and grasslands (Plestenjak et al. 2012), but it is not known if these processes are the consequence of weathering conditions or cave ventilation. The role of karstic cavities in net ecosystem carbon fluxes in semiarid drylands is relatively well understood (Kowalski et al. 2008; Cuezva et al. 2011), but in humid forested areas, soil moisture may play

a crucial role in CO_2 transfer from underground through the soil back to the atmosphere.

2 Materials and methods

2.1 Study sites

This study was conducted at two sampling sites (Fig. 1) within the Velika Jeršanova dolina located in the forest near Postojna, Slovenia (45° 47′ N, 14° 12′ E). The Postojna region has a continental climate with a mean annual temperature of 9.3 °C (period from 1981 to 2010). January has the lowest average temperature (−0.1 °C) and July the highest (19.0 °C). The mean annual precipitation is 1500 mm with no clear seasonal variation, although precipitation is more abundant in autumn (ARSO 2015). The amount or precipitation during the study period is presented in Fig. 2. The site is located at 575 m a.s.l. and is placed on the collapse blocks of the micritic limestone (Šebela and Čar 2000) on the SE edge of Velika Jeršanova dolina. It is surrounded by Omphalodo-Fagetum forest with mainly C3 vegetation.

Two study sites were selected: the first (AC) was located directly above the Rdeča dvorana (hall at the end of Pisani rov), while the second (NC) was a control site located at the bottom of Velika Jeršanova dolina, where no underground cavities are expected. The area was scanned with the ground-penetrating radar. The location with most fractured bedrock was chosen for the AC sampling site as the most suitable location to detect the influence of ventilation from the underlying cave. At this location, soil thickness is ~0.2 m with more than 1 m deep soil pockets. Soil thickness at NC site is deeper than 4 m. Unfortunately, we were not able to determine the absolute soil thickness, since the maximum length of the sampling auger

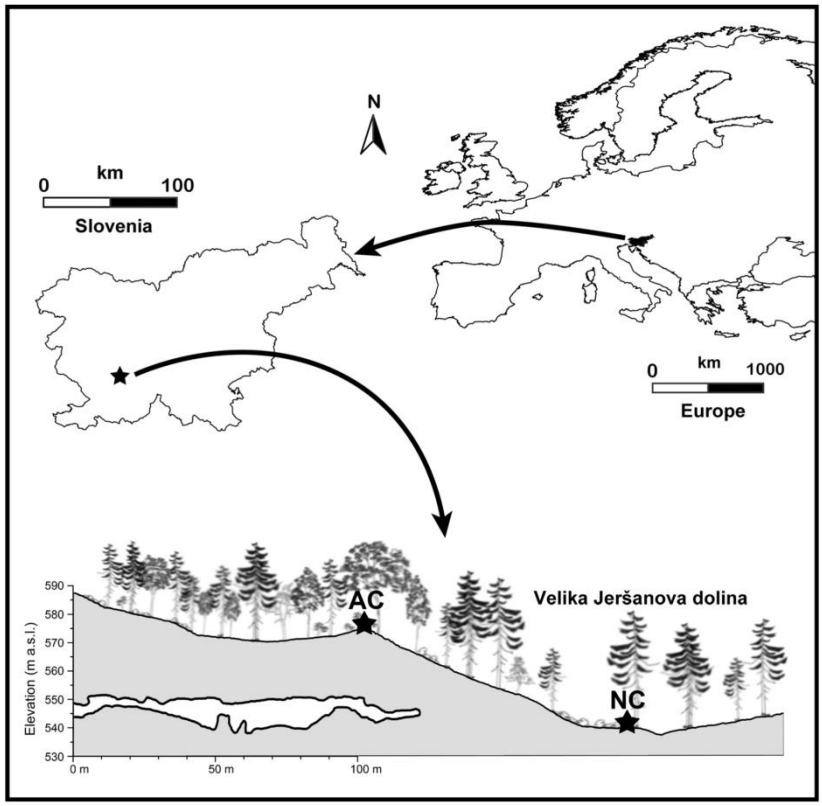


Fig. 1 Location of the study site in Velika jeršanova dolina and Pisni Rov with marked sampling sites. Above the cave (*AC*) and control site (*NC*)

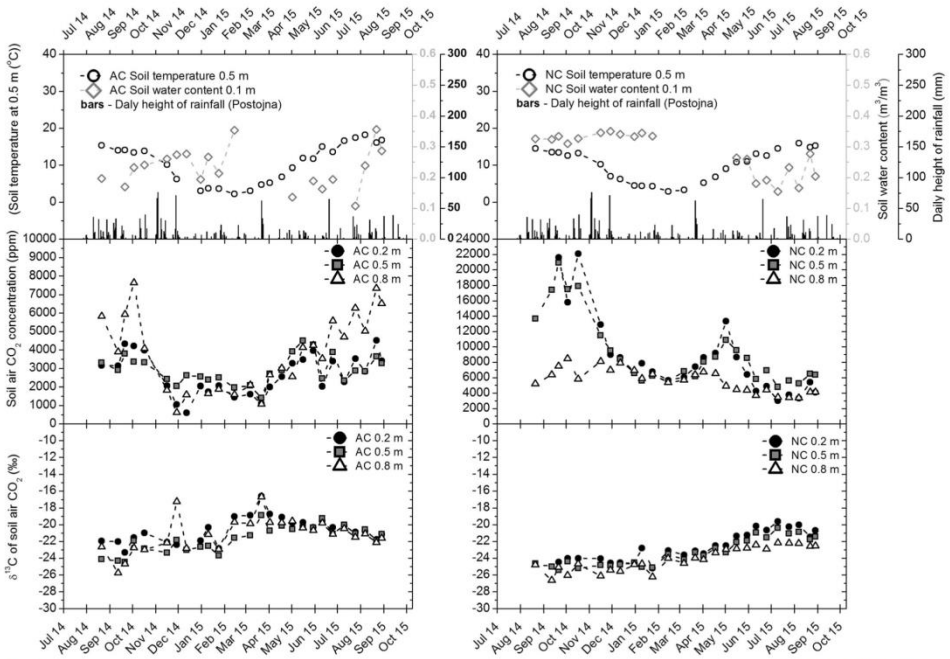


Fig. 2 Time series of soil water content (*SWC*) of the top soil layer, soil temperatures (T_{soil}) at 0.5 m and daily amount of rainfall (ARSO 2015), with soil CO_2 concentrations and $\delta^{13}C$ composition of soil gas CO_2 at three different depths of 0.2, 0.5 and 0.8 m at the AC and NC sites

was 4 m. Pisani rov is a 920-m long dead-end gallery of the Postojna Cave system, which is closed to tourists (Fig. 1). It consists of series of big halls and narrow passages. It deviates from the main Postojna Cave passage to the north and terminates below the slopes of the Velika Jeršanova dolina. Sampling site in Pisani rov is located in Rdeča dvorana at 529 m a.s.l. with cave ceiling ~10 m high. The thickness of the cave ceiling between Rdeča dvorana and the surface is ~30 m (Šebela 2010). The Rdeča Dvorana has very limited ventilation dynamics compared to the rest of the Postojna Caves with some of the highest recorded CO_2 and ^{222}Rn concentrations (Gregorič et al. 2013). The temperature is very stable (8.4 °C) with <0.07 °C thermal change for 5 years (2009–2013) monitoring (Domínguez-Villar et al. 2015).

2.2 Sampling and analyses

Soil gas samples were collected using a Neznal's probe (Barnet et al. 2008) inserted into the soil to a depth of 0.2, 0.5 and 0.8 m. On the top of the probes, a silicone tube with a two-way valve was installed to prevent the direct connection with atmospheric air and to facilitate the sampling. Atmospheric and cave air was sampled directly from the forest air and cave atmosphere in Rdeča dvorana respectively. Sampling was performed every 2 weeks from August 2014 to September 2015. Soil gas and atmospheric and cave air for stable isotope analysis were sampled with 60-ml plastic disposable syringes, injected into pre-evacuated 12-ml septum-capped glass vials (Labco Exetainer®, UK), transported into the laboratory and analysed within 48 h.

Carbon dioxide concentrations in the atmospheric and cave air were measured using a non-dispersive infrared (IR) absorption detector (TESTO-453, TESTO, Germany). The time interval and resolution of each measurement were 10 min and 1 ppm (*v*/v), respectively. The same probe was also used to measure relative humidity and the temperature. Calibration of the CO_2 measurements was performed by the manufacturing company (TESTO, Germany). The accuracy of the measurements was ±50 ppm for measured CO_2 concentrations, lower than 5000 ppm and ±100 ppm for the measured CO_2 concentrations higher than 5000 ppm. All CO_2 measurements were corrected for the influence of standard atmospheric pressure (1013 hPa) as suggested by Spötl et al. (2005). Successive half-hourly mean soil moisture (soil water content—SWC) at a soil depth of 10 cm and soil temperature (TS) at a depth

of 1.0, 0.5, 1.3 and 4 m were obtained using soil FDR sensors and thermocouples, respectively.

The stable isotope composition of CO_2 ($\delta^{13}C_{CO2}$) was determined according to the procedures of Knohl et al. (2004) and Spötl (2004), using a Europa Scientific 20-20 isotope ratio mass spectrometer (IRMS) with ANCA-TG preparation module for trace gas samples. Soil CO_2 concentrations were determined according to Meyer et al. (2014) by IRMS measurements from the soil gas collection volume and the m/z 44 peak area. Calibration was achieved by measuring known volumes of a standard gas.

Soil samples for pedological and stable isotope analyses from the AC and NC sites were taken from the same depths as for gas sampling, using a soil auger. Samples were dried and homogenized according to ISO 11464 (ISO 11464, 2006). Standard pedological analyses were performed at the Laboratory of Slovenian Institute of Hop Research and Brewing, Slovenia, where soil texture, pH, soil organic carbon (SOC) and total nitrogen (N_{tot}) were determined. Subsamples for soil organic carbon stable isotope composition ($\delta^{13}C_{SOC}$) were further treated with 1 M HCl to remove carbonate material. Samples were analysed with IRMS Europa Scientific 20-20 with an ANCA-SL preparation module for solid and liquid samples. Sample analyses were validated against the reference materials NBS 22 and IAEA-CH-7.

Samples for stable carbon isotope analysis of the parent rock material $CaCO_3$ ($\delta^{13}C_{CaCO3}$) were taken from surface rocks and drillings from both sites and from rock material inside the cave. Samples were ground to a powder in an agate mortar, placed into glass vials, flushed with helium and reacted with anhydrous H_3PO_4. The released CO_2 was analysed by IRMS using a Europa Scientific 20-20 instrument with an ANCA-TG preparation module for trace gas samples. Sample analyses were validated against the reference materials NBS 18 and NBS 19. All stable isotope results are reported using the conventional delta (δ)-notation in per mil (‰) relative to the VPDB reference standard. The precision of the measurements was ±0.2 ‰ for $\delta^{13}C_{CO2}$, $\delta^{13}C_{SOC}$ and $\delta^{13}C_{CaCO3}$.

3 Results

3.1 Soil and parent rock characteristics

Soil properties at the selected depth are presented in Table 1. Soils at AC are shallow Rendzic Leptisols and Cambisols with occasional soil pockets and superficial rockiness of about 70 %, while soils at the NC site are deep Chromic Luvisols. The soils have average pH values of 6.0 ± 0.1 and 4.6 ± 0.2, SOC concentrations of 6.3 ± 3.9 and 1.9 ± 1.1 %, N_{tot} concentrations of 0.5 ± 0.26 and 0.17 ± 0.09 %, C/N mass ratio of 11.8 ± 2.4 and 11.3 ± 0.1 at AC and NC, respectively. The $\delta^{13}C_{SOC}$ values show a slight increase toward more positive values with depth with similar average $\delta^{13}C_{SOC}$ values of −25.2 ± 0.1 and −25.7 ± 0.5 ‰ at AC and NC, respectively. The $\delta^{13}C_{CaCO3}$ value of the parent rock is 1.6 ± 0.18 ‰ (SD).

3.2 Soil and atmosphere CO_2 concentrations and stable isotope composition

Soil CO_2 values at the AC site were in the range from 1000 to 7600 ppm with an average value of 3200 ± 1400 ppm, while at NC, the concentrations were higher (from 3000 to 22,000 ppm) with an average value of 7800 ± 4200 ppm. No increase in soil CO_2 with depth was observed at either sampling site. Time series of measured parameters is presented in Fig. 2. Seasonal patterns, i.e. low CO_2 concentrations from November 2014 to March 2015 and higher from May to September 2015 were observed at AC (Fig. 2). The concentration of soil CO_2 follows the same trend as soil temperature. A similar observation was made at NC; however, the soil CO_2 concentrations decrease again in late May together with decreasing SWC. A different behaviour was observed at a depth of 0.8 m at NC. These discrepancies are most likely related to the different processes that govern soil CO_2 production and transport. In the soil auger samples, blue-grey spots were present, which indicate the presence of a pseudogleyic layer due to low water permeability and

Table 1 Description of the soil properties

Location	Depth (m)	pH	N_{tot} (%)	C_{org} (%)	$\delta^{13}C_{SOC}$ (‰)	C/N	Ca^{2+} (mekv/100 g)	Mg^{2+} (mekv/100 g)	Texture			
									Sand (%)	Silt (%)	Clay (%)	Class (USDA)
AC	0.2	5.9	0.58	7.7	−25.3	13.3	44.7	1.38	26.4	31.8	41.8	Clay
	0.5	6.1	0.72	9.5	–	13.2	44.0	1.65	23.4	33.9	42.7	Clay
	0.8	–	0.21	1.9	−25.1	9.0	51.4	0.52	–	–	–	–
NC	0.2	4.4	0.27	3.1	−26.1	11.5	0.86	0.19	23.2	50.8	26.0	Silt loam
	0.5	4.6	0.16	1.8	−25.9	11.3	0.96	0.17	27.8	43.5	28.7	Clay loam
	0.8	4.8	0.08	0.9	−25.2	11.3	6.80	1.06	20.8	43.7	35.5	Clay loam

its stagnation. No influence of the ground water to soil formation is present. Pivka River enters Postojna cave at 510 m a.s.l., and the NC site at the bottom of the Velika Jeršanova dolina is situated at 530 m a.s.l. Stagnation of rainfall water in the soil layers with low permeability is assumed to be the main reason for the formation of the pseudogleyic layer. Low permeability of wet soils affects CO_2 transport and in soil anaerobic conditions can occur due to the lower diffusivity of CO_2 through water-filled pores, smaller oxygen reservoirs and simulation of respiration caused by solubility and movement of nutrients (Tiedje et al., 1984).

The $\delta^{13}C_{CO2}$ values show an opposite trend to the CO_2 concentrations due to the mixing of CO_2 from soil respiration with atmospheric CO_2. The $\delta^{13}C_{CO2}$ were from −26 to −10 ‰ at AC and from −27 to −19 ‰ at NC. The highest $\delta^{13}C_{CO2}$ values at AC were observed in late November 2014 and March 2015, while the highest $\delta^{13}C_{CO2}$ values at NC were observed in July to August 2015. The lowest $\delta^{13}C_{CO2}$ values at both sites were observed in September 2014. A typical negative statistically significant linear correlation exists between log (pCO_2) and $\delta^{13}C_{CO2}$ values. Nevertheless, the correlation coefficients of these two parameters at the depth of 0.5 and 0.8 m are significantly lower at the AC site ($R^2 = 0.02$, $p = 0.454$ and $R^2 = 0.26$, $p = 0.005$, respectively) compared to those at the NC site ($R^2 = 0.33$, $p = 0.001$ and $R^2 = 0.75$, $p < 0.001$, respectively). On the other hand, correlation coefficients between log(pCO_2) and $\delta^{13}C_{CO2}$ values at a depth of 0.2 m were higher at AC than at NC site ($R^2 = 0.60$, $p < 0.001$ and $R^2 = 0.48$, $p < 0.001$; at AC and NC site, respectively). The average atmosphere CO_2 concentration in forest air at both sites was 510 ± 84 ppm with an average $\delta^{13}C_{atm}$ value of −9.6 ± 1.03 ‰.

3.3 Cave atmosphere

The level of CO_2 in cave air shows a seasonal pattern where a cold and warm season can be distinguished (Fig. 3). The CO_2 concentrations were lower during the cold season, where a minimum value of 669 ppm was observed in January 2015. During the warm season, the CO_2 concentrations rose, despite occasional dips, until reaching a maximum of 10,426 ppm in October 2014. In late October 2014, CO_2 concentrations declined and reached minimum values in January and February 2015. The $\delta^{13}C_{CO2}$ values of the cave air also show a seasonal trend with higher values up to −16 ‰ observed in winter and the lowest values down to −25 ‰ obtained in summer. The $\delta^{13}C_{CO2}$ values are in statistically significant negative linear correlation with log (pCO_2) values ($R^2 = 0.63$, $p < 0.001$). Figure 3 shows the relationship between the outside air temperature and the cave air CO_2 concentrations. No significant correlation exists between changes in atmospheric pressure and in cave air CO_2 concentrations. We can assume that during our investigation, ventilation was mainly related to differences in air density as already observed in the study by Gregorič et al. (2013).

4 Discussion

4.1 Soil CO_2 concentrations in relation to T_{soil} and SWC

To gain a deeper perspective about the relationship between soil CO_2, T_{soil} and SWC, we can look at their correlations. If there are only biogenic sources of soil CO_2, its variability can be explained just with T_{soil} and SWC parameters. These parameters are the ones that most commonly affect the temporal

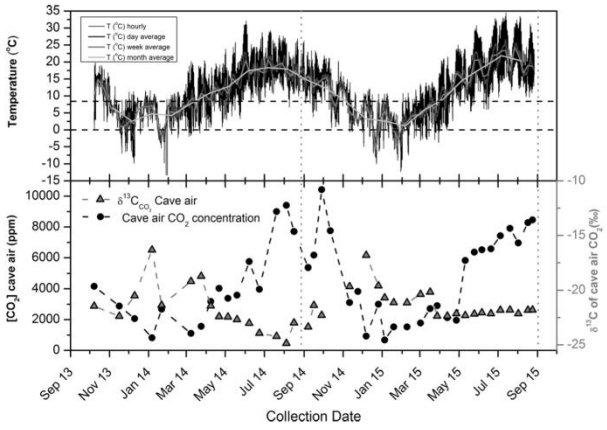


Fig. 3 Time series of cave air CO_2 concentrations and its $\delta^{13}C$ composition along Postojna air temperatures with marked lines of cave temperature of 8.4 and 0 °C. *Place between vertical grey dashed lines* indicates the soil gas measurement period

variation in soil CO_2 concentration (Davidson et al. 2000, Guntiñas et al. 2013). The T_{soil} is considered the most important environmental factor affecting soil respiration (Raich and Potter 1995), with a positive correlation between soil respiration and temperature. In some cases, when low or high SWC restricts soil CO_2 production, SWC can become equal or an even more important factor. With low water contents, the metabolic activity of microbes and roots are inhibited, while at a high soil water content, soil microbial CO_2 production is reduced, since the closed pore space can reduce the content of oxygen (Linn and Doran 1984; Doran et al. 1990; Cook and Orchard 2008). A closed pore space can also cause CO_2 accumulation in soil and an increase in the soil CO_2 concentration.

As expected, the main factors affecting the concentration of soil CO_2 at NC were T_{soil} and SWC. Increased T_{soil} explains 91 and 86 % of the variations in CO_2 concentration at a depth of 0.2 and 0.5 m, respectively, but only until late May 2015, after which time the temperature showed a negative correlation and SWC a positive correlation with soil CO_2. This occurred after a heavy forest sanitation cutting after a Scolytidae outbreak as a consequence of freezing rain damage in February 2014. After cutting, more sunlight reached the forest floor causing a strong growth in ground vegetation, which increased the importance of SWC to soil CO_2 during the spring vegetation period.

No seasonal changes in relation to the T_{soil} and SWC to soil CO_2 concentrations were observed at AC with more scattered datasets compared to NC (Fig. 3). This was expected, since at NC, the main source of CO_2 production is of biogenic origin, while at AC, other sources could influence CO_2 production (Čater and Ogrinc 2011; Plestenjak et al. 2012). A moderate correlation between T_{soil} and CO_2 concentrations was observed at a depth of 0.8 m where temperature explained 67 % of the variation of CO_2 concentrations, while increased T_{soil} explained only 47 and 22 % of the CO_2 variations at a depth of 0.2 and 0.5 m, respectively. No significant correlation exists between SWC and soil CO_2. It was also checked how precipitation data influence the CO_2 distribution. If precipitation, and a resulting increase in soil moisture, was stimulating root or microbial respiration, an increase in CO_2 concentration and lighter soil $\delta^{13}C_{CO2}$ would be expected. Lighter $\delta^{13}C_{CO2}$ compositions were determined at both sites with increasing precipitation (Fig. 2), but an increase in CO_2 concentrations following precipitation was not observed.

4.2 Soil CO_2 sources and mixing

To check if soil CO_2 isotopic composition can be explained by the mixing of two CO_2 sources, i.e. atmospheric and biogenic, a mixing model similar to the one used by Spötl et al. (2005) was applied. The CO_2 content of atmospheric air was on average 510 ppm with an average $\delta^{13}C$ value of −9.6 ‰. These two values were taken as the first endmember. To construct the model, three different "scenarios" for the second "isotopically light" endmembers with three different isotopic compositions were used, i.e. −21, −25 and −30 ‰. These values are well inside the range of isotopic compositions expected for biogenic CO_2 sources at C3 vegetation sites (Kuzyakov 2006) and the $\delta^{13}C_{SOC}$ values observed in our study (Table 1). Model values are represented as lines in Fig. 5. The mathematical expression of the model is

$$\delta^{13}C_{soilCO_2} = \delta^{13}C_{atm} * (X_{atm}/X_{soilCO_2}) + \delta^{13}C_{light} * (1-(X_{atm}/X_{soilCO_2})) \quad (1)$$

where $\delta^{13}C$ are the isotopic compositions and X are the concentrations of CO_2. Subscripts soilCO_2, atm and light represent soil gas CO_2, atmospheric air CO_2 and the isotopically light CO_2 endmember, respectively.

When searching for the isotopic composition of the source of soil CO_2, different diffusivities of $^{12}CO_2$ and $^{13}CO_2$ have to be taken into account. Therefore, the value of an isotopically light biogenic source (Fig. 4) would be ~4.4 ‰ lower, i.e. between −25 and −35 ‰. These values are still within the general isotopic composition range expected for SOC in soils developed under C3 vegetation (Kuzyakov 2006).

Figure 4 shows how sample data from NC follows the modelled lines more closely than the data from AC. This is most obvious at NC during warmer periods where the plotted data follows the shape of the modelled lines in the area between −22 and −25 ‰. Data from both sites are less scattered during warmer periods, when soil CO_2 originates mainly from biogenic sources (as suggested also by the $\delta^{13}C_{CO2}$ values). Some reasons for this scattering can be attributed to the different contributions from the root- or SOM-derived CO_2 or to the changing environmental factors such as plant water availability. Plant water availability can change the $\delta^{13}C$ values by 1–2 ‰ in relation to the biogenic soil CO_2 endmember (Kuzyakov 2006; Hartman and Danin 2010). It should be pointed out that with this model, no definite conclusion regarding different CO_2 sources between AC and NC could be drawn, since values from both sites have roughly the same maximum deviation from the central model line. An approach based on the equation proposed by Davidson (1995) (Eq. 2) was used in the next step to better evaluate the sources of soil CO_2. In this approach, the ^{13}C fractionation between soil CO_2 and its source is not constant but varies due to the difference between atmospheric and soil gas CO_2 concentrations:

$$\delta^{13}C_{light} = \frac{\delta^{13}C_{soilCO_2} - 4.4 + 4.4\frac{X_{atm}}{X_{soilCO_2}} - \delta^{13}C_{atm}\cdot\frac{X_{atm}}{X_{soilCO_2}}}{1.0044\left(1-\frac{X_{atm}}{X_{soilCO_2}}\right)} \quad (2)$$

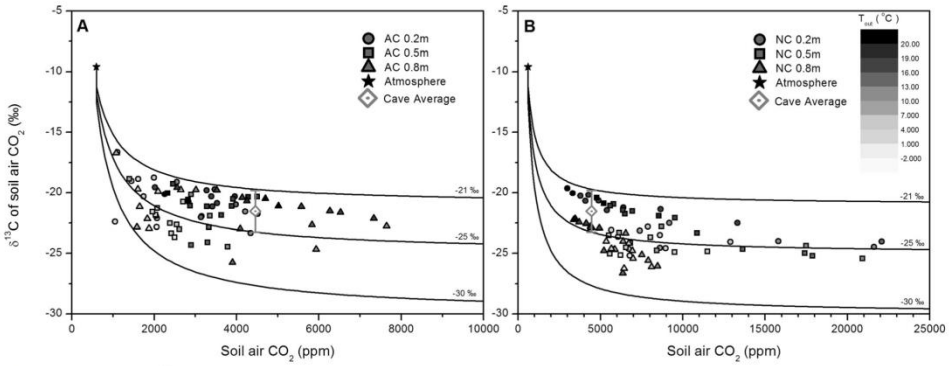


Fig. 4 Scatter plots of $\delta^{13}C$ composition of soil gas CO_2 versus soil gas CO_2 concentration. *Lines* represent modelled values by two-endmember mixing model between the external atmosphere (−9.6 ‰, 510 ppm) and an "isotopically light" endmember with $\delta^{13}C_{CO2}$ compositions of −21, −25 and −30 ‰. The plots include the data for average measured values from the cave atmosphere, where *whisker* represents 1 standard deviation of $\delta^{13}C$ composition of cave air CO_2. Data is colour-mapped with average (24 h before sampling) atmosphere temperatures at Postojna meteorological station (ARSO 2015)

where $\delta^{13}C$ are the isotopic compositions and X are the concentrations of CO_2. Subscripts soilCO_2, atm and light represent soil gas CO_2, atmospheric air CO_2 and the isotopically light CO_2 endmember, respectively. The uncertainty for $\delta^{13}C_{light}$ was estimated to be 11 % based on Gaussian error propagation calculation for a two-component model.

If we assume that soil CO_2 comes from only two sources, the plot line in Fig. 5 should be constant at the value of isotopic composition of the isotopically light endmember ($\delta^{13}C_{light}$). Different environmental factors could eventually shift the $\delta^{13}C_{light}$ endmember for ~1–2 ‰. At AC, this shift is much greater and cannot be attributed solely to the differences in biotic sources caused by environmental factors. At AC, the $\delta^{13}C_{light}$ is relatively constant until late November 2014 and returns to its starting value in April 2015. The $\delta^{13}C_{light}$ value also changes at NC where it increases during the vegetation period and stabilizes or even drops in late August 2015. The change at NC is much smaller than at AC, which we attribute to the aforementioned environmental factors affecting biogenic CO_2 production. Shifts in the $\delta^{13}C_{light}$ value at AC clearly indicate that there must be another source with more positive $\delta^{13}C$ values. Since atmospheric CO_2 has already been taken into account within Eq. 2, this source can be explained by the two main abiotic interpretations: carbonate weathering ($CO_{2(rock)}$) and/or subterranean cavity ventilation ($CO_{2(cave)}$) .

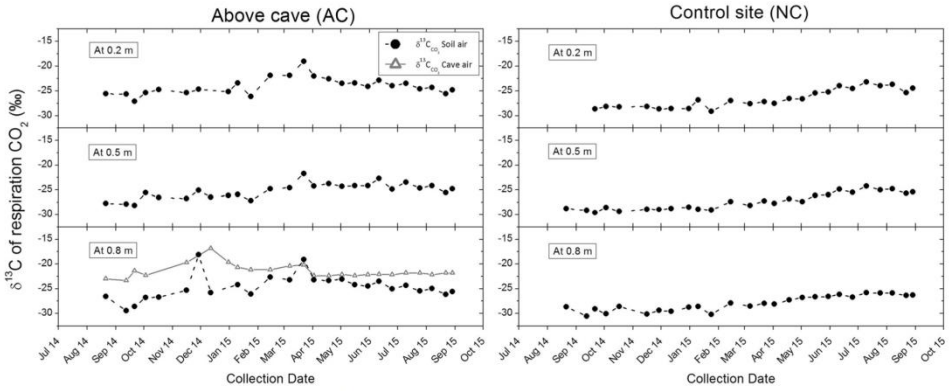


Fig. 5 Time series of calculated light endmember ($\delta^{13}C_{light}$) from two-endmember mixing model (Davidson 1995). Values were calculated from the average values of $\delta^{13}C$ and CO_2 concentration of the atmosphere (−9.6 ‰, 510 ppm) and soil CO_2 measurements at three different sampling depths at the AC and NC sampling sites. *Grey line* represents $\delta^{13}C_{CO2}$ values of cave air

It is known that carbonate weathering is more pronounced during the cold period because of the more dormant state of biotic sources. Contribution of CO_2 from carbonate rock dissolution-precipitation processes can be enhanced due to favourable temperature differences within the soil profile during the cold period. Surface soil layers are colder than deeper layers allowing the infiltrating water to dissolve more CO_2 and $CaCO_3$. When water percolates to deeper and warmer layers, it becomes more saturated, where higher temperatures result in degassing of CO_2 and precipitation of secondary carbonates. This mechanism could be even more pronounced during snow cower when exchange between soil gas and atmosphere is limited and the melting water enters into the soil that is relatively rich in CO_2. This was also the case in our study in January and February 2015 when soil CO_2 concentration was around 2000 ppm (Fig. 2). During the measurement in February 2015, soil temperatures at 0.1, 0.5, 1.3 and 4 m were 0.6, 1.7, 2.8 and 10.6 °C, respectively, and the melting water was infiltrating in the soil. The calcite solubility constants (K_S) ranged from 3.86×10^{-9} at 10.6 °C to 4.14×10^{-9} at 0.6 °C, indicating that calcite is more soluble at lower temperatures.

Under the assumption that the calculated source is a mixture of two sources with different isotopic composition, the relative contribution of each source can be calculated by rearranging the mass balance equation (Eq. 1). Assuming that the isotopic composition of CO_2 from the organic source and limestone are the same as the average measured values for SOC and limestone at the AC site (−25.2 and 1.6 ‰, respectively), we can use the approach used by Jin et al. (2009) and Schindlbacher et al. (2015) to calculate the isotopic composition of DIC ($\delta^{13}C_{DIC}$) of the infiltrating water at certain pH and temperature. In the case when infiltrating water would enter the soil and react with soil CO_2 and carbonate rock material at the upper parts of the soil with the temperature of 1 °C and pH 8, $\delta^{13}C_{DIC}$ values around −10.0 ‰ should be obtained for open or closed system, respectively, using the assumptions proposed by Salomons and Mook (1986) and fractionation factors determined by Zhang et al. (1995). The calculated isotope composition of CO_2 degassing from water would be around −19.4 ‰ at 10.6 °C. This value could not be distinguished from soil $\delta^{13}C_{CO2}$ values of around −20.8 ‰ (−25.2 + 4.4 ‰) with possible variation of few per miles due to the mentioned environmental factors. Thus, it is not possible to determine contribution from these two sources based only on stable carbon isotope composition of soil CO_2. In some cases (e.g. December 2014 at AC at the depth of 0.8 m; Fig. 5), the calculated source values had more positive isotopic composition than did the modelled isotopic composition of CO_2 degassing from DIC, suggesting the presence of other source more enriched in ^{13}C.

Another possible source of isotopically heavier CO_2 in soil is CO_2 from subterranean cavities and caves. Figures 3 and 5 show that during the cold period, the shift in $\delta^{13}C_{light}$ observed at AC coincides with the period of stronger cave ventilation. A rough estimate of the relative contribution of $CO_{2(cave)}$ can be calculated, assuming the advective transport of CO_2 from the cave atmosphere to the soil with negligible fractionation of cave CO_2 during the transport. Under these assumptions, the estimated contribution of cave CO_2 to soil CO_2 was up to 80 %.

5 Conclusions

Our research revealed that there was an abiotic source of CO_2 present in soil above the cave during cold periods and coincided with the period of cave ventilation. A first estimate indicates that cave air CO_2 can account for up to 80 % of the overall soil CO_2. This shows that subterranean cavities act as a temporal storage of CO_2 and can be released during favourable conditions. However, for a more accurate interpretation of carbon cycling over carbonate and karst ecosystems, more knowledge and methodologies are required involving more than one tracer, e.g. ^{14}C and/or ^{222}Rn.

Acknowledgments The study is a part of the PhD thesis of B. Krajnc supported by the Innovative scheme for co-financing of doctoral studies financed by the European Union through the European Social Fund and by the scholarship granted by the World Federation of Scientists. We are grateful to Iztok J. Košir from the Slovenian Institute for Hop Research and Brewing for the pedologic analyses and the Farmland and Forest Fund of the Republic of Slovenia for the permission to do research in the forest. We would also like to thank the Regional Forest Service Postojna of the Slovenian Forest Service and Maksimilijan Gorup for providing information regarding sanitation forest cutting. We appreciate the support of cave guides Stanislav Glažar, Janez Margon and Erik Rebec for their dedication during fieldwork. We would also like to acknowledge the managers of Postojna Jama d.d. and Ministry of Agriculture and Environment of Slovenia for the permission to access and work in the cave.

References

Amundson R (2001) The carbon budget in soils. Annu Rev Earth Pl Sc 1: 535–562

ARSO (2015) ARSO. Available from: http://www.arso.gov.si

Barnet I, Neznal M, Neznal M, Pacherová P (2008) Radon in geological environment—Czech experience. Czech Geological Survey, Prague

Čater M, Ogrinc N (2011) Soil respiration rates and $\delta^{13}C_{CO2}$ in natural beech forest (*Fagus sylvatica L.*) in relation to stand structure. Isot Environ Healt S 47:221–237

Cerling TE, Quade J (1993) Stable carbon and oxygen isotopes in soil carbonates. Climate change in continental isotopic records pp:217–231

Cerling TE, Solomon DK, Quade J, Bowman JR (1991) On the isotopic composition of carbon in soil carbon dioxide. Geochim Cosmochim Acta 11:3403–3405

Cook FJ, Orchard VA (2008) Relationships between soil respiration and soil moisture. Soil Biol Biochem 5:1013–1018

Cuezva S, Fernandez-Cortes A, Benavente D, Serrano-Ortiz P, Kowalski AS, Sanchez-Moral S (2011) Short-term $CO_{2(g)}$ exchange between a shallow karstic cavity and the external atmosphere during summer: role of the surface soil layer. Atmos Environ 7:1418–1427

Davidson EA, Verchot LV, Cattânio JH, Ackerman IL, Carvalho J (2000) Effects of soil water content on soil respiration in forests and cattle pastures of eastern Amazonia. Biogeochemistry 1:53–69

Davidson GR (1995) The stable isotopic composition and measurement of carbon in soil CO_2. Geochimica et Cosmochimica Acta 59(12): 2485–2489

Doerr H, Münnich KO (1986) Annual variations of the ^{14}C content of soil CO_2. Radiocarbon 2A:338–345

Domínguez-Villar D, Lojen S, Krklec K, Baker A, Fairchild IJ (2015) Is global warming affecting cave temperatures? Experimental and model data from a paradigmatic case study. Clim Dyn 3-4:569–581

Doran JW, Mielke LN, Power JF (eds) (1990) Microbial activity as regulated by soil water-filled pore space. Transactions 14th International Congress of Soil Science. Symposium III-3; Ecology of soil microorganisms in microhabital environments. Kyoto, Japan, pp 94–99

GLOBALVIEW-CO2C13 (2009) GLOBALVIEW-CO2C13: cooperative atmospheric data integration project—$\delta^{13}C$ of carbon dioxide. Available from: http://www.esrl.noaa.gov/gmd/ccgg/globalview/co2c13/co2c13_intro.html

Gregorič A, Vaupotič J, Gabrovšek F (2013) Reasons for large fluctuation of radon and CO_2 levels in a dead-end passage of a karst cave (Postojna Cave, Slovenia). Nat Hazards Earth Syst Sci 2:287–297

Guntiñas ME, Gil-Sotres F, Leirós MC, Trasar-Cepeda C (2013) Sensitivity of soil respiration to moisture and temperature. J Soil Sci Plant Nutr 2:445–461

Hartman G, Danin A (2010) Isotopic values of plants in relation to water availability in the eastern Mediterranean region. Oecologia 4: 837–852

ISO 11464 (2006) Soil quality—pretreatment of samples for physio-chemical analysis. ISO, Geneva

Jin L, Ogrinc N, Hamilton SK, Szramek K, Kanduč T, Walter LM (2009) Inorganic carbon isotope systematics in soil profiles undergoing silicate and carbonate weathering (southern Michigan, USA). Chem Geol 1:139–153

Knohl A, Werner RA, Geilmann H, Brand WA (2004) Kel-F discs improve storage time of canopy air samples in 10-mL vials for CO_2-$\delta^{13}C$ analysis. Rapid Commun Mass Spectrom 14:1663–1665

Kowalski AS, Serrano-Ortiz P, Janssens IA, Sánchez-Moral S, Cuezva S, Domingo F, Were A, Alados-Arboledas L (2008) Can flux tower research neglect geochemical CO_2 exchange? Agric For Meteorol 6–7:1045–1054

Kuzyakov Y (2006) Sources of CO_2 efflux from soil and review of partitioning methods. Soil Biol Biochem 3:425–448

Linn DM, Doran JW (1984) Effect of water-filled pore space on carbon dioxide and nitrous oxide production in tilled and nontilled soils. Soil Sci Soc Am J 6:1267–1272

Meyer KW, Feng W, Breecker DO, Banner JL, Guilfoyle A (2014) Interpretation of speleothem calcite $\delta^{13}C$ variations: evidence from monitoring soil CO_2, drip water, and modern speleothem calcite in Central Texas. Geochim Cosmochim Acta 142:281–298

Plestenjak G, Eler K, Vodnik D, Ferlan M, Čater M, Kanduč T, Simončič P, Ogrinc N (2012) Sources of soil CO_2 in calcareous grassland with woody plant encroachment. J Soils Sediments 9:1327–1338

Raich JW, Potter CS (1995) Global patterns of carbon dioxide emissions from soils. Global Biogeochem Cy 1:23–36

Raich JW, Schlesinger WH (1992) The global carbon dioxide flux in soil respiration and its relationship to vegetation and climate. Tellus B 2: 81–99

Raich JW, Potter CS, Bhagawati D (2002) Interannual variability in global soil respiration, 1980–94. Glob Change Biol 8:800–812

Salomons W, Mook WG (1986) Isotope geochemistry of carbonates in the weathering zone. handbook of environmental isotope geochemistry. Elsevier, Amsterdam, pp. 239–269

Schindlbacher A, Borken W, Djukic I, Brandstätter C, Spötl C, Wanek W (2015) Contribution of carbonate weathering to the CO_2 efflux from temperate forest soils. Biogeochemistry 1-3:273–290

Šebela S (2010) Accesses from the surface to the Postojna Cave system. Annales Series historia naturalis 1:55–64

Šebela S, Čar J (2000) Velika Jeršanova doline—a former collapse doline: Velika Jeršanova dolina—nekdanja udornica. Acta carsologica 2: 201–212

Serrano-Ortiz P, Roland M, Sanchez-Moral S, Janssens IA, Domingo F, Godderis Y, Kowalski AS (2010) Hidden, abiotic CO_2 flows and gaseous reservoirs in the terrestrial carbon cycle: review and perspectives. Agric For Meteorol 3:321–329

Spötl C (2004) A simple method of soil gas stable carbon isotope analysis. Rapid Commun Mass Spectrom 11:1239–1242

Spötl C, Fairchild IJ, Tooth AF (2005) Cave air control on dripwater geochemistry, Obir caves (Austria): implications for speleothem deposition in dynamically ventilated caves. Geochim Cosmochim Acta 10:2451–2468

Tiedje JM, Sexstone AJ, Parkin TB, Revsbech NP (1984) Anaerobic processes in soil. Plant Soil 1-3:197–212

Zhang J, Quay PD, Wilbur DO (1995) Carbon isotope fractionation during gas-water exchange and dissolution of CO_2. Geochim Cosmochim Acta 1:107–114

3.4 Scientific Paper: "Sources, pathways and behaviour of cave air CO_2, using carbon isotopes"



In this chapter the paper entitled "Sources, pathways and behaviour of cave air CO_2, using carbon isotopes" by Bor Krajnc, Lixin Jin, Janja Vaupotič, Sonja Lojen, Taichi Nakamura and Nives Ogrinc is presented. The paper is under review in Geochimica et Cosmochimica Acta and represents one of the main researches performed in the scope of the PhD study.

In the following paper the study of sources and dynamics of the cave air CO_2 in Pisani rov, a gallery of Postojna Cave system is presented. This was a two-year study that was conducted from November 2013 to September 2015. During the study the Radon and CO_2 concentrations of cave air at two elevations within the cave chamber were measured together with a stable carbon isotope composition of cave air CO_2. At three occasions also the samples for radiocarbon (^{14}C) were taken. Besides cave air also dripwater (as a possible source of cave CO_2) was sampled. Different geochemical parameters were measured in water, e.g. pH, Total alkalinity, Temperature, $\delta^{13}C$ of dissolved inorganic carbon, $\delta^{18}O$ of dripwater oxygen, concentrations of major ions, etc.

The aim of the study is to further investigate the mechanisms of ventilation and to determinate the origins, pathways and behavior of CO_2 in the cave chamber. This type of approach was used for the first time in the cave air together with dripwater, in Slovenia. Researches of CO_2 dynamics in terrestrial systems are usually focused either on surface soil or, in the case of karst, on the dynamics within the karstic cave. In these areas, systems are inevitably connected and should be studied together, especially in the case of carbon mass balance estimates.

The levels of CO_2 in the cave had a typical seasonal pattern. Accumulation of CO_2 started in spring and reached maximum values in summer. Values started to drop in fall and reached the lowest concentrations in winter. $\delta^{13}C_{CO2}$ were in statistically highly significant negative correlation with $\log(pCO_2)$ values of the cave air, and also radon concentrations showed the same seasonal pattern.

Three important observations were identified in the air composition: (i) CO_2 concentrations correlate with the outside temperatures; (ii) ^{222}Rn concentrations closely follow the CO_2 concentrations; and (iii) both CO_2 and ^{222}Rn concentrations reached higher values at a lower sampling point in the cave chamber. The first and the second observation together strongly indicate that the main factor affecting the CO_2 concentrations in the cave is the outside temperature, triggering the cave ventilation. While the third observation indicates that the cave air is not uniformly mixed. The study of the influence of other meteorological parameters on cave CO_2 did not show any statistically significant influence, with the exception of the NE and SW winds during the winter.

The study of the stable carbon isotopic composition of cave air and dripwater DIC indicated that the major source of cave CO_2 in the studied chamber is the CO_2 originating from soil respiration, coming directly into the cave and that CO_2 which was transported into the cave via dripwater has a minor influence on the cave CO_2 concentration levels. The analysis of the ^{14}C data further supports this assumption

showing that 54-68% of cave air CO_2 originates from young organic matter. The abiotic source contribution of 8% was observed in winter.

In the presented case, the cave atmosphere has a greater influence on the dripwater chemistry (the carbonate equilibrium). This finding was further supported by the observation that other measured dripwater parameters, which are not influenced by CO_2 levels in the cave, showed different behavior than the parameters, which are the main "actors" in the carbonate equilibrium system. A further investigation of these more "conservative" parameters also suggested that the mean residence time of percolating water is around half year.

In this paper, the candidate developed the research question, organized the sampling and performed all necessary measurementsThe filed trips include sample collections, data collections and on-site measurements (temperature, pH, conductivity, CO_2 concentration in cave air, etc.) every two weeks. He collected dripwater samples for stable carbon isotope analysis of dissolved inorganic carbon, samples for cation and anion determination, and samples for stable oxygen isotope analysis. He collected the samples for radon measurements in cave air into scintillation cells, which he analysed later in the laboratory using alpha counter. For $\delta^{13}C$ CO_2 measurements in the cave air the samples were collected into pre-evacuated 12 ml glass vials. He performed all laboratory sample preparation prior to analysis and conducted the analysis using the IRMS. Concentration of cations and anions in waters were measured at the Low-Temperature Geochemistry Laboratory of the University of Texas at El Paso (USA). The candidate collected the sample for ^{14}C analysis into the NaOH solution. ^{14}C analysis was made with Tandetron Accelerator Mass Spectrometer (AMS) at the Japan Atomic Energy Agency in Mutsu, Japan. He performed data analysis, different hydrological, mixing and isotopic fractionation models using different statistical approaches with R statistical environment (R Core Team, 2014), PHREEQC (Parkhurst and Appelo, 2013) and MIX4 (Edgerton et al., 1991) software. The candidate interpreted the data and wrote the manuscript.

Sources, pathways and behaviour of cave air CO_2 using carbon isotopes

Bor Krajnc[1,2] •Lixin Jin[3] • Janja Vaupotič[1,2] • Sonja Lojen[1,2] •Taichi Nakamura[4] • Nives Ogrinc[1,2]

[1]*Jožef Stefan International Postgraduate School, Jamova 39, 1000 Ljubljana, Slovenia*

[2]*Department of Environmental Sciences, Jožef Stefan Institute, Jamova 39, 1000 Ljubljana, Slovenia*

[3]*Department of Geological Sciences, University of Texas at El Paso, El Paso, TX 79968-0555, USA*

[4]*Faculty of Engineering, Hokkaido University, Sapporo 060-8628, Japan*

✉ Bor Krajnc

Tel: +386 1 5885 452

bor.krajnc@ijs.si

Abstract

A 2-year study in a dead-end gallery of Postojna cave in Slovenia investigates dynamics and sources of cave air CO_2. During the investigation, cave air and dripwater composition was monitored at two sampling sites at different elevations: one site at the floor of the cave and one at the celling. Meteorological parameters such as outside temperature, pressure and wind direction in relation to cave air composition (CO_2 and ^{222}Rn concentrations in cave air) were used to investigate the cave ventilation drivers, while carbon isotopes in cave air and dripwater were used to investigate the CO_2 sources. Oxygen stable isotope ratios ($\delta^{18}O$) in precipitation and dripwater, together with major cations and anions were used to investigate the dripwater dynamics and degassing of CO_2 in the cave. Isotopic composition of CO_2 degassed from water was modelled and source partitioning of cave air CO_2 using three end-member model with natural abundances of carbon isotopes (^{12}C, ^{13}C and ^{14}C) was used to distinguish between the major sources: CO_2 from soil respiration, CO_2 from the atmosphere and CO_2 originating from parent rock dissolution/precipitation process. Two regimes of CO_2 concentrations behaviour in cave air were found: the winter ventilation and summer CO_2 accumulation, where spring and fall are considered as transition period between the two regimes. The cave ventilation is mainly driven by the difference in density between the cold outside air and warm cave air. It was found that carbonate mineral has a minor influence on cave air CO_2 amounting at 8% in winter. It was estimated that CO_2 originating from decomposition of young organic matter comprised 54 and 68%, while atmospheric air contribution to cave CO_2 was estimated to be 37 and 24% depending on snow cover. Hydro-chemical parameters show evidence to neglect the explanation that seasonal fluctuations of CO_2 concentrations in soil air are transferred to the cave environment via seepage water. $\delta^{18}O$ values in dripwaters and chemical constituents indicate that mean residence time of dripwater is roughly half a year. Modelled isotopic composition of CO_2 degassing from dripwaters

indicated that CO_2 coming to the cave dissolved in dripwaters can be only a minor source of cave CO_2 at this location and that the major source of CO_2 is originating from decomposition of organic matter transported directly to the cave.

Keywords: CO_2 • CO_2 sources • source partitioning • Karst • Cave air • Ventilation • ^{12}C • ^{13}C • radiocarbon • ^{16}O • ^{18}O • radon • dripwater chemistry • degassing

1. Introduction

A great number of studies are dedicated to CO_2 dynamics in terrestrial ecosystems, focusing on either surface soils or on bedrock cavities (Trumbore 2006; Serrano Ortiz et al., 2010; Bond-Lamberty and Thomson 2010). In karstic areas, both systems exist and are inevitably connected. Soil is produced by roots and decomposition of litter and soil organic matter (SOM), where soil temperature and soil moisture are considered as the most important parameters influencing soil respiration and its underlying processes (Kuzyakov, 2006). Recently it has been found, that abiotic terrestrial CO_2 exchange can temporally even dominate the C fluxes in ecosystems on carbonaceous areas comprising up to 68% of total soil CO_2 flux (Serrano Ortiz et al., 2010). Several studies (Kowalski et al., 2008; Kowalczk and Froelich, 2010; Serrano Ortiz et al., 2010; Were et al., 2010; Plestenjak et al., 2012) consider the possible influence of ventilation of CO_2 from subterranean cracks and caves where substantial amounts of CO_2 can be stored as a possible abiotic source of soil CO_2. Such storing and ventilation of subterranean CO_2 can be explained on an example where rainwater infiltrates and percolates through the soil with higher CO_2 concentration (due to soil respiration) and reduced bicarbonate concentration (due to dilution). Dissolution of soil CO_2 and production of dissolved inorganic carbon (DIC) occurs. This process represents a geochemical CO_2 sink, since the efflux of CO_2 from soil decreases. Soil CO_2 and carbon from carbonate rock are transported in the form of DIC. DIC together with Ca^{2+} and other ions percolates with drainage water and can eventually enter the cave where cave air CO_2 concentrations determine whether the reverse processes precipitates carbonate and degasses CO_2 into the cave atmosphere and therefore augment the local CO_2 cave air concentration. During the events when caves ventilate, gaseous CO_2 escapes from caves (through different paths) into the atmosphere, and can produce sizeable upward fluxes in the atmospheric boundary layer. During the seasons with low cave air ventilation there are high cave CO_2

concentrations, and air in caves can represent sustained belowground sink for gaseous CO_2, whose magnitude may be important for the interpretation of net flux measurements. Another possible transport of CO_2 from soil into deeper layers of soil and eventually caves located near the surface is by molecular diffusion. This mechanism of transported can be even more facilitated during the rain periods when soil pores are saturated by water, and thus the exchange of CO_2 with atmosphere is limited (Wood et al., 1985). Some estimates were made, finding that the CO_2 influx into global karstland is similar to global forest influx (~ 0.5 and 0.6 Pg yr^{-1}, respectively; Liu and Zhao 2000).

Around 44% of the total Slovenian surface is covered by different types of karst (Habič, 1982). Although it is often claimed that our karst is one of the most thoroughly investigated worldwide, we still don't know whether our karst is a source or a sink for atmospheric CO_2. Soil respiration and soil gas have recently been thoroughly investigated in karstic forested areas (Čater and Ogrinc 2011; Ogrinc et al., 2016) and grasslands (Plestenjak et al., 2012), and it was found that a considerable part of the soil CO_2 derives from carbonate weathering, where the contribution of geogenic CO_2 depends upon vegetation, soil type and temperature.

In this study the insights from a 2 years survey of carbon transport in cave waters from Pisani rov, a gallery of Postojna cave system located near Postojna in southwestern Slovenia are presented. Several studies have been already performed in this gallery. First geological surveys of Pisani rov was performed by Gospodarič (1962), followed by several studies such as speleological survey (Gospodarič, 1976) and dripwater quality study (Kogovšek, 1983). Later, geological characteristics of the gallery (Šebela, 1992) and of the geology of collapse dolines and terrain above the cave was described more detailed (Šebela, 1996; Šebela and Čar, 2000; Šebela, 2010). Most recent studies were concerning ventilation characteristics of the gallery (Gregorič et al., 2013) and cave temperature responses to climate changes (Domínguez-Villar et al., 2015). Gregorič et al. (2013) found that ventilation in Pisani rov is

100 manly driven by the difference in density between the cold outside air and warm cave air.
101 Further, it was also shown that accumulated cave CO_2 can represent significant source of soil
102 CO_2 when it is transported back to the soil and atmosphere via advection caused by cave
103 ventilation (Krajnc et al., 2017).
104 The aim of the presented study is to further investigate the mechanisms of ventilation and to
105 determine the origins, pathways and behaviour of CO_2 in the cave chamber including carbon
106 isotopes. This type of approach was used for the first time in cave air and in dripwaters in
107 Slovenia and to our knowledge there are not many studies using these parameters globally.

108 2. Materials and methods

109 *2.1.Study site*

110 Postojna region has a continental climate with mean annual temperature of 9.3 °C (period
111 from 1981-2010), with the mean monthly temperatures of the coolest month of −0.1 °C
112 (January) and at the warmest month of 19.0 °C (July). Mean annual precipitation is 1500 mm
113 with no clear seasonal patterns, although precipitation is more abundant in autumn (ARSO).
114 At the surface above the investigated cave the Omphalodo-Fagetum forest with mainly C_3
115 vegetation prevails. Soil is shallow Leptosol with occasional soil pockets and superficial
116 rockiness of about 80%. Carbon stable isotope composition of soil organic carbon above the
117 cave ($\delta^{13}C_{SOC}$) is −25.2 ± 0.1‰, while the parent rock material has $\delta^{13}C_{rock}$ value of 1.6 ±
118 0.2‰ (Krajnc et al., 2017). Stable isotope composition of atmosphere CO_2 was estimated to
119 be −9.6 ± 1.0‰ during the studying period.

120 The study was conducted at the end of Pisani rov, which is a dead-end horizontal gallery of
121 Postojna Cave system located near Postojna in southwestern Slovenia (Fig.1). The gallery,
122 developed in Turonian limestone (Gospodarič, 1962), is ~600 m long and consists of a series
123 of big halls and narrow passages. It deviates from the main Postojna Cave corridor to the

124 north and terminates below the slopes of the Velika Jeršanova dolina. It is connected to the
125 main Postojna cave corridor by a small entrance (~1 x 1.5 m), which is closed for tourists (Its
126 location is marked with red dot in Figure 1. Study site for this research is located in the last
127 large hall of Pisani rov named "red and white hall" (RiB). RiB is 70 m long with average
128 width of 12 m and average height of 4.5 m (Domínguez-Villar et al., 2015). The thickness of
129 the cave celling is estimated to be around 30 m (Šebela, 2010). Cave air temperature is very
130 stable. In the study done by Domínguez-Villar et al. (2015) it was shown that temperature in
131 RiB is constant at 8.40 ±0.01°C and there was less than 0.07 °C of thermal change during the
132 mentioned study (2009-2013), while daily variability of the temperature was 0.02 °C. It has
133 very limited ventilation dynamics compared to the rest of the caves with some of the highest
134 CO_2 and ^{222}Rn concentrations in Postojna cave recorded (Gregorič et al., 2013).
135

136 *2.2.Meteorological data and oxygen stable isotope composition of local precipitation*

137 Local air temperature, wind direction and speed data was gathered from the nearby
138 Postojna weather station managed by the Environment Agency of Slovenia (533m a.s.l.,
139 45°45'57"N 14°11'35"E (WGS84)). Samples for oxygen stable isotope analysis of local
140 precipitation were collected at the same weather station. The monthly sample was obtained by
141 pooling daily samples collected at 7.00 AM and kept in HDPE container below room
142 temperature until analysis. Air pressure was continuously measured and logged with
143 automatic data logger at the location above the cave during the time of this investigation.
144

145 *2.3.Cave air and dripwater sampling*

146 Cave air samples were collected every two weeks from November 2013 to September
147 2015, at two RiB locations: one on the base of a small hill in RiB (called "Base Hill Air"
148 (BHA)), and the other on the hill (called "On the hill Air" (OHA)) (Fig. 2). Cave air samples

were collected with syringes, injected into the pre-evacuated 12 ml septum-capped glass vials (Labco Exetainer®, UK), and analysed for C isotope ratios. Two samples of cave air CO_2 were collected for $\Delta^{14}C$ analysis in winter (February 2015) on occasions with and without snow cover. During the two winter samplings, also simultaneous sampling of soil air above the cave was performed using the Neznal's probe installed 0.8 m deep in soil. In addition, a soil air sample was collected in late summer (August 2015). All air samples (cave and soil) for $\Delta^{14}C$ analysis were gathered by pumping the air through a Dreschel bottle containing a 1 M NaOH aqueous solution (200 cm^3). The time needed for air sampling depended on the amount of CO_2 in the sampled air.

Since February 2014 cave air samples for ^{222}Rn activity concentration were taken at the same locations as cave air CO_2 samples. Cave air was pumped with a handheld pump into 0.31 dm^3 (Quindós-Poncela et al., 2003) alpha scintillation cell until the air in the cell was exchange by cave air. Cells were transported to laboratory for further measurements.

Dripwater collection locations were at air sampling locations BHA and OHA. First dripwater collection location was under a large stalactite next to the BHA air sampling location, while at the second location (OHA) samples were collected from soda straws. Samples named "large-directly" (LD_BHA) and "straw-directly" (SD_OHA) were collected when the drip rate allowed us to collect enough sample during the visit. Dripwater samples named "large-indirectly" (LI_BHA) and "straw-indirectly" (SI_OHA) were collected into HDPE plastic cup placed under the drip during the time between two visits. Samples for major cation and anion concentration measurements, stable isotope analysis of dripwater oxygen ($\delta^{18}O_{H2O}$) and stable isotopic analysis of dissolved inorganic carbon ($\delta^{13}C_{DIC}$) were taken. Each water sample was filtered through 0.45 μm filters (Minisart® Sartorius, Germany) into 12 ml septum-capped glass vials (Labco Exetainer®, UK). Samples for cation

173 analysis were collected into 15 ml HDPE plastic containers and acidified with ultra-pure
174 concentrated nitric acid (HNO_3).
175
176 *2.4.Cave air analysis*
177 At each location cave air CO_2 concentrations were measured with a non-dispersive
178 infrared absorption detector (TESTO-453, TESTO, Germany), with uncertainty of ± 50 ppmv
179 CO_2. Relative humidity (accuracy= ±2% relative humidity) and air pressure (accuracy ±5 hPa)
180 of the cave air were also measured with this probe. Calibration for CO_2 concentration was
181 performed by the manufacturing company (TESTO K.K., Japan). All CO_2 readings were
182 corrected to a standard atmospheric pressure (1013 hPa) as suggested by Spötl et al. (2005).
183 Radon activity in the scintillation cells was determined using a PRM-145 alpha counter
184 (AMES, Slovenia). The alpha scintillation cells were calibrated in the KR-600 Radon
185 Chamber at the Henryk Niewodniczański Institute of Nuclear Physics, PAN, Kraków, Poland
186 (Kozak et al., 2009). Cell efficiencies are 2 s^{-1} Bq^{-1}, which gives a lower limit of detection of
187 20–50 Bq m^{-3} for 10-minute counting time and 1–2 min^{-1} background.
188 From April 2014 to September 2015 an electronic silicon detector for ^{222}Rn concentration
189 measurements (Radim 5B) was installed at BHA location. Radon concentration measurements
190 were logged every hour and saved to internal memory. Measurement range is from 85 Bq m^{-3}
191 to 50 000 Bq m^{-3} with 20% measurement uncertainty.
192
193 *2.5.Dripwater analysis*
194 Dripwater conductivity (COND) was measured *in-situ* with Ultrameter IITM 6PFCE
195 (Myron L Company, USA) with measurement accuracy of ±1% of measured value. Corning
196 315 high-sensitivity pH meter with an Orion Ross combination pH electrode, calibrated with
197 low ionic strength buffers of 4.01 and 6.97 (corrected for temperature), was used to measure

198 pH in the field as close to the water temperature as possible. Samples for pH measurements
199 were placed in to an airtight container to prevent degassing and measured at least twice to
200 ascertain electrode stability. The reproducibility of field pH determinations was ±0.02 pH
201 units.

202 Total alkalinity of the sample was determined using Gran titration (Gieskes, 1974) with
203 certified 0.05 M HCl. pH during titration was measured with pH meter (OrionTM 3-star pH
204 meter with an Orion™ 8102BNUWP ROSS Ultra™ pH combination electrode, Thermo
205 Fisher Scientific Inc., USA). pH meters were calibrated using buffer solutions traceable to
206 NIST standards with pH values of 4.01 and 7.01 (Hanna Instruments, Inc., USA). Analytical
207 error for alkalinity was estimated to be 10%.

208 Concentrations of cations (Ca^{2+}, Mg^{2+}, Na^{+}, K^{+}, Sr^{2+}, Si^{+}, Fe^{3+} and Al^{3+}) and anions (Cl^{-},
209 SO_4^{2-}, NO_3^{-}, F^{-} and Br^{-}) in the water samples were measured by Perkin Elmer inductively
210 coupled plasma optical emission spectrometry (ICP-OES, DV5300) and Dionex-2100 ion
211 chromatography (IC), respectively at the Low-Temperature Geochemistry Laboratory of the
212 University of Texas at El Paso (UTEP). The precision of IC and ICP analyses was better than
213 ± 3% for major elements and ± 10% for minor elements.
214

215 *2.6. Stable isotopes analysis*

216 CO_2 stable isotope composition ($\delta^{13}C_{CO2}$) of cave air was determined directly from the
217 samples with an isotope ratio mass spectrometer (IRMS) Europa Scientific 20-20 with
218 ANCA-TG preparation module for trace gas samples.

219 For isotope analyses of dissolved inorganic carbon ($\delta^{13}C_{DIC}$) in dripwater, gas evolution
220 method was used (Atekwana and Krishnamurthy, 1998). Briefly, in glass septum tubes
221 (Exetainer Septum Tubes, Labco Limited, UK), 100% phosphoric acid was added (100-200
222 µl) and the septum tubes were purged with pure He. 5 ml of water samples were introduced

223 into the septum tubes using a syringe and the acid-water reaction began immediately upon
224 injection. The isotope ratio of CO_2 was determined directly on gas from the headspace. The
225 optimal extraction procedure was checked using a standard solution with Na_2CO_3 of known
226 $\delta^{13}C_{DIC}$ (–10.8 ± 0.2‰). $\delta^{13}C_{DIC}$ values of cave dripwater were determined by the IsoPrime
227 IRMS with a MultiFlow Bio module.

228 For determination of oxygen isotopic composition of dripwater ($\delta^{18}O_{H2O\_drip}$) and rainfall
229 ($\delta^{18}O_{H2O\_prec}$) the equilibration method was used (Epstein and Mayeda, 1953). 0.2 mL aliquots
230 of water samples were equilibrated with CO_2 at 25°C for 12 h and analysed using IsoPrime
231 continuous-flow isotope ratio mass spectrometer (IRMS; Isoprime Limited, Cheadle, UK)
232 with a Multiflow Bio equilibration unit (VG Instruments Group Limited, Guildford, UK).

233 All stable isotope results are reported using conventional delta (δ)-notation in per mil (‰)
234 relative to VPDB and VSMOW for carbon and oxygen, respectively. In-house working
235 standards (tap water and snow with $\delta^{18}O$ values of −9.1 ± 0.1‰ and −19.7 ± 0.1‰,
236 respectively) calibrated against VSMOW2, SLAP2 and GISP reference materials were used
237 for oxygen in waters and gas standard "CO2 ISO-TOP, High" (Messer) with $\delta^{13}C_{CO2}$ value of
238 –4.3 ± 0.2‰ for CO_2. Reproducibility of the measurements was ±0.1‰ for $\delta^{18}O$, ±0.2‰ for
239 $\delta^{13}C_{DIC}$ and $\delta^{13}C_{CO2}$.

240

241 *2.7.Radiocarbon analysis*

242 NaOH aqueous solution with the $NaCO_3$ formed of CO_2 from cave and soil air during the
243 sampling procedure was transferred into a beaker. The $CaCO_3$ was precipitated after the
244 addition of 1 M $CaCl_2$. The pH was adjusted to 10.5 using a 2 M NH_4Cl solution. The
245 suspension was filtered in the laboratory and the $CaCO_3$ residue was dried in an oven at 45 ˚C
246 during the night. The weight was measured and the carbonate precipitate was retained for
247 carbon isotope analysis. The $\Delta^{14}C$ measurements were made at the Japan Atomic Energy

248 Agency (JAEA, Mutsu, Japan) using a Tandetron Accelerator Mass Spectrometer (AMS)
249 (Model 4130, High Voltage Engineering Europe). The $CaCO_3$ samples (3–100 mg C) were
250 combusted under vacuum overnight at 900 ˚C in the presence of an Ag plate and CuO
251 powder. The released CO_2 was dehydrated using a mixture of ethanol and dry ice and purified
252 with liquid nitrogen. Samples of CO_2 were then reduced to graphite at 650 ˚C with H_2 gas
253 using iron powder (>99.000 %), which was packed in a small aluminium ‘‘target’’ for AMS
254 measurement. A reference ^{14}C oxalic acid (NIST-SRM-4990C) was used to evaluate the
255 carbon isotope data. All the reported $\Delta^{14}C$ values calculated from the $^{14}C/^{12}C$ ratios were
256 corrected for fractionation using the $\delta^{13}C$ value of each sample. The precision of the $\Delta^{14}C$
257 values obtained was typically below ±1.0 (0.3–1.0) % at 1 σ of the counting statistics.
258

259 *2.8.Thermodynamic calculations and data analysis*

260 The partial pressure of CO_2 (pCO_2), DIC and its species concentrations, mineral saturation
261 state (calcite) and carbonate system model were computed using PHREEQC (Parkhurst and
262 Appelo, 2013) and MIX4 (Edgerton et al., 1991) software. Raw data manipulation and
263 statistic calculations were performed using R statistical environment (R Core Team, 2014).

264 **3. Results**

265 *3.1.Cave air composition*

266 The level of CO_2 in cave air shows a typical seasonal pattern. The period of CO_2
267 accumulation in RiB started in March 2014, when cave CO_2 concentrations started to rise and
268 reached maximum values during July and October 2014 (Fig. 3). During summer time the
269 peak CO_2 concentrations at BHA site were always higher (9400-10450 ppmv) than those at
270 OHA site (4300-4500 ppmv). CO_2 concentrations started to drop in late October 2014 and
271 reached minimum values in January 2015, around 700 ppmv at BHA and OHA sites.

Concentrations started to increase again in March 2015 until the end of the measurements. Relative air humidity at BHA and OHA was ≥98% during the measurements.

Radon concentration measured with scintillation cells had similar seasonal pattern as CO_2 concentrations, with the highest and minimum values of 32770 Bq/m^{3}s and 180 Bq/m^{3}s, at BHA site and 19260 Bq/m^{3}s and 630 ppmv at OHA site in summer and winter, respectively (Fig. 3). Continuous radon concentration measurements at BHA sites showed similar seasonal pattern, as scintillation cell measurements, with similar maximum and minimum values of 32020 Bq/m^{3}s and 403 Bq/m^{3}s, respectively.

The $\delta^{13}C_{CO2}$ values of the cave air had a seasonal variation with the less negative values observed from January to April 2014 ranging from −19.2‰ to −16.3‰ at BHA and from −19.8‰ to −17.0‰ at OHA site and from December to February 2015 ranging from −19.6‰ to −11.5‰ at BHA and −18.2‰ to −12.1‰ at OHA site (Fig. 3). The most negative values were obtained from June to September 2014 ranging from −24.3‰ to −23.0‰ at BHA and from −24.3‰ to −22.0‰ at OHA site and from June to September 2015 ranging from −22.4‰ to −21.8‰ at BHA and from −22.1‰ to −20.6‰ at OHA site. The $\delta^{13}C_{CO2}$ values are in statistically highly significant negative linear correlation with log (pCO_2) values of cave air ($R^2_{adj.} = 0.66$, $p < 0.001$ at BHA and $R^2_{adj.} = 0.61$, $p < 0.001$ at OHA site).

$\Delta^{14}C$ values in cave air in winter were −25.5‰ and −12.7‰, during snow cower and without snow cower, respectively. $\Delta^{14}C$ value during summer sampling was −32.2‰. Values for soil air CO_2 were −20.3‰ and −21.9‰ during snow cower and without snow cover respectively.

3.2.Dripwater composition

The seasonal variability of some of the most important parameters of cave dripwater chemistry are presented in Fig. 4 and 5. In dripwater the highest concentrations of Ca^{2+} (from

296 46 to101 mg/l) and NO_3^- (from 8 to 30.6 mg/l) ions were observed, while all other ions were
297 presented in concentrations lower than 3 mg/l: SO_4^{2-} (from 2.2 to 3 mg/l), Mg^{2+} (from 0.7 to
298 1.2 mg/l), Si^+ (from 0.05 to 2 mg/l), Cl^- (from 0.3 to 1 mg/l), Na^+ (from LOD to 2 mg/l), K^+
299 (from LOD to 1.7 mg/l), F^- (from LOD to 0.23 mg/l), Sr^{2+} (from 0.03 to 0.055 mg/l), Al^{3+}
300 (from LOD to 0.09 mg/l), Fe^{3+} (from LOD to 0.05 mg/l), Br^- (from LOD to 0.03 mg/l) and
301 PO_4^{3-} where only one measurement of 0.07 mg/l was above the LOD. After the analyse of the
302 charge balance error (CBE) all samples with error greater than 10% were discarded from
303 further analysis (25 samples out of 125 measured samples).

304 Ions that show typical seasonal variability with the lowest values observed in winter and
305 the highest in summer are Ca^{2+}, Mg^{+2}, Si^+ and Sr^{2+}. Ca^{2+} concentrations are generally lower at
306 SD_OHA and SI_OHA comparing to the sampling site LD_BHA and LI_BHA. Generally
307 higher Ca^{2+} concentrations were observed at SD_OHA then at SI_OHA during the summer.
308 However, during the winter there were occasions when SI_OHA samples had substantially
309 higher Ca^{2+} concentrations than SD_OHA (especially in the 2013-14 winter). Ca^{2+}
310 concentrations showed similar behaviour as HCO_3^- concentrations and opposite as pH, with
311 the highest values of ~ 85 mg/l (4.24 meq/l) for SD_OHA and SI_OHA samples and ~ 100
312 mg/l (5 meq/l) for LD_BHA and LI_BHA samples. The lowest values were observed to be ~
313 50 mg/l (2.5 meq/l) in all four cases.

314 Similar variations, but at much lower concentrations, were observed also for Mg^{2+} and
315 Sr^{2+}. The average Mg^{2+} concentration for all the samples together were 0.94 ± 0.14 mg/l,
316 while the average concentration of Sr^{2+} were 0.04 ± 0.01 mg/l. The Si^+ concentrations show
317 also similar seasonal variations especially for the indirectly sampled samples at both, SI_OHA
318 and LI_BHA sites. Directly sampled samples (SD_OHA and LD_BHA) showed more
319 stochastic behaviour however with notable seasonal variations. While concentrations for

LD_BHA samples were in some occasions similar to “indirectly” sampled samples, this is not the case with SD_OHA samples, where Si^{+} concentrations are substantially higher.

NO_3^- concentrations showed irregular changes during the sampling period. Concentrations for SD_OHA and SI_OHA samples were the highest during the beginning of the investigation in November 2013 and started to drop in January 2014 reaching the lowest values of ~ 8 mg/l in March. Concentrations of NO_3^- were low until July 2014 when they started to increase and in September 2014 they reached again the maximum values of ~ 30 – 40 mg/l. Values started to be lower in November 2014, but after December 2014 the values stayed relatively uniform until the end of the investigation.

Concentrations of SO_4^{2-} and Cl^- decreased with time. At the beginning of the investigations the concentrations were ~2.8 and ~0.7 mg/l, while at the end of the investigations they were ~2.3 and ~0.4 mg/l for SO_4^{2-} and Cl^-, respectively.

K^+ concentrations showed interesting time series behaviour. Concentrations were generally very low at the LOD however three distinctive peaks were observed: in November 2013, July 2014 and August 2014 with the highest concentrations reached at 1.8, 0.8 and 0.6 mg/l, respectively at SD_OHA.

Na^+ and F^- showed very stochastic concentration values during the time of sampling. In both cases higher concentrations were observed for directly sampled than for indirectly sampled samples. However, some of the observed peaks of Na^+ concentrations coincide with peaks observed in K^+ time series. Al^{3+}, Fe^{3+} and Br^- were represented at very low concentrations near LOD and within the measurement error.

Although pH values are very scattered, a seasonal variation, with minimum values close to 7.0 in summer and maximum values close to 7.5 in winter, can be observed at SD_OHA, SI_OHA and LD_BHA. The pH values for LI_BHA samples were the most variable with the

344 minimum observed at pH of 6.69 and maximum at pH of 8.20, with the mean pH value of
345 7.50 ± 0.31.

346 Plotted total alkalinity variation values exhibited the opposite behaviour than pH values,
347 with maximum values observed during summer and the lowest values during the winter. Total
348 alkalinity maximum values for SD_OHA and SI_OHA were ~ 3.8 meq/l, while for LD_BHA
349 and LI_BHA were ~ 4.1 meq/l. The minimum alkalinity values were ~ 2.2 meq/l observed in
350 December at SD_OHA and SI_OHA. Saturation index for calcite indicates that solutions are
351 in equilibrium with calcite, however some seasonal variation have been also observed (Fig.
352 6). The lowest values were reached in late spring (from −0.75 to −0.32, depending on the
353 site), while the highest values of ~ 0.5 were determined in winter, for direct and indirect
354 sampling at both sites. Similarly log(pCO_2) values do not show clear seasonal pattern;
355 although it could be noted that the lowest values were observed in January and February and
356 the highest during September.

357 Time series of $\delta^{13}C_{DIC}$ show opposite behaviour than alkalinity with the less negative
358 values measured in winter: −11.5‰ for SD_OHA and LI_BHA, ~ −9.4‰ for SI_OHA and
359 −12.7 ‰ for LD_BHA. The most negative values were measured in summer: −14.5‰ for
360 SD_OHA, −14.6‰ for SI_OHA and LD_BHA; and −15.0‰ for LI_BHA samples. Mean
361 $\delta^{13}C_{DIC}$ values for SD_OHA, SI_OHA, LD_BHA and LI_BHA were thus as follows: −13.5 ±
362 0.6 ‰, −12.8 ± 1.0 ‰, −13.8 ± 0.5 and −13.7 ± 0.8 ‰ respectively.

363 *3.3.Water isotopes*

364 The variation of amount of precipitation and its $\delta^{18}O_{H2O\_prec}$ values together with the $\delta^{18}O$ of
365 dripwater ($\delta^{18}O_{H2O\_drip}$) can be seen in Figure 5. The $\delta^{18}O_{H2O\_prec}$ values in Postojna show
366 typical seasonal variation, with the most positive values observed in summer and the most
367 negative values during the winter. The weighted average $\delta^{18}O_{H2O\_prec}$ value during the
368 studying period is −7.9‰. The annual average amount of precipitation in Postojna during the

period 1981- 2010 was 1500 mm (ARSO). Although there was no obvious dry seasons or any clear seasonality the precipitation in Postojna tends to be more abundant in fall. The maximal monthly precipitation during the research period was recorded in February 2014 (330 mm), while the minimal monthly precipitation was recorded in April 2015 (36 mm). The year 2014 had more rainy days than other years. The annual precipitation in 2014 was 2069 mm, while for example for the years 2013 and 2015 the annual precipitations were 1622 and 1009 mm, respectively.

Dripwater $\delta^{18}O_{H2O\_drip}$ values show no seasonal pattern with relatively low values at the beginning of the experiment ranging from −10.6‰ for LD_BHA and LI_BHA samples to −9.6‰ found for SD_OHA samples. $\delta^{18}O_{H2O\_drip}$ values started to increase and reached maximum values ~ −8‰ in December 2013 and January 2014. No significant change in $\delta^{18}O_{H2O\_drip}$ values was observed after this period until the end of our study.

4. Discussion

First, Johnson-Wehrly-Mardia correlation coefficient was used to show the correlation between CO_2 concentrations in cave air and the day of the year (Pewsey et al., 2013). Temporal variable indicating day of the year was converted into circular variable by multiplying the sequential number of the day of the year by $2\pi/365$ as done by Jammalamadaka and Lund (2006). Correlation coefficient values of 0.78 ($p < 0.001$) and 0.69 ($p < 0.001$) were calculated for OHA and BHA, respectively. This indicates that it is possible to predict the concentration of CO_2 in cave air by the day of the year.

CO_2 in cave atmosphere can originate from different sources and can be transported through different pathways (Frisia et al., 2011) including: (i) CO_2 from the external atmosphere; (ii) input of CO_2 from the overlaying soil and epikarst; (iii) CO_2 from degassing of dripwaters, (iv) biotic CO_2 production in cave; (v) cave visitors; and (vi) deep CO_2 sources.

393 Biotic and in-situ CO_2 production in the cave is negligible due to the absence of active
394 streams transporting fresh organic material from outside into the cave and the absence of bat
395 colonies. Since Pisani rov is closed to the tourists, and RiB is located at the end of the Pisani
396 rov, the CO_2 exhaled out by tourists of Postojna cave do not affect its air composition.
397 The CO_2 of geologic origin could potentially be released to the caves over the Jeršan fault
398 crossing Pisani rov right in the southern part of RiB in the NW-SE orientation (Šebela and
399 Čar, 2000). The CO_2 of such deep geologic origin is typically ^{13}C-enriched, relative to
400 biological sources. For example, the $\delta^{13}C$ of CO_2 degassing from the upper mantle has values
401 of –6.5‰ (Sano and Marty, 1995) or even higher if deep source CO_2 is undergoing secondary
402 methanogenesis following hydrocarbon biodegradation (Etiope et al., 2011). Our cave CO_2
403 have lower $\delta^{13}C_{CO2}$ values suggesting that CO_2 in RiB has little contribution from CO_2 deep
404 source. Furthermore, $\Delta^{14}C$ values in cave air CO_2 ranged between –25.5‰ and –12.7‰
405 indicative of young CO_2 in RiB.
406 Thus, the main discussion is focused on the major possible sources influencing the cave
407 air CO_2 starting with the mixing CO_2 with external atmosphere in connection to cave
408 ventilation (Fig. 7).
409

410 *4.1. CO_2 from outside atmosphere and cave ventilation*

411 Three important observations were made on the cave air composition (Fig. 3): (i) CO_2
412 concentration curve shows similar behaviour as outside air temperature curve; (ii) ^{222}Rn and
413 CO_2 concentrations are in good positive correlation at BHA and at only moderate positive
414 correlation at OHA site ($R^2_{adj.} = 0.80$ and $R^2_{adj.} = 0.42$) with no distinction between colder and
415 warmer periods; and (iii) both CO_2 and ^{222}Rn concentrations reached higher values at the
416 lower sampling point (BHA). The relation between CO_2 and temperature suggests that either
417 CO_2 concentration in the cave depends on the soil respiration, which is conditioned manly by

418 the temperature or/and that CO_2 concentration in the cave depends on the cave ventilation,
419 which is also influenced by the outside temperature. Since ^{222}Rn production is independent
420 from the soil respiration, the relation between ^{222}Rn and CO_2 further supports the assumption
421 that the cave ventilation (rather than variation of soil respiration) is a driving force influencing
422 both ^{222}Rn and CO_2 concentrations in cave air. The third observation is especially
423 conspicuous when the weekly average temperatures of outside air exceed above the cave air
424 temperature. During the colder period of the year concentrations at OHA were similar than
425 that at BHA and at some occasions also slightly higher. This means that air in RiB is not
426 uniformly mixed and further investigations regarding CO_2 stratification has to be made to
427 develop a useful CO_2 mass balance model to estimate cave air exchange rates with outside
428 atmosphere. Further discussion deals with different parameters affecting CO_2 and ^{222}Rn
429 concentrations in RiB.
430 Gregorič et al. (2013) reported that ventilation in RiB is triggered when outside temperature
431 falls below cave air temperature. In this study, the correlations between measured cave air
432 CO_2 concentration and outside temperatures (Postojna meteorological station) were further
433 tested. Different parameters of the outside air temperature (minimal, maximal and average)
434 during different time periods preceding the CO_2 concentration measurement in the cave air
435 were tested. The calculations were made iteratively for different time lags in daily (24 hours)
436 steps. The highest correlation was found between CO_2 concentrations in RiB and minimal
437 outside temperature over the period of one week before the measurements: $r = 0.82$ ($p <$
438 0.001) and $r = 0.73$ ($p < 0.001$) for BHA and OHA, respectively. Cold air outside of the cave
439 enters the hall and pushes the warm cave air from the cave through vertical cracks and/or
440 fissures. The influence of cave air to soil air was detected and discussed more in detail in
441 Krajnc et al. (2017). Several CO_2 accumulation events also occurred during the cold period
442 when outside temperatures were below 0 °C. The increase in CO_2 concentration in cave air

443 during outside sub-zero temperatures suggested that ventilation of RiB was at least partly
444 driven by hidden air conduits above the cave. These conduits presumably connect RiB and
445 outside atmosphere, but were blocked either by snow or frozen water during the cold winter
446 temperatures. Preliminary measurements of CO_2 concentrations in RiB and airflow direction
447 in Pisani rov corridor performed by Slovenian Karst Research Institute, show that CO_2
448 concentrations decreased when air flows in the direction from the main passage to RiB
449 indicating that fresh air preferentially enters through the main passage. During the warmer
450 periods the ventilation was inhibited and CO_2 starts to accumulate. The stable temperature in
451 RiB is, among others, the result of the dominant role of the heat conduction trough the rock in
452 contrast to the weaker influence of the heat transported by advection. This can happen in
453 caves with limited ventilation (such as Pisani rov) due to the fact that the heat contained in the
454 rock is ~1800 times larger than the heat in the same volume of air (Pflitschand Piasecki,
455 2003). It has been also shown that the direct thermal conduction from the surface temperature
456 changes can be completely muted at depth greater than around 20 m (Pollack and Huang,
457 2000). Similarly, also the transport of heath via percolating water is normally muted within
458 the first 20 m (Anderson, 2005).

459 Continuous monitoring on the radon concentration was used to test if other atmospheric
460 parameters affect cave ventilation, besides atmospheric temperatures. Radon (^{222}Rn) is an α-
461 emitter with half-life ($t_{1/2}$) of 3.82 days. Since it is a noble gas, which can be highly abundant
462 in caves, it is a useful tracer for cave ventilation investigations (e.g. Wilkening and Watkins,
463 1976; Kowalczk and Froelich, 2010; Gregorič et al., 2013; Gregorič et al., 2014). ^{222}Rn
464 concentrations in caves are mainly controlled by a balance of radon emission from cave walls
465 and drip waters, its radioactive decay, and exchange with the outside atmosphere (Wilkening
466 and Watkins, 1976). Correlations of ^{222}Rn concentrations with: wind directions, wind speed,
467 average daily atmospheric pressures, and differences between maximum and minimum daily

atmospheric pressures and rate of change (24 h) of atmospheric pressures were statistically insignificant. Further analysis was made to investigate the wind influence on the cave ^{222}Rn concentrations during different, temperature driven, ventilation regimes in RiB. For this purpose the data was divided in to four subgroups according to the seasons. Winter and summer represent the active and stagnant ventilation regime, respectively; while spring and fall are the transitional periods between them. Winds in Postojna blow mainly from North-East or South-west direction. When comparing ^{222}Rn concentrations with wind directions we observed that in winter ^{222}Rn concentrations rarely reached concentrations over 5000 Bq/m^3s when wind blew from SW direction. When wind blew from N, NE or NEE direction ^{222}Rn concentrations could reach values above 20000 Bq/m^3s. No such observation was noticed for other three seasons. This clearly shows that during the winter, i.e. during the ventilation period, the outside temperature is not the only factor affecting the cave air composition or at least that during the cold period the wind direction has more pronounced effect on cave air composition in RiB. Johnson-Wehrly-Mardia correlation could not be used here since the distribution of wind direction around the year and in each season, was clearly bimodal. Point-biserrial correlation was used instead. Correlation of ^{222}Rn concentrations and winds either from NE or SW was strong and highly significant for winter ($r = 0.63$, $p<0.001$) and low or very low for other seasons in the year. It should be stressed out that except for the wind directions, the correlations of ^{222}Rn continuous data with other parameters were calculated for the whole year and that continuous ^{222}Rn measurements were performed only at BHA site.

A good correlation between ^{222}Rn and CO_2 concentrations at BHA site suggests a common driving force of both gasses e.g. cave ventilation. During warmer periods values are more scattered indicating that other processes controlling these two gasses may become more apparent. Similar behaviour was observed also in the study performed by Gregorič et al. (2013), where the correlation between ^{222}Rn and CO_2 concentrations in warmer periods was

493 even more distinctive from that observed in the colder period. Further it was found that at
494 lower ^{222}Rn and CO_2 concentrations no difference in concentrations between OHA and BHA
495 sites were observed. On the other hand, when thresholds were reached (around 3000 ppmv for
496 CO_2 and around 15000 Bq m^{-3} for ^{222}Rn), concentrations at BHA site become substantially
497 higher than those obtained at OHA. It can be speculated that ventilation of RiB can be roughly
498 divided into two types. First, winter ventilation, which is more rigorous and affects all the RiB
499 air conditions and second, summer ventilation, which is more gentile and directly affects only
500 the upper part of RiB. This, summer ventilation type, may be controlled by other
501 environmental parameters perhaps more important than temperature differences.

502 *4.2.CO_2 from the overlaying soil and epikarst*

503 The second possible sources of cave CO_2 can be soil respired CO_2, which can be transported
504 to the cave dissolved in dripwater or directly transported from soil through cracks into the
505 cave in a gas phase (Ek and Gewelt, 1985; Baldini et al., 2006; Kowalczk and Froelich, 2010;
506 Frisia et al., 2011). During the study, obvious CO_2 gradient was encountered in RiB (i.e.
507 measured CO_2 concentrations were almost always higher at the lower BHA site than at the
508 higher OHA site). The specific compositions of underground air under steady-state conditions
509 are not related to gravity ("weight" of CO_2), but to the absence of air movement around the
510 gas source (Badino, 2009). If CO_2 would be transported into RiB) by diffusion under steady-
511 state conditions, it should be uniformly mixed or at least elevated concentrations should be
512 noticed in its sources. This strongly indicates that CO_2 from soil is not transported to the RiB
513 only by diffusion from the RiB celling or walls, but rather flowing down under transient
514 conditions or diffusing from unknown voids at lower parts of RiB. In either case isotopic
515 composition of cave CO_2 indicates cave CO_2 being a mixture of atmospheric CO_2 and soil
516 respired CO_2. Since soil respired CO_2 can enter the cave also dissolved in dripwaters further
517 discussion about that pathway will follow later in this section.

First, the $\delta^{13}C_{CO2}$ values together with $\Delta^{14}C$ were used to evaluate the relative contribution of different sources to soil and cave CO_2 gas. Three different sources were considered: (i) atmospheric air; (ii) young organic carbon derived from contemporary C3 plants; and (iii) weathered carbonates and carbonate rocks. Thus, a triple mixing model was applied using the following equations:

$$\delta^{13}C_{CO2,atm} F_{CO2,atm} + \delta^{13}C_{CO2,org} F_{CO2,org} + \delta^{13}C_{CO2,CaCO3} F_{CO2,CaCO3} = \delta^{13}C_{CO2,sam} \quad (1)$$

$$\Delta^{14}C_{CO2,atm} F_{CO2,atm} + \Delta^{14}C_{CO2,org} F_{CO2,org} + \Delta^{14}C_{CO2,CaCO3} F_{CO2,CaCO3} = \Delta^{14}C_{CO2,sam} \quad (2)$$

$$F_{CO2,atm} + F_{CO2,org} + F_{CO2,CaCO3} = 1 \quad (3)$$

where subscripts "atm", "org", "CaCO3" and "sam" are related to atmosphere, organic carbon, carbonate rock and sample, respectively. The following isotopic values ($\delta^{13}C$, $\Delta^{14}C$) of individual end-members (–9.6‰, 49.5‰), (–25.2‰, 85.1‰) and (1.6‰, –1000‰) for atmospheric air, young organic carbon and mineral (carbonate rock) sources, respectively, were considered in our calculation. The $\Delta^{14}C$ value of atmospheric air was taken from the literature (Liu et al., 2006; Levin et al., 2010), while $\delta^{13}C_{atm}$, $\delta^{13}C_{CO2,org}$ and $\delta^{13}C_{CO2,CaCO3}$ values were determined in the previous study performed at the same location (Krajnc et al., 2017). Atmospheric CO_2 as well as respiratory sources contain modern ^{14}C from nuclear testing, and since root and most microbial respiration is fuelled by recently synthesized organic matter, the $\Delta^{14}C$ of respiratory CO_2 will be close to that of the atmosphere (ca. +85.1‰) representing the young, ^{14}C-active C. Another source is CO_2 originating from carbonate bedrock, which is composed of ancient, ^{14}C-dead C and has a $\Delta^{14}C$ of –1000‰ (Bond-Lamberty and Thomson 2010). The calculated contributions are presented in Table 1. The data indicate that carbonate mineral has a minor influence on soil and cave CO_2 and the

543 ^{13}C-enrichement in soil CO_2 observed at these sites derives from the atmosphere. Further it
544 was estimated that young organic matter comprised 54 and 68% in cave air, while the highest
545 atmospheric air contribution to CO_2 of 37% was observed in cave sample during the winter
546 under the snow cover. It is interesting to note that in the soil air the lowest atmospheric air
547 contribution was observed during the summer when the degradation of organic matter is more
548 pronounced. Sensitivity analysis was performed by changing $\delta^{13}C$ values of different sources
549 by 1‰ and $\Delta^{14}C$ analysis by the 10‰. The results indicated that the estimated ranges vary
550 only modestly with different choices of source increment and mass balance tolerance
551 parameter values. The highest changes were related to the lowest contribution of atmospheric
552 CO_2 in soil air in summer.
553 At this point a term of "ground air" should be explained. This term was suggested by
554 Atkinson (1977), as a CO_2 in air of the vadose zone below the soil layer. Sources of CO_2 in
555 "ground air" may include same sources as in the cave of interest, since in this regard cave
556 itself can represent a reservoir of "ground air". Additional sources of "ground air" may
557 include CO_2 degassed from the ground water, CO_2 respired from the deep roots, and CO_2
558 from decomposition of organic matter brought by water (Atkinson, 1977; Wood and Petraitis,
559 1984; Wood, 1985; Mattey et al., 2013). In the latter case the decomposition of organic matter
560 at depth of several meters would happen at similar temperatures in all seasons and could
561 therefore represent a constant CO_2 production (Atkinson, 1977). Since "ground air" CO_2 may
562 come from the same sources as soil air CO_2 and it is generally not possible to distinguish it
563 based on isotopic approach; it was not regarded as a separated source in this study but more as
564 a possible mechanism affecting the dynamic of cave CO_2 accumulation. However, this
565 mechanism may be responsible for CO_2 stratification, for its relatively fast "re-accumulation"
566 after ventilation events and for the CO_2 accumulation events in winter during the snow cower.
567

568 *4.3. Dripwater geochemistry and response to the external conditions*

569 Although drip rates from the stalactites were not measured during this investigation, higher
570 drip rates during raining events and lower during drier seasons were observed, except during
571 the vegetation period, when drip rates did not increase during rain events. It seems that there
572 is a direct hydraulic connection with the meteorological signal. To further investigate this
573 observation the $\delta^{18}O_{H2O\_drip}$ was compared with the $\delta^{18}O_{H2O\_prec}$. The aim was to calculate a
574 simple periodic regression analysis, similar to one described by Bliss (1958), to assess the
575 mean residence time of percolating water. Although the precipitation data (2012-2015)
576 showed moderate sinusoidal behaviour with a period of 12 months ($R^2 = 49.6$) there was no
577 such behaviour of the $\delta^{18}O_{H2O\_drip}$ values. There was clear jump of $\delta^{18}O_{H2O\_drip}$ toward more
578 positive values starting to rise in September 2014 suggesting another factor was influencing
579 $\delta^{18}O_{H2O\_drip}$ values: likely near-surface evaporation. Although the absence of sinusoidal
580 behaviour (with the "wave length" of 12 months) of $\delta^{18}O$ values in dripwaters would indicate
581 that the mean residence time of percolating water is more than one year, the observed jump of
582 the values suggests that this is not the case. Possible explanation could be the effect of the
583 "ice rain" and the sanitary cuttings of the forest above the cave that had dramatically exposed
584 the soil to the direct sunlight. This effect could increase the evaporation of rain water
585 percolating into the soil profile and thus affecting the oxygen isotopic composition of water.
586 The "ice rain" event happened in February 2014, while there were several forest cuttings
587 conducted in the subsequent months of 2014 and 2015. With the snow melted until the April
588 the signal of the water enriched in ^{18}O had to travel for roughly half a year, before reaching
589 the cave. Besides that, the spring of 2014 was followed with a highly rainy summer.
590 Together with $\delta^{18}O$ values in dripwaters, also other chemical constituents such as Cl^-, SO_4^{2-},
591 NO_3^- show similar trend (Fig. 5). Cl^- can be used as a conservative tracer for hydrological
592 process since it does not come from weathering of soil naturally present minerals in soil

neither is influenced by biological activity (e.g. Quade et al., 2003; West et al., 2005; Jin et al., 2008). In the present research, Cl^- concentrations in dripwaters do show changes over the time that are in a strong statistically highly significant negative correlation ($R^2_{adj.}$= 0.62, $p<0.001$) with $\delta^{18}O_{H2O\_drip}$ values. This suggests that Cl^-, concentrations and $\delta^{18}O_{H2O\_drip}$ values show the signal transferred from the surface. It is possible that the decrease observed in Cl^- concentrations reflect also the dilution due to increased discharge and/or due to reduced tree water used. Similar observation was also observed for SO_4^{2-} concentrations. Thus, it is likely that we are seeing a change in concentrations of these ions due to a combination of removal from the surface and subsurface, as well as dilution. Similar observation in Cl^- concentrations was also observed in the study performed by Nagra et al. (2016) in a cave dripwater chemistry after post-wildfire in Australia. Even stronger correlation with $\delta^{18}O$ values was observed with NO_3^- concentrations. NO_3^- most strongly correlates with $\delta^{18}O$ for LD_BHA and LI_BHA; $R^2_{adj.}$ = 0.83 and $R^2_{adj.}$ = 0.70 ($p<0,001$), while for SD_OHA and SI_OHA the correlation is weak to moderate. Higher concentrations of NO_3^- observed after tree cutting could be related to the reduction in the tree need for nutrients and thus higher infiltration of NO_3^- into the cave dripwater.

The results on the distribution of carbonate minerals (Ca^{2+}, Mg^{2+} and Sr^{2+}) showed that the "ice rain" event and tree cutting could not be so evident in the carbonate chemistry indicating that other process can have higher impact then hydrology. If we consider mean residence to be roughly half year and noticing that carbonate minerals show obvious seasonal variation with highest values in summer, this suggests to neglect the presence of the so called "classic karst model" (Spötl et al., 2005), where seasonal fluctuations of CO_2 concentrations in soil air are transferred to the cave environment via seepage water (i.e. cave air concentration is higher due to higher soil respiration).

617 Positive correlation was also found between dripwater Na^+ and K^+ concentrations that could
618 be interpreted as controlled by the equilibria between diluted soil solutions and an
619 exchangeable pool associated with clay and organic matter (Berner et al., 1998).
620 Nevertheless, it is very hard to make any firm conclusions for selected sampling drip sites
621 based only on this relatively short monitoring period since karst hydrology can be very
622 complex. Flow of water in karst can be a combination of point and diffuse flow into the
623 ground where again, water can have different flow pathways through the ground, ranging
624 between rapid preferential and slower matrix flow. These water flow pathways depend also on
625 type of porosity water encounters on its way. Three different types of porosity in rock are
626 generally distinguished in karst: **primary** (related to inter-granular void space), **secondary**
627 (joints and fractures) and **tertiary porosity** (conduits) (Ford and Williams, 2007). In addition,
628 water can be withheld and mixed in different voids (water reservoirs) within the epikarst,
629 which can again have different draining types (e.g. drainage with "underflow" or "overflow")
630 that can respond differently depending on the amount of water routed and flowing to them at
631 certain time. Therefore, it can be a very complex system with water following variable
632 pathways before reaching the drip-site under investigation (Bradley et al., 2010).
633 Mg^{2+}/Ca^{2+} ratio is for all measured samples less than 0.1 with the average of 0.02 ± 0.002.
634 This indicates that calcite is the only mineral present i.e. there is only calcite dissolution
635 present in epikarst, showing only minor substitution of Mg^{2+} for Ca^{2+} in calcite. This is further
636 supported by 1000 Sr^{2+}/Ca^{2+} ratios (0.28 ± 0.03) typical for the carbonate fraction. Sr^{2+}
637 concentrations for all sampling sites (except LD_BHA since there were not enough valid data
638 to compare) showed strong to very strong highly significant ($p<0.001$) correlation with Ca^{2+}
639 ($R^2_{adj.}$ ranging 0.51 to 0.76) and therefore also with cave air CO_2 concentration.
640 When discussing has a control on dripwater chemistry a possibility of prior calcite
641 precipitation (PCP) has to be considered. Negative correlation between Ca^{2+} concentration

642 and Mg^{2+}/Ca^{2+} concentrations ratio of the dripwater would indicate the presence of PCP
643 (above cave or inside the cave prior to drip water collection) (Fairchild and Treble, 2009).
644 Data of directly sampled drip water (SD_OHA and LD_BHA) suggested that there was no
645 PCP present at both sampling sites. For the SD_OHA and LD_BHA no statistically
646 significant correlation was found. However, at both sampling sites where water was left in the
647 cave for two weeks before the collection (SI_OHA and LI_BHA), low but significant
648 negative correlations were observed. Correlation strength and significances were $R^2 = 0.31$;
649 $p<0.01$, $R^2 = 0.45$ $p<0.01$ for SI_OHA and LI_BHA site, respectively. This was expected
650 since the water had more than enough time to degas and to precipitate calcite. Furthermore, no
651 seasonal variability was observed for Mg^{2+}/Ca^{2+} and Sr^{2+}/Ca^{2+} ratios in the dripwater neither
652 any statistically significant correlation between Mg^{2+}/Ca^{2+} (and Sr^{2+}/Ca^{2+}) ratios was observed
653 with cave air CO_2 concentrations, its $\delta^{13}C_{CO2}$ values or the surface temperatures. These
654 observations indicate that CO_2 was degassing from dripwaters without forcing a sufficient
655 amount of calcite precipitation to measurably affected dripwaters Mg^{2+}/Ca^{2+} (Sr^{2+}/Ca^{2+}) ratios
656 (Spötl et al. 2005) or/and that recrystallization of calcite within the host rock (not the PCP) is
657 the dominant mechanism affecting Mg^{2+}/Ca^{2+} (Sr^{2+}/Ca^{2+}) variability (Wong et al., 2011).

658 Parameters, which are more susceptible to the changes happening in the cave
659 environment are related to carbonate system and include: pH, alkalinity, HCO^-_3, Ca^{2+}, pCO_2,
660 $\delta^{13}C_{DIC}$ showing more or less obvious seasonal behaviour (Fig. 4 and 5). The changes of pH,
661 alkalinity, HCO_3^-, Ca^{2+}, pCO_2, $\delta^{13}C_{DIC}$ in RiB can be explained as a response to increased
662 CO_2 degassing and consequently by the increased calcite saturation state (SI_{calc}) during the
663 ventilation (Fig.6). This explanation is also supported by higher values of Ca^{2+} in the summer
664 and autumn and the decline of Ca^{2+} following the peak of the winter values of SI_{calc}.
665 Furthermore, this explanation is consistent with the highly significant ($p<0.001$) positive
666 correlation of Ca^{2+} and alkalinity (Pearson's r for SD_OHA, SI_OHA, LD_BHA and

667 LI_BHA were: 0.65, 0.72, 0.87 and 0.72; respectively), and significant negative correlation
668 between Ca^{2+} and pH (Pearson r for SD_OHA, SI_OHA, LD_BHA and LI_BHA were: –0.58,
669 –0.32, –0.81 and –0.48, respectively). Besides that, almost all mentioned parameters are in
670 highly significant, moderate to very strong correlation with the CO_2 concentrations measured
671 in the cave air at both sampling sites. The exceptions are the absence of linear correlation
672 between $\delta^{13}C_{DIC}$ values for SD_OHA with the CO_2 concentrations at OHA site, and HCO^-_3
673 values for LD_BHA with the CO_2 concentrations at BHA site. These findings suggest that
674 reactions occurring in the RiB are decupled from processes happening in the soil and on the
675 way to the cave. These considerations are further supported by the fact that variability of
676 mentioned parameters is in phase with happening at the surface (soil temperature, soil air CO_2
677 concentrations). If these changes were a response to the occurrences at the surface a certain
678 time lag would be expected (Pitty, 1966; Spötl et al., 2005). Therefore, the changes in pH,
679 alkalinity, HCO^-_3, Ca^{2+}, pCO_2, $\delta^{13}C_{DIC}$ in RiB cannot be a consequence of the direct and fast
680 response to the surface conditions but rather a consequence of a mechanism that directly
681 affects the cave environment and is affected with similar environmental parameters as soil
682 respiration, i.e. cave ventilation. Lowering of the CO_2 concentration in cave air causes
683 increased CO_2 degassing, which affects the parameters which are known as the "main actors"
684 in the carbonate equilibria.
685
686 *4.4.CO_2 from degassing of dripwaters*
687 Soil air CO_2 dissolves in infiltrating rain water, which percolates trough the soil profile and
688 the epikarst into the cave. Degassing of CO_2 into the cave air occurs if cave atmosphere has
689 lower pCO_2 than the dripwater that is in equilibrium with the cave air CO_2. CO_2 in infiltrating
690 water forms a weak carbonic acid, which dissolves carbonate bedrock (Reactions 4 and 5),
691 and produces very distinctive isotopic composition:

692 $$CO_{2(g)} + H_2O_{(aq)} \rightleftharpoons H_2CO_{3(aq)} \quad (4)$$

693 $$H_2CO_{3(aq)} + CaCO_{3(s)} \rightleftharpoons 2HCO^-_{3(aq)} + Ca^{2+}_{(aq)} \quad (5)$$

694 $$2HCO^-_{3(aq)} + Ca^{2+}_{(aq)} \rightleftharpoons CO_{2(g)} + CaCO_{3(s)} + H_2O_{(aq)} \quad (6)$$

695

696 The processes of carbonate dissolution during the water percolation can occur somewhere in
697 the range between an open and a closed system. In the open system dissolution, a complete
698 isotopic equilibrium occurs between soil CO_2 and all DIC species in the solution, while the
699 pCO_2 does not change since a large CO_2 reservoir is constantly replenished by the soil
700 respired CO_2. Therefore, the isotopic composition of DIC and subsequently CO_2 degassing
701 from water is not influenced by the isotopic composition of the dissolving $CaCO_3$, but
702 depends only on the isotopic composition of soil CO_2 (Deines et al., 1974; Salomons and
703 Mook, 1986). In a closed system dissolution, the soil water first equilibrates with soil CO_2,
704 and becomes isolated from the soil gas reservoir before the $CaCO_3$ dissolution (Deines et al.,
705 1974; Salomons and Mook, 1986). In this case the stoichiometry of the carbonate dissolution
706 dictates that half of carbon in HCO_3^- originates from $H_2CO_3^*$ and half from $CaCO_3$, which
707 affect the isotopic composition of HCO_3^- according to (Jin et al., 2009):

708

709 $$\delta^{13}C_{DIC} = (\delta^{13}C_{H_2CO_3} + \delta^{13}C_{CaCO_3})/2 \quad (7)$$

710

711 Since the majority of DIC under pH of investigated drip waters is present in the form of
712 HCO_3^- we can assume that $\delta^{13}C_{HCO3} \approx \delta^{13}C_{DIC}$. The isotopic composition of soil respired CO_2
713 ($\delta^{13}C_{CO2} = -25.2 \pm 1.5$‰; Krajnc et al., 2017) and limestone carbonate ($\delta^{13}C_{CaCO3} = 1.6 \pm 0.2$‰;
714 Krajnc et al., 2017) above the cave give similar results for $\delta^{13}C_{DIC}$ if calculation for open and
715 closed system dissolution are considered (−11‰ and −10.3‰ for open and closed systems,

716 respectively). These calculations were made under assumptions that direct contribution from
717 atmospheric CO_2 is negligible, chemical reactions happened at constant temperature of 8.4 ºC
718 where chemical and isotopic equilibrium is achieved and no PCP is occurring. Fractionation
719 factors proposed by Zhang et al. (1995) were used for these calculations. Since in the natural
720 environments a combination of open and closed system dissolution can occur (Hendy, 1971;
721 Fairchild et al., 2006) the actual value of $\delta^{13}C_{DIC}$ is between these two values. However, based
722 on these data it was not possible to make distinction between dissolution in open or closed
723 system, neither to assess the proportion of carbon originating from $CaCO_3$ dissolution.

724 Measured values of $\delta^{13}C_{DIC}$ (SD_OHA and LD_BHA) ranged from ~ −12‰ in winter to ~
725 −14.5‰ in summer. If direct respond of dripwaters to the situation in the soil above the cave
726 was assumed, higher proportion of degradation of organic matter that influences the $\delta^{13}C_{DIC}$
727 values could be expected during the summer. Temperature during chemical reactions also
728 affects the isotopic composition of DIC, where change of temperature to 20 ºC in summer
729 would theoretically change $\delta^{13}C_{DIC}$ value for 1.3‰ (Zhang et al., 1995) towards more
730 negative $\delta^{13}C_{DIC}$ values. To get a better insight into the processes affecting DIC once the
731 water enters the RiB, the measured data were compared with an equilibrium model that is
732 similar to one used by Spötl et al. (2005) (Fig. 8). In the first step measured values were
733 compared with the calculated data explaining DIC concentration against log(pCO_2) values of
734 water. This calculation was performed using a MIX4 software. Values considering only
735 degassing of CO_2 and values considering calcite precipitation after a certain calcite saturation
736 was achieved (+0.35 was used as a realistic saturation index) were calculated (lines D and DP,
737 respectively). The highest measured DIC value of 292 mg/l as HCO_3- (4.79 meq/l) was
738 chosen as a starting point for forward and back modelling of DIC and log(pCO_2) water values.
739 Isotopic composition of DIC was calculated using the linear form of Rayleigh equation
740 (Matthews and Kolodny, 1978) in the similar way as done by Bar-Matthews et al. (1996).

741 Fractionation factors proposed by Zhang et al., (1995) ware used for degassing (line D)
742 whereas for the case where degassing and calcite precipitation occur simultaneously the
743 approach suggested by Bar-Matthews et al. (1996) was used. In this approach, it is assumed
744 that the carbon of dissolved bicarbonate is equally fractionated into $CaCO_3$ and CO_2. Because
745 of this equal split the theoretical fractionation factor is the mean of both fractionation factors.
746 At 8.4 °C: $1000\ln\alpha(CO_2\text{-}HCO_3^-) = -9.8‰$ (Zhang et al 1995) and $1000\ln\alpha(CaCO_3\text{-}HCO_3^-) =$
747 +1.0‰ for calcite (Romanek et al. 1992). Therefore, the theoretical overall fractionation
748 corresponds to $1000\ln\alpha = 4.4‰$.
749 The measured values indicate that majority of changes in dripwater composition happens due
750 to degassing and precipitation under equilibrium conditions. Similarly, the evolution of
751 $\delta^{13}C_{DIC}$ in relation to pCO_2 shows that that majority of measured data follows modelled lines
752 for processes happening under isotopic equilibrium. However, some of the data, especially
753 data from SI_OHA site at hot summer days, plot out from the modelled lines (Fig. 8). The
754 SI_OHA sampling site is located on the hill where lower CO_2 concentrations were recorded
755 (during all seasons) suggesting that this part of RiB is more frequently ventilated also during
756 the warmer periods. At this location larger concentration gradient between CO_2 in dripwater
757 and cave air can occur, which can cause kinetically enhanced isotopic fractionation during
758 degassing.
759 To assess the theoretical isotopic composition of CO_2 degassing from dripwaters a Rayleigh
760 model as described in Appelo & Postma (2005) was applied using PHREEQC software
761 (Parkhurst and Appelo, 2013). To check the hypothesis that CO_2 comes to the cave
762 exclusively via dripwater and from the outside atmosphere, modelled isotopic composition
763 values of degassed CO_2 were used further in the two end-member mixing model (second
764 endmember is atmospheric air) to model the theoretical isotopic composition of cave air CO_2
765 at pCO_2 that were encountered in the RiB during the actual sampling.

766 The comparison of modelled values against the measured ones was used to check the
767 hypothesis (under the assumptions that measured dripwaters are representative for all the
768 RiB). Calculated values are plotted together with the measured cave air $\delta^{13}C_{CO2}$ values in Fig.
769 9. It can be seen that if CO_2 in the cave air would be a mixture of CO_2 degassing from
770 dripwater and atmospheric CO_2, the $\delta^{13}C_{CO2}$ values would be more positive than the measured
771 one. This is the case for both the OHA and BHA. Possible cause for such high $\delta^{13}C_{CO2}$ values
772 could eventually be the kinetically enhanced isotopic fractionation during degassing, but as
773 seen from the Fig. 8 this effect is expected to happen only at certain occasions and only at the
774 OHA site. Nevertheless, modelled $\delta^{13}C_{CO2}$ values are still too high for both OHA and BHA
775 sites indicating that CO_2 degassing from dripwaters could not be a source that would
776 significantly contribute to the overall cave air CO_2 concentrations in RiB. Similar findings
777 were found at Grotta di Ernesto in the study done by Frisia et al. (2011) where CO_2 efflux
778 from dripwater also has only a small effect on the carbon dioxide mass balance in the cave.

779 **5. Conclusions**

780 The conclusions of this study can be summarized as follows:
781 The levels of CO_2 concentrations, $\delta^{13}C_{CO2}$ and ^{222}Rn in the cave air have typical seasonal
782 pattern. Accumulation of CO_2 and ^{222}Rn started in spring and reached maximum values in
783 summer. Values started to drop in fall and reached the lowest concentrations in winter.
784 $\delta^{13}C_{CO2}$ values showed the opposite trend with the lowest $\delta^{13}C_{CO2}$ values observed during the
785 highest CO_2 concentrations. Variations of CO_2 concentrations in cave air are not the function
786 of soil CO_2 productivity, but are mainly caused by the ventilation of the cave that is triggered
787 by the differences between cave and outside air temperature.
788 The analysis of carbon isotope composition of CO_2 and dripwater DIC indicated that the
789 major source of cave CO_2 in the studied chamber is the CO_2 originating from soil respiration,

790 transported directly to the cave, meanwhile the CO_2 transported to the cave in the form of DIC
791 in the dripwaters has minor influence on the cave air CO_2 concentration levels.
792 The DIC concentrations and its isotopic compositions do not have direct response from the
793 variations in soil respiration. The DIC concentrations and its isotopic composition together
794 with Ca^{2+} and Mg^{2+} concentrations in drip waters showed that there was no prior calcite
795 precipitation before the sampling and that forced degassing causing kinetic effects could be
796 possibly present only at certain occasions.

797 **Acknowledgements** The study is a part of PhD thesis of B. Krajnc supported by the
798 Innovative scheme for co-financing of doctoral studies financed by the European Union
799 through the European Social Fund and by the scholarship granted by World Federation of
800 Scientists. This study was performed within H2020 MASTWIN project and within the Japan-
801 Slovenian cooperation. Special thanks goes to professor Franci Gabrovšek for constructive
802 suggestions during the work and to professor Ian Fairchild for enabling us the use of the
803 MIX4 software. We appreciate the support of cave guides Stanislav Glažar, Janez Margon and
804 Erik Rebec for their dedication during fieldwork. We would also like to acknowledge the
805 managers of Postojna Jama d.d. and Ministry of Agriculture and Environment of Slovenia for
806 the permission to access and work in the cave.
807

808 **References**

809 Anderson M. P. (2005) Heat as a Ground Water Tracer. *Ground Water* **43**, 951–968.

810 Appelo C. A. J. and Postma D. (2005) *Geochemistry, groundwater and pollution*. second.,
811 A.A. Balkema Publishers, Leiden.

812 ARSO Postojna climate data (1981-2010). Available at:
813 http://meteo.arso.gov.si/uploads/probase/www/climate/table/sl/by_location/postojna/clim
814 ate-normals_81-10_Postojna.pdf [Accessed October 3, 2016]

815 Atekwana E. . and Krishnamurthy R. . (1998) Seasonal variations of dissolved inorganic
816 carbon and δ13C of surface waters: application of a modified gas evolution technique. *J.*
817 *Hydrol.* **205**, 265–278.

818 Atkinson T. C. (1977) Carbon dioxide in the atmosphere of the unsaturated zone: An
819 important control of groundwater hardness in limestones. *J. Hydrol.* **35**, 111–123.

820 Badino G. (2009) The legend of carbon dioxide heaviness. *J. Cave Karst Stud.* **71**, 100–107.

821 Baldini J. U. L., Baldini L. M., McDermott F. and Clipson N. (2006) Carbon dioxide sources,
822 sinks, and spatial variability in shallow temperate zone caves: Evidence from
823 Ballynamintra Cave, Ireland. *J. Cave Karst Stud.* **68**, 4–11.

824 Bar-Matthews M., Ayalon A., Matthews A., Sass E. and Halicz L. (1996) Carbon and oxygen
825 isotope study of the active water-carbonate system in a karstic Mediterranean cave:
826 Implications for paleoclimate research in semiarid regions. *Geochim. Cosmochim. Acta*
827 **60**, 337–347.

828 Berner R. a., Rao J. L., Chang S., O'Brien R. and Keller C. K. (1998) Seasonal variability of
829 adsorption and exchange equilibria in soil waters. *Aquat. Geochemistry* **4**, 273–290.

830 Bliss C. I. (1958) Periodic Regression in Biology and Climatology. *Connect. Agric. Exp. Stn.*
831 **615**, 3–55.

832 Bond-Lamberty B. and Thomson A. (2010) Temperature-associated increases in the global
833 soil respiration record. *Nature* **464**, 579–582.
834 Bradley C., Baker A., Jex C. N. and Leng M. J. (2010) Hydrological uncertainties in the
835 modelling of cave drip-water δ18O and the implications for stalagmite palaeoclimate
836 reconstructions. *Quat. Sci. Rev.* **29**, 2201–2214.
837 Čater M. and Ogrinc N. (2011) Soil respiration rates and in natural beech forest (Fagus
838 sylvatica L.) in relation to stand structure. *Isotopes Environ. Health Stud.* **47**, 221–237.
839 Deines P., Langmuir D. and Harmon R. S. (1974) Stable carbon isotope ratios and the
840 existence of a gas phase in the evolution of carbonate ground waters. *Geochim.*
841 *Cosmochim. Acta* **38**, 1147–1164.
842 Domínguez-Villar D., Lojen S., Krklec K., Baker A. and Fairchild I. J. (2015) Is global
843 warming affecting cave temperatures? Experimental and model data from a paradigmatic
844 case study. *Clim. Dyn.* **45**, 569–581.
845 Edgerton P., Plummer L. N., Parkhurst D. and Kosiur D. R. (1991) MIX4. Available at:
846 http://www.birmingham.ac.uk/generic/speleothem-science/documents/workshop-
847 files/kr6-workshop-powerpoint.pdf [Accessed September 26, 2017].
848 Ek C. and Gewelt M. (1985) Carbon dioxide in cave atmospheres. New results in belgium and
849 comparison with some other countries. *Earth Surf. Process. Landforms* **10**, 173–187.
850 Epstein S. and Mayeda T. (1953) Variation of O18 content of waters from natural sources.
851 *Geochim. Cosmochim. Acta* **4**, 213–224.
852 Etiope G., Nakada R., Tanaka K. and Yoshida N. (2011) Gas seepage from Tokamachi mud
853 volcanoes, onshore Niigata Basin (Japan): Origin, post-genetic alterations and CH4–CO2
854 fluxes. *Appl. Geochemistry* **26**, 348–359.

855 Fairchild I. J., Smith C. L., Baker A., Fuller L., Spötl C., Mattey D., McDermott F. and
856 E.I.M.F. (2006) Modification and preservation of environmental signals in speleothems.
857 *Earth-Science Rev.* **75**, 105–153.
858 Fairchild I. J. and Treble P. C. (2009) Trace elements in speleothems as recorders of
859 environmental change. *Quat. Sci. Rev.* **28**, 449–468.
860 Ford D. and Williams P. (2007) *Karst Hydrogeology and Geomorphology*., John Wiley &
861 Sons Ltd,., West Sussex, England.
862 Frisia S., Fairchild I. J., Fohlmeister J., Miorandi R., Spötl C. and Borsato A. (2011) Carbon
863 mass-balance modelling and carbon isotope exchange processes in dynamic caves.
864 *Geochim. Cosmochim. Acta* **75**, 380–400.
865 Gieskes J. M. (1974) The alkalinity-total carbon dioxide system in seawater. In *The sea* (ed.
866 E. D. Goldberg). John Wiley and Sons New York. pp. 123–151.
867 Gospodarič R. (1962) K poznavanju Postojnske jame - Pisani rov. *Naše jame* **4**, 9–16.
868 Gospodarič R. (1976) The quaternary caves development between the Pivka basin and polje
869 of Planina. *Acta carsologica* **7**.
870 Gregorič A., Vaupotič J. and Gabrovšek F. (2013) Reasons for large fluctuation of radon and
871 CO2 levels in a dead-end passage of a karst cave (Postojna Cave, Slovenia). *Nat. Hazards*
872 *Earth Syst. Sci.* **13**, 287–297.
873 Gregorič A., Vaupotič J. and Šebela S. (2014) The role of cave ventilation in governing cave
874 air temperature and radon levels (Postojna Cave, Slovenia). *Int. J. Climatol.* **34**, 1488–
875 1500.
876 Habič P. (1982) Pregledna speleološka karta Slovenije: The synoptical speleological map of
877 Slovenia. *Acta carsologica*, 5–22.

878 Hendy C. H. (1971) The isotopic geochemistry of speleothems-I. The calculation of the
879 effects of different modes of formation on the isotopic composition of speleothems and
880 their applicability as palaeoclimatic indicators. *Geochim. Cosmochim. Acta* **35**, 801–824.
881 Jammalamadaka S. R. and Lund U. J. (2006) The effect of wind direction on ozone levels: a
882 case study. *Environ. Ecol. Stat.* **13**, 287–298.
883 Jin L., Hamilton S. K. and Walter L. M. (2008) Mineral weathering rates in glacial drift soils
884 (SW Michigan, USA): New constraints from seasonal sampling of waters and gases at
885 soil monoliths. *Chem. Geol.* **249**, 129–154.
886 Jin L., Ogrinc N., Hamilton S. K., Szramek K., Kanduc T. and Walter L. M. (2009) Inorganic
887 carbon isotope systematics in soil profiles undergoing silicate and carbonate weathering
888 (Southern Michigan, USA). *Chem. Geol.* **264**, 139–153.
889 Kowalczk A. J. and Froelich P. N. (2010) Cave air ventilation and CO2 outgassing by radon-
890 222 modeling: how fast do caves breathe? *Earth Planet. Sci. Lett.* **289**, 209–219.
891 Kowalski A. S., Serrano-Ortiz P., Janssens I. A., Sánchez-Moral S., Cuezva S., Domingo F.,
892 Were A. and Alados-Arboledas L. (2008) Can flux tower research neglect geochemical
893 CO2 exchange? *Agric. For. Meteorol.* **148**, 1045–1054.
894 Kozak K., Mazur J., Vaupotič J., Kobal I., Janik M. and Kochowska E. (2009) Calibration of
895 the IJS-CRn and IFJ-PAN radon measuring devices in the IFJ-KR-600 radon chamber.
896 *Jožef Stefan Inst. Rep. IJS-DP-10103, Ljubljana*.
897 Krajnc B., Ferlan M. and Ogrinc N. (2017) Soil CO2 sources above a subterranean cave-
898 Pisani rov (Postojna Cave, Slovenia). *J. Soils Sediments*, 1–10.
899 Kuzyakov Y. (2006) Sources of CO2 efflux from soil and review of partitioning methods. *Soil*
900 *Biol. Biochem.* **38**, 425–448.
901 Levin I., Naegler T., Kromer B., Diehl M., Francey R., Gomez-Pelaez A., Steele P.,
902 Wagenbach D., Weller R. and Worthy D. (2010) Observations and modelling of the

903 global distribution and long-term trend of atmospheric 14 CO 2. *Tellus B Chem. Phys.*
904 *Meteorol.* **62**, 26–46.
905 Liu W., Moriizumi J., Yamazawa H. and Iida T. (2006) Depth profiles of radiocarbon and
906 carbon isotopic compositions of organic matter and CO2 in a forest soil. *J. Environ.*
907 *Radioact.* **90**, 210–223.
908 Liu Z. and Zhao J. (2000) Contribution of carbonate rock weathering to the atmospheric CO2
909 sink. *Environ. Geol.* **39**, 1053–1058.
910 Mattey D. P., Fisher R., Atkinson T. C., Latin J. P., Durrell R., Ainsworth M., Lowry D. and
911 Fairchild I. J. (2013) Methane in underground air in Gibraltar karst. *Earth Planet. Sci.*
912 *Lett.* **374**, 71–80.
913 Matthews A. and Kolodny Y. (1978) Oxygen isotope fractionation in decarbonation
914 metamorphism: the Mottled Zone event. *Earth Planet. Sci. Lett.* **39**, 179–192.
915 Nagra G., Treble P. C., Andersen M. S., Fairchild I. J., Coleborn K. and Baker A. (2016) A
916 post-wildfire response in cave dripwater chemistry. *Hydrol. Earth Syst. Sci.* **20**, 2745–
917 2758.
918 Ogrinc N., Kanduč T., Krajnc B., Vilhar U., Simončič P. and Jin L. (2016) Inorganic and
919 organic carbon dynamics in forested soils developed on contrasting geology in Slovenia--
920 -a stable isotope approach. *J. Soils Sediments* **16**, 382–395.
921 Parkhurst D. L. and Appelo C. A. J. (2013) *Description of input and examples for PHREEQC*
922 *version 3: a computer program for speciation, batch-reaction, one-dimensional*
923 *transport, and inverse geochemical calculations*., Reston, VA. Available at:
924 http://pubs.er.usgs.gov/publication/tm6A43.
925 Pewsey A., Neuhäuser M. and Ruxton G. D. (2013) *Circular statistics in R*. First edit., Oxford
926 University Press, Oxford.

927 Pflitsch A. and Piasecki J. (2003) Detection of an airflow system in Niedzwiedzia (bear) cave,
928 Kletno, Poland. *J. Cave Karst Stud.* **65**, 160–173.
929 Pitty A. F. (1966) An approach to the study of karst water. *Occ. Pap Geogr* **5**, 70.
930 Plestenjak G., Eler K., Vodnik D., Ferlan M., Čater M., Kanduč T., Simončič P. and Ogrinc
931 N. (2012) Sources of soil CO2 in calcareous grassland with woody plant encroachment.
932 *J. soils sediments* **12**, 1327–1338.
933 Pollack H. N. and Huang S. (2000) Climate Reconstruction from Subsurface Temperatures.
934 *Annu. Rev. Earth Planet. Sci.* **28**, 339–365.
935 Quade J., English N. and DeCelles P. G. (2003) Silicate versus carbonate weathering in the
936 Himalaya: A comparison of the Arun and Seti River watersheds. *Chem. Geol.* **202**, 275–
937 296.
938 Quindos-Poncela L. S., Fernandez P. L., Sainz C., Arteche J., Arozamena J. G. and George A.
939 C. (2003) An improved scintillation cell for radon measurements. *Nucl. Instruments*
940 *Methods Phys. Res. Sect. A Accel. Spectrometers, Detect. Assoc. Equip.* **512**, 606–609.
941 R Core Team (2014) R: A Language and Environment for Statistical Computing. Available
942 at: http://www.r-project.org/.
943 Romanek C. S., Grossman E. L. and Morse J. W. (1992) Carbon isotopic fractionation in
944 synthetic aragonite and calcite: effects of temperature and precipitation rate. *Geochim.*
945 *Cosmochim. Acta* **56**, 419–430.
946 Salomons W. and Mook W. G. (1986) Isotope geochemistry of carbonates in the weathering
947 zone: Chapter 6. In *Handbook of Environmental Isotope Geochemistry* (eds. P. Fritz and
948 Fontes Jean-Charles). Elsevier, Amsterdam. pp. 239–269.
949 Sano Y. and Marty B. (1995) Origin of carbon in fumarolic gas from island arcs. *Chem. Geol.*
950 **119**, 265–274.

951 Serrano-Ortiz P., Roland M., Sanchez-Moral S., Janssens I. A., Domingo F., Godderis Y. and
952 Kowalski A. S. (2010) Hidden, abiotic CO2 flows and gaseous reservoirs in the terrestrial
953 carbon cycle: review and perspectives. *Agric. For. Meteorol.* **150**, 321–329.
954 Spötl C., Fairchild I. J. and Tooth A. F. (2005) Cave air control on dripwater geochemistry,
955 Obir Caves (Austria): Implications for speleothem deposition in dynamically ventilated
956 caves. *Geochim. Cosmochim. Acta* **69**, 2451–2468.
957 Šebela S. (2010) Accesses from the surface to the Postojna Cave system. *Ann. Ser. Hist. Nat.*
958 **20**, 55–64.
959 Šebela S. (1992) Geological characteristics of Pisani rov in Postojna Cave. *Acta carsologica*
960 **21**, 97–116.
961 Šebela S. (1996) The dolines above the colapse chambers of Postojnska jama. *Acta*
962 *carsologica* **25**, 241–250.
963 Šebela S. and Čar J. (2000) Velika Jersanova doline - a former collapse doline = Velika
964 Jersanova dolina - nekdanja udornica. *Acta carsologica* **29**, 201–212.
965 Trumbore S. (2006) Carbon respired by terrestrial ecosystems - Recent progress and
966 challenges. *Glob. Chang. Biol.* **12**, 141–153.
967 Were A., Serrano-Ortiz P., Moreno de Jong C., Villagarcía L., Domingo F. and Kowalski A.
968 S. (2010) Ventilation of subterranean CO2 and Eddy covariance incongruities over
969 carbonate ecosystems. *Biogeosciences* **7**, 859–867.
970 West A. J., Galy A. and Bickle M. (2005) Tectonic and climatic controls on silicate
971 weathering. *Earth Planet. Sci. Lett.* **235**, 211–228.
972 Wilkening M. H. and Watkins D. E. (1976) Air Exchange and 222Rn Concentrations in the
973 Carlsbad Caverns. *Health Phys.* **31**.

974 Wong C. I., Banner J. L. and Musgrove M. (2011) Seasonal dripwater Mg/Ca and Sr/Ca
975 variations driven by cave ventilation: Implications for and modeling of speleothem
976 paleoclimate records. *Geochim. Cosmochim. Acta* **75**, 3514–3529.
977 Wood W. W. (1985) Origin of caves and other solution openings in the unsaturated (vadose)
978 zone of carbonate rocks: a model for CO2 generation. *Geology* **13**, 822–824.
979 Wood W. W. and Petraitis M. J. (1984) Origin and Distribution of Carbon Dioxide in the
980 Unsaturated Zone of the Southern High Plains of Texas. *Water Resour. Res.* **20**, 1193–
981 1208.
982 Zhang J., Quay P. D. and Wilbur D. O. (1995) Carbon isotope fractionation during gas-water
983 exchange and dissolution of CO_2. *Geochim. Cosmochim. Acta* **59**, 107–114.
984

985 **Table Captions**

986 **Table 1.** Concentrations and carbon isotope composition in soil and cave air

987

Table 1: Concentrations and carbon isotope composition in soil and cave air

Sampling location	Date	Snow	CO_2 ppm	$\delta^{13}C_{CO2}$ ‰	$\Delta^{14}C$ ‰	Org	Air	$CaCO_3$
Soil	3.2.2015	Yes	2362	−20.5	−20.4	0.77	0.14	0.09
Soil	3.2.2015	Yes	2213	−20.6	−20.3	0.78	0.13	0.09
Cave	28.1.2015	Yes	1521	−16.8	−25.5	0.54	0.37	0.09
Soil	18.2.2015	No	1516	−19.0	−18.0	0.67	0.24	0.09
Soil	18.2.2015	No	1673	−19.7	−21.9	0.72	0.19	0.09
Cave	18.2.2015	No	1658	−19.2	−12.7	0.68	0.24	0.08
Soil	26.8.2015	-	8275	−21.8	−32.2	0.86	0.03	0.11

988

989

990 **Fig. 1:** Location of the study site in in the last hall of Pisani rov in Postojna cave. Entrance to
991 Pisani rov that is closed for tourist visits is marked with the red dot. The sampling location
992 in Red and White hall is marked with a star.

993

994 **Fig. 2:** Lateral view of the Red and White hall. Cave air and dripwater sampling locations on
995 the base of the hill (BHA) and on the hill (OHA) are marked with stars. Elevation
996 difference between the sampling locations is cca. 6 m. The ovals above the cave represent
997 the collapsed blocks (Adapted after Šebela and Čar (2000)).

998

999 **Fig. 3:** Variations of cave air CO_2 concentrations, its isotopic composition and ^{222}Rn
1000 concentrations along Postojna air temperatures with marked lines of cave air temperature
1001 of 8.4 and 0°C. BHA and OHA are cave air sampling locations on the base of the hill and
1002 on the hill, respectively.

1003

1004 **Fig. 4:** Variations in dripwater carbonate system parameters monitored at two different sites,
1005 using two different collection methods in Red and White hall. SD_OHA and SI_OHA
1006 stands for "directly" and "indirectly" sampled samples at the OHA location, while
1007 LD_BHA and LI_BHA stands for directly and indirectly sampled samples ad BHA
1008 location, respectively. The HCO_3^- values were computed using PHREEQC (Parkhurst and
1009 Appelo, 2013).

1010

1011 **Fig 5:** Comparison between seasonal variations of monthly mean surface temperature, surface
1012 precipitation (monthly surface precipitation amount and its oxygen stable isotopic
1013 composition, $\delta^{18}O_{H2O\_prec}$), oxygen stable isotope composition ($\delta^{18}O_{H2O\_drip}$), Cl^-, SO_4^{2-} and
1014 NO_3^- concentrations in cave dripwaters from two stalactites (S and L) at two locations

(OHA and BHA) and within each of the two collecting procedures ("direct" and "indirect" sampling D and I).

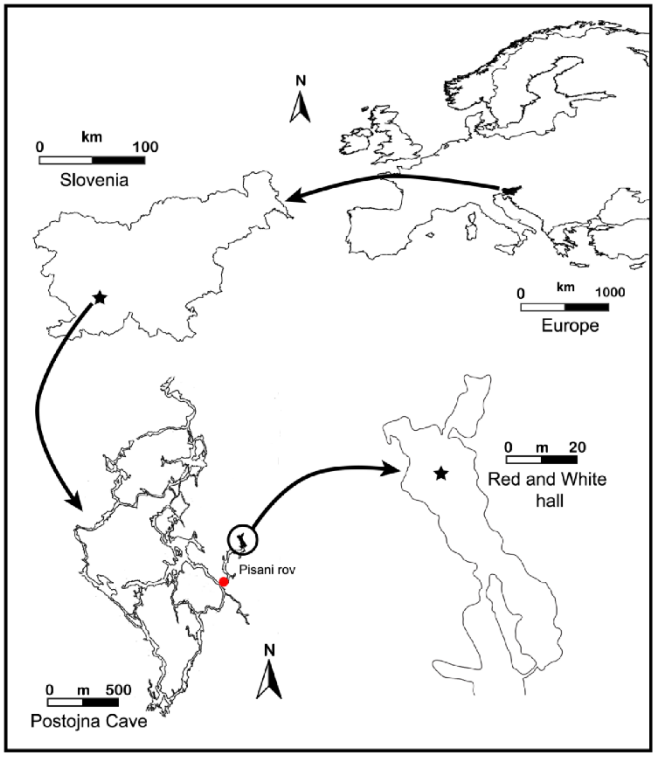
Fig 6: Saturation of dripwaters with respect to calcite log(IAP/K) in relation to pCO_2 of dripwaters in Red and White hall. The grey area at the plots represents the uncertainty of saturation for the samples based on errors associated with pH, alkalinity and ion measurement errors. The colours represent the season in which the sample was collected

Fig 7: Simplified schematic illustration of summer (A) and winter (B) cave atmosphere dynamics showing cave air CO_2 sources and sinks together with ventilation dynamics typical for chimney effect type that is less effective or even absent during the summer. The value of isotopic composition of CO_2 degassing from dripwaters is average of values modelled within presented study. Described $\delta^{13}C$ and pCO_2 values for organic matter, soil respiration, limestone bedrock and atmosphere are taken from previous study and are specific for this location (Krajnc et al., 2017). Values of $\Delta^{14}C$ are general values taken from the literature (Liu et al., 2006; Levin et al., 2010).

Fig. 8: Modelled and measured values of dripwater dissolved inorganic carbon (DIC) (A) and its $\delta^{13}C_{DIC}$ values (B) in relation to log(pCO_2). Modelled values of DIC concentrations were derived using MIX4. Line D represents values if only degassing of CO_2 was considered while line DP represents the values considering also calcite precipitation after the achieved calcite saturation (+0.35 was used as a realistic saturation index). DIC and log (pCO2) values were calculated from alkalinity and pH data of measured samples. Modelled $\delta^{13}C_{DIC}$ values were calculated using the linear form of Rayleigh equation (Matthews and Kolodny, 1978) in the similar way as done by Bar-Matthews et al. (1996).

Fractionation factors proposed by Zhang et al. (1995) and Romanek et al. (1992) were used.

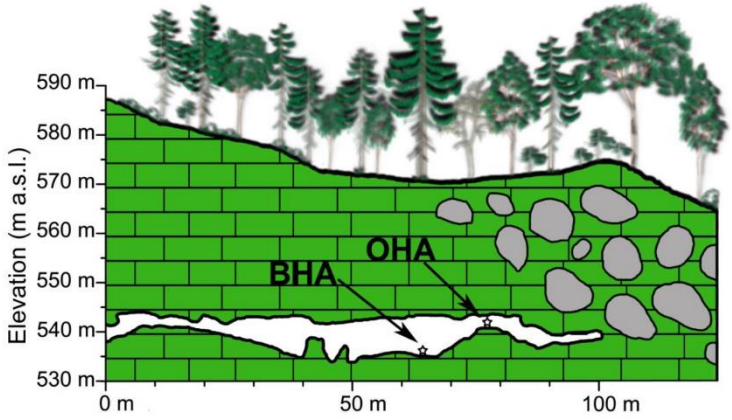
Fig. 9: Variations of measured cave air CO_2 isotopic composition along with the modelled isotopic composition for OHA and BHA site in Red and White hall. Model assumed that cave air CO_2 is exclusively a mixture of CO_2 degassed from dripwaters and CO_2 from the outside atmosphere. Modelled values for model A and B were calculated using two endmember mass balance model. Firs endmember is the CO_2 from the outside atmosphere and the second is the modelled isotopic composition of CO_2 degassing from the dripwater (SD_OHA and LD_BHA). Isotopic composition of CO_2 degassing from dripwaters was calculated in the similar way as described in Appelo and Postma (2005). Two possible scenarios were used. In the first scenario, which outputs were used for Model A, the rates for degassing and for calcite precipitation approach equilibrium at the same pace, while in the second one, which outputs were used for Model B the rates for degassing, are 100 fold greater than calcite precipitation. Note that modelled data has almost always more positive $\delta^{13}C_{CO2}$ values compared to the measured ones.



1057

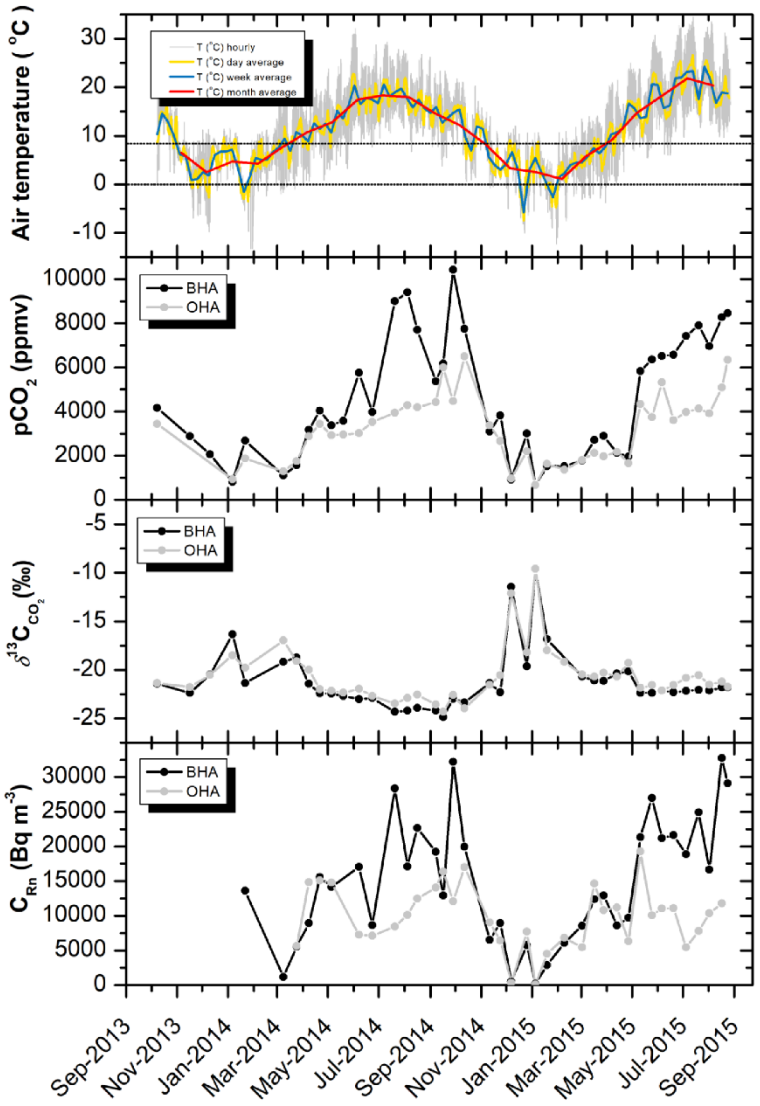
1058 Figure 1.

1059



1060

1061 Figure 2.



1062

1063 Figure 3.

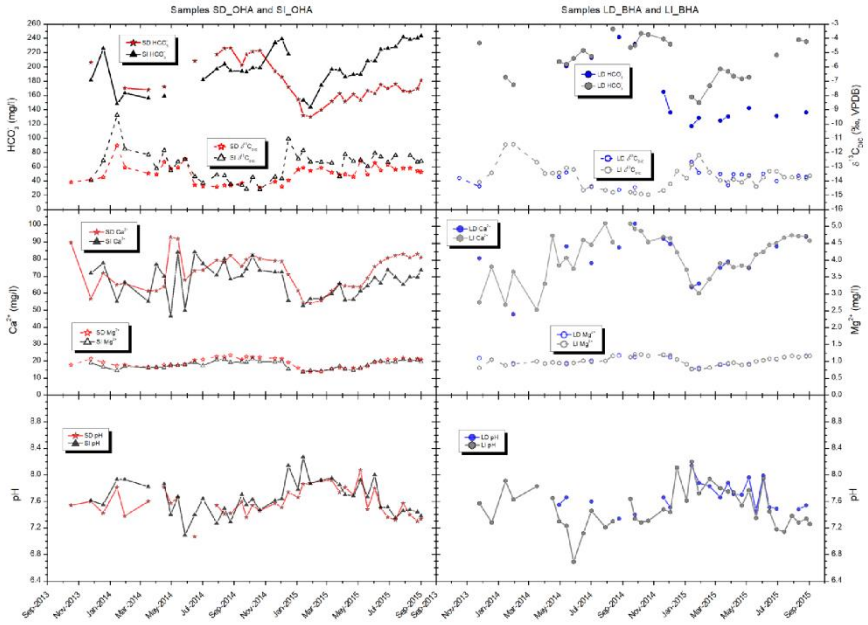

Samples SD_OHA and SI_OHA
Samples LD_BHA and LI_BHA
SD HCO3
SI HCO3
SD δ13CDIC
SI δ13CDIC
LD HCO3
LI HCO3
LD δ13CDIC
LI δ13CDIC
SD Ca2+
SI Ca2+
SD Mg2+
SI Mg2+
LD Ca2+
LI Ca2+
LD Mg2+
LI Mg2+
SD pH
SI pH
LD pH
LI pH
HCO3- (mg/l)
δ13CDIC (‰, VPDB)
Ca2+ (mg/l)
Mg2+ (mg/l)
p-I
Sep-2013
Nov-2013
Jan-2014
Mar-2014
May-2014
Jul-2014
Sep-2014
Nov-2014
Jan-2015
Mar-2015
May-2015
Jul-2015
Sep-2015

Figure 4.

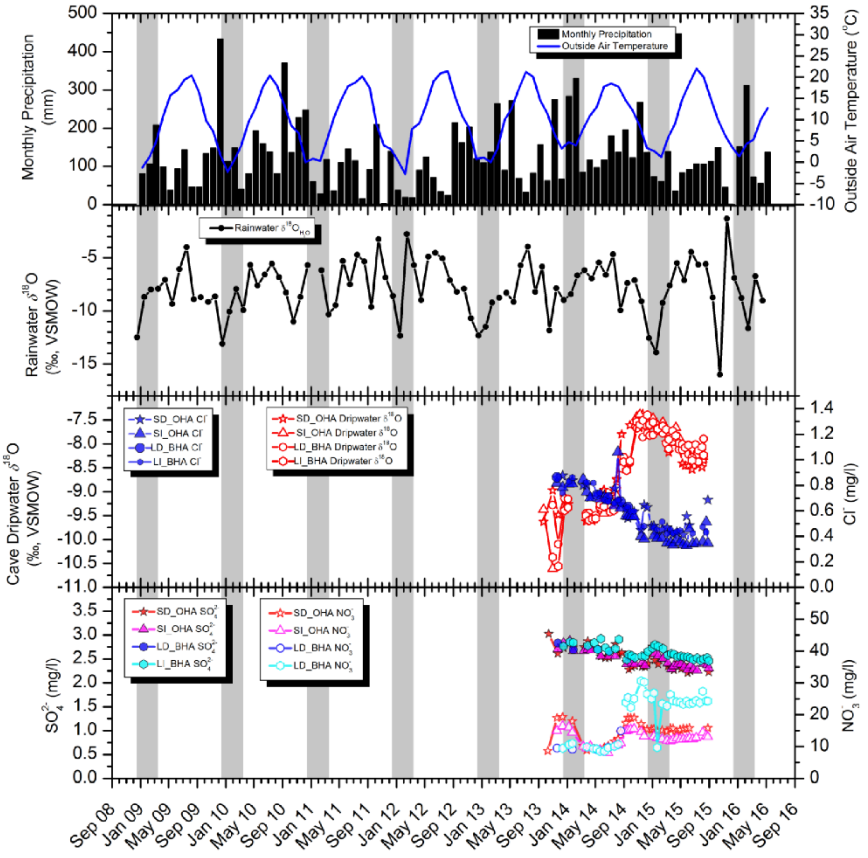
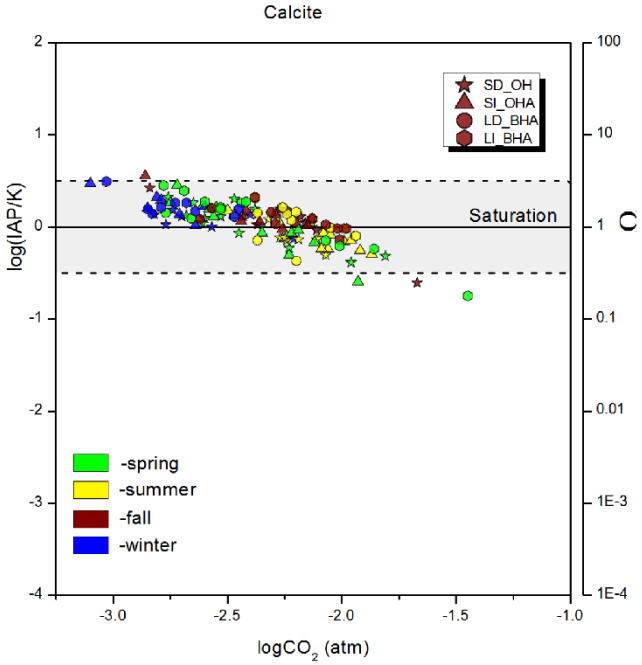
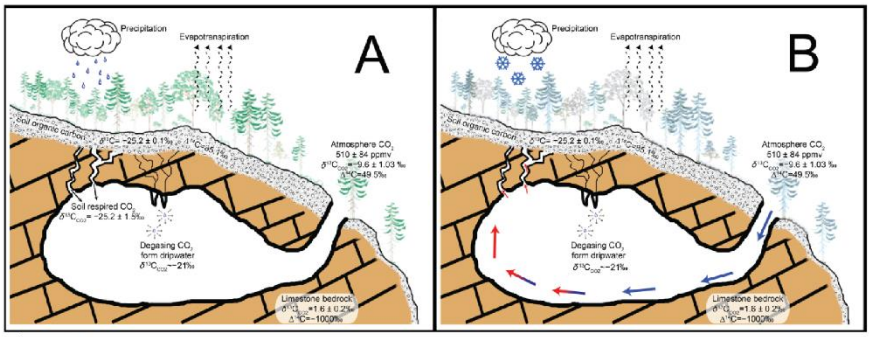

Monthly Precipitation (mm)
Outside Air Temperature (°C)
Monthly Precipitation
Outside Air Temperature
Rainwater δ18OH2O
Rainwater δ18O (‰, VSMOW)
Cave Dripwater δ18O (‰, VSMOW)
SD_OHA Cl-
SI_OHA Cl-
LD_BHA Cl-
LI_BHA Cl-
SD_OHA Dripwater δ18O
SI_OHA Dripwater δ18O
LD_BHA Dripwater δ18O
LI_BHA Dripwater δ18O
Cl- (mg/l)
SD_OHA SO42-
SI_OHA SO42-
LD_BHA SO42-
LI_BHA SO42-
SD_OHA NO3-
SI_OHA NO3-
LD_BHA NO3-
LD_BHA NO3-
SO42- (mg/l)
NO3- (mg/l)
Sep 08
Jan 09
May 09
Sep 09
Jan 10
May 10
Sep 10
Jan 11
May 11
Sep 11
Jan 12
May 12
Sep 12
Jan 13
May 13
Sep 13
Jan 14
May 14
Sep 14
Jan 15
May 15
Sep 15
Jan 16
May 16
Sep 16

Figure 5.

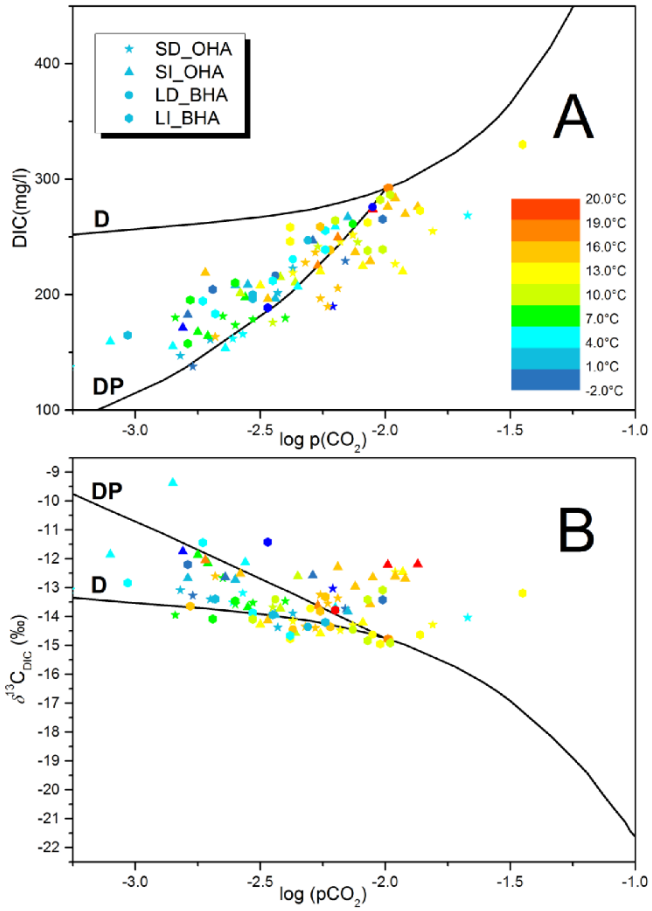


1068
1069 Figure 6.

1070



1071
1072 Figure 7.



1073
1074 Figure 8

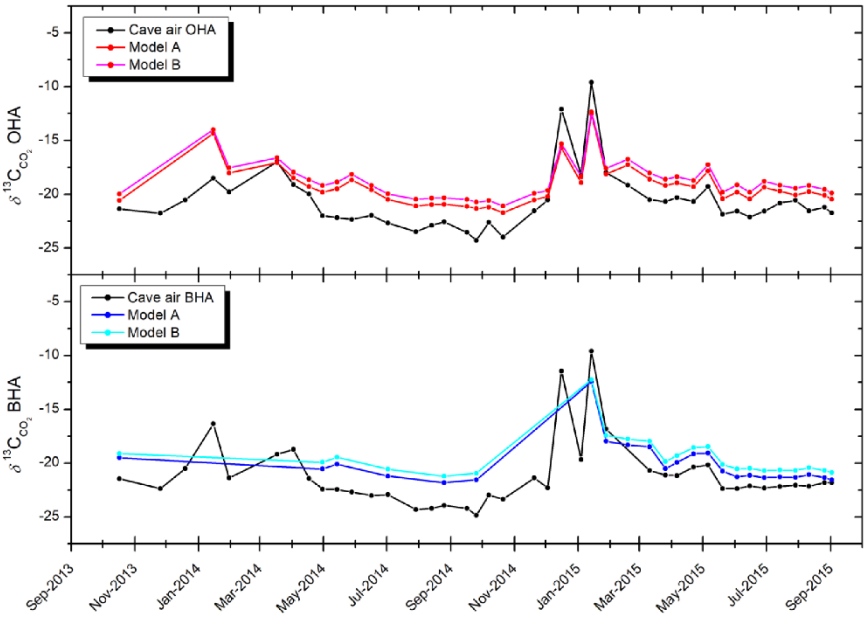

Cave air OHA
Model A
Model B
δ 13C CO2 OHA
Cave air BHA
Model A
Model B
δ 13C CO2 BHA
-5
-10
-15
-20
-25
Sep-2013
Nov-2013
Jan-2014
Mar-2014
May-2014
Jul-2014
Sep-2014
Nov-2014
Jan-2015
Mar-2015
May-2015
Jul-2015
Sep-2015

Figure 9

3.5 Scientific Paper: "Temporal analysis of $\delta^{13}C_{CO2}$ and CO_2 efflux in soil gas emissions at Mt. Etna: a new tool for volcano monitoring"

In this chapter the paper entitled "Temporal analysis of $\delta^{13}C_{CO2}$ and CO_2 efflux in soil gas emissions at Mt. Etna: a new tool for volcano monitoring" by Salvatore Giammanco, Bor Krajnc, Jože Kotnik and Nives Ogrinc is presented. The paper is accepted in the Annals of Geophysics.

In the presented study the soil gas emission of CO_2 from four study sites of mountain Etna volcano in Italy were monitored. The aim of the present work was to study the temporal variations of CO_2 efflux and the associated stable carbon isotope composition of CO_2 with the main objectives to better define the correlation between CO_2 efflux and its isotopic composition in the selected high-degassing sites of the volcano and to recognize possible influences on soil degassing due to volcanic activity.

Etna is one of the most active volcanoes in the world and is also known as one of the main sources of magmatic CO_2. Beside the active summit vents, where most of the release of CO_2 occurs, also a substantial amount of this gas is released from volcano flanks. Most of the CO_2 released from flanks is produced by magma outgassing from reservoirs located at intermediate to great depths beneath the volcano and is transported to the surfaces through volcano-tectonic faults.

One of the study sites was located on the southwestern flank at the elevation of 115 m a.s.l. and other three sites at the eastern flank of Mt. Etna at elevations between 320 m and 510 m a.s.l. At all four sites soil CO_2 effluxes and its stable carbon isotopic composition were measured, while the meteorological data was gathered from the nearby meteorological stations.

The site on the southwestern flank had the highest values of CO_2 efflux, most positive $\delta^{13}C_{CO2}$ values (between +1.6‰ and +3.1‰) and very small variation with time, despite wide ranges of CO_2. The isotopic composition of CO_2 at this site was explained as being a consequence of strong interaction between deep magmatic fluids and hydrothermal aquifer (T> 120 °C). Fractionation of carbon isotopes in water between gaseous CO_2 and dissolved HCO_3^- favors enrichment of the heavier carbon isotope in the residual gas phase that passes through the water. Besides that also the small variation of $\delta^{13}C_{CO2}$ points to a relative stability of the hydrothermal system that effectively buffers the magmatic fluids coming from depths within the volcano and does not allow for large changes in the isotopic composition of the escaping CO_2.

$\delta^{13}C_{CO2}$ values at the sites at eastern flanks were more negative and showed wider variations with time (from about −18‰ to about +1‰). A general positive correlation existed between $\delta^{13}C_{CO2}$ and CO_2 efflux at these sites. Higher effluxes corresponded to higher $\delta^{13}C_{CO2}$ values i.e. values similar to the magmatic CO_2 at this volcano. More negative $\delta^{13}C_{CO2}$ values during lower effluxes indicate a higher degree of mixing of the magmatic component with the shallow non-magmatic fluid (e.g. groundwater) and/or the organic source of the soil gas. No influence of meteorological parameters on the variation of the CO_2 effluxes and its isotopic composition was found, suggesting that the observed changes can be attributed to variations in volcanic activity. As a matter of fact, the largest anomalies in the monitored parameters preceded the opening of the southeast crater in late 2009 and therefore they could represent a key to unveiling the dynamics of the volcano.

The results of the study are encouraging for the future monitoring of the eruptive activity of Mt. Etna, where the chosen sampling sites are easily accessible, the sampling procedure is simple and the analytical methods are precise and reliable.

In this paper, the candidate performed stable isotope measurements of the soil gas CO_2 using the IRMS and helped to write the manuscript, which was written by Salvatore Giammanco.

Temporal analysis of $\delta^{13}C_{CO2}$ and CO_2 efflux in soil gas emissions at Mt. Etna: a new tool for volcano monitoring

Shortened title: $\delta^{13}C_{CO2}$ and CO_2 efflux in soil gases of Mt. Etna

S. Giammanco[(1)], B. Krajnc[(2,3)], J. Kotnik[(3)], N. Ogrinc[(2,3)]

[1] *Istituto Nazionale di Geofisica e Vulcanologia, Osservatorio Etneo, Catania, Italy*

[2]*Jožef Stefan International Postgraduate School, Jamova 39, 1000 Ljubljana, Slovenia*

[3]*Jožef Stefan Institute, Department of Environmental Sciences, Jamova 39, 1000 Ljubljana, Slovenia*

*Corresponding author: Salvatore Giammanco, Istituto Nazionale di Geofisica e Vulcanologia, Osservatorio Etneo, Catania, Italy.

Phone: +39 095 7165829; E-mail: salvatore.giammanco@ingv.it

***Subject classification**:* 03.04.02. Carbon Cycling; 03.04.06. Hydrothermal Systems; 04.04.12. Fluid Geochemistry; 04.08.01. Gases; 04.08.06. Volcano monitoring.

ABSTRACT

We monitored the soil gas emission of CO_2 from selected sites of Mt. Etna volcano during the period February 2009 to December 2010 by measuring periodically the soil CO_2 efflux together with the associated stable carbon isotope composition of CO_2 from February 2009 to December 2010. Correlation between the two parameters showed distinct behaviors depending on the sites as a reflection of the different interactions between crustal and sub-crustal fluids. Where deep CO_2 interacted with shallow cold ground water and/or with shallow biogenic CO_2, a positive correlation between soil CO_2 effluxes and carbon isotopes was evident and it depended strongly on the velocity of gas through the soil. In these cases, the highest CO_2 effluxes corresponded to $\delta^{13}C_{CO2}$ values similar to those of the deep magmatic CO_2 emitted from the crater and peri-crateric gas emissions at the summit. In areas where a shallow hydrothermal system was presumed, then a similar correlation was less evident or even absent, suggesting strong control on C isotopes arising from the interactions between CO_2 gas and dissolved HCO_3^- that occur in aquifers at T>120 °C. Marked temporal variations were observed in both parameters at all sites. No significant effect of meteorological parameters was found, so the observed changes were reasonably attributed to variations in volcanic activity of Mt. Etna. In particular, the variations were attributed to increased degassing of CO_2 from incoming new magma, possibly coupled with increased hydrothermal activity in at least some of the shallow aquifers of the volcano. The largest anomalies in the monitored parameters preceded the opening of the New Southeast crater in late 2009 and therefore they could represent a key to unveiling the dynamics of the volcano.

1. Introduction

Mt. Etna volcano, one of the most active volcanoes in the world, is also known as a one of the main sources of magmatic CO_2. The total emission rate has been recently estimated at

about 60,000 $t \cdot d^{-1}$ (Hernández et al., 2015). Most of the release of CO_2 occurs through the active summit vents of the volcano, but a remarkable fraction of this gas (about 10 % of the total amount according to D'Alessandro et al., 1997b and Hernández et al., 2015) is released from its flanks. In this case, CO_2 emissions at the surface occur in diffuse form through volcano-tectonic faults (e.g., Giammanco et al., 1998; Aiuppa et al., 2004) and they are produced by magma outgassing from reservoirs located at intermediate to great depths beneath the volcano (Bruno et al., 2001; Aiuppa et al., 2004; Giammanco et al., 2013). Studies on soil gas carried out in the last 17 years at Mt. Etna showed that the central eastern flank and the lower southwestern flank of the volcano are characterised by the strongest anomalies in both soil gas concentration and soil CO_2 efflux and by the highest content of magmatic CO_2, which dissolves into local groundwater (Anzà et al., 1989; Giammanco et al., 1995, 1996; Allard et al., 1997; Brusca et al., 2001; Aiuppa et al., 2004; Giammanco and Bonfanti, 2009).

The aim of the present work was to study the temporal variations of soil CO_2 efflux and the associated stable carbon isotope composition of CO_2 over a time span of several months, covering the period between the end of the 2008-2009 flank eruption and the opening and eruption of the New Southeast Crater (NSEC), today the most active summit crater of Mt. Etna (Fig. 1). The main objectives of our study are: i) to better define the correlation between the above two parameters in selected high-degassing sites of the volcano; ii) to model the dynamics of geochemical interactions between CO_2 and the surrounding environment and iii) to recognize possible influences of volcanic activity on soil degassing.

2. Eruptive phenomena at Mt. Etna during the studied period

Mt. Etna is a large Quaternary composite volcano, which grew to its present elevation of 3320 m by accumulation of lavas and tephra erupted during the last 200 kyr (Gillot et al., 1994). At present, its activity is represented by summit and/or flank eruptions, the former being mostly

75 short-lived and characterized mainly by production of tephra with minor lavas, the latter being,
76 on average, long-lived and mostly producing lava effusions that may emplace voluminous lava
77 flow fields.

78 Our study began during the final stages of the long-standing 2008-2009 flank eruption.
79 Details on this eruption are given in Bonaccorso et al. (2011) and in Corsaro and Miraglia
80 (2014). The eruption started on May 13th from a fissure that developed from the SE Crater
81 towards the Valle del Bove (VB in Fig. 1), a morphological depression that occupies a large
82 part of the east flank of Mt. Etna. Lava flows from this fissure expanded inside the VB, reaching
83 a maximum length of about 6 km and a total volume of about $70 \pm 20 \times 10^6$ m^3 (Branca S.,
84 quoted in Corsaro and Miraglia, 2014). The eruption ended on July 7th, 2009, 419 days after its
85 onset.

86 Just a few months later, on November 6th, 2009, a new vent opened on the lower eastern
87 slopes of the Southeast Crater, one of the four summit craters of Mt. Etna and the most active
88 one in the last thirty years (e.g., Behncke et al., 2014). This new vent, named New Southeast
89 Crater (NSEC), appeared as a relatively small open pit emitting hot pressurised gas. Its birth
90 marked the end of the eruptive activity at the SE Crater, thus virtually "replacing" it as a new
91 opening in the conduit of the previous SE cone. The vigorous degassing activity of NSEC
92 continued until the end of 2010, without appreciable changes.

93 In the meantime, since August 25th, 2010, some isolated explosive episodes occurred at
94 the Bocca Nuova crater (BN), the westernmost of the four summit craters of Etna (for details
95 on this and on the following volcanological information, see
96 http://www.ct.ingv.it/en/rapporti.html). The strong gas and ash explosion of August 25th, 2010
97 at the BN was followed by several smaller explosive events that produced short-lived emissions
98 of volcanic ash. Seven major explosions occurred at BN until August, 29th, although with less
99 intensity than the first one. Other significant explosive events took place at BN on October 7th

and on November 1st, both producing minor ash plumes. After more than one month of relative quiescence at Etna, a new strong explosion occurred at BN on December 22nd, 2010. This explosion was probably less powerful than the one on August 25th, but certainly stronger than the numerous events between late August and November 2010.

On the afternoon of December 23rd, 2010, Strombolian activity apparently started for the first time inside the NSEC since its formation. However, bad weather conditions prevented clear observation of the summit area, so this activity could not be followed in detail. On the late afternoon of January 2nd, 2011 mild Strombolian activity appeared again within the pit of NSEC, preceded by several days of repeated emissions of hot gas. Strombolian explosions, although with variable intensity, continued through January 6th and then ceased. Mild explosive activity resumed on January 11th, and its intensity began to increase on January 12th until producing a small lava outflow. Finally, a paroxysmal eruption occurred during the night between January 12 and 13, with lava fountains and voluminous lava flows. The event ceased completely after about two hours. This was the first of a long and complex sequence of eruptive events that characterized the evolution and growth of the NSEC until 2015 (Behncke et al., 2014; De Beni et al., 2015).

3. Materials and methods

3.1.Sampling sites

For the purposes of this study, we selected the sites most representative of soil degassing (Fig. 1), as they are all characterized by anomalous high emissions of soil CO_2. In particular, site P39 is located on the southwestern flank at an altitude of 115 m a.s.l., ~2 km SW of the town of Paternò, in an area with visible absence of vegetation due to the intense gas emissions

124 from the soil. The other three sites (P78, ZAF06 and ZAF08) are located on the eastern flank
125 of Mt. Etna, at altitudes between 320 m and 510 m a.s.l..
126 Apart from CO_2, the chemical composition of the gas released from all sites, but
127 especially at P39, shows trace amounts of CH_4, He and sometimes H_2 and CO (Giammanco et
128 al., 1998). Previous geochemical studies on the gases emitted at sites P39 and P78 indicated
129 that the origin of these gases is dominantly magmatic (D'Alessandro et al, 1997a; Giammanco
130 et al., 1998; Pecoraino and Giammanco, 2005). In particular, the chemical and isotope features
131 of gases emanating at site P39 show evidence of their direct origin from the mantle source of
132 Mt. Etna basalts (Giammanco et al., 1998a; Caracausi et al., 2003a, 2003b). This site is located
133 on a NE-SW-directed regional fault that is thought, based mainly on geochemical data, to be
134 part of the deep feeder system of Mt. Etna (>10 km; Caracausi et al., 2003a, 2003b). Sites P78,
135 ZAF06 and ZAF08 are part of an anomalous degassing zone that is aligned on a WNW-ESE
136 fault system (Anzà et al., 1993; Giammanco et al., 1995). A recent study on soil CO_2 emissions
137 in the central eastern flank of Mt. Etna (Giammanco and Bonfanti, 2009), recognized this line
138 as a major fault characterized by clear anomalous degassing whose changes in time are linked
139 to volcanic activity. Gases from this site are assumed to derive from a shallower portion (5 –
140 10 km) of the magma feeder system of Mt. Etna (Giammanco et al., 1998; Bruno et al., 2001).
141
142 *3.2.Soil CO_2 efflux*
143 Soil CO_2 effluxes (expressed in g m^{-2} d^{-1}) were measured at all selected sampling sites
144 using the method of the dynamic accumulation chamber (e.g., Parkinson, 1981; Chiodini et al.,
145 1998; Farrar et al., 1995). CO_2 effluxes were measured in at least duplicate during each survey,
146 and the arithmetic average of the values was considered for the temporal analysis of data. The
147 sampling frequency was variable but, on average, once every 20-30 days. The data cover the
148 period from February 2nd, 2009 to December 12th, 2010. In order to evaluate the possible

149 influence of the main meteorological parameters on the temporal variations of CO_2 efflux,
150 values of air temperature, total daily rainfall, minimum and maximum relative humidity and
151 wind speed at a height of 2 m above the ground were also acquired thanks to the monitoring
152 network of the Servizio Informativo Agrometeorologico Siciliano (SIAS). In particular, we
153 chose the station of Paternò, representative of the weather conditions of the low SW flank of
154 Mt. Etna, and the station of Riposto, representative of the weather conditions of the low E flank
155 of Mt. Etna (see Figure 1).

156 Because the CO_2 efflux data are log-normally distributed (Ahrens, 1954; Giammanco et
157 al, 2010), all graphic analyses of these data in the present paper have been performed on a $\log_{10}$
158 scale.

159

160 *3.3.Stable carbon isotope composition of CO_2*

161 Samples for stable isotope analysis were collected in the soil at a depth of 50 cm using a 5
162 mm ID teflon tube connected to a syringe. The gas aliquots were immediately injected into pre-
163 evacuated 12-ml glass serum vials. To avoid possible contamination with gas from the sampler
164 tube, the system was purged twice with the soil gas. The septum penetration needles allow
165 direct delivery of the gas sample into the pre-evacuated vial thereby minimizing possible
166 contamination with atmospheric air (Torn et al., 2003). The stable isotope composition of CO_2
167 was determined according to the methods of Knohl et al. (2004) and Spötl (2004). These
168 methods have been applied successfully in various forest soils in Slovenia (Čater and Ogrinc,
169 2011; Krajnc et al., 2016; Krajnc et al., 2017). Measurements were made directly from vials
170 using a Europa Scientific 20–20 continuous flow isotope ratio mass spectrometer (IRMS)
171 coupled to an ANCA-TG preparation module for gas samples. Stable isotope results are
172 reported using the conventional delta—notation (δ), in per ml (‰) relative to the VPDB
173 reference standard - $\delta^{13}C_{CO2}$. The accuracy of the measurements was checked using "CO2 ISO-

174 TOP, High" CO_2 standard with $\delta^{13}C_{CO2}$ value of –4.3 ± 0.2‰. The precision of measurements
175 was ±0.2‰.
176
177
178 **4. Results and discussion**
179
180 *4.1.Geochemical characterization of sites*
181 The results of the measurements carried out during our study are shown in Table 1. Figure
182 2 shows the correlation plot between the $\delta^{13}C_{CO2}$ values and the corresponding $\log_{10}$ values of
183 CO_2 efflux measured at all sites. Site P39 displays the highest levels of CO_2 efflux (up to about
184 32,000 g m^{-2} d^{-1}) and the most positive values of $\delta^{13}C_{CO2}$ (between +1.6 and +3.1‰).
185 Furthermore, the isotope composition of carbon showed very small variation with time, despite
186 the wide range of CO_2 effluxes measured. This is in line with previous measurements of both
187 parameters at this site (Giammanco et al., 1998; Pecoraino and Giammanco, 2005). The isotopic
188 shift of carbon observed at this site was explained as being due to strong interaction between
189 deep magmatic fluids and a hydrothermal aquifer at T° > 120 °C because, in this case, the
190 fractionation factor in water between gaseous CO_2 and dissolved HCO_3^- favors enrichment of
191 the heavier carbon isotope in the residual gas phase that passes through the ground water (Mook
192 et al., 1974). Higher water temperature causes a larger positive isotopic shift in $\delta^{13}C_{CO2}$ values.
193 In fact, the presence of a geothermal aquifer beneath the area of Paternò has already been
194 postulated by Chiodini et al. (1996), who calculated a temperature of water of up to about 150
195 °C, based on liquid and gaseous geothermometers. In our case, the deep CO_2 that interacts with
196 the hydrothermal aquifer at about 150 °C should undergo an isotopic shift of about +2‰ (Mook
197 et al., 1974). Therefore, the estimated $\delta^{13}C_{CO2}$ values of the pristine deep CO_2 before interaction
198 with thermal water would be very similar to those measured in the high-temperature fumaroles

199 near the summit of Mt. Etna (Giammanco et al., 1998; Aiuppa et al., 2004), assumed as
200 representative of the C-isotope composition of magmatic CO_2 of this volcano (grey horizontal
201 band in Figure 2). However, the C isotope values found in this study at site P39 are slightly
202 more positive than those found at the same site in previous work (Giammanco et al., 1998;
203 Pecoraino and Giammanco, 2005). If we assume a pristine C-isotope composition in the range
204 of -2.5 to -1‰ as representative of the magmatic CO_2 emitted from Etna (Giammanco et al.,
205 1998; Pecoraino and Giammanco, 2005), then the range of values that we observed would be
206 compatible with an isotopic shift of +3 to +4‰. According to Mook et al. (1974), such a
207 fractionation factor would be due to interaction between CO_2 and the hydrothermal system at a
208 water temperature of 180-200 °C. A summary of the above geochemical interactions for site
209 P39 is shown in the graphic model of Figure 3a.
210 The other monitored sites showed a distinct and generally coherent behavior. Figure 2
211 highlights that, differently from site P39, $\delta^{13}C_{CO2}$ values at sites P78, ZAF06 and ZAF08
212 showed a wider range of variations with time (from about -18‰ to about +1‰), although with
213 a smaller deviation (from about -6‰ to about +1‰) at site ZAF06. The most negative $\delta^{13}C_{CO2}$
214 value clearly points to a marked influence of an organic component in the emitted CO_2,
215 produced from a shallow biogenic source of gas in the thick and well-structured soil in these
216 sites (e.g., Giammanco et al., 1998). It must be considered, however, that a shift towards more
217 negative values of $\delta^{13}C_{CO2}$ may also occur as consequence of fractionation of C-isotopes
218 between gaseous CO_2 and dissolved HCO_3^- when deep CO_2 reacts with cold ground water for
219 a long time. The eastern flank of Mt. Etna is characterized by the ubiquitous presence of large
220 unconfined aquifers. Therefore, deep CO_2 rising at high pressure (>> 100 kPa) through faults
221 inevitably encounters ground water and at least in part reacts with it, both chemically and
222 isotopically. The entity of these reactions is more or less marked as a function of the contact
223 time between gas and water. A long reaction time occurs because of long pathways of CO_2 gas

224 through a thick aquifer or more generally because of low gas flux conditions. Given enough
225 contact time between high-pressure dissolved CO_2 and water, the fractionation factor ranges
226 from -9.6 to -8.5‰ in the temperature interval between 10° and 25°C (Mook et al., 1974). The
227 above geochemical interactions for sites ZAF06, ZAF08 and P78 are summarized in the graphic
228 model of Figure 3b. The slightly more positive values observed at site ZAF06 may be due at
229 least to partial interaction between deep magmatic CO_2 and thermal ground water, similar to
230 that observed at site P39. It should be noted that this site is located very close to a water well
231 ("Petrulli" well) with water temperature constantly a little higher than the average temperature
232 of Mt. Etna ground water and the highest among the ground waters of the east flank of the
233 volcano (Bonfanti et al., 1996; Brusca et al., 2001; Aiuppa et al., 2004).
234 A general positive correlation exists between the $\delta^{13}C_{CO2}$ values measured at sites P78,
235 ZAF06 and ZAF08 and the corresponding values of soil CO_2 efflux (on a $\log_{10}$ scale) (Figure
236 2). In detail, assuming a $\log_{10}$ fit of data on the plots, the correlation coefficients (R^2) between
237 the pairs of parameters for each site were calculated as +0.40 for site P78, +0.07 for site ZAF06
238 and +0.66 for site ZAF08. These results also confirm preliminary results based on previous
239 measurements performed in the same area. A similar positive correlation was found at site P78
240 by Giammanco et al. (1998) and by Pecoraino and Giammanco (2005). According to these
241 authors, when CO_2 effluxes from site P78 were the highest, the corresponding values of $\delta^{13}C_{CO2}$
242 became very similar to the pristine magmatic ones assumed for Mt. Etna. More negative values
243 of $\delta^{13}C_{CO2}$ would then indicate a higher degree of mixing between the magmatic component
244 and the biogenic source in the soil gas, particularly evident at low CO_2 efflux values. This
245 indicates that when CO_2 efflux becomes higher, magmatic CO_2 can reach the surface more
246 efficiently, thus surmounting the shallow biogenic component of the gas. This in turn confirms
247 the transport of free gas (mostly CO_2) along preferential pathways in the crust that correspond
248 to tectonic faults, where the local permeability is much higher than in the surrounding volcanic

249 rocks (values of permeability in Etna rocks are in the range from 2.5×10^{-11} to 2.9×10^{-10} m^2,
250 according to Aureli, 1973 and Ferrara, 1975) and where local ground water quickly becomes
251 saturated with CO_2.

252 This behavior appears to be valid, more or less, for all three sites of the east flank of Mt.
253 Etna investigated during this study. Interestingly, our findings are also in agreement with those
254 of similar studies carried out at the Solfatara crater (Phlaegrean Fields, Italy) by Chiodini et al
255 (2008), who found a similar positive correlation between CO_2 efflux and the $\delta^{13}C_{CO2}$ values of
256 the corresponding soil CO_2 efflux (i.e., C isotopes were not measured in soil gas samples, but
257 at the outlet of the CO_2 efflux measurement device) from fumaroles located inside the crater
258 and from diffuse emissions occurring both inside and outside of the crater. They explained the
259 correlation as being due to a combination of three distinct statistical populations of samples: i)
260 a high-flux population with a mean $\delta^{13}C$ value of -2.3±0.9‰, representative of pure
261 hydrothermal degassing of CO_2 (this value was actually very similar to that of local fumarolic
262 CO_2, that is -1.48‰); ii) a low flux population with a mean $\delta^{13}C$ value of about -19.4±2.1‰,
263 representative of biogenic degassing of CO_2 (from microbial decomposition of organic matter
264 in the soil, from plant residues or from root respiration); iii) an intermediate efflux population
265 with a mean $\delta^{13}C$ value of about -9.8±3.7‰, representative of a mixture of the two above.
266
267 *4.2.Temporal changes of the monitored parameters*
268 The temporal patterns of the soil CO_2 efflux values for each site monitored, plotted on a
269 $\log_{10}$ scale (Fig. 4), show some common features between sites. A marked and sharp decrease
270 was observed in mid-February 2009 simultaneously at sites P78, ZAF06 and ZAF08, to then
271 give way to a steady increase since the end of March 2009. Further decreases were recorded, in
272 a more scattered way, from November 2009 to March 2010 and finally, following a sudden
273 drop, in late October-December 2010, the latter observed only at sites ZAF08 and P78. The

highest effluxes were observed during June-July 2009 at most of the sites, more evidently at P39. High effluxes were also recorded in April 2010 at site ZAF06, in July 2010 at P39 and, during September-October 2010, at more or less all sites. Site ZAF06 showed slightly more stable CO_2 effluxes after the above mentioned period of very low values from January to March 2009. In order to determine whether the above changes were at least in part caused by variations in the main meteorological parameters, we performed a linear cross-correlation analysis of all the data, divided into areas (SE flank and E flank). The resulting correlation matrixes (Tables 3 and 4 for the area near Paternò and for that near Riposto, respectively), show no significant correlation between the considered parameters. All correlation coefficients were in the range between -0.56 and +0.7 and, apart from a very weak direct correlation between CO_2 efflux and air temperature at site P78 (R = +0.61), all other coefficients between soil CO_2 efflux and meteorological parameters had values between -0.56 and +0.51. This clearly suggests a non-environmental, probably volcanic, cause for the observed temporal changes in soil CO_2 efflux values (and by reflection also in $\delta^{13}C_{CO2}$ values) at all monitored sites.

The temporal patterns of $\delta^{13}C_{CO2}$ values (Fig. 5) show dissimilar behavior between site P39 and the other three sites. As noted above, the $\delta^{13}C_{CO2}$ values at site P39 in general varied within a much narrower range (only about 1‰) than at the other sites and showed no appreciable correlation with the CO_2 efflux values. This points to a marked geochemical stability of the hydrothermal system beneath site P39, likely due to its large volume that makes it less sensitive, at least in terms of isotopic composition of the escaping CO_2, to changes in the input of high-enthalpy magmatic fluids coming from depth.

The other sites show, instead, a consistent behavior, marked by a more or less sharp positive shift of $\delta^{13}C$ values in April-May 2009, followed by a slower trend towards even more positive values. Carbon isotope values remained quite stable or decreased slightly from June to

October 2010 to show a fairly more marked shift towards negative values in October-November 2010.

The overall picture arising from the above data indicates the significant arrival of deep magmatic CO_2 just before the end of the 2008-2009 flank eruption, reasonably related to emplacement of new gas-rich magma within relatively deep portions of the volcano and along conduits that were not directly connected with those feeding the ongoing flank eruption. This interpretation is strongly supported by other geochemical and geophysical parameters that were measured during the same period by the monitoring network of the Istituto Nazionale di Geofisica e Vulcanologia (Mattia et al., 2015). In particular, the behavior observed in the temporal pattern of soil CO_2 efflux in early 2009 can be interpreted according to geochemical studies made both on soil CO_2 emissions from Mt. Etna (Giammanco et al., 1995; Bruno et al., 2001), and on crater fumarole emissions at Vulcano Island (Nuccio and Valenza, 1992, 1998). Strong decreases in the CO_2 output from soils or from fumaroles accompany early stages of magma motion towards the surface. In those cases, magma undergoes sudden pressure decreases, which causes marked exsolution of a separate vapor phase in the volatile-saturated melt and consequent partition of volatiles into the newly formed bubbles according to the different gas solubilities. Because of its low solubility in magma, CO_2 will be highly enriched in the separate vapor phase. The consequent decrease in the concentration of residual dissolved CO_2 in the uppermost portion of a magma body produces a kinetic diffusion effect that translates into an inward and upward migration of dissolved gas. This process results in an initial decrease of volatile fluxes released from the deep magma towards the surface. Subsequently, when CO_2-rich gas bubbles are able to escape from magma, outward advective fluxes of magmatic volatiles through the main pathways across the structure of the volcano (i.e., volcanic conduits, degassing faults) will markedly increase. The sequence observed in our data in early 2009, therefore, would represent a complete cycle of fresh magma transfer from deeper to shallower

323 levels in the volcano. The simultaneous change in C isotope values would simply reflect the
324 isotopic shift related with the above mention changes in the degree of mixing between the
325 magmatic component and the biogenic source as function of CO_2 efflux.

326 After the end of the 2008-2009 eruption a further slow increase in magmatic CO_2
327 degassing was in general observed, suggesting that deep-coming magma moved further upward
328 and accumulated into shallower portions of the volcanic system, thus releasing higher amounts
329 of fluids. This in turn produced a higher input of high-enthalpy fluids into the shallow aquifers
330 of Mt. Etna, thus raising the temperature of water in the sub-surface hydrothermal systems
331 within the volcano. This process would explain the further isotopic shift towards positive $\delta^{13}C$
332 values observed during the summer of 2010. Besides, the progressive pressurization of the
333 shallow volcanic system as consequence of magma accumulation also reasonably led to the
334 opening of the NSEC in early November 2009 and prepared for its following eruptive activity.

335 The sharp decrease in CO_2 efflux, combined with the slight negative shift of $\delta^{13}C$ values,
336 observed since October 2010 at sites P78, ZAF08 and, to a lesser extent, also at ZAF06, might
337 be the consequence of a sudden upward migration of magma. Marked transient decreases in
338 soil CO_2 emissions at Mt. Etna were interpreted by Giammanco et al. (1995) as an indication
339 of rapid upward migration of the gas source (i.e., a CO_2-oversaturated magma). Shallow magma
340 up-rise produces a greater gas pressure gradient between the source of gas and the summit of
341 the volcano, which greatly overcomes the gradient existing between the gas source and the
342 peripheral areas. This large contrast favors the release of magmatic gas along the direction
343 source-summit of the volcano, thus significantly dampening diffuse flank degassing. This
344 hypothesis is also strongly supported by the following occurrence both of Strombolian activity
345 at NSEC in late December 2010 and, mostly, of the long sequence of eruptive episodes since
346 January 12, 2011; the latter episodes would testify the final arrival of magma at the surface.
347

5. Concluding remarks

The results of this study will help to better understand and define the physico-chemical mechanisms that rule the interactions occurring between deep CO_2 deriving from magma degassing inside Mt. Etna feeder conduit and the shallow fluids within the volcano. The observed temporal variations of the studied parameters are explained in terms of variable degrees of geochemical interaction between high-enthalpy magmatic fluids and shallow ground water, as a function of the supply of magmatic gas from depth.

At high soil CO_2 effluxes, $\delta^{13}C_{CO2}$ values in the peripheral sites are similar to those found in the fumarole gases emitted close to the active summit craters of Mt. Etna. When this occurs, we can reasonably hypothesize that new gas-rich magma is accumulating in relatively deep (5-10 km) volumes within the volcano, causing a strong pressure increase in the whole volcanic system. Conversely, when flank CO_2 emission is low, values of $\delta^{13}C_{CO2}$ become more negative, pointing to a greater interaction with shallow non-magmatic fluids, in our case cold ground water and biogenic CO_2 (Giammanco et al., 1998; Pecoraino and Giammanco, 2005).

Our results are encouraging for future monitoring of the eruptive activity of Mt. Etna. The sampling sites chosen are always easy to access under most weather conditions. Further, the sampling procedure is simple and the analytical methods are precise and reliable. A higher sampling frequency will certainly improve the temporal resolution on the studied parameters, thus permitting their use also as short-term indicators of the dynamics of Mt. Etna.

Acknowledgements

We wish to thank S. Consoli, F. Calvagna and M. Lopez for their help during the field work. We also thank the “Regione Siciliana - SIAS - Servizio Informativo Agrometeorologico Siciliano” for kindly providing the meteorological data used in this work. We acknowledge the financial support of Slovenian Research Programme “Cycling of substances in the environment,

373 mass balances, modelling of environmental processes and risk assessment" (P1-0143) and
374 bilateral Slovenian-Italian Cooperation "Mercury emissions, its influence and correlation with
375 Rn on Etna area". Special thanks are given to Prof Roger H. Pain for linguistic corrections.

376

377 **References**

378 Aiuppa, A., Allard, P., D'Alessandro, W., Giammanco, S., Parello, F., and M. Valenza (2004).
379 Magmatic gas leakage at Mount Etna (Sicily, Italy): relationships with the volcano-
380 tectonic structures, the hydrological pattern and the eruptive activity, in Mt. Etna:
381 Volcano Laboratory, A.G.U. Geophysical Monograph Series 143, 129-145, doi:
382 10.1029/143GM09.
383 Allard, A., Jean-Baptiste, P., D'alessandro, W., Parello, F., Parisi, B., and C. Flehoc (1997).
384 Mantle-derived helium and carbon in groundwaters and gases of Mount Etna, Italy, Earth
385 Planet, Sci. Let., 148, 501–516.
386 Anzà, S., Dongarrà, G., Giammanco, S., Gottini, V., Hauser, S. and M. Valenza (1989).
387 Geochimica dei fluidi dell'Etna: Le acque sotterranee, Miner. Petrogr. Acta, 32, 231-251
388 (in Italian).
389 Ahrens, L.H. (1954). The lognormal distribution of the elements (A fundamental law of
390 geochemistry and its subsidiary). Geochim. Cosmochim. Acta, 5, 49-73.
391 Aureli, A. (1973). Idrogeologia del fianco occidentale etneo, proc. 2nd Int.l Congress on
392 Underground Waters, Palermo, Italy, 425-487 (in Italian).
393 Behncke, B., Branca, S., Corsaro, R.A., De Beni, E., Miraglia, L. and C. Proietti (2014). The
394 2011–2012 summit activity of Mount Etna: birth, growth and products of the new SE
395 crater. J. Volcanol. Geotherm. Res., 270, 10–21.
396 http://dx.doi.org/10.1016/j.jvolgeores.2013.11.012.

397 De Beni, E., Behncke, B., Branca, S., Nicolosi, I., Carluccio, R., D'Ajello Caracciolo, F. and
398 M. Chiappini (2015). The continuing story of Etna's New Southeast Crater (2012–2014):
399 Evolution and volume calculations based on field surveys and aerophotogrammetry. J.
400 Volcanol. Geotherm. Res., 303, 175–186.
401 http://dx.doi.org/10.1016/j.jvolgeores.2015.07.021.
402 Bonaccorso, A., Bonforte, A., Calvari, S., Del Negro, C., Di Grazia, G., Ganci, G., Neri, M.,
403 Vicari, A. and E. Boschi (2011). The initial phases of the 2008–2009 Mount Etna
404 eruption: A multidisciplinary approach for hazard assessment. J. Geophys. Res., 116,
405 B03203, doi:10.1029/2010JB007906.
406 Bonfanti, P., D'Alessandro, W., Dongarrà, G., Parello, F. and M. Valenza (1996). Medium-term
407 anomalies in groundwater temperature before 1991-1993 Mt. Etna Eruption, J. Volcanol.
408 Geotherm. Res., 73, 303-308.
409 Bruno N, Caltabiano T, Giammanco S and R. Romano (2001). Degassing of SO_2 and CO_2 at
410 Mount Etna (Sicily) as an indicator of pre-eruptive ascent and shallow emplacement of
411 magma, J. Volcanol. Geotherm. Res., 110, 137-153.
412 Brusca, L., Aiuppa, A., D'alessandro, W., Parello, F., Allard, P., and A. Michel (2001).
413 Geochemical mapping of magmatic gas-water-rock interactions in the aquifer of Mount
414 Etna volcano, J. Volcanol. Geotherm. Res., 108, 199–218.
415 Caracausi, A., Favara, R., Giammanco, S., Italiano, F., Nuccio, P.M., Paonita, A., Pecoraino,
416 G. and A. Rizzo (2003°). Mount Etna: Geochemical signals of magma ascent and
417 unusually extensive plumbing system, Geophys. Res. Lett., 30, 1057-1060,
418 doi:10.1029/2002GL015463.
419 Caracausi, A., Italiano, F., Nuccio, P.M., Paonita, A. and A. Rizzo (2003b). Evidence of deep
420 magma degassing and ascent by geochemistry of peripheral gas emissions at Mount Etna

421 (Italy): Assessment of the magmatic reservoir pressure, J. Geophys. Res., 108, B10, 2463,
422 doi: 10.1029/2002JB002095.
423 Chiodini, G., D'Alessandro, W. And F. Parello (1996). Geochemistry of gases and waters
424 discharged by the mud volcanoes at Paternò, Mt. Etna (Italy), Bull. Volcanol., 58, 51-58.
425 Chiodini, G., Cioni, R., Guidi, M., Raco, B. and L. Marini (1998). Soil CO_2 flux measurements
426 in volcanic and geothermal areas, App. Geochem., 13, 543– 552.
427 Chiodini, G., Caliro S., Cardellini C., Avino R., Granieri D. and A. Schmidt (2008). Carbon
428 isotopic composition of soil CO2 efflux, a powerful method to discriminate different
429 sources feeding soil CO_2 degassing in volcanic-hydrothermal areas, Earth Planet. Sci.
430 Lett., 274, 372-379, doi:10.1016/j.epsl.2008.07.051.
431 Corsaro, R.A. and L. Miraglia (2014). The transition from summit to flank activity at Mt. Etna,
432 Sicily (Italy): Inferences from the petrology of products erupted in 2007–2009, J.
433 Volcanol. Geotherm. Res., 275, 51-60, doi:10.1016/j.jvolgeores.2014.02.009.
434 Čater M. and N. Ogrinc (2011). Soil respiration rates and $\delta^{13}C_{CO2}$ in natural beech forest (*Fagus*
435 *sylvatica L.*) in relation to stand structure, Isot. Environ. Health, S 47, 221–237.
436 D'Alessandro, W., De Gregorio, S., Dongarrà, G., Gurrieri, S., Parello, F. and B. Parisi (1997a).
437 Chemical and isotopic characterization of the gases of Mount Etna (Italy), J. Volcanol.
438 Geotherm. Res., 78, 65-76.
439 D'Alessandro, W., Giammanco, S., Parello, F. and M. Valenza (1997b). CO_2 output and
440 $\delta^{13}C(CO_2)$ from Mount Etna as indicators of degassing of shallow asthenosphere, Bull.
441 Volcanol., 58, 455-458.
442 Farrar, C.D., Sorey, M.L., Evans, W.C., Howle, J.F., Kerr, B.D., Kennedy, B.M., King, C.Y.
443 and J.R Southon (1995). Forest-killing diffuse CO_2 emission at Mammoth Mountain as a
444 sign of magmatic unrest, Nature, 376, 675-678.

445 Ferrara, V. (1975). Idrogeologia del versante orientale dell'Etna, proc. 3rd Int.l Congress on
446 Underground Waters, Palermo, Italy, 91-144 (in Italian).
447 Giammanco, S., Gurrieri, S., and M. Valenza (1995). Soil CO_2 degassing on Mt. Etna (Sicily)
448 during the period 1989-1993: discrimination between climatic and volcanic influences,
449 Bull. Volcanol., 57, 52-60.
450 Giammanco, S., Inguaggiato, S. and M. Valenza (1998). Soil and fumarole gases of Mount
451 Etna: Geochemistry and relations with volcanic activity, J. Volcanol. Geotherm. Res., 81,
452 297-310.
453 Giammanco, S. and P. Bonfanti (2009). Cluster analysis of soil CO_2 data from Mt. Etna (Italy)
454 reveals volcanic influences on temporal and spatial patterns of degassing, Bull. Volcanol.,
455 71, 201-218, doi: 10.1007/s00445-008-0218-x.
456 Giammanco, S., Bellotti, F., Groppelli, G. and A. Pinton (2010). Statistical analysis reveals
457 spatial and temporal anomalies of soil CO2 efflux on Mount Etna volcano (Italy), J.
458 Volcanol. Geotherm. Res., 194, 1-14, doi:10.1016/j.jvolgeores.2010.04.006.
459 Giammanco, S., Neri, M., Salerno, G.G., Caltabiano, T., Burton, M.R and V. Longo (2013).
460 Evidence for a recent change in the shallow plumbing system of Mt. Etna (Italy): gas
461 geochemistry and structural data during 2001-2005, J. Volcanol. Geotherm. Res., 251,
462 90–97, doi:10.1016/j.jvolgeores.2012.06.001.
463 Gillot., P.-Y., Kieffer, G. and R. Romano (1994). The evolution of Mount Etna in the light of
464 potassium-argon dating, Acta Vulcanol., 5, 81-87.
465 Hernández, P.A., Melián, G., Giammanco, S., Sortino, F., Barrancos, J., Pérez, N.M., Padrón,
466 E., López, M., Donovan, A., Mori, T. and K. Notsu (2015). Contribution of CO_2 and H_2S
467 emitted to the atmosphere by visible and non-visible degassing from volcanoes: The Etna
468 Volcano case study, Surv. Geophys., 36 (3), 327-349, doi: 10.1007/s10712-015-9321-7.

469 Knohl, A., Werner, R.A., Geilmann, H. and W.A. Brand (2004). Kel-F discs improve storage
470 time of canopy air samples in 10-mL vials for CO_2-$\delta^{13}C$ analysis, Rapid Commun. Mass.
471 Spectrom., 14, 1663–1665, doi: 10.1002/rcm.1528.
472 Krajnc, B., Fujiyoshi, R., Vaupotič, J., Amano, H., Sakuta, Y., Gregorič, A. and N. Ogrinc
473 (2016). Using ^{222}Rn and carbon isotopes (^{12}C, ^{13}C and ^{14}C) to determine CO_2 sources in
474 forest soils developed on contrasting geology in Slovenia, Environ. Earth. Sci., 75, 1068
475 doi: 10.1007/s12665-016-5866-0.
476 Krajnc, B., Ferlan, M. and N. Ogrinc (2017). Soil CO_2 sources above a subterranean cave—
477 Pisani rov (Postojna Cave, Slovenia), J. Soils Sed., 17, 1883–1892. doi: 10.1007/s11368-
478 016-1543-x.
479 Mattia, M., Bruno, V., Caltabiano, T., Cannata, A., Cannavò, F., D'Alessandro, W., Di Grazia,
480 W., Federico, C., Giammanco, S., La Spina, A., Liuzzo, M., Longo, M., Monaco, C.,
481 Patanè, D. and Salerno, G. (2015). A comprehensive interpretative model of slow slip
482 events on Mt. Etna's eastern flank, Geochem. Geophys. Geosyst., 16, 635-658,
483 doi:10.1002/2014GC005585.
484 Mook, W.G., Bommerson, J.C., and W.H. Staverman (1974). Carbon isotope fractionation
485 between dissolved bicarbonate and gaseous carbon dioxide, Earth Planet. Sci. Lett., 22,
486 169-176.
487 Nuccio, P.M. and Valenza, M. (1992). Modification of geochemical parametres during magma
488 ascent: The case of Vulcano, Aeolian Islands. Publ. I.G.F. - CNR, Palermo, Italy, 7, 1-23.
489 Nuccio, P.M. and Valenza, M. (1998). Magma degassing and geochemical detection of its
490 ascent, in Water-Rock Interaction, Balkema Rotterdam, 475-478.
491 Parkinson, K.J. (1981). An improved method for measuring soil respiration in the field, J. App.
492 Ecol., 18, 221-228.

493 Pecoraino, G. and S. Giammanco (2005). Geochemical Characterization and Temporal
494 Changes in Parietal Gas Emissions at Mt. Etna (Italy) During the Period July 2000 - July
495 2003, Terr. Atmosph. Ocean. Sci., 16, 805-841.
496 Spötl C. (2004). A simple method of soil gas stable carbon isotope analysis, Rapid Commun.
497 Mass Spectrom., 18, 1239–1242, doi: 10.1002/rcm.1468.
498 Torn, M.S., Davis, S., Bird, J.A., Shaw, M.R. and M.E. Conrad (2003). Automated analysis of
499 C-13/C-12 ratios in CO_2 and dissolved inorganic carbon for ecological and environmental
500 applications, Rapid Commun. Mass Spectrom., 17, 2675–2682. doi:10.1002/rcm.1246.
501

502 **Table Captions**

503 Table 1. Values of soil CO_2 efflux (in g m^{-2} d^{-1}) and $\delta^{13}C_{CO2}$ (in per mil vs. PDB) measured at
504 sites ZAF06, ZAF08 and P78 during the study period. Also shown are the corresponding
505 meteorological data measured at the station located at Riposto. n.d. = not determined.
506
507 Table 2. Values of soil CO_2 efflux (in g m^{-2} d^{-1}) and $\delta^{13}C_{CO2}$ (in per ml vs. PDB) measured at
508 site P39 during the studied period. Also shown are the corresponding meteorological data
509 measured at the station located at Paternò. n.d. = not determined.
510
511 Table 3. Correlation matrix between the soil CO_2 efflux values measured at site P39 and the
512 corresponding meteorological parameters measured at the station of Paternò.
513
514 Table 4. Correlation matrix between the soil CO_2 efflux values measured at sites ZAF06,
515 ZAF08 and P78 and the corresponding meteorological parameters measured at the station of
516 Riposto.
517
518
519
520
521
522
523
524
525
526
527
528
529

Table 1. Values of soil CO_2 efflux (in g m^{-2} d^{-1}) and $\delta^{13}C_{CO2}$ (in ‰ vs. PDB) measured at sites ZAF06, ZAF08 and P78 during the studied period. Also shown are the corresponding meteorological data measured at the station located at Riposto. n.d. = not determined.

Date	ZAF06		ZAF08		P78		T_{air}	Rain	RH min	RH max	Wind
	CO_2 flux	$\delta^{13}C_{CO2}$	CO_2 flux	$\delta^{13}C_{CO2}$	CO_2 flux	$\delta^{13}C_{CO2}$	°C	mm	%	%	m/s
02/03/09	3753	-5.10	233	-7.37	514	-12.93	14.70	0.00	55.00	100.00	1.09
02/16/09	12.4	-3.94	9.10	-17.69	5.30	-15.12	7.87	0.00	33.00	72.00	0.88
02/26/09	28.2	-6.17	7.60	-14.98	7.80	-14.43	9.20	0.20	30.00	73.00	1.95
03/12/09	77.5	-4.72	82.3	-16.21	68.5	-14.08	12.06	0.00	31.00	92.00	3.21
03/24/09	115	-4.42	39.1	-17.17	169	-16.18	10.96	0.00	38.00	79.00	0.98
04/09/09	2369	-5.10	62.3	-11.92	47.8	-11.03	13.23	2.80	66.00	100.00	0.53
04/20/09	n.d.	n.d.	493	-6.92	406	-10.58	14.38	9.00	78.00	100.00	0.69
04/29/09	798	-5.00	280	-5.83	145	-12.43	15.98	0.00	39.00	98.00	0.75
05/13/09	709	-3.00	1480	-4.13	909	-9.02	18.22	0.00	40.00	92.00	0.87
06/01/09	587	-2.10	882	-3.62	1075	-6.00	21.14	0.00	64.00	100.00	0.80
06/15/09	2534	-2.62	548	-3.34	676	n.d.	23.69	0.00	27.00	69.00	0.89
06/26/09	1212	n.d.	515	-3.81	427	-4.80	21.80	0.00	41.00	79.00	0.81
07/13/09	2017	-2.37	991	-4.41	856	n.d.	24.00	0.00	37.00	84.00	0.98
07/30/09	920	-2.39	968	-3.14	1118	-4.39	26.46	0.00	34.00	78.00	0.97
08/10/09	736	-2.16	1493	-3.44	1188	-4.36	25.95	0.00	52.00	94.00	0.74
08/25/09	603	-2.31	764	-3.16	1104	-4.31	26.07	0.00	55.00	100.00	0.65
09/07/09	667	-1.90	619	-3.22	702	-4.22	23.46	6.40	38.00	100.00	1.17
10/22/09	2604	-1.91	2138	-3.12	1887	-6.52	20.15	8.00	83.00	100.00	0.42
11/01/09	1921	-1.11	232	-2.52	491	-4.95	13.53	0.00	43.00	82.00	0.77
11/16/09	757	-1.04	2104	-2.54	396	-5.06	17.65	0.00	25.00	74.00	0.80
12/10/09	534	-0.55	52.2	-7.06	338	-4.37	13.13	0.00	39.00	76.00	2.88
12/30/09	601	-1.00	2722	-2.35	678	-4.71	15.34	0.00	48.00	89.00	0.64
01/19/10	272	-1.03	37.3	-15.60	198	-5.44	9.99	1.60	42.00	100.00	1.20
01/29/10	3200	-1.76	408	-3.18	727	-6.67	9.51	0.00	59.00	90.00	0.68
02/12/10	193	-0.08	10.8	-16.91	29.0	-4.05	9.19	0.00	16.00	100.00	2.49
03/01/10	1540	-1.31	895	-2.57	740	-4.82	14.53	0.00	52.00	100.00	0.63
03/19/10	220	-0.53	18.8	-13.05	111	-5.90	11.28	0.00	40.00	81.00	1.05
04/09/10	1487	-0.87	336	-2.45	697	-4.09	14.10	0.00	50.00	85.00	0.56
04/26/10	4638	-0.74	670	-2.77	556	-3.31	16.83	0.00	55.00	100.00	0.72
06/08/10	2158	1.16	661	-2.96	949	-1.32	21.25	0.00	42.00	100.00	0.48
06/22/10	1479	1.01	312	-4.52	1223	-0.94	19.87	0.00	43.00	100.00	0.15
07/14/10	608	0.83	685	-2.16	2506	-0.85	25.93	0.00	48.00	100.00	0.93
07/29/10	521	0.72	422	-1.74	1362	-0.92	23.98	0.00	53.00	83.00	0.90
08/26/10	614	0.71	1156	-1.49	2415	-1.08	26.45	0.00	44.00	100.00	0.78
09/09/10	3037	0.55	550	-2.69	2723	-1.02	23.68	104.20	53.00	100.00	1.09
09/23/10	281	0.13	321	-2.29	605	-1.28	20.33	0.40	61.00	100.00	0.57
10/06/10	2777	-0.30	1971	-1.45	4606	-1.79	21.67	0.00	72.00	100.00	0.59
10/22/10	838	-0.30	8.40	-5.91	24.2	-3.85	16.95	0.80	75.00	100.00	0.75
11/19/10	176	-0.08	34.9	-6.92	224	-1.83	14.74	0.00	52.00	95.00	0.76
12/07/10	167	-0.80	281	-2.98	709	-3.04	13.19	0.00	63.00	100.00	0.86

Table 2. Values of soil CO_2 efflux (in g m^{-2} d^{-1}) and of $\delta^{13}C_{CO2}$ (in per mil vs. PDB) measured at site P39 during the studied period. Also shown are the corresponding meteorological data measured at the station located at Paternò. n.d. = not determined.

Date	P39		T_{air}	Rain	RH min	RH max	Wind
	CO_2 flux	$\delta^{13}C_{CO2}$	°C	mm	%	%	m/s
05/13/09	568	2.79	18.59	0.00	13.00	91.00	0.48
06/01/09	31608	2.53	22.09	0.00	15.00	87.00	1.77
06/15/09	11384	n.d.	23.15	0.00	12.00	77.00	1.08
06/26/09	24468	2.50	22.58	0.00	12.00	86.00	1.07
07/13/09	22838	2.30	24.57	0.00	12.00	90.00	1.04
07/30/09	15143	2.33	26.73	0.00	18.00	82.00	1.49
08/10/09	10446	n.d.	26.78	0.00	26.00	82.00	1.49
08/25/09	7213	2.16	26.97	0.00	19.00	94.00	1.26
09/07/09	5288	2.13	24.38	0.00	26.00	94.00	1.24
11/16/09	1378	2.47	15.53	0.00	22.00	98.00	0.50
12/10/09	3076	2.44	13.36	0.00	38.00	80.00	1.90
12/30/09	3054	2.58	15.77	0.00	25.00	95.00	0.63
01/07/10	1777	2.94	12.81	0.00	43.00	96.00	1.64
01/29/10	1160	2.65	9.57	0.00	53.00	90.00	0.69
02/12/10	307	2.90	7.05	1.00	42.00	97.00	0.84
03/01/10	904	3.10	14.88	0.00	41.00	97.00	1.00
03/19/10	733	2.87	10.46	0.00	30.00	97.00	0.88
04/09/10	5124	2.92	13.87	0.00	40.00	93.00	1.72
04/26/10	5027	2.68	16.19	3.00	27.00	97.00	1.04
06/08/10	2374	2.99	22.44	0.00	26.00	91.00	1.83
06/23/10	3297	1.60	22.65	0.00	25.00	66.00	1.46
07/14/10	4227.12	2.79	27.23	0.00	18.00	79.00	1.80
07/29/10	10535.88	2.64	24.88	0.00	23.00	93.00	1.23
08/26/10	7871.28	2.65	27.30	0.00	20.00	87.00	1.74
09/09/10	4362.12	2.66	24.50	5.60	47.00	94.00	1.64
09/23/10	3699.48	2.47	19.85	1.20	52.00	95.00	1.38
10/06/10	5419.92	2.55	21.49	0.00	47.00	94.00	0.50
10/22/10	3044.40	2.31	16.12	1.40	61.00	93.00	0.95
11/19/10	1991.04	2.29	13.44	0.00	39.00	99.00	0.40
12/07/10	2339.04	2.31	13.59	0.00	42.00	99.00	0.45

Table 3. Correlation matrix between the soil CO_2 efflux values measured at sites P39 and the corresponding meteorological parameters measured at the station of Paternò.

	P39	T_{air}	Rain	RH min	RH max	Wind
P39	1.00	0.51	-0.13	-0.55	-0.31	0.27
T° air		1.00	0.02	-0.56	-0.48	0.45
Rain			1.00	0.34	0.21	0.11
RH min				1.00	0.41	-0.15
RH max					1.00	-0.49
Wind						1.00

Table 4. Correlation matrix between the soil CO_2 efflux values measured at sites ZAF06, ZAF08 and P78 and the corresponding meteorological parameters measured at the station of Riposto.

	ZAF06	ZAF08	P78	T_{air}	Rain	RH min	RH max	Wind
ZAF06	1.00	0.18	0.32	0.16	0.26	0.29	0.19	-0.31
ZAF08		1.00	0.51	0.45	0.00	0.18	0.07	-0.34
P78			1.00	0.61	0.33	0.35	0.31	-0.28
T° air				1.00	0.18	0.14	0.18	-0.35
Rain					1.00	0.11	0.17	0.02
RH min						1.00	0.56	-0.49
RH max							1.00	-0.24
Wind								1.00

566 **Figure Captions**

567 **Figure 1.** Map of the study area. The red circles indicate the location of soil CO_2 sampling
568 points. The three main rift zones (NE, W and S) are also shown. VB = Valle del Bove
569 morphological depression. The blue squares indicate the location of the two SIAS
570 meteorological stations used for the purposes of this study. The yellow star shows the location
571 both of the SE Crater and of the nearby NSEC.

572

573 **Figure 2.** Correlation plot between $\delta^{13}C_{CO2}$ values and the corresponding $\log_{10}$ values of CO_2
574 efflux measured at all sites. The horizontal bands indicate the ranges of $\delta^{13}C_{CO2}$ values related
575 to the main sources of CO_2 found at Mt. Etna (i.e., biogenic, magmatic and hydrothermal).

576

577 **Figure 3.** Schematic graphic models of the geochemical interactions between magmatic CO_2
578 gas and shallow fluids in the monitored sites: a) interaction between magmatic CO_2 and
579 hydrothermal fluids (depicted as an orange horizontal layer) at site P39, with consequent
580 positive shift of $\delta^{13}C$ values due to partition of ^{12}C into the liquid phase as HCO_3^-; b) interaction
581 between magmatic CO_2 and cold ground water (depicted as a blue horizontal layer) at sites
582 ZAF06, ZAF08 and P78, causing partition of ^{13}C into the liquid phase, followed by mixing with
583 shallow biogenic CO_2 produced in the soil (depicted as a green horizontal layer) and consequent
584 enrichment in ^{12}C in the gas phase.

585

586 **Figure 4.** Temporal pattern of the soil CO_2 effluxes measured in the monitored sites during the
587 study period: a) P39; b) P78; c) ZAF08; d) ZAF06. The pink area indicates the period of the
588 2008-2009 flank eruption. The vertical red line indicates the moment of the opening of the
589 NSEC.

590

591 **Figure 5.** Temporal pattern of the $\delta^{13}C_{CO2}$ values measured in the monitored sites during the
592 studied period: a) P39; b) P78; c) ZAF08; d) ZAF06. The pink area indicates the period of the
593 2008-2009 flank eruption. The vertical red line indicates the moment of the opening of the
594 NSEC.
595
596
597
598
599
600
601
602
603
604
605
606
607
608
609
610

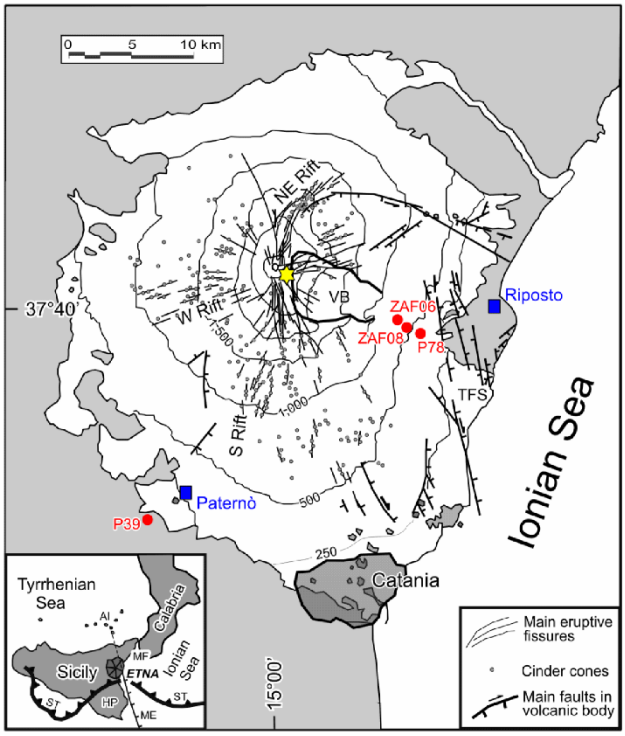
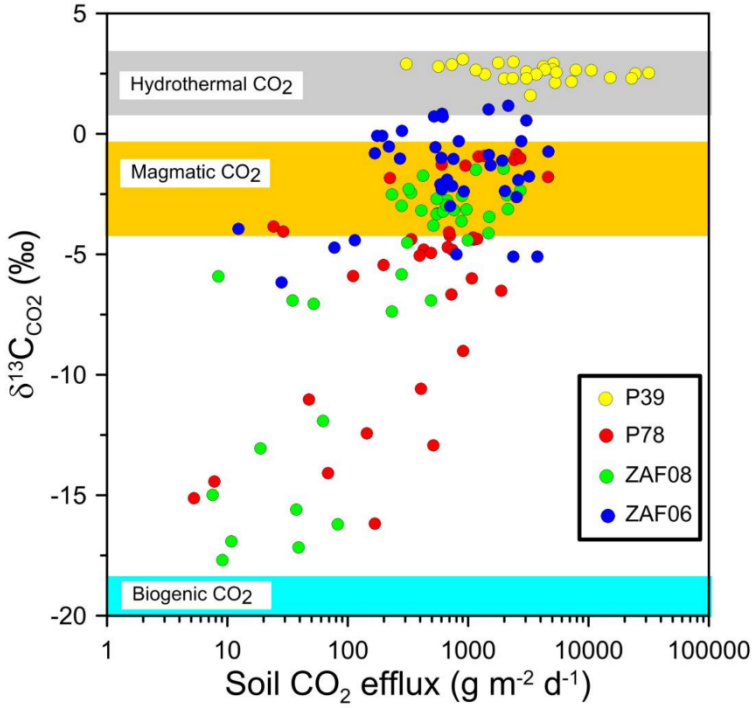

0 5 10 km
NE Rift
VB
W Rift
S Rift
ZAF06
ZAF08
P78
P39
Riposto
Paternò
Catania
TFS
Ionian Sea
37°40'
15°00'
1-500
1-000
500
250
Tyrrhenian Sea
Sicily
Calabria
Ionian Sea
AI
MF
ETNA
HP
ST
ME
Main eruptive fissures
Cinder cones
Main faults in volcanic body

Figure 1.



623

624 Figure 2.

625

626

627

628

629

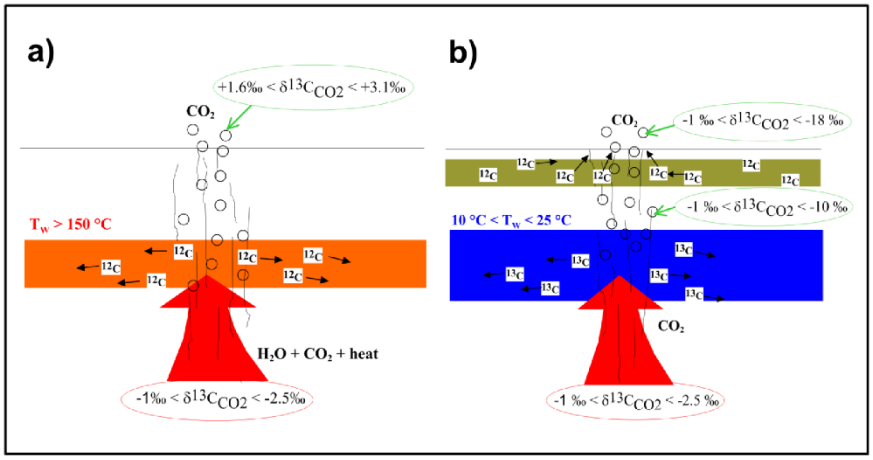
630

631

632

633

634



635

636 Figure 3.

637

638

639

640

641

642

643

644

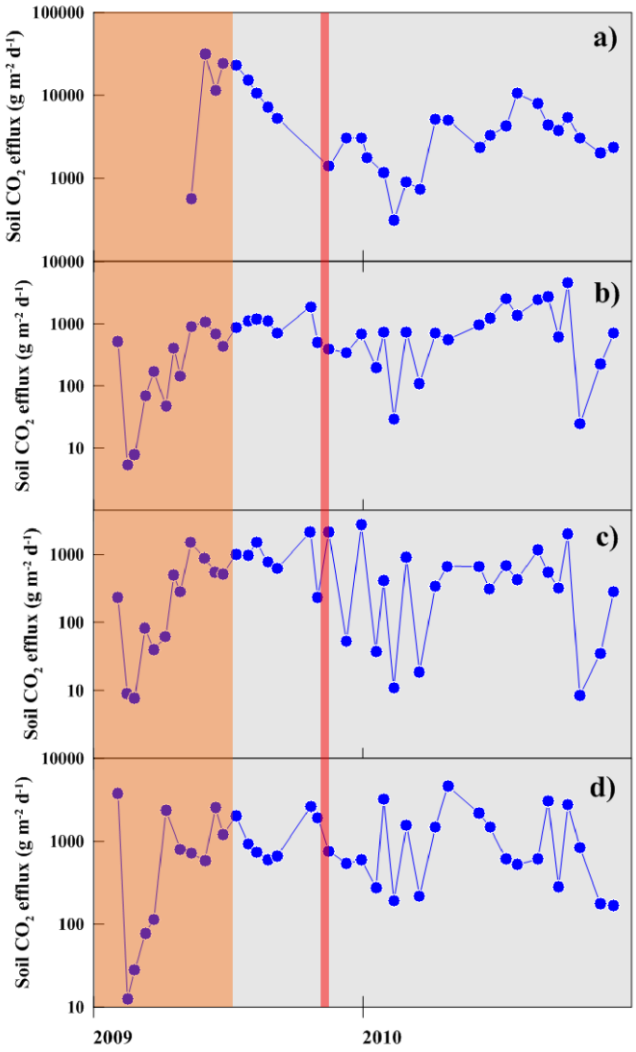
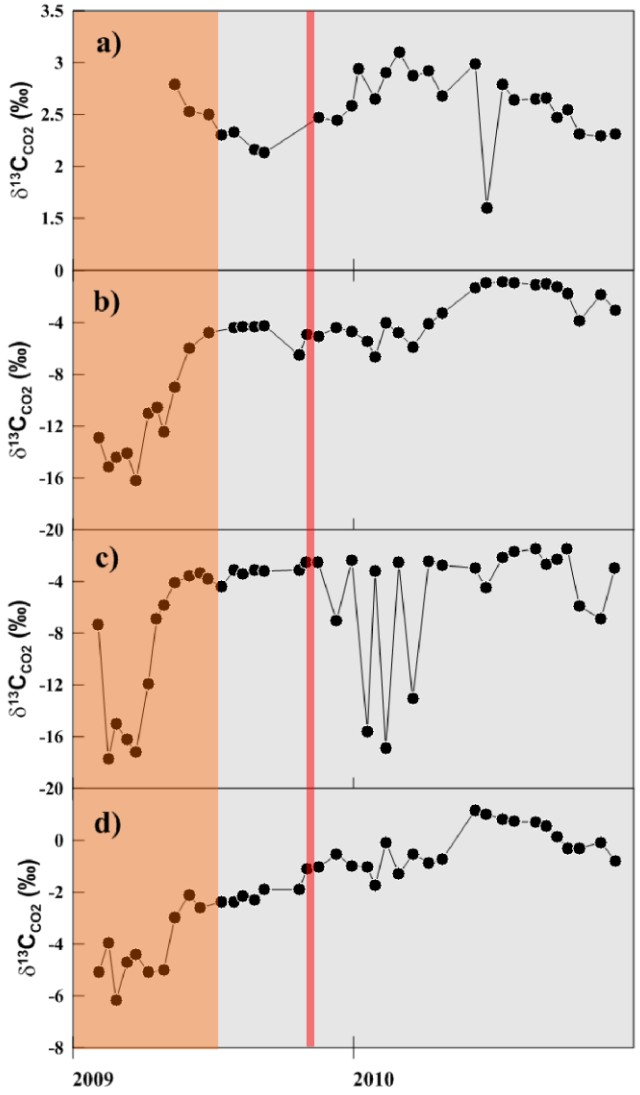

a)
b)
c)
d)
Soil CO_2 efflux (g m^{-2} d^{-1})
100000
10000
1000
100
10
2009
2010

Figure 4.



651

652 Figure 5

Chapter 4

Conclusions

This study contributes to the scientific knowledge of the CO_2 exchanges between the atmosphere and the soil, and processes occurring below the soil. The emphasis is placed on the different sources and factors involved in its transport. The present study of soil CO_2 fluxes on different parent rock materials, and its contribution from abiotic sources is the first comprehensive study of the soil CO_2 sources in Slovenia (and to our knowledge one of the few globally), which combines conventional tools with carbon isotope (stable and radioactive) and ^{222}Rn analysis. The research contributes to one of the major scientific challenges in achieving societal goals of the 21st century: "the categorization and quantification of major surface types as sources or sinks of CO_2". The mechanisms in the biogeochemical carbon cycling that influence the CO_2 dynamics between soil and the atmosphere are at present not completely understood, especially in the Karst area. This work provides qualitative-quantitative information on the contribution of geogenic processes, i.e. carbonate weathering and precipitation, as well as ventilation of belowground cavities, to the carbon cycle. Although the proposed dissertation consists of several case studies, the approach is rather context-sensitive than site-specific. It is flexible enough to be transferrable; therefore its replication will enable us to build a solid knowledge basis to construct the spatial database of net natural CO_2 fluxes (sources and sinks) for the Slovenian territory.

The contribution to the science performed within this study has resulted in three published, one accepted and one paper under review in SCI international journals. The work has been presented at 10 international conferences (See Bibliography) with 4 oral presentations. The main conclusions of the present research that consisted of several consecutive steps that roughly follow the order of scientific articles presented in this dissertation can be summarized as follows:

1. The first investigation dealing with the CO_2 sources in forest soils developed on contrasting geology with two sampling sites located on soils formed above carbonate bedrock, one above metamorphic bedrock and the remainder above clastic sedimentary rocks showed that:
   - **Carbon dioxide was consistently young at all sampling sites independent of the parent rock material** (carbonate vs. non-carbonate). The carbonate minerals had no influence on soil CO_2 isotopic composition.
   - At certain soil types, even at relatively deep soil the influence of atmospheric air has to be taken into account, since the **^{13}C-enrichment** of soil CO_2 can be a **consequence of the mixing of soil CO_2 with atmospheric CO_2**. In these cases it is important to include also ^{222}Rn measurements. The ^{13}C-enrichment of soil CO_2 that appears together with

the highest radon concentrations (if the soil itself contributes little to soil gas radon concentration) indicates the influence of subterranean CO_2 from e.g. pores, fissures and cavities; rather than the direct influence of atmospheric CO_2. This observation already indicates the adoption of the first hypothesis of the thesis showing that **cave ventilation is a significant source of soil CO_2 in the karst region**.

- At this stage it was shown that the soil–air ventilation system is too complex to explain the sources of the gaseous components only with one measurement therefore more measurements at different parts of the year have to be performed. Ideally, a continuous measurement system has to be applied.

2. The second investigation dealt with the transport of carbon in the forest soils (developed on different parent rock materials: one plot on magmatic granodiorite bedrock, two plots on carbonate bedrock in the karstic-dinaric area and one situated on Pleistocene coalluvial terraces) in the form of dissolved inorganic and organic carbon (DIC and DOC) in the infiltrating waters as a mechanism, which transports soil carbon from soil CO_2 and soil organic matter within and out of the soil carbon pool. The aim was to understand better the carbon dynamics and processes in the soil profiles, sources and transformation of DIC and DOC in soil waters, and the CO_2 consumption by chemical weathering. The main conclusions of this investigation were drawn as follows:
   - **The loss of DOC at 5 cm was in the order of 1 mol m^{-2} $year^{-1}$ at all four study sites**, although the vegetation coverage varies among sites. Only a small fraction of the DOC remained in soil waters with the majority either sorbed on mineral surfaces, respired, or re-assimilated.
   - A sharp decrease in DOC fluxes observed at locations with sandy soil texture is related to the amount of water percolating through the soil. **The drainage of water via macro pores in sandy soils can flush out a substantial amount of DOC.**
   - Highest DIC fluxes were observed at deeper soils (50 cm), where dolomite and calcite dissolution dominates. Indeed, the C isotope composition of DIC at those places suggested that half of the DIC was from soil CO_2 and the other half from carbonate minerals. **2 to 5 mol m^{-2} $year^{-1}$ of CO_2 was estimated to be lost through soil waters in dissolved inorganic form**.
   - **Soil waters above dolomite and calcite parent rock material remained unsaturated with respect to dolomite and calcite**, and the continuous dissolution of these carbonate minerals can continue to dissolve more CO_2 until equilibration is reached and thus **acting as a sink of C**.
   - At soils developed over non-carbonate parent rock material DIC fluxes were much lower, ~0.2 mol m^{-2} $year^{-1}$, which is consistent with slow silicate dissolution kinetics.
   - This investigation clearly identified local lithology (carbonate-bearing vs. carbonate free rocks), types of vegetation (spruce, beech), soil texture (clay, silt, sand), and climate (i.e., water fluxes through balances of precipitation and evapotranspiration) as important factors controlling the magnitude of carbon losses in dissolved organic and inorganic forms.

3. The third part of the PhD thesis uses the knowledge gathered during the first period to investigate the carbon sources in forest soil above known subterranean cave. During this investigation larger sampling frequency was used with continuous measurements of soil CO_2 fluxes and bimonthly sampling of soil and cave air (as a possible CO_2 source). This research has led to the following conclusions:
   - There was an **abiotic source of CO_2 present in soil** above the cave during cold periods and **coincided with the period of cave ventilation**.
   - It was estimated that cave air CO_2 can account for up to 80% of the overall soil CO_2 during the cave ventilation periods, and potentially up to 20% of annual CO_2 flux from soil above the cave. With this observation, the first hypothesis of this work was accepted indicating **that cave ventilation can be a significant source of soil CO_2 in the karst region**. Here it must be stressed out that this applies for the soils above caves, mainly during the ventilation of the cave and that a greater number of investigations above caves has to be made to generalize this observation.
   - It was shown further that subterranean cavities can act as a temporal storage of CO_2 and can be released during favorable conditions.
   - Results reveal that CO_2, which has accumulated underground can be quickly released to the atmosphere due to the processes of ventilation and therefore such processes should be included into the models of CO_2 exchange between soil and atmosphere. Thus, the future studies orientated into the determination of the **net CO_2 exchange between soil and atmosphere** at such areas should not base only on the assumption of **diffusive CO_2 flux**. The possibility of **advective CO_2 flux** from soils has to be taken into account when applying different CO_2 flux measurement methods (e.g. profile methods assuming only diffusive fluxes).

4. The forth investigation was performed in parallel with the previously described study. Here the CO_2 dynamics and dripwater geochemistry were investigated in the cave located below the investigated soil. The conclusions of this study can be summarized as follows:
   - The levels of CO_2, $\delta^{13}C_{CO2}$ and ^{222}Rn in the cave had a typical seasonal pattern. Accumulation of CO_2 and ^{222}Rn started in spring and reached maximum values in summer. Values started to drop in fall and reached the lowest concentrations in winter. $\delta^{13}C_{CO2}$ values showed the opposite trend with the lowest $\delta^{13}C_{CO2}$ values observed during the highest CO_2 concentrations.
   - **Variations of CO_2 concentrations** are not the function of soil CO_2 productivity, but **are mainly caused by the ventilation of the cave** that is **triggered by the differences between cave and outside air temperature**.
   - The analysis of carbon isotope composition of CO_2 and dripwater DIC indicated that the major source of cave CO_2 in the studied chamber is the CO_2 originating from soil respiration, transported directly to the cave. However, **the CO_2 transported to the cave in the form of DIC in**

the dripwaters has a minor influence on the cave air CO_2 concentration levels. This finding supports the second hypothesis of this thesis showing that **soil CO_2 is the main source of cave air CO_2 transported by diffusion or flowing down from the soil**.

- The DIC concentrations and its isotopic composition do not have a direct response from the variations in soil respiration.
- The DIC concentrations and its isotopic composition together with Ca^{2+} and Mg^{2+} concentrations in drip waters showed that there was no prior calcite precipitation before the sampling and that forced degassing causing kinetic effects could be possibly present only at rare occasions. **These findings deny the third hypothesis** stating that: **the process of cave ventilation forces degassing of CO_2 from the dripwater, prior to any calcite precipitation, causing kinetic isotope fractionation**. However, it should be pointed out that this study was performed only in one cave chamber and since different caves can have very different mechanisms affecting their dripwater and cave air composition, this conclusion cannot be generalized.

5. The fifth investigation was oriented to the characterization of deep CO_2 source and the possibility to use a stable isotope approach as a tool for volcano emissions. The study contributed to a better understanding of the physio-chemical interactions occurring between deep CO_2 derived from magma degassing inside Mt. Etna feeder conduit and the shallow environment of the volcano. It has also helped to understand better the temporal variations of CO_2 effluxes that take place as a consequence of the dynamics of magma release and transport to the surface through the volcano flanks. Based on the obtained results, the conclusions are summarized as follows:
   - At high soil CO_2 effluxes, $\delta^{13}C_{CO2}$ values in the peripheral sites are similar to those found in the fumarole gases emitted close to the active summit craters. Therefore it can be reasonably hypothesizing **that new gas-rich magma is accumulating in relatively deep (5-10 km) volumes within the volcano**, causing a strong pressure increase in the whole volcanic system.
   - When flank CO_2 emission is low, values of $\delta^{13}C_{CO2}$ become more negative, pointing to a greater interaction with shallow non-magmatic fluids i.e. cold ground water and biogenic CO_2.
   - Results are encouraging **for future monitoring of the eruptive activity of Mt. Etna**. The sampling sites chosen are always easy to access under most weather conditions. Further, **the sampling procedure is simple and the analytical methods are precise and reliable**. A higher sampling frequency will certainly improve the temporal resolution on the studied parameters, thus permitting their use also as short-term indicators of the dynamics of Mt. Etna.

The findings of this study demonstrate that isotope geochemistry is a very useful tool with which to address the sources of CO_2 in soil. However, stable isotopes can be considered as a complementary tool and are therefore recommended to use also other traces such as radiocarbon and radon to support the stable isotopic data. It was also shown that this knowledge has a potential usefulness in short term prediction of volcanic activity. It was also shown that in karst areas abiotic processes, such as weathering and

storage/ventilation of karst systems, should be considered as mechanisms that, together with biological processes (photosynthesis and respiration), can contribute to the annual Net Ecosystem Carbon Balance (NECB) and should be considered to be of equal importance to organic C. However, their contributions are site specific and vary seasonaly. The major issues and therefore motivations for further development were encountered in regard of the providing energy for the automated field instruments, where systems depending on the photovoltaic panels lack performance in shadowed forests and cannot be used in the cave environment. Therefore, one part of future improvement for the methods used in this investigation will focus in overcoming the energy consumption problems. Besides that several techniques that required manual sampling could be automated in future investigations. For example, for gathering high frequency data for stable isotope composition of cave and soil CO_2 using portable optical devices and using sensors that continuously measure other parameters such as CO_2 concentrations in cave and at different depths within the soil profile.

The results of the present PhD thesis are also important from the socioeconomic aspect. It is expected that they will contribute to the estimation of the advantages and deficiencies of the present environmental status of soils on Karstic areas, which is important for the monitoring, planning and mitigating due to future environmental changes. Generally, the research outcomes enable a better understanding of the various sinks and sources of carbon in the Karstic environment in relation to the land use. Today this is an important priority in the EU policy and could also be applied in the IPCC revision of CO_2 emissions to the atmosphere where, following the IPCC 2013 Summary for policy makers, a large fraction of anthropogenic climate change resulting from CO_2 emissions is irreversible on a multi-century to millennial time scale, except in the case of a large net removal of CO_2 from the atmosphere over a sustained period.

Further, it was shown that these tools can be used for monitoring soil CO_2 above subterranean Carbon Capture and Storage facilities (CCS-Carbon Capture Sites), to detect a possible leakage of captured CO_2. CCS is regarded as one of the most important long-term measures for reducing carbon globally (International Energy Agency) and it has been suggested as a mitigation to counteract atmospheric CO_2 build up (Wilkinson, Haszeldine, Mackay, Smith, & Sargeant, 2013). Thus, the outcomes of the proposed PhD can represent an important scientific basis for planning of monitoring strategies in terrestrial management of CCS sites.

References

Allison, C. E., Francey, R. J., & Krummel, P. B. (2003). δ13C in CO2 from sites in the CSIRO Atmospheric Research GASLAB air sampling network. In *Trends: A Compendium of Data on Global Change, Carbon Dioxide Information Analysis Center, Oak Ridge National Laboratory, US Department of Energy, Oak Ridge, TN, USA* (Vol. 10). Oak Ridge: Carbon Dioxide Information Analysis Center, Oak Ridge National Laboratory, U.S. Department of Energy. Retrieved from http://cdiac.ess-dive.lbl.gov/trends/co2/allison-csiro/allcsiro_gaslab.html

Amundson, R. (2001). The Carbon Budget in Soils. *Annual Review of Earth and Planetary Sciences*, *29*(1), 535–562. https://doi.org/10.1146/annurev.earth.29.1.535

Amundson, R., & Davidson, E. (1990). Carbon dioxide and nitrogenous gases in the soil atmosphere. *Journal of Geochemical Exploration*, *38*(1–2), 13–41. https://doi.org/10.1016/0375-6742(90)90091-N

Amundson, R., Stern, L., Baisden, T., & Wang, Y. (1998). The isotopic composition of soil and soil-respired CO2. *Geoderma*, *82*(1–3), 83–114. https://doi.org/10.1016/S0016-7061(97)00098-0

Appelo, C. A. J., & Postma, D. (2005). *Geochemistry, groundwater and pollution* (second). Leiden: A.A. Balkema Publishers.

Arrhenius, S. (1889). Über die Reaktionsgeschwindigkeit bei der Inversion von Rohrzucker durch Säuren. *Zeitschrift Für Physikalische Chemie*, *4U*(1), 226–248. https://doi.org/10.1515/zpch-1889-0416

Arya, S. P. (1988). *Introduction to micrometeorology*. New York, NY: Academic Press Inc.

Aubinet, M., Grelle, A., Ibrom, A., Rannik, Ü., Moncrieff, J., Foken, T., … Vesala, T. (1999). Estimates of the Annual Net Carbon and Water Exchange of Forests: The EUROFLUX Methodology. In *Advances in ecological research* (Vol. 30, pp. 113–175). https://doi.org/10.1016/S0065-2504(08)60018-5

Badino, G. (2010). Underground meteorology-"what's the weather underground?" *Acta Carsologica*, *39*(3).

Bahn, M., Rodeghiero, M., Anderson-Dunn, M., Dore, S., Gimeno, C., Drösler, M., … Flechard, C. (2008). Soil respiration in European grasslands in relation to climate and assimilate supply. *Ecosystems*, *11*(8), 1352–1367.

Bar-Matthews, M., Ayalon, A., Matthews, A., Sass, E., & Halicz, L. (1996). Carbon and oxygen isotope study of the active water-carbonate system in a karstic Mediterranean cave: Implications for paleoclimate research in semiarid regions. *Geochimica et Cosmochimica Acta*, *60*(2), 337–347. https://doi.org/10.1016/0016-7037(95)00395-9

Barillon, R., Özgümüs, A., & Chambaudet, A. (2005). Direct recoil radon emanation from crystalline phases. Influence of moisture content. *Geochimica et Cosmochimica Acta*, *69*(11), 2735–2744.

Benson, S., Lennard, C., Maynard, P., & Roux, C. (2006). Forensic applications of isotope ratio mass spectrometry-a review. *Forensic Science International*, *157*(1), 1–22.

Berner, R. (1975). The role of magnesium in the crystal growth of calcite and aragonite from sea water. *Geochimica et Cosmochimica Acta*, *39*(4), 489IN3495-494504.

Berner, R. (2003). The long-term carbon cycle, fossil fuels and atmospheric composition. *Nature*, *426*(6964), 323.

Bertolini, T., Inglima, I., Rubino, M., Marzaioli, F., Lubritto, C., Subke, J.-A., … Cotrufo, M. F. (2006). Sampling soil-derived CO2 for analysis of isotopic composition: A comparison of different techniques. *Isotopes in Environmental and Health Studies*, *42*(1), 57–65.

Bond-Lamberty, B., & Thomson, A. (2010). Temperature-associated increases in the global soil respiration record. *Nature*, *464*(7288), 579–582. https://doi.org/10.1038/nature08930

Burba, G., & Anderson, D. (2010). A Brief Practical Guide to Eddy Covariance Flux Measurements: Principles and Workflow Examples for Scientific and Industrial Applications. Retrieved from http://www.gburba.com/science/publications.html

Bütz, D. E., Casperson, S. L., & Whigham, L. D. (2014). The emerging role of carbon isotope ratio determination in health research and medical diagnostics. *Journal of Analytical Atomic Spectrometry*, *29*(4), 594–598.

Carter, J. F., & Barwick, V. J. (2011). Good practice guide for isotope ratio mass spectrometry. *FIRMS Network*.

Cerling, T. E., & Quade, J. (1993). Stable carbon and oxygen isotopes in soil carbonates. *Climate Change in Continental Isotopic Records*, 217–231.

Cerling, T. E., Solomon, D. K., Quade, J., & Bowman, J. R. (1991). On the isotopic composition of carbon in soil carbon dioxide. *Geochimica et Cosmochimica Acta*, *55*(11), 3403–3405. https://doi.org/10.1016/0016-7037(91)90498-T

Cheng, W., Coleman, D. C., Carroll, C. R., & Hoffman, C. A. (1993). In situ measurement of root respiration and soluble C concentrations in the rhizosphere. *Soil Biology and Biochemistry*, *25*(9), 1189–1196.

Cigna, A. (1968). An analytical study of air circulation in caves. *International Journal of Speleology*, *3*(1/2), 41–54. https://doi.org/10.5038/1827-806X.3.1.3

Cigna, A. (2003). The distribution of radon concentration in caves. *International Journal of Speleology*, *32*(1/4), 113–115. https://doi.org/10.5038/1827-806X.32.1.8

Cigna, A. (2005). Radon in caves. *International Journal of Speleology*, *34*(1/2), 1–18. https://doi.org/10.5038/1827-806X.34.1.1

Clark, I. D., & Fritz, P. (1997). *Environmental isotopes in hydrogeology*. Boca Raton: Lewis Publishers.

Cole, J. J., Caraco, N. F., Kling, G. W., & Kratz, T. K. (1994). Carbon dioxide supersaturation in the surface waters of lakes. *Science-AAAS-Weekly Paper Edition*, *265*(5178), 1568–1569.

Coplen, T. B. (2011). Guidelines and recommended terms for expression of stable-isotope-ratio and gas-ratio measurement results. *Rapid Communications in Mass Spectrometry*, *25*(17), 2538–2560.

Covington, M. D., & Perne, M. (2016). Consider a cylindrical cave: A physicist's view of cave and karst science. *Acta Carsologica*, *44*(3). https://doi.org/10.3986/ac.v44i3.1925

Craig, H. (1957). Isotopic standards for carbon and oxygen and correction factors for mass-spectrometric analysis of carbon dioxide. *Geochimica et Cosmochimica Acta*, *12*(1–2), 133–149.

Cunningham, K. I., & LaRock, E. J. (1991). Recognition of microclimate zones through radon mapping, Lechuguilla Cave, Carlsbad Caverns National Park, New Mexico. *Health Physics*, *61*(4), 493–500.

Čater, M., & Ogrinc, N. (2011). Soil respiration rates and in natural beech forest (Fagus sylvatica L.) in relation to stand structure. *Isotopes in Environmental and Health Studies*, *47*(2), 221–237.

Davidson, E. A., & Trumbore, S. E. (1995). Gas diffusivity and production of CO 2 in deep soils of the eastern Amazon. *Tellus B: Chemical and Physical Meteorology*, *47*(5), 550–565. https://doi.org/10.3402/tellusb.v47i5.16071

Davidson, E., Belk, E., & Boone, R. D. (1998). Soil water content and temperature as independent or confounded factors controlling soil respiration in a temperate mixed hardwood forest. *Global Change Biology*, *4*(2), 217–227.

Davidson, E., Savage, K., Verchot, L. V, & Navarro, R. (2002). Minimizing artifacts and biases in chamber-based measurements of soil respiration. *Agricultural and Forest Meteorology*, *113*(1), 21–37.

Dawson, T. E., & Brooks, P. D. (2001). Fundamentals of stable isotope chemistry and measurement. In M. Unkovich, J. Pate, A. McNeill, & J. Gibbs (Eds.), *Stable Isotope Techniques in the Study of Biological Processes and Functioning of Ecosystems* (pp. 1–18). Dordrecht: Springer Netherlands.

Dawson, T. E., Mambelli, S., Plamboeck, A. H., Templer, P. H., & Tu, K. P. (2002). Stable isotopes in plant ecology. *Annual Review of Ecology and Systematics*, *33*(1), 507–559.

de Jong, E., Redmann, R. E., & Ripley, E. A. (1979). A comparison of methods to measure soil respiration. *Soil Science*, *127*(5), 300–306.

Deines, P. (1980). The isotopic composition of reduced organic carbon. In P. Fritz & J.-C. Fontes (Eds.), *Handbook of environmental isotope geochemistry* (Vol. 1, pp. 329–406). New York: Elsevier.

Deines, P., Langmuir, D., & Harmon, R. S. (1974). Stable carbon isotope ratios and the existence of a gas phase in the evolution of carbonate ground waters. *Geochimica et Cosmochimica Acta*, *38*(7), 1147–1164. https://doi.org/10.1016/0016-7037(74)90010-6

Dickson, A. G. (1981). An exact definition of total alkalinity and a procedure for the estimation of alkalinity and total inorganic carbon from titration data. *Deep Sea Research Part A. Oceanographic Research Papers*, *28*(6), 609–623.

Dioumaeva, I., Trumbore, S., Schuur, E. A. G., GOULDEN, M. L., Litvak, M., & HIRSCH, A. I. (2002). Decomposition of peat from upland boreal forest: Temperature dependence and sources of respired carbon. *Journal of Geophysical Research: Biogeosciences*, *107*(D3).

Dörr, H., & Münnich, K. O. (1986). Annual variations of the 14C content of soil CO2. *Radiocarbon*, *28*(2A), 338–345.

Drewitt, G. B., Black, T. A., & Jassal, R. S. (2005). Using measurements of soil CO2 efflux and concentrations to infer the depth distribution of CO2 production in a forest soil. *Canadian Journal of Soil Science*, *85*(2), 213–221.

Dreybrodt, W. (2011). Comments on processes contributing to the isotope composition of 13C and 18O in calcite deposited to speleothems. *Acta Carsologica*, *40*(2).

Dulinski, M., & Rozanski, K. (1990). Formation of 13 C/12 C isotope ratios in speleothems: a semi-dynamic model. *Radiocarbon*, *32*(1), 7–16.

Eiler, J. M. (2007). "Clumped-isotope" geochemistry-The study of naturally-occurring, multiply-substituted isotopologues. *Earth and Planetary Science Letters*, *262*(3), 309–327.

Ekblad, A., & Högberg, P. (2001). Natural abundance of 13C in CO2 respired from forest soils reveals speed of link between tree photosynthesis and root respiration. *Oecologia*, *127*(3), 305–308. https://doi.org/10.1007/s004420100667

Emerson, S., & Hedges, J. (2008). *Chemical oceanography and the marine carbon cycle*. Cambridge University Press.

Emmerich, W. E. (2003). Carbon dioxide fluxes in a semiarid environment with high carbonate soils. *Agricultural and Forest Meteorology*, *116*(1), 91–102.

Etiope, G., & Martinelli, G. (2002). Migration of carrier and trace gases in the geosphere: an overview. *Physics of the Earth and Planetary Interiors*, *129*(3–4), 185–204. https://doi.org/10.1016/S0031-9201(01)00292-8

Etiope, G., Nakada, R., Tanaka, K., & Yoshida, N. (2011). Gas seepage from Tokamachi mud volcanoes, onshore Niigata Basin (Japan): Origin, post-genetic alterations and CH4–CO2 fluxes. *Applied Geochemistry*, *26*(3), 348–359. https://doi.org/10.1016/j.apgeochem.2010.12.008

Fairchild, I. J., & Baker, A. (2012). *Speleothem Science*. Chichester, UK: John Wiley & Sons, Ltd. https://doi.org/10.1002/9781444361094

Fairchild, I. J., & Treble, P. C. (2009). Trace elements in speleothems as recorders of environmental change. *Quaternary Science Reviews*, *28*(5–6), 449–468. https://doi.org/10.1016/j.quascirev.2008.11.007

Fang, C., & Moncrieff, J. B. (1998). An open-top chamber for measuring soil respiration and the influence of pressure difference on CO2 efflux measurement. *Functional Ecology*, *12*(2), 319–325.

Fang, C., & Moncrieff, J. B. (1999). A model for soil CO2 production and transport 1: Model development. *Agricultural and Forest Meteorology*, *95*(4), 225–236.

Farquhar, G. D., Ehleringer, J. R., & Hubick, K. T. (1989). Carbon isotope discrimination and photosynthesis. *Annual Review of Plant Physiology and Plant Molecular Biology*, *40*(1), 503–537.

Farquhar, G. D., O'Leary, M. H., & Berry, J. A. (1982). On the relationship between carbon isotope discrimination and the intercellular carbon dioxide concentration in leaves. *Functional Plant Biology*, *9*(2), 121–137.

Foken, T., & Wichura, B. (1996). Tools for quality assessment of surface-based flux measurements. *Agricultural and Forest Meteorology*, *78*(1), 83–105.

Freijer, J. I., & Leffelaar, P. A. (1996). Adapted Fick's law applied to soil respiration. *Water Resources Research*, *32*(4), 791–800.

Frisia, S., Fairchild, I. J., Fohlmeister, J., Miorandi, R., Spötl, C., & Borsato, A. (2011). Carbon mass-balance modelling and carbon isotope exchange processes in dynamic caves. *Geochimica et Cosmochimica Acta*, *75*(2), 380–400. https://doi.org/10.1016/j.gca.2010.10.021

Froment, A. (1972). Soil respiration in a mixed oak forest. *Oikos*, 273–277.

Gaudinski, J. B., Trumbore, S. E., Davidson, E. A., & Zheng, S. (2000). Soil carbon cycling in a temperate forest: Radiocarbon-based estimates of residence times, sequestration rates and partitioning of fluxes. *Biogeochemistry*, *51*(1), 33–69.

Gillmore, G. K., Phillips, P. S., Denman, A. R., & Gilbertson, D. D. (2002). Radon in the Creswell Crags Permian limestone caves. *Journal of Environmental Radioactivity*, *62*(2), 165–179.

GLOBALVIEW-CO2C13. (2009). Cooperative Atmospheric Data Integration Project - δ13C of Carbon Dioxide. Retrieved April 14, 2017, from http://www.esrl.noaa.gov/gmd/ccgg/globalview/co2c13/co2c13_intro.html

Godwin, H. (1962). Half-life of radiocarbon. *Nature*, *195*(4845), 984. https://doi.org/10.1038/195984a0

Gregoric, A., Zidansek, A., & Vaupotic, J. (2011). Dependence of radon levels in Postojna Cave on outside air temperature. *Natural Hazards and Earth System Sciences*, *11*(5), 1523.

Gregorič, A., Vaupotič, J., & Gabrovšek, F. (2013). Reasons for large fluctuation of radon and CO2 levels in a dead-end passage of a karst cave (Postojna Cave, Slovenia). *Natural Hazards and Earth System Science*, *13*(2), 287–297. https://doi.org/10.5194/nhess-13-287-2013

Gregorič, A., Vaupotič, J., & Šebela, S. (2014). The role of cave ventilation in governing cave air temperature and radon levels (Postojna Cave, Slovenia). *International Journal of Climatology*, *34*(5), 1488–1500. https://doi.org/10.1002/joc.3778

Griffis, T. J. (2013). Tracing the flow of carbon dioxide and water vapor between the biosphere and atmosphere: A review of optical isotope techniques and their application. *Agricultural and Forest Meteorology*, *174*, 85–109.

Hakl, J., Csige, I., Hunyadi, I., Várhegyi, A., & Géczy, G. (1996). Radon transport in fractured porous media-experimental study in caves. *Environment International*, *22*, 433–437.

Hakl, J., Hunyadi, I., Csige, I., Géczy, G., Lénárt, L., & Várhegyi, A. (1997). Radon transport phenomena studied in karst caves-international experiences on radon levels and exposures. *Radiation Measurements*, *28*(1), 675–684.

Handley, L. L., & Raven, J. A. (1992). The use of natural abundance of nitrogen isotopes in plant physiology and ecology. *Plant, Cell & Environment*, *15*(9), 965–985.

Hirsch, A. I., Trumbore, S. E., & Goulden, M. L. (2003). Direct measurement of the deep soil respiration accompanying seasonal thawing of a boreal forest soil: Comparison of carbon exchange between boreal black spruce forests and the atmosphere for a wildfire age sequence (FIRE-EXB). *Journal of Geophysical Research*, *108*(D3), WFX2-1.

Hoefs, J. (2008). *Stable isotope geochemistry*. Springer Science & Business Media.

Högberg, P. (1998). Tansley Review No. 95: 15N natural abundance in soil-plant systems. *New Phytologist*, *139*(3), 595.

Inglima, I., Alberti, G., Bertolini, T., Vaccari, F. P., Gioli, B., Miglietta, F., … Peressotti, A. (2009). Precipitation pulses enhance respiration of Mediterranean ecosystems: the balance between organic and inorganic components of increased soil CO2 efflux. *Global Change Biology*, *15*(5), 1289–1301.

IPCC. (2013). *Climate change 2013: The physical science basis: Working Group I contribution to the Fifth assessment report of the Intergovernmental Panel on Climate Change*. (P. Stocker, Thomas; Qin, Dahe; Plattner, Gian-Kasper; Tignor, Melinda; Allen, Simon; Boschung, Judith; Nauels, Alexander; Xia, Yu; Vincent, Bex; Midgley, Ed.). Cambridge University Press.

Iskandar, D., Yamazawa, H., & Iida, T. (2004). Quantification of the dependency of radon emanation power on soil temperature. *Applied Radiation and Isotopes*, *60*(6), 971–973.

Jassal, R., Black, A., Novak, M., Morgenstern, K., Nesic, Z., & Gaumont-Guay, D. (2005). Relationship between soil CO2 concentrations and forest-floor CO2 effluxes. *Agricultural and Forest Meteorology*, *130*(3–4), 176–192. https://doi.org/10.1016/j.agrformet.2005.03.005

Jaynes, D. B., & Rogowski, A. S. (1983). Applicability of Fick's law to gas diffusion. *Soil Science Society of America Journal*, *47*(3), 425–430.

Jin, L., Ogrinc, N., Hamilton, S. K., Szramek, K., Kanduc, T., & Walter, L. M. (2009). Inorganic carbon isotope systematics in soil profiles undergoing silicate and

carbonate weathering (Southern Michigan, USA). *Chemical Geology*, *264*(1–4), 139–153. https://doi.org/10.1016/j.chemgeo.2009.03.002

Johansson, O., & Wedborg, M. (1982). On the evaluation of potentiometric titrations of sea-water with hydrochloric-acid. *Oceanologica Acta*, *5*(2), 209–218.

Kardos, R., Gregorič, A., Jónás, J., Vaupotič, J., Kovács, T., & Ishimori, Y. (2015). Dependence of radon emanation of soil on lithology. *Journal of Radioanalytical and Nuclear Chemistry*, *304*(3), 1321–1327. https://doi.org/10.1007/s10967-015-3954-3

Kaufmann, G., & Dreybrodt, W. (2007). Calcite dissolution kinetics in the system CaCO3-H2O-CO2 at high undersaturation. *Geochimica et Cosmochimica Acta*, *71*(6), 1398–1410. https://doi.org/https://doi.org/10.1016/j.gca.2006.10.024

Kawagucci, S., Tsunogai, U., Kudo, S., Nakagawa, F., Honda, H., Aoki, S., … Gamo, T. (2005). An analytical system for determining δ17O in CO2 using continuous flow-isotope ratio MS. *Analytical Chemistry*, *77*(14), 4509–4514. https://doi.org/10.1021/ac050266u

Kivastik, J. (1998). Paediatric reference values for spirometry. *Clinical Physiology and Functional Imaging*, *18*(6), 489–497. https://doi.org/10.1046/j.1365-2281.1998.00135.x

Koehler, B., Zehe, E., Corre, M. D., & Veldkamp, E. (2010). An inverse analysis reveals limitations of the soil-CO2 profile method to calculate CO2 production for well-structured soils. *Biogeosciences Discussions*, *7*(2). https://doi.org/10.5194/bg-7-2311-2010

Kovács, T., Szeiler, G., Fábián, F., Kardos, R., Gregorič, A., & Vaupotič, J. (2013). Systematic survey of natural radioactivity of soil in Slovenia. *Journal of Environmental Radioactivity*, *122*, 70–78. https://doi.org/https://doi.org/10.1016/j.jenvrad.2013.02.007

Kowalczk, A. J., & Froelich, P. N. (2010). Cave air ventilation and CO2 outgassing by radon-222 modeling: how fast do caves breathe? *Earth and Planetary Science Letters*, *289*(1), 209–219. https://doi.org/https://doi.org/10.1016/j.epsl.2009.11.010

Kowalski, A. S., & Sánchez-Cañete, E. P. (2010). A new definition of the virtual temperature, valid for the atmosphere and the CO2-rich air of the vadose zone. *Journal of Applied Meteorology and Climatology*, *49*(8), 1692–1695. https://doi.org/https://doi.org/10.1175/2010JAMC2534.1

Kowalski, A. S., Serrano-Ortiz, P., Janssens, I. A., Sánchez-Moral, S., Cuezva, S., Domingo, F., … Alados-Arboledas, L. (2008). Can flux tower research neglect geochemical CO2 exchange? *Agricultural and Forest Meteorology*, *148*(6–7), 1045–1054. https://doi.org/10.1016/j.agrformet.2008.02.004

Krajnc, B., Ferlan, M., & Ogrinc, N. (2017). Soil CO2 sources above a subterranean cave-Pisani rov (Postojna Cave, Slovenia). *Journal of Soils and Sediments*, 1–10.

Kristiansson, K., & Malmqvist, L. (1982). Evidence for nondiffusive transport of 222Rn in the ground and a new physical model for the transport. *GEOPHYSICS*, *47*(10), 1444–1452. https://doi.org/10.1190/1.1441293

Kucera, C., & Kirkham, D. R. (1971). Soil respiration studies in tallgrass prairie in Missouri. *Ecology*, *52*(5), 912–915. https://doi.org/10.2307/1936043

Kutsch, W., Bahn, M., & Heinemeyer, A. (2009). *Soil carbon dynamics: An integrated methodology / edited by Werner L. Kutsch, Michael Bahn, Andreas Heinemeyer*. Cambridge: Cambridge University Press.

Kuzyakov, Y. (2002). Review: Factors affecting rhizosphere priming effects. *Journal of Plant Nutrition and Soil Science*, *165*(4), 382–396. https://doi.org/10.1002/1522-2624(200208)165:4<382::AID-JPLN382>3.0.CO;2-#

Kuzyakov, Y. (2006). Sources of CO2 efflux from soil and review of partitioning methods. *Soil Biology and Biochemistry*, *38*(3), 425–448. https://doi.org/10.1016/j.soilbio.2005.08.020

Kuzyakov, Y., Leinweber, P., Sapronov, D., & Eckhardt, K.--U. (2003). Qualitative assessment of rhizodeposits in non-sterile soil by analytical pyrolysis. *Journal of Plant Nutrition and Soil Science*, *166*(6), 719–723. https://doi.org/10.1002/jpln.200320363

Lambert, W. J., & Aharon, P. (2011). Controls on dissolved inorganic carbon and δ13C in cave waters from DeSoto Caverns: implications for speleothem δ13C assessments. *Geochimica et Cosmochimica Acta*, *75*(3), 753–768.

Lasslop, G., Reichstein, M., Papale, D., Richardson, A. D., Arneth, A., Barr, A., … Wohlfahrt, G. (2010). Separation of net ecosystem exchange into assimilation and respiration using a light response curve approach: Critical issues and global evaluation. *Global Change Biology*, *16*(1), 187–208.

Lee, X., Sargent, S., Smith, R., & Tanner, B. (2005). In situ measurement of the water vapor 18O/16O isotope ratio for atmospheric and ecological applications. *Journal of Atmospheric and Oceanic Technology*, *22*(5), 555–565.

Levin, I., Naegler, T., Kromer, B., Diehl, M., Francey, R., Gomez-Pelaez, A., … Worthy, D. (2010). Observations and modelling of the global distribution and long-term trend of atmospheric 14 CO 2. *Tellus B: Chemical and Physical Meteorology*, *62*(1), 26–46. https://doi.org/10.1111/j.1600-0889.2009.00446.x

LGR. (2013). OA-ICOS Technology: The Most Successfully Method for Trace Gas and Isotope Analysis. Retrieved March 1, 2013, from http://www.lgrinc.com/advantages/oa-icos.php

Liang, N., Nakadai, T., Hirano, T., Qu, L., Koike, T., Fujinuma, Y., & Inoue, G. (2004). In situ comparison of four approaches to estimating soil CO2 efflux in a northern larch (Larix kaempferi Sarg.) forest. *Agricultural and Forest Meteorology*, *123*(1), 97–117.

Liu, W., Moriizumi, J., Yamazawa, H., & Iida, T. (2006). Depth profiles of radiocarbon and carbon isotopic compositions of organic matter and CO2 in a forest soil. *Journal of Environmental Radioactivity*, *90*(3), 210–223. https://doi.org/10.1016/j.jenvrad.2006.07.003

Livingston, G. P., & Hutchinson, G. L. (1995). Enclosure-based measurement of trace gas exchange: Applications and sources of error. *Biogenic Trace Gases: Measuring Emissions from Soil and Water*, 14–51.

Lloyd, J., & Taylor, J. A. (1994). On the temperature dependence of soil respiration. *Functional Ecology*, 315–323.

Luetscher, M., & Jeannin, P.--Y. (2004). Temperature distribution in karst systems: the role of air and water fluxes. *Terra Nova*, *16*(6), 344–350.

Lund, C. P., Riley, W. J., Pierce, L. L., & Field, C. B. (1999). The effects of chamber pressurization on soil-surface CO2 flux and the implications for NEE measurements under elevated CO2. *Global Change Biology*, *5*(3), 269–281.

Luo, Y., & Zhou, X. (2006). *Soil respiration and the environment*. Amsterdam and London: Academic Press. Retrieved from http://www.loc.gov/catdir/enhancements/fy0665/2006024416-d.html

Michener, R. H., & Lajtha, K. (2008). *Stable isotopes in ecology and environmental science* (2nd ed.). Malden, Mass. [etc.]: Blackwell Publishing.

Millero, F. J. (1995). Thermodynamics of the carbon dioxide system in the oceans. *Geochimica et Cosmochimica Acta*, *59*(4), 661–677.

Monger, H. C., & Gallegos, R. A. (2000). Biotic and abiotic processes and rates of pedogenic carbonate accumulation in the southwestern United States-relationship to atmospheric CO2 sequestration. In R. Lal, J. M. Kimble, H. Eswaran, & B. A. Stewart (Eds.), *Global climate change and pedogenic carbonates* (pp. 273–289). Boca Raton: Lewis Publishers CRC Press.

Mörner, N.-A., & Etiope, G. (2002). Carbon degassing from the lithosphere. *Global and Planetary Change*, *33*(1), 185–203.

Muller, P. (1994). Glossary of terms used in physical organic chemistry (IUPAC Recommendations 1994). *Pure and Applied Chemistry*, *66*(5). https://doi.org/10.1351/pac199466051077

Nakamura, K., Schoeller, D. A., Winkler, F. J., & Schmidt, H. L. (1982). Geographical variations in the carbon isotope composition of the diet and hair in contemporary man. *Biomedical Mass Spectrometry*, *9*(9), 390–394. https://doi.org/10.1002/bms.1200090906

Nay, S. M., Mattson, K. G., & Bormann, B. T. (1994). Biases of chamber methods for measuring soil CO2 efflux demonstrated with a laboratory apparatus. *Ecology*, *75*(8), 2460–2463.

NOAA. (2017). Globally averaged marine surface annual mean data. (Ed Dlugokencky, Ed.). Retrieved from ftp://aftp.cmdl.noaa.gov/products/trends/CO2/CO2_annmean_gl.txt

O'Leary, M. H. (1988). Carbon isotopes in photosynthesis. *Bioscience*, *38*(5), 328–336.

Ogrinc, N., Simončič, P., & Kovač, N. (2012). Soil organic matter characterization at different forest stands in Slovenia. In P. A. Björklund & F. V Mello (Eds.), *Soil organic matter* (pp. 89–110). Hauppauge, N.Y.: {Nova Science} and {Lancaster : Gazelle [distributor]}.

Ota, M., & Yamazawa, H. (2010). Forest floor CO2 flux estimated from soil CO2 and radon concentrations. *Atmospheric Environment*, *44*(36), 4529–4535.

Papale, D., Reichstein, M., Aubinet, M., Canfora, E., Bernhofer, C., Kutsch, W., … Vesala, T. (2006). Towards a standardized processing of Net Ecosystem Exchange measured with eddy covariance technique: Algorithms and uncertainty estimation. *Biogeosciences*, *3*(4), 571–583.

Peet, M. M., & Krizek, D. T. (1997). Carbon Dioxide: Chapter 4. In R. W. Langhans & T. W. Tibbitts (Eds.), *Plant Growth Chamber Handbook* (pp. 65–80). Ames. Retrieved from https://ncera.phytotron.ncsu.edu/wp-content/uploads/sites/6/2017/06/Ch04.pdf

Perrier, F., Richon, P., Crouzeix, C., Morat, P., & Le Mouël, J.-L. (2004). Radon-222 signatures of natural ventilation regimes in an underground quarry. *Journal of Environmental Radioactivity*, *71*(1), 17–32.

Phillips, D. L., & Gregg, J. W. (2003). Source partitioning using stable isotopes: coping with too many sources. *Oecologia*, *136*(2), 261–269.

Pingintha, N., Leclerc, M. Y., Beasley Jr, J., Zhang, G., & Senthong, C. (2010). Assessment of the soil CO2 gradient method for soil CO2 efflux measurements: comparison of six models in the calculation of the relative gas diffusion coefficient. *Tellus B*, *62*(1), 47–58.

Plestenjak, G., Eler, K., Vodnik, D., Ferlan, M., Čater, M., Kanduč, T., … Ogrinc, N. (2012). Sources of soil CO2 in calcareous grassland with woody plant encroachment. *Journal of Soils and Sediments*, *12*(9), 1327–1338.

Plummer, L. N., & Busenberg, E. (1982). The solubilities of calcite, aragonite and vaterite in CO2-H2O solutions between 0 and 90oC, and an evaluation of the

aqueous model for the system CaCO3-CO2-H2O. *Geochimica et Cosmochimica Acta*, *46*(6), 1011–1040.

Raich, J. W., & Potter, C. S. (1995). Global patterns of carbon dioxide emissions from soils. *Global Biogeochemical Cycles*, *9*(1), 23–36.

Raich, J. W., & Schlesinger, W. H. (1992). The global carbon dioxide flux in soil respiration and its relationship to vegetation and climate. *Tellus B: Chemical and Physical Meteorology*, *44*(2), 81–99.

Rao, M. S. (2012). Stable isotopic analysis using mass spectrometry and laser based techniques: A review. In S. Sathiyamoorthy, B. E. Caroline, & J. G. Jayanthi (Eds.), *Emerging Trends in Science, Engineering and Technology* (pp. 523–538). India: {Springer India} and {Imprint Springer}.

Reichstein, M., Falge, E., Baldocchi, D., Papale, D., Aubinet, M., Berbigier, P., … Granier, A. (2005). On the separation of net ecosystem exchange into assimilation and ecosystem respiration: Review and improved algorithm. *Global Change Biology*, *11*(9), 1424–1439.

Richardson, A. D., & Hollinger, D. Y. (2007). A method to estimate the additional uncertainty in gap-filled NEE resulting from long gaps in the CO2 flux record. *Agricultural and Forest Meteorology*, *147*(3), 199–208.

Risk, D., Kellman, L., & Beltrami, H. (2008). A new method for in situ soil gas diffusivity measurement and applications in the monitoring of subsurface CO2 production. *Journal of Geophysical Research: Biogeosciences*, *113*(G2).

Robinson, D. (2001). δ15N as an integrator of the nitrogen cycle. *Trends in Ecology & Evolution*, *16*(3), 153–162.

Romanek, C. S., Grossman, E. L., & Morse, J. W. (1992). Carbon isotopic fractionation in synthetic aragonite and calcite: effects of temperature and precipitation rate. *Geochimica et Cosmochimica Acta*, *56*(1), 419–430.

Rosman, K. J. R., & Taylor, P. D. P. (1998). Isotopic compositions of the elements 1997 (Technical Report). *Pure and Applied Chemistry*, *70*(1), 217–235.

Sakoda, A., Hanamoto, K., Ishimori, Y., Kataoka, T., Kawabe, A., & Yamaoka, K. (2010). First model of the effect of grain size on radon emanation. *Applied Radiation and Isotopes*, *68*(6), 1169–1172.

Salomons, W., & Mook, W. G. (1986). Isotope geochemistry of carbonates in the weathering zone: Chapter 6. In P. Fritz & Fontes Jean-Charles (Eds.), *Handbook of Environmental Isotope Geochemistry* (pp. 239–269). Amsterdam: Elsevier.

Sánchez-Cañete, E. P., Kowalski, A. S., Serrano-Ortiz, P., Pérez-Priego, O., & Domingo, F. (Eds.). (2013). Deep CO2 soil inhalation/exhalation in a carbonated semiarid steppe induced by atmospheric pressure fluctuations (Vol. 15).

Sano, Y., & Marty, B. (1995). Origin of carbon in fumarolic gas from island arcs. *Chemical Geology*, *119*(1–4), 265–274. https://doi.org/10.1016/0009-2541(94)00097-R

Schimel, D. S. (1993). *Theory and application of tracers*. Academic Press.

Schlesinger, W. H. (1985). The formation of caliche in soils of the Mojave Desert, California. *Geochimica et Cosmochimica Acta*, *49*(1), 57–66.

Schlesinger, W. H., & Andrews, J. A. (2000). Soil respiration and the global carbon cycle. *Biogeochemistry*, *48*(1), 7–20.

Serrano-Ortiz, P., Roland, M., Sanchez-Moral, S., Janssens, I. A., Domingo, F., Godderis, Y., & Kowalski, A. S. (2010). Hidden, abiotic CO2 flows and gaseous reservoirs in the terrestrial carbon cycle: review and perspectives. *Agricultural and Forest Meteorology*, *150*(3), 321–329.

Singh, J. S., & Gupta. (1977). Plant decomposition and soil respiration in terrestrial ecosystems. *The Botanical Review*, *43*(4), 449–528.

Spötl, C., Fairchild, I. J., & Tooth, A. F. (2005). Cave air control on dripwater geochemistry, Obir Caves (Austria): Implications for speleothem deposition in dynamically ventilated caves. *Geochimica et Cosmochimica Acta*, *69*(10), 2451–2468. https://doi.org/10.1016/j.gca.2004.12.009

Stabel, H.-H. (1986). Calcite precipitation in Lake Constance: Chemical equilibrium, sedimentation, and nucleation by algae. *Limnology and Oceanography*, *31*(5), 1081–1094. https://doi.org/10.4319/lo.1986.31.5.1081

Stranden, E., Kolstad, A. K., & Lind, B. (1984). The influence of moisture and temperature on radon exhalation. *Radiation Protection Dosimetry*, *7*(1–4), 55–58.

Stumm, W., & Morgan, J. J. (1981). *Aquatic chemistry: chemical equilibria and rates in natural waters* (Second Edi). New York: John Wiley & Sons.

Tranvik, L. J., Downing, J. A., Cotner, J. B., Loiselle, S. A., Striegl, R. G., Ballatore, T. J., … Weyhenmeyer, G. A. (2009). Lakes and reservoirs as regulators of carbon cycling and climate. *Limnology and Oceanography*, *54*(6part2), 2298–2314. https://doi.org/10.4319/lo.2009.54.6{\textunderscore }part{\textunderscore }2.2298

Wang, L., Caylor, K. K., & Dragoni, D. (2009). On the calibration of continuous, high-precision δ18O and δ2H measurements using an off-axis integrated cavity output spectrometer. *Rapid Communications in Mass Spectrometry*, *23*(4), 530–536.

Webb, E. K., Pearman, G. I., & Leuning, R. (1980). Correction of flux measurements for density effects due to heat and water vapour transfer. *Quarterly Journal of the Royal Meteorological Society*, *106*(447), 85–100.

Were, A., Serrano-Ortiz, P., Moreno de Jong, C., Villagarcía, L., Domingo, F., & Kowalski, A. S. (2010). Ventilation of subterranean CO2 and Eddy covariance incongruities over carbonate ecosystems. *Biogeosciences*, *7*(3), 859–867.

Wigley, T. (1967). Non-steady flow through a porous medium and cave breathing. *Journal of Geophysical Research*, *72*(12), 3199–3205. https://doi.org/10.1029/JZ072i012p03199

Wigley, T., & Brown, M. (1976). The Physics of Caves. In Ford, Trevor, D. & Cullingford, Cecil, Howard, Dunstan (Eds.), *The Science of Speleology* (pp. 329–358). New York: Academic Press.

Wilkening, M. (1990). *Radon in the Environment* (Vol. 40). Elsevier.

Wilkinson, M., Haszeldine, R. S., Mackay, E., Smith, K., & Sargeant, S. (2013). A new stratigraphic trap for CO2 in the UK North Sea: Appraisal using legacy information. *International Journal of Greenhouse Gas Control*, *12*, 310–322. https://doi.org/10.1016/j.ijggc.2012.09.013

Witkamp, M. (1966). Decomposition of leaf litter in relation to environment, microflora, and microbial respiration. *Ecology*, *47*(2), 194–201.

Wood, W. W. (1985). Origin of caves and other solution openings in the unsaturated (vadose) zone of carbonate rocks: a model for CO2 generation. *Geology*, *13*(11), 822–824.

Yakir, D., & Wang, X.-F. (1996). Fluxes of CO2 and water between terrestrial vegetation and the atmosphere estimated from isotope measurements. *Nature*, *380*(6574), 515.

Zhang, J., Quay, P. D., & Wilbur, D. O. (1995). Carbon isotope fractionation during gas-water exchange and dissolution of CO2. *Geochimica et Cosmochimica Acta*, *59*(1), 107–114.

Bibliography

Publications Related to the Thesis

Journal Articles

Krajnc, B., FujiyoshI, R., Vaupotič, J., Amano, H., Sakuta, Y., Gregorič, A., Ogrinc, N. (2016). Using ^{222}Rn and carbon isotopes (^{12}C, ^{13}C and ^{14}C) to determine CO_2 sources in forest soils developed on contrasting geology in Slovenia. *Environmental earth sciences*, 75(3),1068-1-1068-10. doi: 10.1007/s12665-016-5866-0

Ogrinc, N., Kanduč, T., Krajnc, B., Vilhar, U., Simončič, P., Jin, L. (2016) Inorganic and organic carbon dynamics in forested soils developed on contrasting geology in Slovenia - a stable isotope approach. *Journal of soils and sediments : protection, risk assessment and remediation*, 16(2), 382-395. doi: 10.1007/s11368-015-1255-7

Krajnc, B., Ferlan, M., Ogrinc, N. (2017) Soil CO_2 sources above a subterranean cave : Pisani rov (Postojna Cave, Slovenia). *Journal of soils and sediments : protection, risk assessment and remediation*, 17(7), 1883-1892. doi: 10.1007/s11368-016-1543-x

Giammanco, S., Krajnc B., Kotnik, J., Ogrinc N. Temporal analysis of $\delta^{13}C_{CO2}$ and CO_2 efflux in soil gas emissions at Mt. Etna: a new tool for volcano monitoring. *Journal Annals of Geophysics*, in press.

Krajnc, B., Jin, L., Vaupotič, J., Lojen, S., Nakamura, T., Ogrinc N. Sources, pathways and behaviour of cave air CO_2, using carbon isotopes. *Geochimica et Cosmochimica Acta*, under review.

Conference Paper

Krajnc, B., Lojen, S., Vaupotič, J., Dominiguez-Villar, D., Ogrinc, N.(2014). Dynamics of cave air ventilation in a dead - end passage of Postojna Cave (Pisani rov - Colourful gallery). In *Proceedings of 6th Jožef Stefan International Postgraduate School Students' Conference*. Ljubljana, Slovenia: Jožef Stefan International Postgraduate School.

Krajnc, B., Ferlan, M., Ogrinc, N. (2016). Evidence of cave ventilation and its contribution to soil CO_2 flux. In *Proceedings of 8th Jožef Stefan International Postgraduate School Students' Conference*. Ljubljana, Slovenia: Jožef Stefan International Postgraduate School.

Published scientific conference contribution abstract (invited lecture)

Lojen, S., Kanduč, T., Zavadlav, S., Krajnc, B., Ogrinc, N., Mezga, K.(2015). Carbon cycling in karstic areas: application of traditional and potential of non-traditional stable isotopes. In: *Book of abstracts of ESIR Isotope Workshop XIII*. Zadar, Croatia: Ruđer Bošković Institute.

Jin, L., Ortiz, A., Ogrinc, N., Krajnc, B., Kaye, J.P.(2017). Agricultural irrigation in drylands leads to development of pedogenic carbonate and release of soil CO_2. In: *Book of abstracts of Goldschmidt Conference.* Paris, France: European Association of Geochemistry & Geochemical Society.

Published scientific conference contribution abstract

Krajnc, B., Ferlan, M., Lojen, S., Vaupotič, J., Ogrinc, N.(2014). Can soil CO_2 efflux be affected by subterranean cave systems?. In: *Program and abstract book of 8th Young Researchers' Day.* Ljubljana, Slovenia: Jožef Stefan Institute.

Krajnc, B., Ferlan, M., Ogrinc, N. (2014). Method for flux and stable isotope measurements of soil CO_2. In: *Programme and abstracts of IASWS 13th International Symposium.* Grahamstown, South Africa: IASWS International Symposium

Krajnc, B., Ferlan, M., Ogrinc, N.(2015). Automated method for continuous soil CO_2 flux measurements. In *9th Young researchers' day.* Ljubljana, Slovenia: Jožef Stefan Institute.

Krajnc, B., Ferlan, M., Vaupotič, J., Jin, L., Lojen, S., Gabrovšek, F., Ogrinc, N.(2015). Soil-cave CO_2 dynamics and interactions. In *Dynamics of Biogeochemical Systems : processes and modeling : conference program and abstracts.* Piran, Slovenia: National Institute of Biology & Jožef Stefan Institute.

Krajnc, B., Ferlan, M., Ogrinc, N.(2015). Can subterranean cave system affect soil CO_2 fluxes?. In *European Geosciences Union, General Assembly 2015.* Vienna, Austria: European Geosciences Union.

Krajnc, B., Fujiyoshi, R., Vaupotič, J., Amano, H., Sakuta, Y., Gregorič, A., Ogrinc, N.(2016). Forest soil CO_2 source determination on diverse parent material using natural tracers (^{222}Rn, stable carbon isotopes ^{12}C, ^{13}C and ^{14}C). In *Program and abstract book of 10th Young researchers' day.* Ljubljana, Slovenia: Jožef Stefan Institute

Ortiz, A., Jin, L., Ogrinc, N., Krajnc, B., Kaye, J.(2016). Understanding the repercussions of dryland irrigation on pedogenic carbonate development. In *26th Goldschmidt Conference, 26.* Yokohama, Japan: European Association of Geochemistry & Geochemical Society

Kikaj, D., Krajnc, B., Črnič, B., Gregorič, A., Vaupotič, J.(2017). Radon as a tool in studying ventilation in the Postojna cave. In:*, Book of abstracts of III. East European Radon Symposum,* Sofia, Bulgaria: European Radon association

Krajnc, B., Nakamura, T., Ogrinc, N.(2017). Determining sources of CO_2 in Pisani rov (Postojna cave) using carbon isotopes ^{12}C, ^{13}C and ^{14}C). In *Program and abstract book of 11th Young researchers' day.* Ljubljana, Slovenia: Jožef Stefan Institute

Unpublished conference contribution

Krajnc, B., Ferlan, M., Lojen, S., Gabrovšek, F., Vaupotič, J., Ogrinc, N.(2015). Cave air dynamics and drip water geochemistry in Pisani rov-Postojna cave (Slovenia): presented at KG@B 2015, International Conference on Groundwater in Karst 20-26 June 2015, Birmingham, UK: University of Birmingham.

Biography

The author of this thesis Bor Krajnc was born on May 4, 1983 in Ljubljana, Slovenia. He finished his primary and secondary education in Ljubljana, Slovenia. He started his studies at the Biotechnical Faculty, University of Ljubljana, Slovenia, in 2002. In 2011, he was awarded a Diploma degree in Forestry for the thesis entitled "Forest soil bulk density and carbon stock on hard carbonate parent materials of Slovenia" from the University of Ljubljana. In 2012, he was selected as a PhD candidate at the Jožef Stefan International Postgraduate School, Ljubljana, Slovenia, under the supervision of Prof. Dr. Nives Ogrinc at the Department of Environmental Sciences. His research focuses on different sources and fluxes of CO_2 in natural ecosystems. For his work he uses different flux measurement techniques and naturally present tracers, such as stable and radioactive isotopes of carbon, stable isotopes of oxygen, and 222-radon. During the PhD studies he attended several workshops on the topic of isotope measurement techniques, use of stable isotopes in environmental sciences, geochemistry, cave systems, carbon cycle, data processing and visualization, and presented his work at several international conferences.